UNIVERSIDAD AUTÓNOMA DE MADRID
FACULTAD DE MEDICINA
DEPARTAMENTO DE BIOQUÍMICA

OVERCOMING MULTI-DRUG RESISTANCE IN FBXW7-DEFICIENT TUMOURS

LAURA SÁNCHEZ BURGOS
BSc, BIOLOGY
MSc, LIFE SCIENCES & TECHNOLOGIES

The work presented in this Doctoral Thesis has been carried out at the Genomic Instability Group in the Spanish National Cancer Research Centre (CNIO, Madrid), under the direction and supervision of Dr. Óscar Fernández-Capetillo Ruiz and funded by the La Caixa Foundation and the Marie Skłodowska-Curie European Union's Horizon 2020 actions (INPhINIT fellowship LCF/BQ/IN17/11620001).

Madrid, 2021

SPANISH NATIONAL CANCER RESEARCH CENTRE

June 1st 2021

To whom it might concern:

Dr. Óscar Fernández-Capetillo Ruiz, head of the Genomic Instability Group at the Spanish National Cancer Research Centre (CNIO) and Professor of Cancer Therapy at the Department of Medical Biochemistry and Biophysics (Karolinska Institutet), certifies that the Doctoral Thesis entitled: "Overcoming multi-drug resistance in FBXW7-deficient tumours", developed by Laura Sánchez Burgos, BSc, MSc, meets all the requirements to obtain the PhD (Doctor of Philosophy) degree in Molecular Biology and that it will be defended at the Universidad Autónoma de Madrid with the aforementioned objective. This Thesis has been carried out under my direction and I authorise its presentation to the Tribunal.

Dr. Óscar Fernández-Capetillo Ruiz
PhD Thesis Director

Deputy Director
Genomic Instability Group
Spanish National Cancer Research Centre (CNIO)
C/Melchor Fernández Almagro, 3
28029 Madrid
Spain

Professor of Cancer Therapy
Department of Medical Biochemistry and Biophysics
Karolinska Institutet
Solnavägen, 1
17177 Stockholm
Sweden

"*The scientist only imposes two things, namely* ***truth and sincerity****,*
imposes them upon himself and upon other scientists"
Erwin Schrödinger

"*There was truth and there was untruth,*
and if you clung to the truth even against the whole world, you were not mad"
1984, George Orwell

"*Once you do learn about the truth,*
you end up having to take a certain responsibility for it"
1Q84, Haruki Murakami

A Antonio, Sonia e Ignacio
A Diego

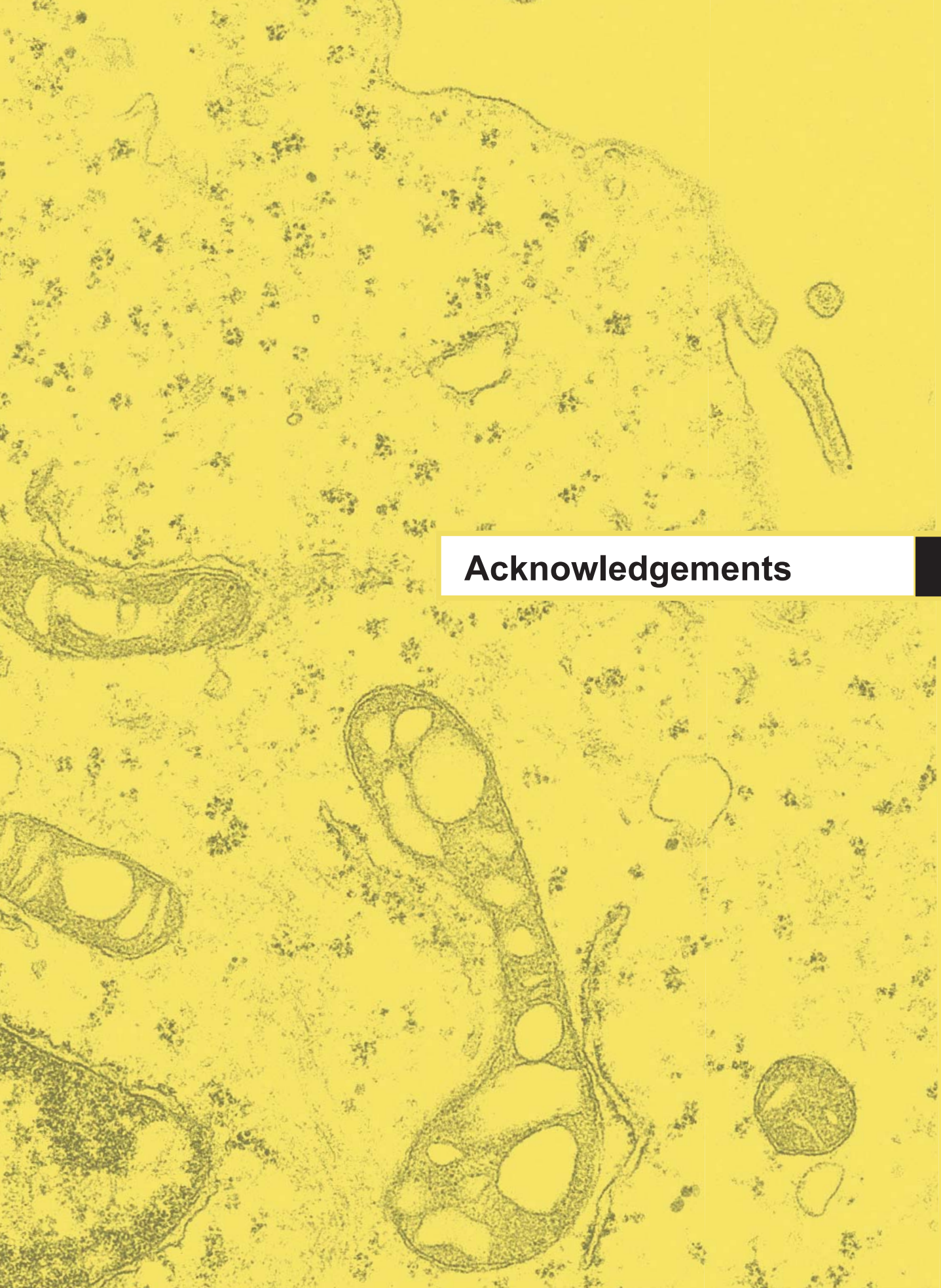

Acknowledgements

ACKNOWLEDGEMENTS

Hace ya 4 años que empecé con una grandísima ilusión este viaje. Pasado este tiempo, he descubierto tres cosas esenciales, que no son directamente mis resultados científicos, pero que están enormemente ligadas a ellos. La primera, es una manera de hacer y entender la ciencia, que me ha cambiado y que me llevo para el resto de mis futuros viajes. Otra, es el camino en sí: me enorgullece casi a la par que haber llegado al final, el que pese a los baches que han surgido, haber sabido disfrutar hasta los más pequeños resultados y, sobre todo, mantener intacta la llama de esta ilusión por la ciencia. Por último, y muy relacionada con las anteriores, los compañeros de viaje que he tenido a lo largo de este camino y a los que debo agradecer inmensamente el resultado de esta tesis.

Sin duda, el primer y más grandísimo gracias va dirigido hacia mi director de tesis, Óscar. Gracias en primer lugar por darme la oportunidad de hacer la tesis aquí y de poder empezar y realizar este proyecto. Por supuesto, por tu guía día a día que ha sacado adelante el proyecto, gracias por confiar en mí y por enseñarme tanto, en especial a saber centrarme en lo importante, a avivar mi curiosidad hacia cualquier tema interesante, a saber plantear las preguntas más adecuadas y a pensar siempre out-of-the-box. Y es que lo que agradezco más sin duda, es haberme trasmitido tu visión de la ciencia, que me llevo para el futuro. Estoy muy agradecida de haber podido tener el mejor mentor para mi doctorado, pero, sobre todo, para el camino que está por venir.

A mi familia de Inestabilidad Genómica, gracias por todos estos preciosos años y por enseñarme tanto, y no solo en el plano científico. Mati, el motor del lab, gracias por tu energía y positivismo contagiosos, por enseñarme a trabajar con el método Mati con el que todo funciona SIEMPRE, por amenizarnos tanto en el lab, y es que, sin duda, sin ti, se para el laboratorio. Vane, gracias por estar siempre dispuesta a echar una mano y aportar siempre ideas y soluciones a cualquier problema, y sobre todo por tu optimismo y alegría que me ha hecho sentirme siempre increíble en el lab. Bárbara, gracias por enseñarme a trabajar como una máquina en cultivos, y por acompañarme en los largos ratos ahí, por tu espíritu generación Z, y por tu dulzura y ánimos. Sergio, gracias por ayudarme y enseñarme al principio y por ser un staff tan genial. Emilio, gracias por la ayuda esencial con los Westerns y todo el mundo proteínas, y con cualquier otra cosa. Marta, la gurú de cualquier técnica, o películas y series, gracias por la ayuda con los ratones, por escucharme y ayudarme con cualquier cosa, por tu buen humor y la diversión constante en el pasillo, ha sido fantástico estar en el pasillo guay contigo. Sara, gracias por echarme una mano con las PCRs y con cualquier favor que he necesitado, por facilitar tanto el trabajo con tu orden, por preocuparte tanto por mí, y por tu buen corazón. Ali, gracias por toda la ayuda con todas las cuestiones administrativas o científicas, por tu generosidad y por preocuparte y animarme siempre. María, gracias por enseñarme todas las técnicas cuando entré al lab, y por ser una gran compi de mesa.

Una de las cosas que más agradezco es haber compartido esta tesis con unos grandísimos amigos. Tere, I cannot be more grateful to you, thanks for all your help at the beginning of this project, with your “consultorio” always open for me, and for being such an amazing and loving person, I was really lucky to share with you most of my PhD. Antonio, por enseñarme que con pocas palabras se puede demostrar mucho, gracias por la ayuda en el lab, pero sobre todo por estar siempre en todas y hasta el cierre, ha sido muy divertido compartir tesis contigo. Sasha, mi esencial; mi compi de resistencia millennial, de rincón del pasillo, y de tesis de principio al final; gracias por ayudar en la corrección de la tesis, por aconsejarme e impedirme hacer experimentos locos, por todas las ideas que me has aportado y por las confidencias y charlas no científicas que me han ayudado tanto, gracias por tu sentido humor y todas las risas que hemos compartido en estos años. Pablo, gracias por estar siempre dispuesto a ayudar con todo, por compartir conmigo tu energía positiva y sobre todo por hacer cada día en el lab único y especial, por llenarlo de tu fantasía, locura, intensidad máxima y alegría, sin ti no imagino todos estos momentos en la tesis. Elena, compartir la tesis contigo ha sido sentirse en casa, gracias por tu honestidad, buenos consejos y correcciones, porque sé que puedo confiarte cualquier cosa, por estar siempre dispuesta a ayudarme, y sobre todo por todo tu cariño y la diversión continua a tu lado; estoy muy feliz de haber encontrado a una persona tan fantástica y buena como tú gracias a esta tesis. Gema, que en poco tiempo y te has convertido en la experta de los screens, del espionaje y de un deporte en particular (se nota la clase), pero, sobre todo, te has ganado todo mi corazón; gracias por venir con las pilas cargadas para revolucionar el lab y llenarlo de alegría y diversión.

Por supuesto, también a los que estáis por venir: Belén, muchísimas gracias por ayudarme con mis experimentos en los veranos, y por darme la oportunidad de poder guiarte y enseñarte para tu proyecto de máster, aunque con una persona tan brillante y trabajadora como tú ha sido muy fácil; creo que he aprendido mucho más yo en este proceso que al revés, gracias de corazón, también por tu entusiasmo y positivismo con todo en la vida. Jorge, gracias por la frescura y las risas que en tan poquito tiempo has traído al lab, estoy encantada de que te hayas unido a tope. Ivó, gracias por los consejos sobre la ISR, te va a ir genial en el lab. Y también a todos vosotros con los que compartí tan buenos momentos, aunque fueran más cortos. Judith, fue fantástico conocer a una persona tan alegre y buena como tú, me dio mucha pena que no te quedaras más tiempo. Isa y Cris, un placer tremendo haber coincidido con vosotras y por esas increíbles fiestas de tesis. Elena y Patri, que por suerte os puedo seguir viendo por el CNIO.

Thanks a lot also to the Karolinska Capetillos for the great scientific collaboration, special thanks to Jordi, Bartek and Alba. Bartek and Wanda it was pleasure to work with you in the COVID project. Alba, ha sido un placer compartir todo este tiempo de tesis contigo, por la gran sinergia en cosillas de bioinformática y por todas las conversaciones de ciencia y de no ciencia.

Sin duda esta tesis es fruto de la colaboración con varios grupos del CNIO, cuya ayuda ha sido esencial en los puntos más clave del proyecto. A Fátima, Héctor, Santiago, Gonzalo y Carlos de Bioinformática. Ha sido un placer trabajar con todos vosotros por vuestra calidad científica, pero también humana. Fátima, gracias por coordinar y aportar tantas ideas de análisis de bioinformática que hemos llevado a cabo en este proyecto y en nuestro proyecto COVID (gracias ahí también a Gonzalo). Héctor, gracias por los análisis de CTRP y con la estadística del Xenabrowser, esenciales. Santiago, gracias por el análisis del CCLE de proteómica que tanto valor ha dado a este proyecto. Carlos muchas gracias por el tutorial de bases de datos, y por tantos años de amistad. A Javier y Eduardo de Proteómica, gracias por la realización de los experimentos de proteómica que fueron clave para avanzar con el proyecto. A Joaquín, Sonia, Carmen y Javier del grupo de Experimental Therapeutics, por proveernos con la librería de FDA antitumoural drugs y otras tantas siempre que hemos necesitado, y ¡por descubrirnos el CMap! A Jaska y a Johanne de Microscopía Electrónica del CNIO, y a Fernando del CIB, aunque todo vuestro trabajo no ha llegado a tiempo para esta tesis, sé que va a ser esencial para cerrar algunas preguntas que nos quedan pendientes. Thanks a lot also to Bruno Amati and his lab, for their inspirational work and the helpful discussions for this project.

También agradecer a las Unidades del CNIO por haberme facilitado el trabajo. A la Unidad de Microscopía Confocal: Diego, Manu, Jesús y Gadea; por ser siempre tan agradables y hacer todo tan fácil, es un placer siempre bajar allí con vosotros. A la Unidad de Citometría: Lola, Julia, Sara y Tania; por toda la ayuda con los sorters y con los cientos de veces que me dio fallo el citómetro pasando las placas. Al Animalario, en especial gracias a Sheila por la paciencia para enseñarme a trabajar con ratones, y a Virginia y Flor por su labor directa y ayuda. También gracias a la Unidad de Genómica por la ayuda en la parte de secuenciación y a la Unidad de Edición Genómica de Ratón, por la preparación de los medios de las mESCs. También como no a nuestros vecinos de cultivos de Monoclonales, que aparte de ser una gran compañía para los largos ratos en cultivos, han sido mi gran proveedor de líneas celulares (¡gracias Sere!). Gracias también a Paloma, que es ella una Unidad en sí misma, por toda la ayuda con el papeleo y por gestionar mis miles de envíos. ¡Y gracias al resto de Unidades y personal que hace que el CNIO funcione!Gracias, como no, a todos aquellos que alguna vez contestasteis un “alguien tiene”. Y es que el CNIO, aparte del increíble ambiente científico, me ha hecho sentirme en casa: gracias a todos los demás con los que he tenido la suerte de poder compartir estos 4 magníficos años. Gracias en especial al equipo chupito CNIO, Alberto y Pedro, al que sin duda sumaría a Nerea, Ana Belén, Tere y ¡al resto del grupo que no habéis fallado a una sola Beer Hour! Por todas esas fiestas hasta la 1h en la Social, o hasta las mil en el sótano del bar cutre (¿nombre?) siendo DJs o, cómo no, en el fantástico karaoke de Plaza Castilla.

Gracias también a la Fundación La Caixa, en especial a Gisela por toda la ayuda. Mis agradecimientos se extienden no solo a la beca que me ha permitido hacer este doctorado, sino también a la oportunidad que me ha brindado de conocer a tanta gente increíble, y sobre todo a grandes amigos. En especial, gracias al grupo de la Caixa Madrid, por los miles de quedadas, fiestas, cine, futbolín o risas en los webinars, ¡sois lo más! Lorena y Natalia, sé que me llevo a dos grandes amigas de aquí, ha sido increíble compartir esta tesis con vosotras.

Y por último debo dar las gracias a una colaboración muy especial y esencial para mi proyecto con mis amigos Xiaotong, Nacho y Bea. Gracias por la ayuda con toda la parte de caracterización de mitocondrias: reactivos, análisis, ideas. Xiaotong, thanks a lot for the protocols, and all your energy and the joy that you shared all this time with me from Lausanne to Madrid! Nacho, gracias por tu generosidad y estar siempre dispuesto a ayudar con lo que sea, por ese arrojo que tienes, y por todos los increíbles buenos ratos. Bea, gracias por ayudarme a todos los niveles posibles, incluyendo la lectura de esta tesis, por haber estado todos los días a mi lado siguiendo esta tesis, por tu coraje y corazón, por tu risa contagiosa, y por ser la definición de amistad.

Y es que tengo que agradecer a muchos amigos el haber podido tirar de esta tesis. Sus, gracias por ser esencial día a día, por tu optimismo y por convertir cualquier momento en una explosión de alegría y felicidad. Pau, por tu cariño y tu energía que me ha ayudado a lo largo de esta tesis. Aida, por estar siempre dispuesta a defenderme, y porque compartir piso contigo ha sido hogar. Vic, gracias por la ayuda administrativa con la tesis, y sobre todo por ser mi comparti de vida desde el primer día de uni: de Yugas, de tesis, de piso, de festivales, de viajes, y de muchísimas alegrías.

Gracias a mis amigos de siempre, por supuesto. Marcos, no ha sido fácil acabar la tesis sin uno de mis más grandes y mejores amigos; sin embargo, tu fuerza y energía me ha acompañado todo este camino. Car, gracias por ser mi persona, mi fan número 1 haga lo que haga, por las Jungles que juntas pueden ser en cualquier sitio y por

nuestra manera de vivir too fast too furious. Ángel, gracias por interesarte tanto por la 100sia, por tus bromas y el cachondeo constante, por tu apoyo incondicional y por querer tenerme siempre cerca. Andrea, al final se cumplió aquella promesa hecha con 8 años de que cuando fueras arquitecta me construirías mi casa, aunque sea un sentido más figurado: gracias por diseñar y maquetar esta tesis, y por supuesto por tu grandísima amistad estos más de 20 años. Jorge, gracias por todos los consejos y ayuda; a los Pablos, Javi, a los demás de Collado, a todos vosotros gracias, por todos los chocoviajes y por vuestra preciosa amistad. A mis chicas de Moral, gracias por la felicidad constante a vuestro lado; a Ali(ta), por las tardes de gordeo y por estar siempre apoyándome. Ali (A), gracias a mi amiga más antigua, por estar siempre en todas, y por animarme siempre a seguir adelante (con nuestra cabezonería típica) a lograr cualquier cosa; en definitiva, por ser familia.

Also, to all my friends from Switzerland, who followed me to Madrid or stayed in other parts of the world, but with whom I could always feel forever young in Balélec, Torino (thanks for the invitations as a speaker Marco and prof. Surace), Bucharest or Vienna, thanks! Cómo no, también a Silvia, Ale, Carlos, Pily, Dani, y demás Nostálgicos, por tantas noches en el Space Monkey o donde sea, porque con vosotros cualquier plan es siempre maravilloso; en nada esto está ardiendo en San Juan. Gracias al LIM, por las consultas de estadística y por supuesto por las grandísimas parrilladas argentinas. También gracias Matilde, por ayudarme a gestionar mis emociones de cara a esta tesis.

This has been my great scientific journey, but before that, I had many small but long adventures that lead the way to follow. To my previous labs and mentors, I am profoundly grateful: since my introduction in research in meiosis and biophysics, (gracias Mónica, Juan Luis, Fernando), to all that I learnt at EPFL on bioinformatics and stem cells (merci Didier, Olaia, Marine).

A los Romero Miguel, que ya son familia, gracias por hacerme estar siempre tan a gusto. Isabel y Luis, gracias por cuidarme desde el primer día, por todo el cariño y por estar siempre pendientes, interesados y orgullosos de todo este trabajo. A Rober, gracias por tu enorme corazón, por tu humor y porque sin duda hacemos un gran equipo.

A mi familia. Juan, has sido un motor para realizar esta tesis. Gracias a todos los Sánchez y Burgos por ayudarme a seguir adelante en todo momento, me da mucha alegría poder compartir con vosotros este momento (primera Doctora de ambas familias), en especial a los que habéis seguido muy de cerca todo este trabajo. En especial, gracias a mi abuela Puri y a mi tía Mari, y como no, a mis padres y a mi hermano.

Mamá, papá, no habría logrado alcanzar ninguna meta sin vosotros, gracias por animarme siempre a hacer lo que más me gustara y a impulsar mi curiosidad y creatividad. Mamá, gracias por enseñarme a ser perseverante y paciente, y por animarme siempre a creer que puedo construir cualquier castillo. Papá, gracias por ayudarme a relativizar todos los problemas y a ver la vida siempre de una manera positiva. Igna, gracias por ayudarme con mis preguntas tontas de química, también por ayudarme a ser más segura de mí misma y a ser siempre la mejor versión de mí, gracias por cuidarme en todas nuestras aventuras, conciertos y en la vida en general; y, en resumen, gracias por ser mi ejemplo a seguir, aun siendo mi hermano pequeño.

Y sin duda, esta tesis es Diego. Diego, sé que preferirías que cayera en lo atípico, y simplemente te diera un agradecimiento formal por ser mi manager de salud durante la escritura de esta tesis, mi co-autor de charlas divulgativas, y por leer, sugerir, corregir y aportar a esta tesis. O, incluso, un agradecimiento más informal por las discusiones científicas, los violin plots o los tuppers. Pero te voy a dar igualmente las gracias a mi manera. Gracias por seguir día a día cada experimento, por tu paciencia, y por tu amor. Gracias por hacer mía también tu visión entusiasta de la vida y de cada cosa nueva que haces, y, en definitiva, por darme tanta felicidad. Gracias por compartir esta tesis conmigo, por otros tantos años más antes, y, por supuesto, por el viaje que está por comenzar. GRACIAS.

Index

ACKNOWLEDGEMENTS 1
INDEX 4
RESUMEN 9
ABSTRACT 10
ABBREVIATIONS 11
INTRODUCTION 13
1. RESISTANCE TO ANTITUMOURAL AGENTS 13
1.1. Drug resistance: a major challenge in the oncology field 13
1.2. Mechanisms of resistance to antitumoural compounds 14
1.2.1. Pre-target mechanisms of resistance 14
1.2.2. On-target mechanisms of resistance: altered drug targets 14
1.2.3. Post-target mechanisms of resistance 15
1.2.4. Off-target mechanisms and other factors involved in resistance 16
1.3. Approaches to overcome drug resistance 16
1.3.1. Approaches to improve the rationale behind therapeutic interventions 16
1.3.2. Approaches for the identification of novel resistance-related genes and their vulnerabilities 16
1.3.3. Forward genetic screens 17
2. FBXW7 18
2.1. FBXW7 biology 18
2.1.1. FBXW7: a component of the ubiquitin-proteasome system 18
2.1.2. FBXW7 substrates 20
2.1.3. FBXW7 regulators 20
2.1.4. FBXW7 in physiology and pathology 21
2.2. FBXW7 deregulation in cancer 21
2.2.1. FBXW7: the ultimate tumour suppressor 21
2.2.2. Oncogenic FBXW7 substrates 22
2.2.3. Roles of FBXW7 in the response to antitumoural compounds 23
3. MITOCHONDRIA AND CANCER 24
3.1. Mitochondria 24
3.1.1. An overview of mitochondrial organization 24

3.1.2. OXPHOS 25
3.1.3. Mitochondrial translation 25
3.2. Targeting mitochondria in cancer 27
3.2.1. Mitochondrial translation and OXPHOS in cancer 27
3.2.2. Targeting OXPHOS 28
3.2.3. Targeting mitochondrial translation 28
3.3.4. Mechanism of action of mitochondrial translation inhibitors 29
OBJECTIVES 32
MATERIAL AND METHODS 33
1. CELLULAR BIOLOGY 33
1.1. Cell culture 33
1.2. Generation of knock-out, knockdown and fluorescent-proteins-expressing cell lines 33
1.2.1. Lentiviral production 33
1.2.2. Generation of knock-out cell lines 33
1.2.3. Generation of cell lines expressing fluorescent proteins 34
1.2.4. Knockdown experiments 35
1.3. CRISPR-Cas9 screens 35
1.4. Compounds 35
1.5. Flow cytometry and Flow Activated Cell Sorting (FACS) 38
1.5.1. Flow cytometry and High-Throughput flow cytometry for competition-two-colour assays .. 38
1.5.2. Flow Activated Cell Sorting (FACS) of fluorescent-proteins-expressing cells 38
1.6. Cell viability assays 38
1.6.1. Clonogenic assays 38
1.6.2. Cell-Titer Glo assays 38
1.6.3. Cell viability measurement by High Throughput Microscopy 39
1.7. Immunofluorescence stainings 39
1.7.1. ATF4 nuclear localisation by High Throughput Microscopy 39
1.7.2. Mitochondrial staining by Confocal Microscopy 39
2. MOLECULAR BIOLOGY 39
2.1. CRISPR-Cas9 screens sgRNA sequencing 39
2.2. Western Blot 40
2.3. Mass spectrometry 41

2.3.1. Samples preparation 41
2.3.2. High pH reverse phase chromatography 41
2.3.3. Liquid Chromatography with tandem mass spectrometry (LC-MS/MS) 41
2.4. Quantitative RT-PCR 41
3. MOUSE BIOLOGY 42
3.1. Xenograft experiments 42
4. BIOINFORMATICS, DATA ANALYSIS AND REPRESENTATION 42
4.1. Identification of CRISPR-Cas9 screens sgRNA sequences using Galaxy 42
4.2. *FBXW7* mutations/expression and drug response analysis 42
4.2.1. Representation of the most FBXW7-mutated cancer types 42
4.2.2. Analysis of the multi-drug resistance phenotype of FBXW7 mutated cancer cells 42
4.2.3. Patients' survival, drug treatment, and FBXW7 gene expression correlation 43
4.3. Proteomics data analysis 43
4.3.1. Mass spectrometry data analysis 43
4.3.2. Cancer Cell Line Encyclopaedia (CCLE) proteomics analysis 43
4.4. Connectivity Map (CMap) analysis 44
4.4.1. CMap data analysis 44
4.4.2. Drug "Gene Set Enrichment Analysis" (GSEA) 44
4.5. Other graphical representations and statistical analyses 44
RESULTS 45
1. IDENTIFICATION OF NOVEL MECHANISMS OF RESISTANCE TO GENOTOXIC THERAPIES THROUGH CRISPR-CAS9 SCREENS 45
1.1. CRISPR-Cas9 screens for mediators of cisplatin-resistance 45
1.2. CRISPR-Cas9 screens for modulators of UV-light sensitivity 46
1.3. Validation of CRISPR-Cas9 screens hits: *Ptpn2* 46
1.4. Identification of *Fbxw7* as a recurrent hit in CRISPR-Cas9 screens 47
2. FBXW7 DEFICIENCY AS A MULTI-DRUG RESISTANCE AND POOR PROGNOSIS MARKER IN CANCER 48
2.1. *Fbxw7* deletion is associated with multi-drug resistance 48
2.1.1. Loss of Fbxw7 is associated to multi-drug resistance in mESCs 48
2.1.2. FBXW7 deficiency is associated with multi-drug resistance in human cancer cell lines 50
2.1.3. FBXW7 deficiency is associated with poor therapy response in cancer patients 51

2.2. Mechanisms of therapy resistance driven by FBXW7-deficiency 52

2.2.1. MCL1 52

2.2.2. ABCB1 52

3. PROTEOMIC APPROACHES IDENTIFIED MITOCHONDRIAL TRANSLATION AND OTHER MITOCHONDRIAL PROCESSES AS A VULNERABILITY FOR FBXW7-DEFICIENT CELLS 55

3.1. Proteomic comparison between *FBXW7*-mutated and WT cells revealed an upregulation of mitochondrial processes in FBXW7-deficient cells 55

3.2. Mitochondrial translation and other mitochondrial processes are upregulated in FBXW7-deficient cells 57

3.3. Targeting mitochondrial activity is selectively toxic for FBXW7-deficient cells 60

3.3.1. Genetic and pharmacological inhibition of mitochondrial activity 60

3.3.2. Mechanism of action of the sensitivity to mitochondrial poisons: MYC and the ISR 63

3.4. Efficacy of tigecycline in preclinical models of FBXW7-deficient tumours 65

4. DISCOVERY OF ADDITIONAL COMPOUNDS SELECTIVELY KILLING *FBXW7*-DEFICIENT CELLS 66

4.1. A focused chemical screen identifies the B-RAF inhibitor PLX-4720 as a compound selectively killing *FBXW7* KO cells 66

4.2. Connectivity Map (CMap) tool identified more compounds similar to PLX-4720 in the ability to selectively kill *FBXW7* KO cells 67

4.3. Compounds preferentially toxic for FBXW7-deficient cells activate the ISR 68

4.4. Activating the ISR as a general strategy to target FBXW7-deficient tumours 71

DISCUSSION 74

1. SHEDDING LIGHT ON THE MECHANISMS BEHIND DRUG RESISTANCE IN CANCER 74

1.1. Studying the mechanisms of cancer drug resistance 74

1.2. CRISPR-Cas9 screens as a powerful technique to discover novel resistance-related genes 74

1.3. FBXW7 deficiency as a multi-drug resistance mediator 76

1.4. FBXW7 deficiency mechanism of MDR may be multifactorial and drug-dependent 78

1.4.1. MCL1 78

1.4.2. ABCB1 78

1.4.3. Cellular phenotype 78

2. OVERCOMING RESISTANCE 79

2.1. General strategies to overcome drug resistance 79

2.2. Current potential strategies to overcome therapy resistance in FBXW7-deficient cells 79

2.3. Novel ideas to overcome therapy resistance in FBXW7-deficient cells 80

2.3.1. Increase FBXW7-substrate binding affinity 80

2.3.2. Targeting of FBXW7 regulators 81

2.3.3. Targeting of downstream oncoproteins 81

2.3.4. Discovery of synthetic-lethal strategies 81

2.3.5. This Thesis approach 82

2.4. Final considerations to overcome therapy resistance in FBXW7-deficient cells 82

3. TARGETING MITOCHONDRIAL TRANSLATION **82**

3.1. Targeting the mitochondria to overcome resistance in FBXW7-deficient cells 82

3.2. Clinical use of tigecycline 83

3.3. New strategies to target mitochondrial translation 84

4. TARGETING THE ISR **84**

4.1. Role of the ISR in the toxicity of mitochondrial translation inhibitors 84

4.2. Discovery of novel drugs activating the ISR 85

4.3. Other tumour types or diseases that may be targeted by activating the ISR 87

4.4. Dissecting the induction of the ISR in FBXW7-deficient cells 87

CONCLUSIONES **89**

CONCLUSIONS **90**

ANNEX **91**

1. ANNEX FIGURES **91**

2. ANNEX TABLES **94**

BIBLIOGRAPHY **106**

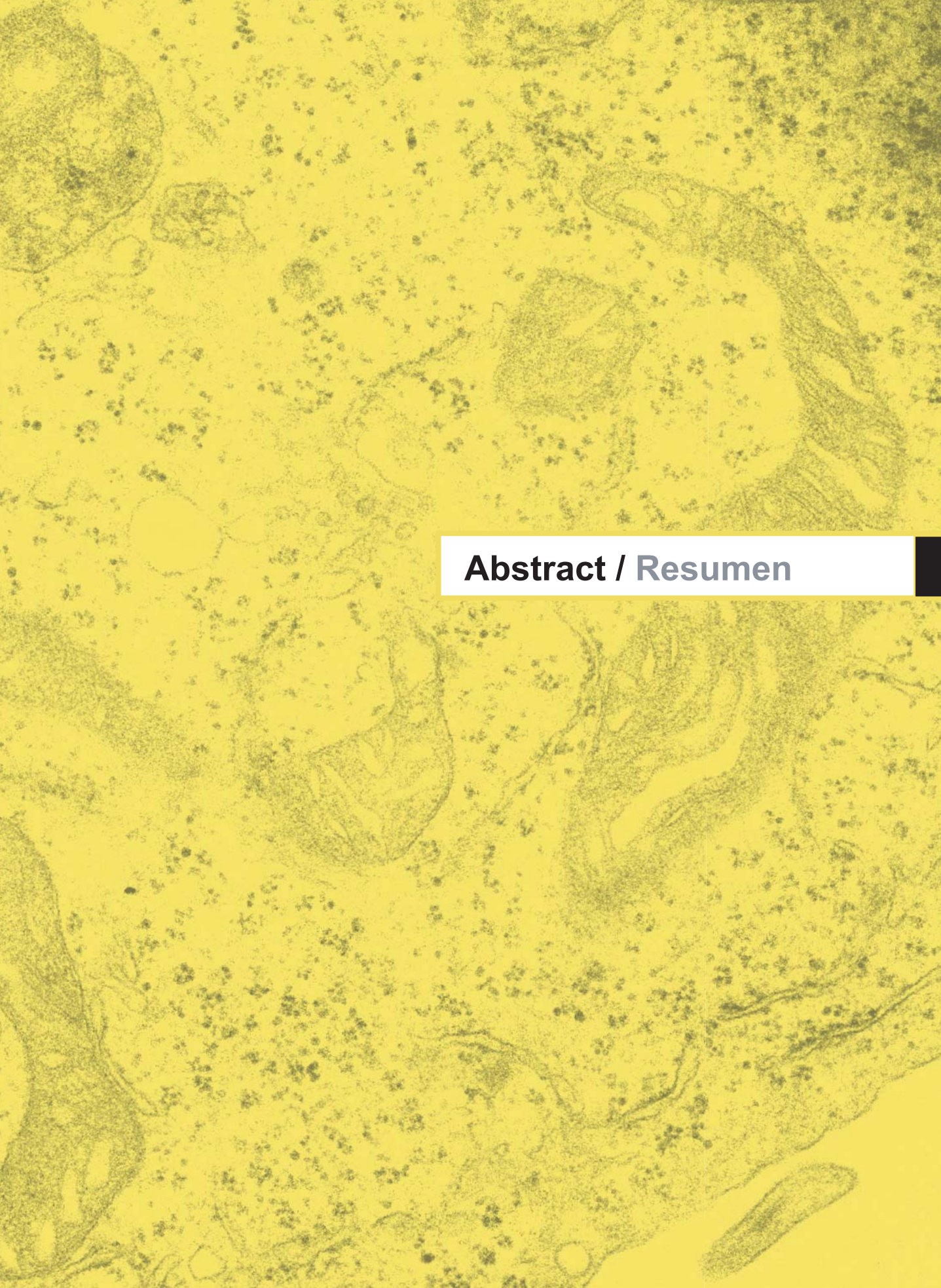

Abstract / Resumen

La **resistencia a los fármacos** supone la principal limitación para el éxito terapéutico de los tratamientos antitumorales, contribuyendo al fracaso de estas terapias en aproximadamente el 90% de los pacientes con metástasis. Sin embargo, nuestra comprensión de los mecanismos que contribuyen a esta resistencia es limitada. En ese sentido, el descubrimiento de las mutaciones causantes de la resistencia puede ayudar a identificar nuevos marcadores de respuesta a terapias, así como opciones terapéuticas para superarla. La tecnología CRISPR-Cas9 supone, a tal efecto, una herramienta con un gran potencial para descubrir mutaciones relacionadas con resistencia a fármacos a través de cribados genómicos. Al realizar dicho cribado en busca de mecanismos de resistencia a cisplatina, radiación ultravioleta y varios fármacos citotóxicos, encontramos que las deleciones del gen FBXW7, un componente de reconocimiento de sustrato del complejo E3 ubiquitina ligasa, eran un hallazgo recurrente. Posteriormente, pudimos confirmar que las células deficientes para FBXW7 son **resistentes a la gran mayoría de los agentes antitumorales** usados actualmente. Este hallazgo es de gran importancia, ya que las mutaciones en *FBXW7* son una de las más frecuentes en cáncer y, tras realizar un análisis bioinformático de bases de datos, confirmamos que bajos niveles de FBXW7 se correlacionan con un peor pronóstico para pacientes de cáncer que están recibiendo cualquier terapia. Nuestro trabajo muestra que el mecanismo de resistencia a múltiples fármacos observado en células deficientes para FBXW7 es **multifactorial y dependiente del fármaco**, estando MCL1 y ABCB1 relacionados con la resistencia a algunos fármacos concretos. Además, otro de nuestros objetivos fue tratar de neutralizar esta resistencia mediante la búsqueda de vulnerabilidades genéticas o farmacológicas en células deficientes para FBXW7. De este modo, dos análisis de proteómica diferentes mostraron que varios elementos de distintos procesos mitocondriales, como la traducción mitocondrial, se encontraban sobre-expresados en células deficientes para FBXW7. De manera destacada, la **inhibición de la traducción mitocondrial con el antibiótico tigeciclina**, así como otras estrategias tanto genéticas como farmacológicas cuya diana es el metabolismo mitocondrial, eliminaban selectivamente tumores deficientes en FBXW7 *in vitro* e *in vivo*. Estos efectos eran dependientes de C-MYC y de la activación de la respuesta integrada al estrés (ISR), ya que su disminución o su inhibición en células deficientes para FBXW7 anulaba los efectos ya mencionados. Finalmente, y a través de un enfoque independiente, encontramos otro grupo de fármacos, todos activadores de la ISR, que era selectivamente tóxico para las células deficientes para FBXW7. De manera colectiva, este trabajo ha contribuido al descubrimiento de la deficiencia de FBXW7 como nueva mutación relacionada con multi-resistencia a fármacos y ha puesto de manifiesto que la sobre-regulación de la traducción mitocondrial es una vulnerabilidad que puede ser explotada para neutralizar esta resistencia.

Drug resistance is a major limitation for the therapeutic success of antitumoural treatments, estimated to contribute to treatment failure in 90% of metastatic patients. However, our understanding of the mechanisms involved in therapy resistance is still incomplete. The discovery of the mutations driving resistance can help in the identification of new therapy-response markers and therapeutic options that overcome such resistance. The advent of CRISPR-Cas9 technology has now provided significant potential through genome-wide screens to discover resistance-related mutations. During our efforts to screen for mechanisms of resistance towards cisplatin, UV and other cytotoxic drugs, we found **deletions of *Fbxw7***, a substrate recognition component of an E3 ubiquitin-protein ligase complex, as a recurrent hit. We subsequently observed that FBXW7-deficient cells are **resistant to the vast majority of currently-used antitumoural agents**. Importantly, *FBXW7* mutations are one of the most frequent in cancer, and dataset analysis indicate that low FBXW7 levels correlated with poor prognosis in cancer patients undergoing therapy. Our work indicates that the multi-drug resistance observed in FBXW7-deficient cells is **multifactorial and drug-dependent**, with MCL1 and ABCB1 being involved in the resistance to some specific drugs. Next, we aimed to overcome such resistance by the discovery of genetic or chemical vulnerabilities in *FBXW7*-deficient cells. Proteomic analyses showed that some components of mitochondrial processes such as mitochondrial translation were overexpressed in FBXW7-deficient cells. Importantly, **inhibition of mitochondrial translation by repurposing the antibiotic tigecycline** and other genetic and pharmacological approaches that target mitochondrial metabolism, selectively killed FBXW7-deficient cells *in vitro* and *in vivo*. These effects were dependent on C-MYC and the integrated stress response (ISR), as their downregulation or inhibition in FBXW7-deficient cells abrogated the aforementioned effects. Finally, and through an independent approach, we found another set of compounds that were also preferentially toxic for FBXW7-deficient cells, all of which were found to be activators of the ISR. Collectively, this work has contributed to the discovery of FBXW7 deficiency as a novel mutation related to multi-drug resistance, and has discovered the upregulation of mitochondrial translation as a vulnerability that can be exploited for targeting this resistance.

Abbreviations

-/-	Homozygous
+/-	Heterozygous
2'CMeA	2'-C-methyladenosine
5-FU	Fluorouracil
β-TrCP Ligase	β-Transducing Repeat Containing E3 Ubiquitin Protein
ABC	ATP-binding cassette
ABCB1	ABC subfamily B member 1
ADP	Adenosine diphosphate
AGO	Argonaute protein
ALL	Acute Lymphoblastic Leukaemia
AML	Acute Myeloid Leukaemia
AMP	Adenosine monophosphate
AMPK	5' AMP-activated protein kinase
ATCC	American Type Culture Collection
ATF	Activating Transcription Factor (4, 5, 6)
ATP	Adenosine triphosphate
ATR	Ataxia Telangiectasia and Rad3 related
a.u.	Arbitrary units
AUC	Area Under the Curve
BCL2	B-Cell Lymphoma 2
BFP	Blue Fluorescent Protein
BRCA	Breast Cancer Type (1, 2)
BSA	Bovine serum albumin
CAS9	CRISPR-Associated Protein 9
CCLE	Cancer Cell Line Encyclopaedia
CCNE1	Cyclin E1
CDC4	Cell Division Control protein 4
CDC25A	Cell Division Cycle 25A
C/EBPδ	CCAAT Enhancer Binding Protein delta
CHOP	C/EBP Homologous Protein
CMap	Connectivity Map
CML	Chronic Myeloid Leukaemia
CPD	Cdc4 Phosphodegron
CRISPR	Clustered Regularly Interspaced Short Palindromic Repeats
CS	Citrate Synthase
CSC	Cancer stem cell
CTLA4	Cytotoxic T-Lymphocyte-Associated protein 4
CTRP	Cancer Therapeutics Response Portal
CUL1	Cullin-1
DAB2IP	DAB2 Interacting Protein
DAB-III	10-Desacetylbaccatin-III
DAPI	4′,6-diamidino-2-phenylindole
dCas9	Dead Cas9
DELE1	DAP3 Binding Cell Death Enhancer 1
DMEM	Dulbecco's Modified Eagle's Medium
DMF	Dimethyl formamide
DMSO	Dimethyl sulfoxide
DSB	Double Strand Break
dsRNA	Double Stranded RNA
DNA	Deoxyribonucleic acid
dpc	Days post coitum
DTT	Dithiothreitol
E1	Ubiquitin-activating enzyme
E2	Ubiquitin-conjugating enzyme
E3	Ubiquitin-protein ligase
EDTA	Ethylenediaminetetraacetic acid
EFs	Elongation factors
EGFR	Epidermal Growth Factor Receptor
eIF2α	Eukaryotic Initiation Factor-2α (eIF2α)
ER	Endoplasmic Reticulum
esiRNA	Endoribonuclease-prepared siRNA
EMT	Epithelial-Mesenchymal Transition
ENU	N-ethyl-N-nitrosourea
ERK	Extracellular signal-regulated kinase
ETC	Electron Transport Chain
EtOH	Ethanol
FACS	Flow Activated Cell Sorting
FAD	Flavin Adenine Dinucleotide
FBS	Fetal Bovine Serum
FBXL	F-box coupled with LRRs
FBXWO	F-box with other motifs
FBXW	F-box coupled with WD repeats
FBXW7	F-Box and WD Repeat Domain Containing 7
FC	Fold-change
FDA	U.S. Food and Drug Administration
FDR	False-Discovery Rate
GCN2	General Control Non-derepressible 2
GDA	Genomics and Drugs Integrated Analysis
GDC	NCI Genomic Data Commons
GFP	Green Fluorescent Protein
GO	Gene Ontology
GSEA	Gene Set Enrichment Analysis
GSK3	Glycogen Synthase Kinase 3
Gy	Gray
H	Hour
HCD	Higher-energy collisional dissociation
HEPES	4-(2-hydroxyethyl)-1-piperazineethanesulfonic acid
HRI	Heme-Regulated Inhibitor
HRP	Horseradish peroxidase
HSP	Heat-shock Protein
HU	Hydroxyurea
i	Inhibitor
IF	Immunofluorescence
IFs	Initiation Complex Factors
IMTs	Inhibitors of Mitochondrial Transcription
i.p.	Intraperitoneal
IR	Ionizing Radiation
IRE1α	Inositol-requiring transmembrane kinase / endoribonuclease 1α
ISR	Integrated Stress Response
ISRIB	ISR inhibitor
KD	Knock-down
KLF	Kruppel-Like Factor
KO	Knock-out
LC-MS/MS	Liquid Chromatography with tandem mass spectrometry
LIF	Leukaemia Inhibitory Factor
lncRNA	Long non-coding RNA

LPS	Lipopolysaccharides
LRR	Leucine-Rich Repeats
MAPK	Mitogen-Activated Protein Kinase
MCL1	Myeloid Cell Leukaemia 1
MDR	Multi-drug resistance
MED	Mediator Complex
MEF	Mouse Embryonic Fibroblast
mESC	Mouse Embryonic Stem Cell
Min	Minutes
miRNA	microRNA
MITF	Melanocyte Lineage Transcription Factor
MMR	DNA mismatch repair
MOA	Mechanism of action
MOI	Multiplicity of infection
MOMP	Mitochondrial Outer Membrane Permeabilization
MRP(L/S)	Mitochondrial Ribosomal Protein large/small
mtDNA	Mitochondrial DNA
mTOR	Mechanistic Target of Rapamycin
MUT	Mutation
MYH9	Myosin Heavy Chain 9
NAD	Nicotinamide Adenine Dinucleotide
NCI60	US National Cancer Institute 60 human tumour cell line anticancer drug screen
NER	Nucleotide Excision Repair
NES	Normalized Enrichment Score
NLS	Nuclear Localisation Signal
n.s.	Non-significant
OMA1	Overlapping Activity with M-AAA Protease
OXPHOS	Oxidative Phosphorylation
padj	adjusted p-value
PARP	Poly [ADP-Ribose] Polymerase
PBS	Phosphate-buffered saline
PCR	Polymerase chain reaction
PD1	Programmed Death 1
PDL1	Programmed Death Ligand 1
PERK	PKR-like Endoplasmic Reticulum Kinase
PFA	Paraformaldehyde
PGC1α	PPARγ Coactivator-1α
PI3K	Phosphoinositide 3-kinase
PKMYT1	Membrane-associated tyrosine- and threonine-specific cdc2-inhibitory kinase
PKR	Protein Kinase R
PLK1	Polo Like Kinase 1
POLRMT	mtRNA polymerase
PRMT5	Protein Arginine Methyltransferase 5
PROTAC	Proteolysis-Targeting Chimera
PTEN	Phosphatase and Tensin homolog
PTPN2	Protein Tyrosine Phosphatase Non-Receptor Type 2
qRT-PCR	Real-Time Quantitative Reverse Transcription PCR
pval	p-value
RAF	Rapidly Accelerated Fibrosarcoma
RAS	Rat sarcoma
RB1	Retinoblastoma 1
RBX1/2	RING Box Protein 1/2
RFs	Release factors
ROS	Reactive oxygen species
RNA	Ribonucleic acid
RNAi	Interference RNA
rRNA	Ribosomal RNA
RT	Room temperature
SCF	Skp, Cullin, F-box (containing complex)
SD	Standard Deviation
SDH	Succinate Dehydrogenase
SDS	Sodium dodecyl sulphate
Secs	Seconds
SEL-10	Suppressor/Enhancer of Lin-12 10
SKP1	S-phase Kinase-associated Protein 1
sgRNA	Single Guide RNA
shRNA	Short hairpin RNA
siRNA	Small Interfering RNA
SREBP1	Sterol regulatory element-binding protein 1
STAT3	Signal transducer and activator of transcription 3
STYX	Serine/Threonine/Tyrosine Interacting Protein
TALEN	Transcription Activator-Like Effectors
T-ALL	T-lineage acute lymphoblastic leukaemia
TCA	Tricarboxylic acid
TC-PTP	T-cell protein tyrosine phosphatase
TGF-β	Transforming Growth Factor Beta
TGIF	TGFB Induced Factor Homeobox 1
TMD	Transmembrane Domain
TP53	Tumour Protein P53
TRIP12	Thyroid Hormone Receptor Interactor 12
tRNA	Transfer RNA
UQCR	Ubiquinol-cytochrome c reductase
UPS	Ubiquitin-Proteasome System
USP	Ubiquitin Specific Protease
UV	Ultraviolet
VCP/p97	Valosin Containing Protein
WB	Western Blot
WD rep.	Tryptophan and aspartic acid repeat
WNT	Wingless-related integration site
WRN	Werner syndrome ATP-dependent helicase
WT	Wild-Type
XRCC4	X-Ray Repair Cross Complementing 4
ZEB	Zinc Finger E-Box Binding Homeobox
ZFN	Zinc-Finger Nucleases

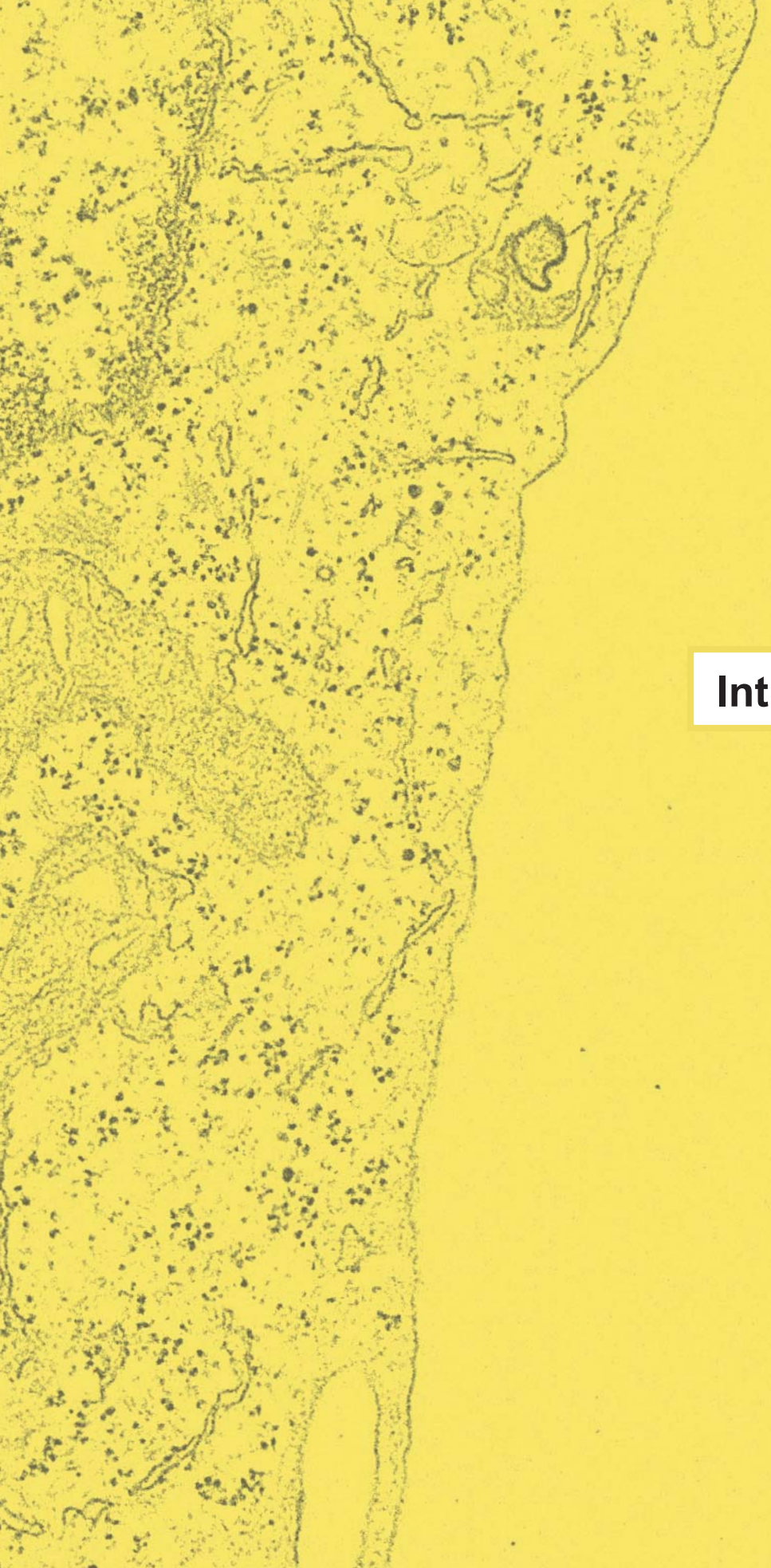

Introduction

Resistance to antitumoural agents constitutes one of the most difficult conundrums for the oncology field. While performing genetic screens to identify novel mechanisms of resistance to anticancer drugs, we found deletions of *Fbxw7* as a recurrent hit. Apart from characterising the resistance mechanisms in *FBXW7*-deleted cells, we identified a vulnerability of these cells that linked to mitochondria organelles. Concomitantly, **these three topics** (resistance to antitumoural agents, FBXW7 and mitochondria) will be covered in this introduction to provide the theoretical framework required for the comprehension of the Thesis results.

1. RESISTANCE TO ANTITUMOURAL AGENTS

1.1. Drug resistance: a major challenge in the oncology field

Cancer is a large group of diseases characterised by an abnormal cell growth that eventually leads to invasion of surrounding tissues and spreading to distant organs (metastasis). It is the second leading cause of death globally, being responsible for an estimated 9.5 million deaths in 2018 (WHO, 2018). The relevance of the disease explains the extensive efforts that have been devoted during the last century to try to cure cancer.

Initially, tumour resection was the only therapy that offered any hope of stopping the disease (**Figure 1**). It was not until World War II that the widespread use of focused X-rays as a cancer therapy (radiotherapy) started, together with the first chemical treatments or **chemotherapies**: nitrogen mustard (Goodman et al., 1946) and aminopterin (Farber et al., 1948), which showed success in reducing lymphoma tumour growth, bringing a lot of excitement to the field (**Figure 1**). However, although tumours went to remission rapidly after treatment, they eventually became resistant, resulting in disease relapse (Vasan et al., 2019) (**Figure 1**).

The first solution to address the drug resistance problem was taken from the rulebook of antimicrobial therapy, **polychemotherapy** (**Figure 1**), through combination of single agents with non-overlapping mechanisms of action. It worked well for some cancer types (Bonadonna et al., 1976, Devita et al., 1980, Bosl et al., 1986), but the success achieved soon reached a plateau, explained in part by the lack of fixed rules or rationale behind the design of the combinations, and the reduced efficacy of each single compound due to the dosage reduction required for avoiding systemic toxicity. Most importantly, most multi-drug treatments were limited by the appearance of multi-drug resistance (MDR) (Shoemaker et al., 1983), which allowed mutant cells to survive to any type of compound (**Figure 1**).

The discovery in 1975 of the first oncogene (c-src) (Stehelin et al., 1976) was a milestone (**Figure 1**) that triggered the identification of the drivers of cancer and the development of **targeted therapies** against them (Hanahan and Weinberg, 2000, Hanahan and Weinberg, 2011). Nevertheless, among the thousands of cancer-driving genes described, only 43 small molecule inhibitors have been approved (Bedard et al., 2020), and some are just considered “undruggable”. Importantly, even if some of these “undruggable targets” are eventually targeted, we may expect resistance: resistance mechanisms are often described even for agents that are not yet in the clinic (Ruiz et al., 2016, Mayor-Ruiz et al., 2018). For instance, the initial successes of BCR-ABL (Kantarjian et al., 2002) and EGFR inhibitors (Fukuoka et al., 2003, Kris et al., 2003), were rapidly followed by resistance (Gorre et al., 2001, Sawyers et al., 2002, Shah et al., 2002, Kobayashi et al., 2005, Pao et al., 2005) (**Figure 1**). **Immunotherapies** with anti-CTLA4 (Leach et al., 1996) or anti-PD1/PDL1 (Iwai et al., 2002) monoclonal antibodies that disable adaptive immune system negative checkpoints, despite unprecedented long-term clinical responses, were no exception to this: the majority of patients directly fail to respond, while others ultimately experienced relapse (Sharma et al., 2017, Fares et al., 2019) (**Figure 1**). Hence, targeted therapies and immunotherapy faced the same challenge as conventional chemotherapies: treatment failure due to drug resistance. Therefore, nowadays, drug resistance remains one of the main challenges in the oncology field in order to achieve a successful curative cancer therapy.

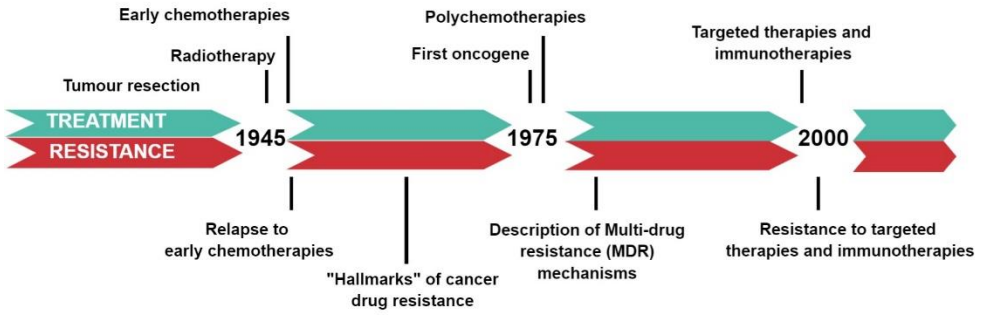

Figure 1: Drug treatment versus resistance timeline. Timeline displaying the milestones in cancer treatment development (green, up) and the subsequent observation of drug resistance (red, down).

1.2. Mechanisms of resistance to antitumoural compounds

Resistance mechanisms are divided in intrinsic, already present in the tumour prior to treatment, and acquired, that arise during the treatment period. Regardless of the time of appearance, the molecular basis of both types of resistance can be encompassed into different **"hallmarks"**. The mechanisms of resistance can be categorised into these hallmarks depending on whether they occur before the compound reaches its target (pre-target) or after (post-target); or if they produce the effects directly on the target (on-target) or off-target (Brockman, 1963, Longley and Johnston, 2005, Holohan et al., 2013, Housman et al., 2014, Mansoori et al., 2017) (**Figure 2**). The main mechanisms belonging to these categories will be further described below.

1.2.1. Pre-target mechanisms of resistance

Pre-target mechanisms involve those that can prevent the active compound from reaching its target in sufficient amounts to exert its function, and can be divided into two:

Altered membrane transport. Mechanisms that reduce the amount of available drug in the cell include reduced absorption, by decreased expression or inactivating mutations of the carriers that some drugs utilise for entering the cell (Holohan et al., 2013), or increased drug efflux (**Figure 2**). The physiological role of the ATP-binding cassette (ABC) transporter family proteins is to prevent the accumulation of toxins within the cell by promoting their transport across the membrane. Their overexpression or increased activity in cancerous cells has been linked to resistance to single agents or multiple drugs producing MDR (Shoemaker et al., 1983), due to exacerbated expulsion of compounds (**Figure 2**). Indeed, the ABC Subfamily B Member 1 (**ABCB1**; also known as P-glycoprotein and MDR1) was the first MDR mechanism to be identified (Kartner et al., 1983a, Kartner et al., 1983b). Its overexpression in tumour cells has been associated with chemoresistance *in vitro* (Kartner et al., 1983a, Kartner et al., 1983b) and with treatment failure in many cancers (Nooter et al., 1997, Triller et al., 2006). Importantly, the mechanisms of ABCB1 overexpression have proven to be not only intrinsic to the tumour, but also acquired after long-exposure to chemotherapeutic agents (Abolhoda et al., 1999). ABCB1 substrates include major cancer chemotherapeutics, such as taxanes, anthracyclines, topoisomerase inhibitors or antimetabolites, and even kinase inhibitors used in targeted therapies (Shukla et al., 2012, Housman et al., 2014, Mansoori et al., 2017).

Altered drug metabolism. This mechanism of resistance relates to the downregulation or inactivation of pathways that convert pro-drugs into their active form to acquire clinical efficacy (Schwartz et al., 1985, Malet-Martino and Martino, 2002), or that promote an excessive catabolism of the drugs (Townsend and Tew, 2003, Pljesa-Ercegovac et al., 2018) (**Figure 2**).

1.2.2. On-target mechanisms of resistance: altered drug targets

Drug efficacy can also be diminished or blunted if there is less of the target protein or if it is mutated in such a way that the compounds cannot bind or exert their effects (**Figure 2**). This has been reported for many chemotherapeutic agents, but is especially relevant for targeted therapies, as they

are even more sensitive to point mutations of the target that may reduce drug binding and hamper efficacy (Gorre et al., 2001, Shah et al., 2002).

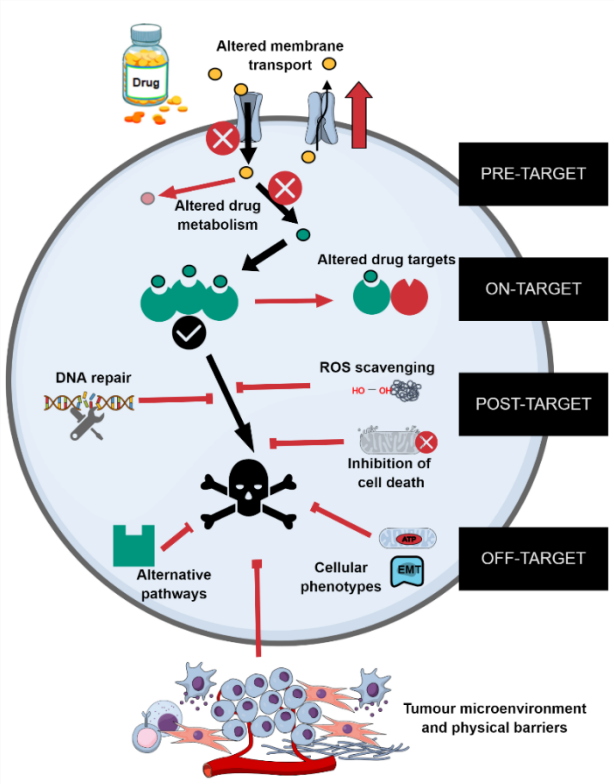

Figure 2: Hallmarks of cancer drug resistance. Black lines represent the normal mechanism of action of an antitumoural drug, from its entry into the cell, conversion to an active form (if needed), binding to its cellular target, and execution of the cell death programme by different means. The different pre-target (altered membrane transport, altered drug metabolism and altered drug targets), on-target (altered drug targets), post-target (DNA repair, ROS scavenging and inhibition of cell death) and off-target (alternative pathways, cellular phenotypes and tumour microenvironment and physical barriers) mechanisms of resistance are marked in red.

1.2.3. Post-target mechanisms of resistance

Treatment outcome depends ultimately on how cancer cells respond to the insults. Alterations in repair or death pathways can lead to treatment failure even if there was sufficient active drug in the cell and it correctly inhibited its cellular targets.

Enhanced DNA damage repair and reactive oxygen species (ROS) scavenging. The effectiveness of agents that produce DNA damage or ROS depend on the repair and scavenging capacity of cancer cells. Thus, if this is generally increased or altered, this would allow cancer cells to present an MDR phenotype to genotoxic therapies (**Figure 2**).

Inhibition of cell death. Deregulation of apoptosis is often involved in MDR, as induction of cell death via apoptosis is a shared mechanism of action among many drugs (**Figure 2**). One of the master regulator of this process is the *TP53* tumour-suppressor gene, which responds to DNA damage by promoting DNA repair, cell cycle arrest, or apoptosis. In *TP53* mutated tumours, drug resistance occurs as cells can continue growing despite DNA damage (Aas et al., 1996). Regarding the apoptotic pathway itself, it is divided into two interconnected pathways: an extrinsic pathway that involves death receptors on the cell surface, and an intrinsic pathway mediated by the mitochondria and, more specifically, by modulating the mitochondrial outer membrane permeabilisation (MOMP) (Letai, 2008). The latter is more closely related to chemoresistance, as many cytotoxic drugs promote cell death through it. The MOMP, once triggered, initiates the activation of the executioners of apoptosis, the caspases, being considered the point of no return towards death by apoptosis (Kalkavan and Green, 2018). In fact, the clinical response to many genotoxic drugs correlates with the mitochondrial proximity to the apoptotic threshold marked by the MOMP: mitochondrial priming (Chonghaile et al., 2011). The interplay between **anti-apoptotic and pro-apoptotic** proteins is what regulates mitochondrial priming, preventing or inducing the MOMP, respectively. Alongside, the upregulation of anti-apoptotic proteins, such as BCL2 or MCL1, or the downregulation of pro-apoptotic proteins, have been implicated in chemoresistance (Miyashita and Reed, 1992, Kitada et al., 1998, Nita et al., 1998, Wang et al., 2001, Chonghaile et al., 2011).

1.2.4. Off-target mechanisms and other factors involved in resistance

There are also off-target mechanisms that may reduce drug efficacy even if they are not directly engaged on the main signalling pathway of the target.

Alternative pathways. Alterations in pathways not directly engaged by the drug can also have an impact on drug responses (**Figure 2**). For instance, the activation of other prosurvival routes, the presence of redundant pathways, or the activation of alternative proteins (oncogenic bypass), may compensate or rescue the inhibition of a specific protein (Holohan et al., 2013).

Cellular phenotypes. There are general specific cellular contexts that have been related recently to chemoresistance (**Figure 2**), such as the Epithelial-Mesenchymal Transition (EMT) and an upregulated mitochondrial metabolism (later discussed in **Introduction 3.2.**). Both are related to tumour stemness (Mani et al., 2008, Lonergan et al., 2007, Vega-Naredo et al., 2014, Hirpara et al., 2019), another context related to resistance (Dean et al., 2005, Nunes et al., 2018, Hepburn et al., 2019, Lettnin et al., 2019). EMT allows cancer cells to lose their apical-basal polarity and intracellular junctions, and acquire migration and invasion capabilities. Accordingly, the EMT has generally been related to tumour metastasis. The link between EMT inducing pathways (TGF-β, Wnt, Hedgehog, Notch) or transcription factors (SNAIL1/2, TWIST, ZEB1/2) and drug resistance, proposed for the first time in the 1990s (Sommers et al., 1992), has progressively been reported in different cancer types (Cheng et al., 2007, Arumugam et al., 2009, Oliveras-Ferraros et al., 2012, Ren et al., 2013b, Song et al., 2018, Li et al., 2019). The actual relevance of the role of EMT in metastasis *in vivo* has even been challenged in favour of its importance in cancer drug resistance (Fischer et al., 2015, Zheng et al., 2015).

Tumour microenvironment and physical barriers. The adjacent space of stromal, vascular and immune cells, may mediate resistance by thwarting immune clearance of tumour cells, obstructing drug absorption, and by providing growth factor and cytokines signalling cues (Junttila and de Sauvage, 2013, Sharma et al., 2017) (**Figure 2**). Other external factors affecting drug response and resistance include physical barriers imposed by general anatomy (blood-brain barrier) or by the tumour itself (large tumour size) (Vasan et al., 2019).

1.3. Approaches to overcome drug resistance

1.3.1. Approaches to improve the rationale behind therapeutic interventions

Efforts to overcome the aforementioned drug resistance mechanisms and achieve curative responses have been attempted through different general strategies. The most straight-forward one is to **begin the treatment before** tumour size and clonal diversity start to increase. Large population screens can help to detect pre-malignant tumoural lesions, and moderately increased patient survival in some tumour types (Andrae et al., 2008, Bleyer and Welch, 2012). Still, strategies of early tumour detection must be coupled with the most effective way of **reaching deep responses** by optimisation of the delivery schedules, compound potency (Peters et al., 2017, Soria et al., 2017), and therapeutic index. Furthermore, treatment and regimen selection **should be rapidly adapted** if there are evidences that the initial option is not reducing tumour growth effectively. That includes not only patient surveillance of tumour growth, but also the use of *ex vivo* culture platforms (Jung et al., 2013, Majumder et al., 2015), patient-derived-xenografts (Fiebig et al., 1985, Hidalgo et al., 2014), or even of *in vivo* implantable microdevices that may predict tumour therapeutic response (Jonas et al., 2015).

1.3.2. Approaches for the identification of novel resistance-related genes and their vulnerabilities

Identifying the genes and mutations involved in resistance provides useful prognostic value, and avoids using unnecessary medication. Most importantly, a better understanding of these mechanisms can lead the development of inhibitors against the drivers of resistance, as well as the discovery of vulnerabilities or synthetic lethalities to overcome resistance. For instance, after the discovery of ABCB1 or BCL2-family alterations in MDR, inhibitors against both have been developed (Cornwell et al., 1987, Starling et al., 1997, Roe et al., 1999, Oltersdorf et al., 2005, van Delft et al.,

2006, Souers et al., 2013, Friberg et al., 2013). On the other hand, the concept of **synthetic lethality**, largely illustrated by the inhibition of PARP in *BRCA*-mutant tumours (Farmer et al., 2005, Bryant et al., 2005), leads to cell death through a combination of deficiencies in two or more gene functions, while individual deficiencies are not detrimental. Identification of these cancer dependencies (Tsherniak et al., 2017, McDonald et al., 2017, Dharia et al., 2021) and vulnerabilities of resistant cells (Ruiz et al., 2016, Hangauer et al., 2017, Liu et al., 2019, Alasiri et al., 2019, Mariniello et al., 2020, Moens et al., 2021) is a powerful emerging field that may help to overcome drug resistance in cancer patients (Finn et al., 2016).

While a detailed knowledge on the mediators of resistance in tumour cells is required, the picture is still incomplete. The main gold-standards to identify **novel unknown resistance-related** genes and mutations have been OMICS analyses from patients samples and data, as well as proteomic and genomic characterizations of already resistant cell lines (Garraway and Janne, 2012). On the other hand, forward genetic screens have recently become one of the best approaches to identify and select for individuals that possess a resistant phenotype within a mutagenised population of cells.

1.3.3. Forward genetic screens

The use of loss-of-function **genome-wide screen** techniques in haploid organisms has helped to further the exhaustive study of multiple signalling pathways and other cellular processes (Giaever et al., 2002, Costanzo et al., 2016). In diploid cells, both copies of the gene need to be inactivated, implicating an additional difficulty. Screens in diploid cells were initially performed by exposing cells to chemical agents, like ENU (Russell et al., 1979, Acevedo-Arozena et al., 2008). However, the fact that ENU generates multiple and random mutations complicated the identification of the causal mutation. Later, reagents that enable near genome-scale systematic mutagenesis simplified analysis and expanded the scope of this technology. After its discovery, interference RNA (RNAi) became the predominant approach (Fire et al., 1998, Brummelkamp et al., 2002). However, for genetic screens in diploid cells, it produced only a partial suppression and had substantial off-target effects (Kaelin, 2012, Booker et al., 2011), limiting its usefulness.

In the last decades, four different strategies of **targeted nuclease-mediated mutagenesis** have been engineered: zinc-finger nucleases (ZFNs) from eukaryotic transcription factors (Urnov et al., 2005), meganucleases encoded by mobile genetic elements (Smith et al., 2006), transcription activator-like effectors (TALENs) from *Xanthomas* bacteria (Boch et al., 2009, Moscou and Bogdanove, 2009), and Clustered Regularly Interspaced Short Palindromic Repeats (CRISPR)-CRISPR-Associated Protein 9 (Cas9) (Jinek et al., 2012, Cong et al., 2013, Mali et al., 2013, Hwang et al., 2013). These customisable nucleases can be exploited for genome editing as they generate specific-site DNA double-strand breaks (DBSs), that, when repaired with error-prone mechanisms, can introduce mutations at specific sequences.

The main **drawback** of ZNFs, meganucleases and TALENs is that they recognize DNA sequences by protein-DNA interactions, limiting their production, especially on a genome-wide scale. On the contrary, CRISPR-Cas9 recognises the target DNA by base pairing with a single guide RNA (sgRNA) that can be synthesised for each custom sequence. It is highly efficient, has limited off-target effects, and its simplicity has enabled the expansion of its application to the genome-scale.

Very recently, **sgRNAs libraries** that target thousands of genes have been developed to be used for genome-wide screenings in human (Shalem et al., 2014, Sanjana et al., 2014, Wang et al., 2014b, Zhou et al., 2014, Doench et al., 2016) and mouse cells (Koike-Yusa et al., 2014, Tzelepis et al., 2016). Also, gain-of-function or gene inactivation screens have also been performed, using the tools provided by an inactive dead Cas9 fused to transcription enhancers o repressors, respectively (Gilbert et al., 2014, Konermann et al., 2015, Sanson et al., 2018). Moreover, sgRNA or Cas9 multiplexing strategies have allowed the performance of combinatorial screens (Wong et al., 2016, Han et al., 2017, Shen et al., 2017, Najm et al., 2018), and the introduction of *in vivo* CRISPR screens have allowed the identification of hits in a more relevant physiological setting (Chen et al., 2015, Manguso et al., 2017, Huang et al., 2021).

Regardless of specific considerations, most **CRISPR-Cas9 screens** follow a similar strategy (Wang et al., 2016b) (**Figure 3**): (**1**) generation of sgRNA constructs by array-based synthesis of oligonucleotide libraries, (**2**) packaging into lentiviral vectors and production of lentiviral particles, (**3**) infection of target cells and selection of infected cells, (**4**) use of the library of mutant cells to perform the screens and, (**5**) detection of the enriched or depleted sgRNAs by sequencing. The usual read-out of the screens is cell viability, but cell populations expressing specific can be selected according to the expression of proteins or markers (Parnas et al., 2015, Breslow et al., 2018, Potting et al., 2018, Condon et al., 2021).

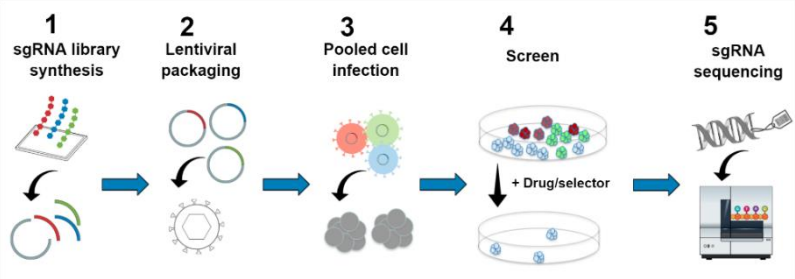

Figure 3: General strategy steps of CRISPR-Cas9 screens. Summary of the principal steps, explained in the text above: (1) sgRNA library synthesis, (2) lentiviral packaging, (3) pooled cell infection, (4) screen performance, and (5) sgRNA detection by sequencing.

The use of these libraries for different screens have allowed an exhaustive study and **identification of genes** implicated in multiple signalling pathways and physiological or pathological processes. Screens have been performed to detect advantageous mutations (positive selection screens) or those that lead to the loss of a property such as viability or expression of a gene (negative selection screens). Their main applications and some representative examples are summarised in **Annex Table 1** and **Annex Table 2**. Overall, negative selection screens have allowed the discovery of negative regulators of pathways, essential fitness genes, therapy-sensitising genes, or tumour dependencies (**Annex Table 1-2**). On the other hand, positive selection screens have allowed the identification of novel positive regulators of pathways, drivers of tumourigenesis and therapy-resistance genes (**Annex Table 1-2**).

Specifically, CRISPR-screens have been vastly used for **identifying drug resistance** (or sensitivity) mechanisms. The first CRISPR-Cas9 screens ever performed focused on the identification of resistance genes for chemotherapeutic agents like 6-thioguanine (Wang et al., 2014b, Koike-Yusa et al., 2014), etoposide (Wang et al., 2014b), or the BRAF inhibitors vemurafenib (Shalem et al., 2014) and PLX-4720 (Konermann et al., 2015). A summary of other mutations identified in drug resistance CRISPR-screens can be found in **Annex Table 2**. One example of this strategy comes from our own group. The use of loss-of-function CRISPR-Cas9 libraries in murine embryonic stem cells (mESCs) (Ruiz et al., 2016) allowed the identification of mechanisms of resistance to an ATR inhibitor previously developed by the laboratory (Toledo et al., 2011). The screen revealed that the loss of *CDC25A* conferred resistance to ATR inhibitors, and the authors showed that the combination of ATR inhibitors and WEE1 inhibitors can overcome such resistance (Ruiz et al., 2016).

In this Thesis, during our efforts to screen for additional mechanisms of resistance, we found deletions of ***Fbxw7*** as a recurrent hit. Thus, we will now focus on enlighten about the biology of FBXW7, and its deregulation in cancer and drug resistance.

2. FBXW7

2.1. FBXW7 biology

2.1.1. FBXW7: a component of the ubiquitin-proteasome system

Ubiquitin conjugation is an essential tag required for protein degradation by the proteasome (Komander and Rape, 2012). The **ubiquitin-proteasome system** (UPS) plays an essential role in maintaining cellular proteostasis as well as in regulating many cellular processes like cell cycle progression, DNA damage repair, or apoptosis (Hershko and Ciechanover, 1998). Ubiquitin binding to a lysine residue in the target protein requires a sequential chain of three enzymatic reactions mediated by a ubiquitin-activating enzyme (E1), an ubiquitin-conjugating enzyme (E2), and an ubiquitin-protein

ligase (E3) (Hochstrasser, 2009) (**Figure 4**). The E1 activates ubiquitin and transfers it to the E2 (**Figure 4**). E3 provides substrate specificity and finally catalyses the deposition of ubiquitin from the loaded E2 onto the target protein, leading to its subsequent degradation by the 26S proteasome (**Figure 4**).

The Skp-Cullin-F-box (**SCF**) **complex** is one of the main and most widely studied E3 ligases. It is composed of four components (Zheng et al., 2002, Cardozo and Pagano, 2004) (**Figure 4**): a CUL1 domain-containing protein, which is the catalytic core; a Rbx1/2 domain protein, which also aids in catalytic function and binds to the E2; a SKP1 domain protein, which joins the F-box with CUL1; and finally an F-BOX domain-containing protein which provides substrate recognition specificity. In humans, 72 **F-box proteins** have been identified to date (Yumimoto and Nakayama, 2020). All of them possess an F-box motif that binds to the Skp1 component, while they can present tryptophan and aspartic acid repeats (WD), leucine-rich repeats (LRR) or other protein interaction domains to recognise a large array of proteins for ubiquitylation (Yumimoto and Nakayama, 2020). Based on this, the F-box protein family is classified in FBXW (F-box coupled with WD repeats), FBXL (F-box coupled with LRRs) and FBXO (F-box with other motifs) proteins (Jin, 2004).

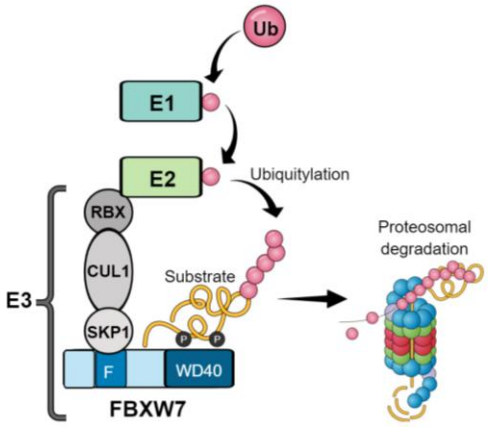

Figure 4: The SCF^{FBXW7} complex and ubiquitylation of protein substrates by the ubiquitin-proteasome system (UPS). The E1 enzyme activates ubiquitin and transfers it to the E2. The E3 enzyme is composed of catalytic Cul1 and Rbx1/2 proteins, a Skp1 protein, which joins Cul1 and, in this case, FBXW7, that mediates substrate recognition. E3 provides substrate specificity and catalyses the deposition of ubiquitin from E2 to the target protein for its degradation by the 26S proteasome. FBXW7 binds to the SKP1 domain through an F-box motif (F), and the WD40 repeats allow the recognition of specific phosphorylated (P) substrate-proteins. Ubiquitin (Ub, red circles).

F-Box and WD Repeat Domain Containing 7 (FBXW7; also known as Cdc4 in yeast, SEL-10 in worms, and AGO in flies) is a member of FBXW subfamily (**Figure 4**). First identified in yeast in 1973 as *Cdc4* (Hartwell et al., 1973), human *FBXW7* was discovered together with many other human F-box proteins (Winston et al., 1999, Cenciarelli et al., 1999). The identification of *Fbxw7/FBXW7* as the mouse and human orthologues of *Cdc4* came from two independent approaches: isolation of mammalian counterparts of *C. elegans* SEL-10 in relationship with NOTCH regulation (Oberg et al., 2001, Wu et al., 2001, Gupta-Rossi et al., 2001, Maruyama et al., 2001) and the identification of FBXW7 as the ubiquitin ligase that mediated degradation of cyclin-E in tumour cell lines (Moberg et al., 2001, Strohmaier et al., 2001, Koepp et al., 2001).

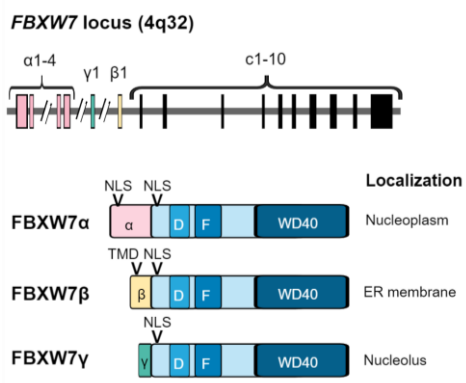

Figure 5: Structure of *FBXW7* genomic locus and domain organisation of the encoded protein isoforms. Alternative transcriptional initiation produces three FBXW7 transcripts and proteins: FBXW7α, β and γ. They share 10 common exons (c1-10), FBXW7β and γ present one isoform-specific first exon β1 and γ1 (respectively), and FBXW7α present four specific exons α1-4. Common domains are F-box motif (F), the WD40 repeats and a dimerization domain (D). They share a nuclear localisation signal (NLS), and, in addition, FBXW7α contains another NLS and FBXW7β a transmembrane domain (TMD).

The **genomic organisation** of *FBXW7* is highly conserved in mammals, and produces three transcripts, FBXW7α, β and γ, expressed from their own promoter and produced by alternative splicing of the first exon (Spruck et al., 2002), while the other ten exons are shared (**Figure 5**). There is only

one isoform-specific first exon for FBXW7 β and γ, whereas for FBXW7α, there are four (**Figure 5**). Each isoform contains the same WD40, F-box and dimerization domains, and just differs in the N-terminal localisation domain (**Figure 5**), explaining their **different subcellular localisations** (Kimura et al., 2003, Welcker et al., 2004a) (**Figure 5**): FBXW7α in the nucleoplasm, FBXW7β in the cytoplasm or endoplasmic reticulum (ER), and FBXW7γ in the nucleolus. Their independent promoters allow for differential expression in tissues: **FBXW7α, the main isoform**, is expressed in most human and mouse tissues, whereas FBXW7β has been detected only in brain and testes, and FBXW7γ in heart and skeletal muscle (Spruck et al., 2002, Matsumoto et al., 2006). The prevalence of each isoform is consistent with the fact that FBXW7α regulates a wider range of substrates than FBXW7β and FBXW7γ (Grim et al., 2008, Ekholm-Reed et al., 2013, Trausch-Azar et al., 2015, Koo et al., 2015, Xu et al., 2016, Vazquez-Dominguez et al., 2019).

2.1.2. FBXW7 substrates

All the substrates of FBXW7 identified to date are displayed in **Annex Table 3** (Yumimoto et al., 2012, Yumimoto and Nakayama, 2020). Interestingly, among FBXW7 substrates, XRCC4 (Zhang et al., 2016a) and γ-catenin (Li et al., 2018b), are polyubiquitylated but not degraded. The ubiquitin mark has signalling functions in DNA damage repair and cell cycle progression. As FBXW7α is the main isoform, most FBXW7 substrates are polyubiquitylated in the nucleoplasm.

The WD40 motif of FBXW7 is composed of three arginine residues that bind substrates through recognition of a conserved phosphorylated domain, called **Cdc4 phosphodegron (CPD)** (Nash et al., 2001, Perkins et al., 2001, Koepp et al., 2001). The consensus CPD contains a Thr or Ser at position 0, Pro at positions +1 and +2, Thr, Ser, Glu, or Asp at position +4, and hydrophobic amino acids at positions -5, -3, -2, and -1. CPD phosphorylation of several, if not all, substrates is performed by glycogen-synthase-kinase 3 (GSK3) upon PI3K pathway activation (Welcker and Clurman, 2008). Most of FBXW7 substrates contain one or even more CPDs, but others present suboptimal CPDs that differ at more than half of the residues of the consensus sequence (**Annex Table 3**). There are other proteins that have been proposed to be regulated by FBXW7, but due to absence of a CPD it remains unclear if their stability is mediated through indirect means (Yumimoto and Nakayama, 2020) (**Annex Table 3**).

2.1.3. FBXW7 regulators

FBXW7 can be regulated in several ways, mainly by its transcriptional regulation and by its protein stabilisation/ destabilisation. Regarding the **transcriptional regulation** of *FBXW7*, C/EBPδ tumour suppressor is a transcriptional inhibitor of FBXW7α (Balamurugan et al., 2010), and a FBXW7 substrate (Balamurugan et al., 2013). In contrast, p53 is an inducer of FBW7β following genotoxic insults as ultraviolet irradiation (Kimura et al., 2003, Mao et al., 2004). At an epigenetic level, PRMT5 can silence *FBXW7* expression (Qin et al., 2019), and there are multiple miRNA (miRNA-223 and miRNA 27-a the main ones) that can downregulate FBXW7, as well as some lncRNAs that counteract the action of these miRNAs (Lin et al., 2019, Yumimoto and Nakayama, 2020).

Another layer of regulation of FBXW7 function is through its **stabilisation** by PI3K phosphorylation (Schulein et al., 2011). However, other phosphorylation marks generate the opposite effect on FBXW7: its ubiquitylation and destabilisation. Those phosphorylations are mediated by the ERK/MAPK kinases (Ji et al., 2015, Zhang et al., 2020a), or by PLK1 triggered by MYC overexpression (Xiao et al., 2016). The antagonistic actions of ubiquitylases (TRIP12) and deubiquitylases (USP9X, USP28) also regulate FBXW7 stability (Khan et al., 2018, Khan et al., 2021). In particular, the actions of the deubiquitylase USP28 are dual (Popov et al., 2007, Schulein-Volk et al., 2014): it reverses FBXW7-dependant substrate ubiquitylation, but also stabilises FBXW7 by reversing its self-ubiquitylation and, therefore, increases its actions. In addition, a direct protein inhibitor of FBXW7 has been described: STYX (Reiterer et al., 2017, Liu et al., 2020). Finally, the monomeric and dimeric status of FBXW7 protein, which is regulated by some proteins (Lan et al., 2019), influences certain FBXW7 substrates degradation (Tang et al., 2007, Welcker et al., 2013).

2.1.4. FBXW7 in physiology and pathology

The first evidences of the crucial role of FBXW7 in mammalian physiology came from **mouse biology**. *Fbxw7*$^{-/-}$ mouse embryos present premature embryonic lethality as a consequence of impaired vascular development in the brain and yolk sac caused by a deregulation of NOTCH (Tetzlaff et al., 2004, Tsunematsu et al., 2004). *Fbxw7*$^{+/-}$ mice are healthy and fertile but have increased susceptibility to radiation-induced tumourigenesis, exacerbated in *Tp53*$^{+/-}$ or *Pten*$^{+/-}$ backgrounds (Mao et al., 2004, Kwon et al., 2012). Conditional deletion, downregulation or knock-in (KI) mutations of *Fbxw7* in **different tissues** resulted in different outcomes, mostly mediated by an accumulation of NOTCH or MYC. In haematopoietic stem cells, *Fbxw7* mutations lead to the loss of self-renewal, exhaustion of the quiescent stem cell pool, and leukaemia (Thompson et al., 2008, Matsuoka et al., 2008). In neurons, it caused perinatal death due to impaired neuronal differentiation that affected brain morphology and suckling behaviour (Matsumoto et al., 2011). In spermatogonial stem cells, differentiation was blunted (Kanatsu-Shinohara et al., 2014). In liver, a variety of phenotypes was observed: tissue inflammation, cholangiocarcinomas, non-alcoholic fatty liver disease, and diabetes (Onoyama et al., 2011, Ikenoue et al., 2018, Zhao et al., 2018, Zhang et al., 2019a). In addition, *Fbxw7* alterations in thymus, lung, stomach, and intestine induced tumour development (Onoyama et al., 2007, Ruiz et al., 2019, Jiang et al., 2017, Babaei-Jadidi et al., 2011, Davis et al., 2014a).

Due to the vast number and relevance of FBXW7 substrates, FBXW7 is involved directly or indirectly in virtually all cellular processes. Consistently, **its deregulation** has been associated with the aforementioned processes and pathologies observed in mice, as well as with others such as inflammation (Balamurugan et al., 2013, He et al., 2019, Zhang et al., 2019a, Gstalder et al., 2020), circadian clock regulation (Zhao et al., 2016) or Parkinson's disease (Ekholm-Reed et al., 2013, Wang et al., 2018). Nevertheless, *FBXW7* alterations have been particularly studied in cancer.

2.2. FBXW7 deregulation in cancer

2.2.1. FBXW7: the ultimate tumour suppressor

The human *FBXW7* gene is located at chromosome 4q31q.3, a region deleted in 30% of human cancers (Spruck et al., 2002). *FBXW7* is the **9th most mutated gene** in cancer (Lawrence et al., 2013), harbouring mutations in around 3-6% of human cancers (Akhoondi et al., 2007), and is by far the most mutated F-box protein (Yumimoto and Nakayama, 2020). Most cases are point-mutations or deep deletions, and regarding tumour types, the most altered types are endometrial (15-20%) and colorectal (15%) cancers or adenocarcinomas, followed by T-lymphoblastic leukemia/lymphoma (13%), cervical (8-12%) and bladder (8-10%) carcinomas (**Figure 6**). Most point-mutations are concentrated at the arginine residues of the WD40-repeat domain responsible for substrate binding, preferentially at R^{465}, R^{479}, and R^{505}, whereas few mutations have been detected in the dimerization and F-box domains of FBXW7 (**Figure 7**). *FBXW7* downregulation or CPD domain mutations in FBXW7 substrates, especially in MYC and KLF5, are also very abundant in human cancers (Yumimoto and Nakayama, 2020).

Loss of *FBXW7* function, through mutation, deletion or downregulation, has been related to tumoural processes such as tumour initiation and progression (Mao et al., 2004, Akhoondi et al., 2007, Ikenoue et al., 2018, Zhang et al., 2016b, Jiang et al., 2017, Davis et al., 2014a), metastasis (Huang et al., 2018, Kourtis et al., 2015, Li et al., 2018a, Yang et al., 2015, Yumimoto et al., 2015, Zhang et al., 2018b), and resistance to certain cancer chemotherapies (**Introduction 2.2.3.**). Of note, *FBXW7* deletions have been identified in different forward genome-wide screens as a cancer driver (Kas et al., 2017, Huang et al., 2019, Takeda et al., 2019). All of these evidences support the nomination of FBXW7 as the "ultimate tumour suppressor" (Yeh et al., 2018).

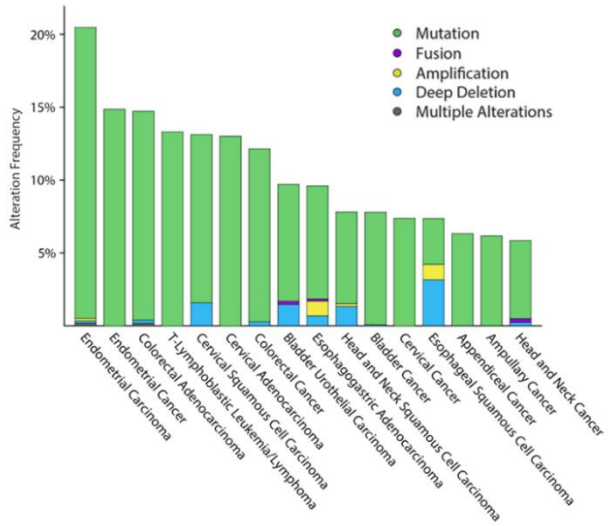

Figure 6: *FBXW7* mutation frequency for different human cancer types. CBioPortal curated set of non-redundant studies was used. Cancer types, including a minimum of 40 total cases and a minimum of 5.5% of alterations, are represented. The different types of alterations are shown in the figure legend.

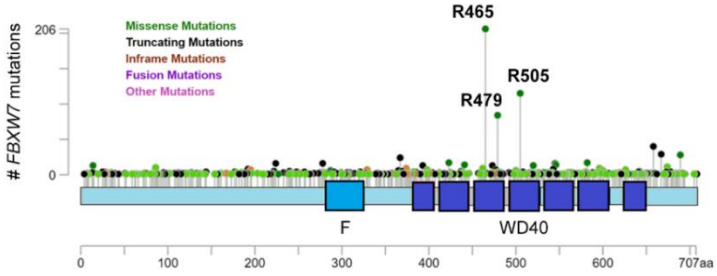

Figure 7: Distribution of *FBXW7* mutations. CBioPortal curated set of non-redundant studies was used. The different types of mutations are shown in the figure legend. F-box motif (F). In WD40 repeats (WD40), most mutations concentrate in the R465, R479 and R505 residues.

2.2.2. Oncogenic FBXW7 substrates

The tumoural phenotypes of *FBXW7*-altered cells should not be surprising taking into account the molecular functions of FBXW7; among which, its role in substrate recognition of **multiple oncoproteins** (**Annex Table 3**). Consequently, when *FBXW7* is deleted, these oncoproteins cannot be correctly degraded and accumulate in the cell, promoting tumourigenesis. Some of the most critical oncoproteins regulated by FBXW7 are MYC, MCL1, CCNE1, NOTCH, and JUN.

C-MYC is a bHLH-LZ family transcription factor, which by gain-of function mutations and overexpression has been vastly shown to promote tumourigenesis (Meyer and Penn, 2008, Tansey, 2014). Increased activity of MYC induces the transcription of genes involved in general cellular transcription, RNA and protein biosynthesis, glycolysis, and nuclearly-encoded mitochondrial function genes (Miller et al., 2012, Menssen and Hermeking, 2002, Li et al., 2005). The result of these effects at the cellular level is the promotion of cell proliferation, metabolic transformation, and metastasis, which have been described as MYC-dependant in MYC CPD-mutated tumours or in *FBXW7*-altered cancers (Yada et al., 2004, Welcker et al., 2004b, Onoyama et al., 2007, Reavie et al., 2013). Phosphorylation of MYC by GSK3 at residues Thr^{58} and Ser^{62} is the mark recognized by FBXW7 for C-MYC degradation and, in fact, the Thr^{58} site is the most mutated residue in C-MYC in B-cell lymphomas (Bahram et al., 2000).

MCL1 is an anti-apoptotic BCL2-family member that induces carcinogenesis and drug resistance when upregulated (Inuzuka et al., 2011, Wertz et al., 2011), as cells become resilient to cell death by apoptosis. FBXW7 deposits ubiquitin on MCL1 for its proteasomal degradation after Ser^{159} and Thr^{163} sites have been phosphorylated by GSK3 (Ren et al., 2013a).

Another relevant oncoprotein substrate of FBXW7 is **Cyclin E** (CCNE1), which controls G1/S cell cycle progression. The accumulation of CCNE1 due to *FBXW7* mutations breaks the tight regulation of the cell cycle and results in chromosome instability and aneuploidy (Rajagopalan et al., 2004), and

also promotes uncontrolled growth and carcinogenesis (Koepp et al., 2001, Moberg et al., 2001, Strohmaier et al., 2001).

NOTCH and C-JUN CPD mutation or protein overexpression due to *FBXW7* alterations have been described to be broadly linked to tumour development (Malyukova et al., 2007, O'Neil et al., 2007, Wei et al., 2005, Babaei-Jadidi et al., 2011).

Finally, other interesting FBXW7 substrates related to cancer are; **MED13**, component of the Mediator complex which recruits the CDK8 oncogene for transcriptional activation (Davis et al., 2013); PPARγ Coactivator-1α (**PGC1α**) transcriptional co-activator that harmonises mitochondrial biogenesis and energetics (Olson et al., 2008); Kruppel-Like Factor 5 (**KLF5**) transcription factor, holding key roles in proliferation and tumourigenesis (Zhao et al., 2010); and **TGIF1**, a transcriptional repressor that inhibits TGF-β signalling oncogenic pathway (Bengoechea-Alonso and Ericsson, 2010a).

2.2.3. Roles of FBXW7 in the response to antitumoural compounds

Besides their role as cancer drivers, *FBXW7* alterations have also been involved in resistance to several antitumoural compounds. Studies reporting this link, as well as the **potential FBXW7 substrates that mediate resistance** are summarised in **Figure 8** and **Annex Table 4**. Among others, MCL1 overexpression has emerged as a key mediator of resistance upon *FBXW7* loss. MCL1 deregulation was firstly described as the mechanism of resistance of *FBXW7*-mutant cells to vincristine, taxol, nocodazole, etoposide and the BCL2 inhibitor ABT-737 BCL2, in colorectal and T-Cell Acute Lymphoblastic Leukaemia (T-ALL) (Wertz et al., 2011, Inuzuka et al., 2011), and later expanded to many other cells and compounds (**Figure 8** and **Annex Table 4**). Besides MCL1, upregulation of the EMT has been linked to resistance to doxorubicin, sorafenib, 5-FU and cisplatin in *FBXW7*-altered cells (**Figure 8** and **Annex Table 4**). C-MYC and NOTCH are also involved in resistance to more than one compound, but the rest of FBXW7 substrates associated with chemoresistance promote resistance only to one compound (**Figure 8** and **Annex Table 4**). All of these data is concordant with the hypothesis that the resistance mediator in *FBXW7*-deleted cells **may be drug-dependent** (Yan et al., 2020b). Moreover, there are compounds for which several mediators have been reported, complicating the landscape of FBXW7 resistance and the possibility of overcoming resistance.

In addition to studies in cancer cells, several CRISPR-Cas9 genome-wide genetic screens have identified *FBXW7* deletions as a **resistance hit**. These include resistance screens to JQ1 (Liao et al., 2018), pterostilbene and resveratrol (Benslimane et al., 2020), MNNG and Duocarmycin (Olivieri et al., 2020) and erlotinib (Zeng et al., 2019). Moreover, in a very recent report (Hundley et al., 2021), CRISPR-Cas9 screens were performed against 41 different antitumoural compounds, utilizing a sgRNA library against UPS-components. *FBXW7* deletion was isolated as a resistance hit for 5 compounds (flavopiridol, palbociclib, rivociclib, pictilisib, pravastatin). Interestingly, it was also found **as a sensitiser** for 11 compounds (BI-2536 PLK1 inhibitor, JG-231 HSP70 inhibitor, colchicine, CB-5083 VCP/p97 inhibitor, pladienolide B, TTFA mitochondrial electron chain complex II inhibitor, dichloroacetic acid, BAPTA-AM, brefeldin A, camptothecin, MMS). A venetoclax screen similarly found *FBXW7* deletions as sensitisers (Chen et al., 2019b). Nevertheless, none of these manuscripts validated any of these observations, so the role of FBXW7 in response to these compounds is yet to be determined.

Despite its general link with resistance, *FBXW7*-altered cells have been reported to display **sensitivity towards some compounds** (**Annex Table 5**). Compounds such as MCL1 inhibitors, rapamycin and MS-275 have been described to reverse the resistance phenotype for regorafenib, gefinitib and taxol (Tong et al., 2017b, Xiao et al., 2018b, Yokobori et al., 2014) (**Annex Table 5**). Of note, drugs for which *FBXW7*-mutated tumours seemed to be especially sensitive are contradictory to other reports linking these drugs to resistance (**Figure 8** and **Annex Table 4**). Other sensitising compounds included some targeting mitochondrial metabolism, or MCL1 and C-MYC overexpression in FBXW7-deficient tumours (**Annex Table 5**). In the case of mitochondrial metabolism inhibitors, two compounds were described, but their efficacy was cell line dependent (Davis et al., 2018). On the other hand, C-MYC overexpression was shown to force leukaemia-initiating cells or other cancer stem cells (CSCs) to enter the cell cycle, and for those types of cancer cells, treatments that eliminate dividing

cells, such as imatinib, supposed a vulnerability for *FBXW7*-ablated tumours (Takeishi et al., 2013) (**Annex Table 5**). However, to date, no effective drug that selectively eradicates *FBXW7*-mutant cells has progressed to the clinic.

In this Thesis, we found that targeting the **mitochondria** supposed a vulnerability for FBXW7-deficient tumours. Therefore, we will further focus on discussing about the main mitochondrial processes, their role in cancer, and the different compounds targeting mitochondria.

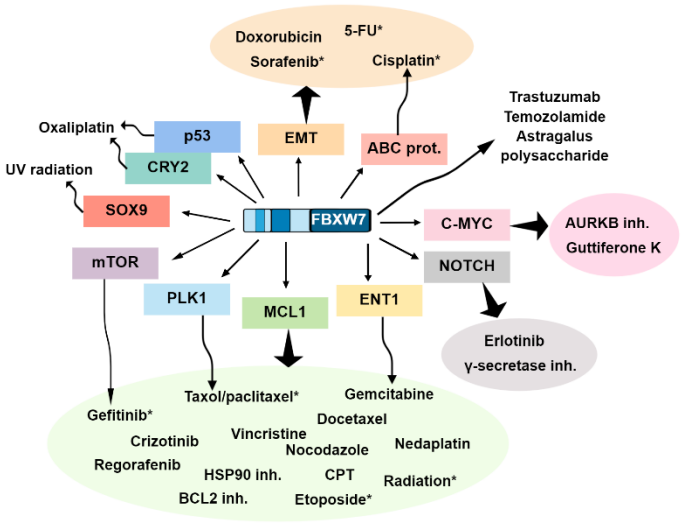

Figure 8: FBXW7 resistance mediators. Compounds for which *FBXW7* deletion or downregulation has been linked to resistance, as well as the resistance mediator. For the mediators MCL1, EMT, NOTCH and C-MYC, compounds are highlighted in green, orange, grey and pink, respectively. MTOR, PLK1 and ENT1 have been described to be related to resistance to some compounds typically related to MCL1; same for an ABC protein and EMT, both related to cisplatin resistance. Other mediators and insults are shown, as well as compounds for which the mediator has not yet been described. (*) indicates compounds that have also been related to sensitivity in FBXW7-deficient cells. For complete data and references, see **Annex Table 4**.

3. MITOCHONDRIA AND CANCER

3.1. Mitochondria

Mitochondria are double membrane-bound cellular organelles found in the cytoplasm of almost all eukaryotic cells. They originated from ancestral α-proteobacteria, which were incorporated into and synchronized with an proto-eukaryotic cell via endosymbiosis (Margulis, 1970, Gray et al., 1999). Their functional role has long been summarised as the **powerhouse of the cell** (Siekevitz, 1957), manufacturing the basic unit of cellular energy, adenosine triphosphate (ATP), through oxidative phosphorylation (OXPHOS) (van der Bliek et al., 2017). Still, the functions of mitochondria range far beyond bioenergetics and include the production of metabolic precursors of lipids, proteins, DNA and RNA; the preservation of ion homeostasis; heat generation; and finally the metabolism of toxic by-products (ammonium and ROS). Additionally, mitochondria are known to coordinate multiple signalling pathways and adaptation to stressors, and they are the central regulator node of the intrinsic pathway of apoptosis.

3.1.1. An overview of mitochondrial organization

Mitochondrial dynamics. Mitochondria are in continuous movement along cytoskeletal tracks and constantly change shape, length and form networks through fission and fusion events. Fission and fusion rates are dependent on the metabolic demands and signalling pathways, and may be unbalanced in pathogenic conditions such as cancer (Dai and Jiang, 2019). In general, cells with a higher dependence on OXPHOS metabolism tend to present large fused mitochondrial networks, while glycolytic cells normally present multiple fissioned mitochondria (Yao et al., 2019, Dai and Jiang, 2019).

Mitochondrial components. Mitochondria are composed of an outer membrane and an inner membrane, separated by a mitochondrial intermembrane space, and a mitochondrial matrix, which is compartmentalised by both membranes (Alberts et al., 2005). The inner membrane is folded multiple times forming cristae structures. The outer membrane of mitochondria is highly permeable, due to its similar composition to the cell membrane and the presence of porines and translocases. On the other hand, the inner membrane does not contain porines, and is highly impermeable to all molecules. This property acts as an electric insulator and chemical barrier that allows the creation of an electric

membrane potential gradient and a proton gradient between the intermembrane space and the matrix, which is used by the five protein complexes of the mitochondrial electron transport chain (ETC) to generate energy via OXPHOS (van der Bliek et al., 2017). Finally, the matrix contains the mitochondrial DNA (mtDNA), mitochondrial ribosomes, tRNAs and enzymes for the different processes that take place there: mtDNA replication, transcription and translation, the assembly of OXPHOS complexes, as well as reactions such as tricarboxylic acid (TCA) cycle, urea cycle or transamination (Alberts et al., 2005).

3.1.2. OXPHOS

In brief, OXPHOS is the anabolic route in which pyruvate (metabolised from glucose in the cytosol by glycolysis) and other nutrients like glutamine or galactose are metabolised and oxidised through the TCA cycle in the mitochondrial matrix (Nolfi-Donegan et al., 2020) (**Figure 9**). The electrons resulting from these reactions are stored in the reduced intermediates NADH and $FADH_2$, which then provide a pair of electrons to the complexes I (NADH-ubiquinone oxidoreductase) and II (succinate dehydrogenase subunits, SDH), respectively. The electrons are then sequentially transferred to ubiquinone, to complex III (ubiquinol-cytochrome c reductase subunits, UQCR), to cytochrome C and, finally, to complex IV (cytochrome c oxidase subunits), where oxygen acts as the terminal electron acceptor and is reduced to water. The transfer of electrons from complex I to ubiquinone, from complex III to cytochrome C and from complex IV to oxygen results in the pumping of protons to the intermembrane space. The re-entry of protons into the matrix through complex V (ATP synthase subunits) dissipates the created membrane potential and couples it to the production of ATP from ADP by the very same complex V.

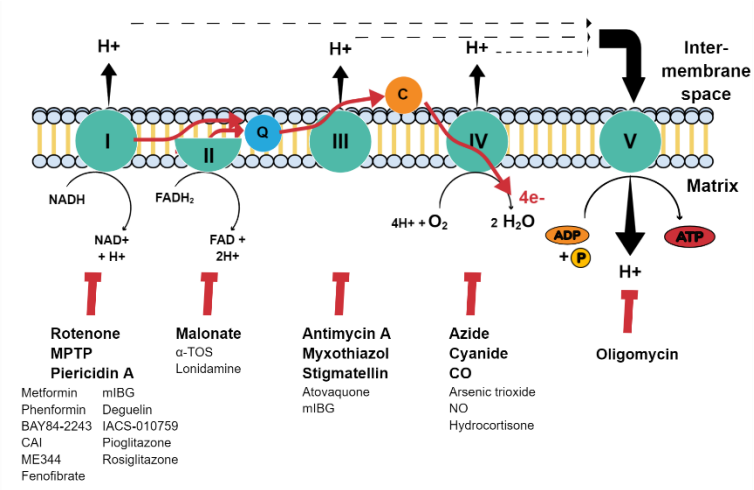

Figure 9: OXPHOS and its inhibitors. OXPHOS representation as explained in the text. (Q) ubiquinone, (C) cytochrome C. Red lines indicates the electron transfer flow; black thin lines, the different processes; and the dotted and thick lines, the proton gradient. Below, the different inhibitors of each complex. In bold, the classical mitochondrial poisons, while the rest indicates novel inhibitors that have been developed or repurposed since.

3.1.3. Mitochondrial translation

Most mitochondrial proteins are encoded by the nuclear genome, transcribed and translated in the nucleus and cytoplasm, and then exported to the mitochondria (**Figure 10**). However, a fraction of mitochondrial proteins is encoded by the mtDNA and need to be synthesised by the mitochondrial transcription and translation machinery.

mtDNA is a double-stranded circular molecule of 16659 base pairs that is continuously replicated independently of the cell cycle (**Figure 10**). It lacks introns and codes for 37 genes: 22 tRNAs, 2 rRNAs and 13 subunits of the OXPHOS complexes I, III, IV and V (Anderson et al., 1981).

For their transcription, mitochondria use specific mitochondrial **transcription** machinery: an mtRNA polymerase (POLRMT), a series of transcription factors, including TFAM, TFB1M, and TFB2M, as well as the transcription termination factors MTERF1-4 (Smits et al., 2010) (**Figure 10**). Mitochondrial transcripts are polycistronic RNA molecules that are later processed and subjected to polyadenylation.

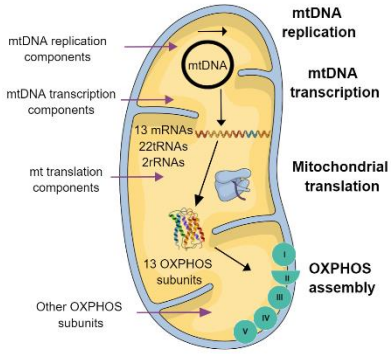

Figure 10: Overview of the processes involved in mitochondrial translation and biogenesis of OXPHOS system. Before translation takes place, the mtDNA needs to be maintained, replicated and transcribed to a polycistronic mRNA molecule. It lacks introns and codes for 37 genes: 22 tRNAs, 2 rRNAs and 13 subunits of the OXPHOS complexes I, III, IV and V. The 13 OXPHOS subunits will be later assembled with other subunits imported from the cytosol. For the three processes to take place (replication, transcription and translation), the machinery components and factors need to be also imported from the cytosol (purple arrows).

Despite several unique features (**Table 1**), mitochondrial translation is similar to other translation processes, especially prokaryotic translation (Smits et al., 2010) (**Figure 11**): (**1**) **Initiation**. Mitochondrial translation begins with the recognition and binding of the mRNA to the ribosome, followed by the union of methionine tRNA and deposition of that first amino acid, aided by initiation complex factors (IFs). (**2**) **Elongation**. Polypeptide elongation occurs through sequential union of tRNAs, which bring and deposit more amino acids in the acceptor site. These processes are supported by different elongation factors that, together with the ribosome itself facilitate elongation by: (a) protecting tRNAs from hydrolysis and carry them to the acceptor site (EFTus); (b) catalysing peptide bond formation; (c) promoting the exit of tRNAs and the translocation of the mRNA through the ribosome to start a new cycle (EFGs); (d) supporting the conversion of other elongation factors into their active form (EFTs). (**3**) **Termination**. Mitochondrial translation termination occurs via the recognition of stop codons by release factors (RFs), producing the release of the complete polypeptide and the disassembly of the translation complex and the ribosomal subunits, aided by RFF and EFT proteins.

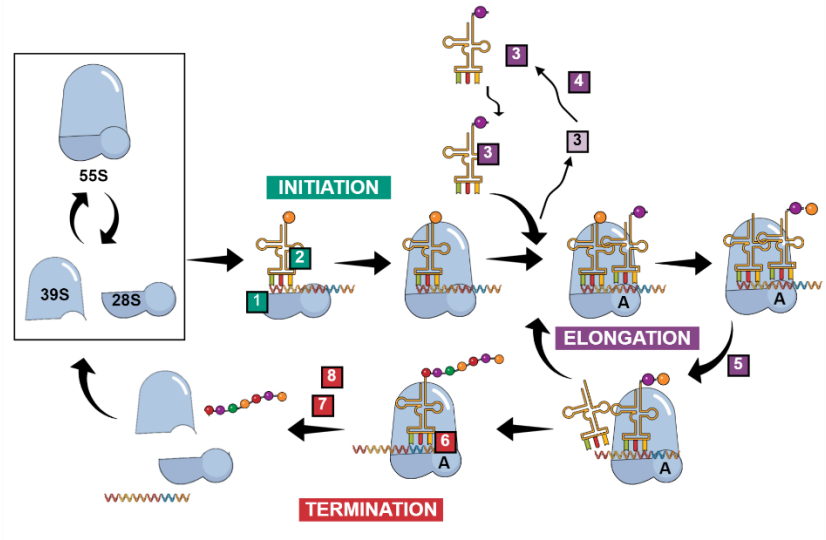

Figure 11: Process of protein synthesis in mammalian mitochondria. For detailed description see the text description. (A) is the acceptor site. Initiation factors (in green) are mtIF3 (1) and mtIF2 (2). Elongation factors (in purple) are mtEFu or TUFM (3), mtEFs (4) and mtEGF1 (5). Termination factors (in red) are mtRFs (6), and mtEFG2 (7) and mtRFF (8).

The **differential features** of mitochondrial translation versus bacterial translation are represented in **Table 1**. Most of the components of the translation machinery are orthologues of prokaryotic factors. However, some eukaryotic factors perform functions of two different bacterial proteins (mtIF2 as bacterial IF1 and IF2), or the role of one prokaryotic protein is distributed between two different mitochondrial proteins (mtEFG1 and mtEFG2). There is some variability between species in the composition of the mitoribosomes. Specifically, mammalian mitoribosomes are composed of a large subunit (LSU, 39S), formed by a 16S rRNA, a structural tRNA and 50 MRPs (MRPLs); and a small subunit (SSU, 28S), which contains a 12S rRNA and 29 MRPs (MRPSs). Interestingly, mitochondrial translation is tethered to the inner membrane to promote co-translational insertion into the membrane of the newly synthetized proteins and their assembly into OXPHOS complexes.

Table 1: Differential features of mitochondrial translation.

Differential features of mitochondrial translation	
mRNAs (Grohmann et al., 1978, Montoya et al., 1981, Liao and Spremulli, 1989)	Contain no or few 5' untranslated nucleotides
	Are uncapped
	Poly-A forms part of the stop codon
	Mitoribosomes bind independently of the sequence or presence of initiation components
tRNAs (Barrell et al., 1980, Anderson et al., 1981, Mikelsaar, 1983, Osawa et al., 1992)	Universal code changes: AGG/AGA for stop codons, AUA for methionine, UGA for tryptophan
	Translates all codons using only 22 tRNAs instead of 31
	Single methionine tRNA
	Shorter and with size variations in the loop domains
Components of the translation machinery (Smits et al., 2010)	2 initiation factors: mtIF2 and mtIF3
	3 types of elongation factors: mtEFTu or TUFM, mtEFTs and mtEFGs
	2 release factors: mtRF1 and mtRF1a
	1 recycling factor mtRRF
	Other essential but with unknown function: PTCD3 and HsPDF
Mitoribosome (55S) (Smits et al., 2010)	Reduced amount of rRNA
	Double number of mitochondrial ribosomal proteins (MRPs)

3.2. Targeting mitochondria in cancer

3.2.1. Mitochondrial translation and OXPHOS in cancer

Mitochondrial alterations have been involved in aging (Chan, 2006) and certain pathologies, such as diabetes (Højlund et al., 2008), Parkinson's disease (Mandemakers et al., 2007), and cancer (Dai and Jiang, 2019, Kim et al., 2017a). In cancer, alterations in ROS production and apoptotic signalling have been vastly studied, as discussed in **Introduction 1.2.3**. Nonetheless, the contribution of OXPHOS and mitochondrial metabolism to cancer has been largely ignored, due to **flawed reasoning from Warburg's** observation that cancer cells present an upregulated glycolysis and high lactate production from glucose (Warburg et al., 1927, Warburg, 1956). The presence of Warburg's effect in many tumours is unquestionable, what is more, it has been exploited to detect metabolically active tumours by imaging (Palaskas et al., 2011) and to specifically kill cancer cells using inhibitors of glucose metabolism enzymes. However, Warburg assumed that this metabolic switch arises from a universal mitochondrial OXPHOS downregulation or functional impairment in tumours (Warburg, 1956). Although true for some tumours with mtDNA mutations (Pedersen, 1978, Larman et al., 2012), or in low oxygen conditions inside solid tumours (Moreno-Sanchez et al., 2007), this concept has been challenged since its initial communication (Weinhouse et al., 1956) by evidences from the last half century proving that mitochondria are fully functional and that, undeniably, many tumours rely on OXPHOS metabolism for their growth and survival.

Already in the 80s, there were evidences that **OXPHOS was preferentially used** by HeLa cervical carcinoma cells to generate ATP (Reitzer et al., 1979). It was later proven for other cancer cell types, not only in basal conditions, but also under limiting glucose conditions, where cancer cells suffered a metabolic adaptation from aerobic glycolysis to OXPHOS (Jose et al., 2011, Ashton et al., 2018). These functional assays have been extended and complemented with the description of an upregulation of OXPHOS proteins and mtDNA levels in many tumours, including breast cancer, Hodgkin lymphoma, B-cell lymphomas, and acute myeloid leukaemia (AML) (Whitaker-Menezes et al., 2011, Caro et al., 2012, Lagadinou et al., 2013, Scotland et al., 2013, Birkenmeier et al., 2016, Zacksenhaus et al., 2017, Hu et al., 2013). Noteworthy, and apart from an upregulation of ETC/OXPHOS proteins, a global **upregulation of mitochondrial translation** has been found in many tumour cells, including breast cancer cells (Sotgia et al., 2012) or in the Pan-Cancer Human Protein Atlas Project, where an excess of mitoribosomal proteins and assembly factors was reported in human cancers (Kim et al., 2017a).

Importantly, mitochondrial transcription, translation and OXPHOS upregulation can be **driven by oncogenes**. For instance, *H-Ras*^{V12} increases mitochondrial metabolism (Telang et al., 2007, Yao et al., 2019), as does its downstream effector B-RAF which, when inhibited, renders tumours addicted to OXPHOS metabolism (Haq et al., 2013). Inhibition of B-RAF increases the levels of the master regulator of mitochondrial metabolism, PGC1α, via melanocyte lineage transcription factor (MITF), which globally induces the expression of OXPHOS and mitochondrial biogenesis genes. Interestingly, PGC1α overexpression via MITF, regardless of the levels of B-RAF, was also shown to be an inducer of global mitochondrial expression in melanoma (Vazquez et al., 2013). Other oncogenic alterations promoting mitochondrial protein translation, OXPHOS and mitochondrial metabolism dependence are *RB1* loss (Jones et al., 2016, Zacksenhaus et al., 2017), *PTEN* loss (Naguib et al., 2018), and MCL1 and C-MYC overexpression (Lee et al., 2017b, D'Andrea et al., 2016). Despite its known roles in promoting glycolysis, C-MYC also induces a global mitochondrial gene expression and function programme (Miller et al., 2012, Menssen and Hermeking, 2002, Li et al., 2005, Skrtic et al., 2011, D'Andrea et al., 2016, Oran et al., 2016). Of note, *FBXW7* mutations have also been recently associated to an enhanced mitochondrial gene transcriptional program in a MITF-dependent manner in melanoma (Abbate et al., 2018), and in broader pan-cancer signatures (Davis et al., 2018).

Interestingly, certain chemotherapies like 5-FU (Vellinga et al., 2015, Yun et al., 2019), topoisomerase inhibitors (Fu et al., 2008), and targeted agents as B-RAF inhibitors (Haq et al., 2013), can also promote mitochondrial biogenesis, mainly through activation of AMPK or PGC1α. Indeed, **resistance** to these agents and to many others, like AraC (Farge et al., 2017), paclitaxel/docetaxel (Farnie et al., 2015, Ippolito et al., 2016), cisplatin (Xu et al., 2018, Cruz-Bermudez et al., 2019), other ROS-inducing agents (Vazquez et al., 2013), gefinitinib/vemurafenib (Hirpara et al., 2019), sorafenib (Messner et al., 2020), venetoclax (Chen et al., 2019b), and ibrutinib (Zhang et al., 2019b) have been associated with an enhancement of mitochondrial processes and metabolism, and, in fact, rely on OXPHOS metabolism for chemoresistance and survival. Importantly, increased mitochondrial activity has also been linked to MDR (Roesch et al., 2013, Lee et al., 2017b). In light of this data, targeting either OXPHOS or mitochondrial translation have emerged as promising therapeutic strategies to overcome drug resistance in cancer.

3.2.2. Targeting OXPHOS

There are multiple drugs that can inhibit the mitochondrial ETC at different points, and that have proven efficacy to reduce growth in tumours where OPXHOS is a vulnerability. Classical **mitochondrial poisons**, as well as newer compounds that have been repurposed for inhibiting OXPHOS, are displayed in **Figure 9** (Ashton et al., 2018). Representative examples are malonate for complex II inhibition, antimycin A for complex III, cyanide and azide for complex IV, and oligomycin for complex V. In the case of complex I inhibition, there are multiple additional inhibitors that have been repurposed, such as the classical diabetic drugs metformin and phenformin, or the poisons rotenone, piericidin A, and MPTP. A very recent case is the discovery of IACS-010759, a clinical-grade, highly potent and selective small-molecule inhibitor of complex I (Molina et al., 2018, Tsuji et al., 2020), which was proven to be successful for exploiting OXPHOS dependence of certain hematologic malignancies (Molina et al., 2018, Zhang et al., 2019b, Donati et al., 2020).

3.2.3. Targeting mitochondrial translation

Due to **conserved evolutionary similarities** between bacterial and mitochondrial ribosomes, antibiotics that interfere with bacterial protein synthesis have the potential to inhibit mitochondrial translation (Riesbeck et al., 1990, Zhang et al., 2005). This property opened the window to repurpose several antibiotic families targeting the bacterial ribosomes such as tetracyclines, glycylcyclines, oxazolidinones, and chloramphenicol, for cancer therapies.

Even though some tetracyclines were already known since over 40 years ago to exert antitumoural effects (Leezenberg et al., 1979, Kroon et al., 1984), it was not until recently that their repurposing has really expanded. Pioneer work, from Škrtić *et al.*, identified the glycylcycline

tigecycline in a chemical screen for FDA-approved agents targeting AML cells (Skrtic et al., 2011). Tigecycline inhibition of mitochondrial translation was selectively lethal for leukemic cells in *in vitro* and *in vivo* models; as cancerous cells, in comparison with normal haematopoietic cells, rely heavily on the increase in mitochondrial metabolism that come together with an increase in mitochondrial biogenesis. Later work identified MYC as the driver of mitochondrial translation upregulation, and indeed, two pieces of work identified a mitochondrial translation protein (Ptcd3) (D'Andrea et al., 2016), and the mitochondrial RNA polymerase (POLRMT) (Oran et al., 2016) as synthetic lethal interactors of MYC. Consistently, MYC-overexpressing lymphomas were selectively sensitive to several antibiotics such as chloramphenicol and linezolid, but none were as effective as tigecycline (D'Andrea et al., 2016). RB1-deficient breast (Jones et al., 2016) and *K-RAS* mutant colorectal cancer cells (Martin et al., 2017) were later shown to be also exceedingly sensitive to tigecycline.

Tigecycline has been shown to present antitumoural properties in **other tumour types**, like gastric cancer (Tang et al., 2014), cervical carcinoma (Li et al., 2015a), oral squamous cell carcinoma (Ren et al., 2015), B-cell lymphomas (D'Andrea et al., 2016, Norberg et al., 2017), melanoma (Hu et al., 2016), neuroblastoma (Zhong et al., 2016), glioma (Yang et al., 2016), lung cancer (Jia et al., 2016, Yan et al., 2020a), therapy-resistant chronic myeloid leukaemia (CML) (Kuntz et al., 2017, Lu et al., 2017), acute lymphoblastic leukaemia (ALL) (Fu et al., 2017), multiple myeloma (Ma et al., 2018), retinoblastoma (Xiong et al., 2018), ovarian cancer (Hu and Guo, 2019), thyroid cancer (Wang et al., 2019), osteosarcoma (Chen et al., 2019a), and sorafenib-resistant (Messner et al., 2020) and non-resistant hepatocellular carcinoma (Tan et al., 2017). Importantly, tigecycline has been shown to **work synergistically** in combination with chemotherapy (Tan et al., 2017, Wang et al., 2019, Hu and Guo, 2019), and with the targeted therapy imatinib (Kuntz et al., 2017) or a combination of the BCL2 inhibitor venetoclax with rituximab (Ravà et al., 2018). The last case is of key relevance, as BCL2 activation limited the efficacy of tigecycline, which was only restored by a combined treatment with venetoclax. Likewise, targeting mitochondrial essential proteins was shown to reinstate venetoclax sensitivity in resistant cells (Chen et al., 2019b, Sharon et al., 2019). Inhibition of autophagy has also been shown to synergise with tigecycline to eliminate cancerous cells (Lu et al., 2017, Ma et al., 2018).

At the clinical level, tigecycline has already proved safety in AML patients in a **phase I trial** (Reed et al., 2016)(NCT01332786), despite a lack of response which was attributed to the short half-life of the drug (9.5h). Fortunately, a novel formulation containing ascorbic acid and pyruvate maintains the stability of this drug for at least a week (Jitkova et al., 2014). Two other clinical trials, not yet recruiting, are prospected to evaluate the efficacy of tigecycline in cancer. The first evaluates its use in urogenital cancer patients (NCT03962920), while the second in tumour cells from patients with CML, in order to correlate the *in vitro* sensitivity of cells to tigecycline with the patients' clinical parameters and survival outcome (NCT02883036).

Besides tigecycline, **other mitochondrial translation inhibitors** have proven to be successful antitumoural treatments in *in vitro* and *in vivo* models: tetracyclines including doxycycline (Leezenberg et al., 1979, Kroon et al., 1984, Lamb et al., 2015, Dijk et al., 2020) and minocycline, which importantly is able to cross the blood-brain barrier (Sotomayor et al., 1992, Markovic et al., 2011, Garrido-Mesa et al., 2013, Romero-Miguel et al., 2021); the inhibitor of HsPDF actinonin (Sheth et al., 2014, Lee et al., 2015); POLRMT inhibitors 2'-C-methyladenosine (2'CMeA) (Oran et al., 2016) and the novel specific inhibitors of mitochondrial transcription (IMTs) (Bonekamp et al., 2020); as well as the oxazolidinone tedizolid (Sharon et al., 2019).

3.3.4. Mechanism of action of mitochondrial translation inhibitors

The main mechanism of action of tigecycline is to **block mitochondrial translation**; however, the exact target of tigecycline in the mitoribosome has not yet been identified. In bacterial ribosomes, it is known to bind to both large and small subunits (Jenner et al., 2013, Schedlbauer et al., 2015), blocking the binding of the aminoacyl-tRNA to the acceptor site. Therefore, due to conservation, it is expected to bind similarly to mitoribosomes. Consistently, genetic inhibition of mitochondrial translation by EF-Tu knockdown, mimics the inhibitory effects of tigecycline (Skrtic et al., 2011). The other inhibitors

of mitochondrial translation are known to work similarly or in other branches of the process. Regardless of the specific inhibitory point, mitochondrial translation inhibition converges in the downregulation of mitochondrial-encoded OXPHOS complexes, with the subsequent depolarization of the mitochondrial membrane and **dampening of mitochondrial respiration** and ATP production via OXPHOS, as well as an exacerbated ROS production and induction of P53-independent apoptosis (D'Andrea et al., 2016). Other works have pointed out **independent actions** of tigecycline in the cell, such as ß-catenin inhibition (Li et al., 2015a), autophagy induction by activation of AMPK, downregulation of the PI3K-AKT-mTOR pathway (Tang et al., 2014, Zhong et al., 2016, Lu et al., 2017, Ma et al., 2018, Hu and Guo, 2019), and downregulation of p21 (Hu et al., 2016).

More recently, an induction of the **integrated stress response (ISR)** has been related to the mechanism of cell death induced by mitochondrial inhibition. The ISR is a physiological cell response that attempts to restore cellular homeostasis following different stressors; however, excessive and prolonged ISR activation eventually causes cell death (**Figure 12**). Different kinases are in charge of sensing diverse stressors in the cell, converging at the phosphorylation of the protein eIF2α (**Figure 12**): GCN2, which is stimulated by depletion of amino acids; PERK, which is activated upon ER stress; PKR, which detects dsRNA following viral infections; and HRI, which is triggered upon heme deprivation and **mitochondrial stress**, as recently shown (Guo et al., 2020a, Fessler et al., 2020). Specifically, the activation of HRI following mitochondrial stress has been described to occur through the binding of a fragment of DELE1 protein. This fragment is generated after the cleavage of the complete DELE1 protein by the mitochondrial stress-activated protease OMA1 (Guo et al., 2020a, Fessler et al., 2020) (**Figure 12**). The downstream effects of phosphorylation of eIF2α are a reduction of total protein synthesis, and the nuclear translocation and activation of the ISR effectors ATF4, ATF5, and CHOP; ATF4 being the main regulator of mitochondrial stress response in the cell (Quirós et al., 2017) (**Figure 12**). ATF4-dependent activation of CHOP, or directly ATF4, may promote cell death by upregulating different pro-apoptotic family members, among many other mechanisms (Pakos-Zebrucka et al., 2016) (**Figure 12**). Concomitantly, mitochondrial stressors, such as the complex I inhibitor IACS-010759 (Donati et al., 2020), depletion of a mitochondrial chaperonin (Chen et al., 2019b), and the mitochondrial translation inhibitor tedizolid (Sharon et al., 2019) can activate the ISR. Moreover, cell death provoked by these insults can be rescued by an ISR inhibitor (ISRIB). Importantly, venetoclax has also been shown to suppress mitochondrial respiration and to activate the ISR (Sharon et al., 2019), implying a possible antitumoural mechanism of action for certain targeted therapies through the generation of mitochondrial stress and activation of the ISR. In the case of tedizolid and venetoclax (Sharon et al., 2019), the authors reported a suppressed glycolytic capacity as the ultimate mechanism of cell death, while for IACS-010759, toxicity due to the lowering of the apoptotic threshold via CHOP induction was proposed (Donati et al., 2020).

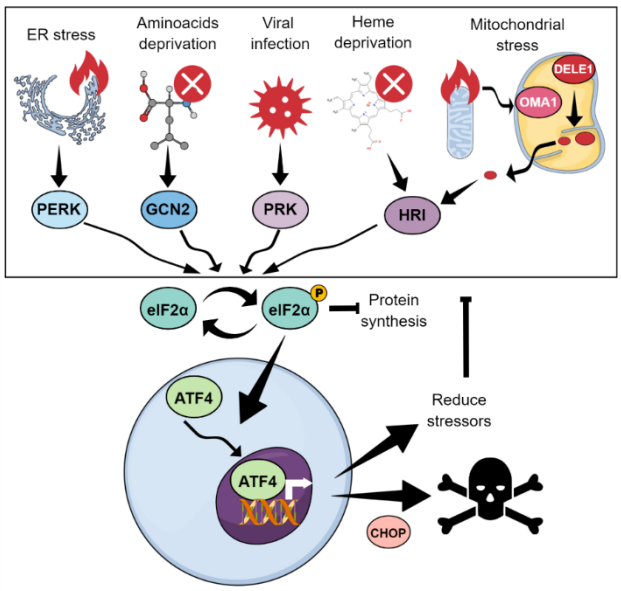

Figure 12: The integrated stress response (ISR). ISR kinases sense different stressors and converge at the phosphorylation of the protein eIF2α: GCN2, by depletion of amino acids; PERK, by ER stress; PKR, by viral infection; and HRI, by heme deprivation and by mitochondrial stress. Specifically, OMA1, a mitochondrial protein, senses the stress and cleaves DELE1, a fragment of which goes to the cytosol and activates HRI. eIF2α-P blocks protein synthesis and activates ATF4, which translocates to the nucleus to activate stress-response pathways or, via intense signalling, to kill cells (aided by CHOP).

In this Doctoral Thesis, we will further explore mechanisms of resistance to antitumoural therapies, as it is one of the main challenges in the cancer research field. For this aim, we will utilise one of the most powerful recent technologies to identify novel resistance-related mediators: CRISPR-Cas9 screens. We found among our hits *FBXW7*-deletions. Consistent with the importance of *FBXW7* mutations in cancer, and, more specifically, in drug resistance, we followed on this hit. Not only did we try to solve the underlying cause of the resistance, but also investigated ways to overcome it and specifically eliminate *FBXW7*-mutated tumours. Research in this direction brought us to the mitochondria and the novel targeting of mitochondrial translation as an effective cancer treatment. Moreover, we dug into the mechanisms of action of these compounds and found a possible involvement of the ISR pathway.

Objectives

1. To perform CRISPR-Cas9-based genome-wide genetic screens in order to identify novel determinants of the sensitivity to genotoxic agents and other cytotoxic insults.
2. To characterise the mechanisms behind the resistance associated to mutations found in the CRISPR-Cas9 screens.
3. To use the knowledge about the mechanisms of resistance associated to the identified mutations to discover ways to overcome such resistance *in vitro* and in *in vivo*.

Material and Methods

1. CELLULAR BIOLOGY

1.1. Cell culture

All **cells were grown** at 37ºC in a humidified air atmosphere with 5% CO_2 unless specified.

mESCs were grown on gelatin and feeder layers, using Dulbecco's Modified Eagle's Medium (DMEM) (high glucose) (Invitrogen) supplemented with 15% knockout serum replacement (Invitrogen), Leukemia Inhibitory Factor (LIF) (1000 U/ml), 0.1 mM non-essential amino acids, 1% glutamax, and 55mM β-mercaptoethanol. For the drug treatment experiments, mESCs were plated only on gelatin. R1 mESCs were obtained from the American Type Culture Collection (ATCC). mESCs Cas9 clones and mESCs loss-of-function libraries had been previously generated (Ruiz et al., 2016). The mouse embryonic fibroblasts (MEFs) needed for feeder production were obtained from 13.5 days post coitum (dpc) embryos by standard methods and cultured in standard DMEM (high glucose) (Sigma, D5796), 15% Fetal Bovine Serum (FBS), and 0.1mM non-essential amino acids in low-oxygen conditions. To generate feeder layers, MEFs at early passages were growth arrested by ionizing irradiation (IR) with 80 Gray (Gy) for 30 minutes (min). MEFs were immortalized by lentiviral expression of the SV40-T121 antigen following standard procedures.

Human cancer cell lines HEK293T, DLD1 and HeLa were cultured in standard DMEM (high glucose) (Sigma, D5796) supplemented with 10% FBS and 1% penicillin/streptomycin. A2780 cell line was maintained in RPMI 1640 medium (EuroClone, ECM2001L), 10% FBS and 1% penicillin/streptomycin. HEK293T and HeLa cell lines were obtained from the ATCC; while DLD1 and A2780 were kindly provided by the CNIO Monoclonal Antibodies Unit.

1.2. Generation of knock-out, knockdown and fluorescent-proteins-expressing cell lines

1.2.1. Lentiviral production

Lentiviral vectors were individually co-transfected with third generation packaging vectors in HEK293T cells, using Lipofectamine 2000 (Invitrogen) to generate viral supernatants as previously described (Ruiz et al., 2011).

1.2.2. Generation of knock-out cell lines

To generate *Ptpn2* and *Fbxw7* knock-out (KO) mES R1 cells and *FBXW7* KO DLD1, HeLa and A2780 cell lines, **CRISPR-Cas9 gene editing** was used. The sequences of the sgRNAs used were designed using the MIT CRISPR design tool (http://www.genome-engineering.org/crispr/) and cloned into a pLentiCRISPR v2 lentiviral vector (Addgene, 52961), as described (Sanjana et al., 2014). Only sgRNAs with the highest scores and lowest probability of generating off-target effects were selected. The sequences of the sgRNAs can be found in **Table 2**.

Cells were independently infected with the different lentiviral supernatants **encoding the corresponding sgRNAs** against *Ptpn2/Fbxw7/FBXW7.* Each cell line was also infected with the empty pLentiCRISPR v2 vector to generate working-control wild-type (WT) cell lines. 48 hours (h) after infection, the cells were selected for three days with 2µg/ml puromycin (Sigma, P8833). To obtain pure KO clones, the pool of cells was single-cell grown, expanded and expression of PTPN2/FBXW7 was verified by Western Blot to select the KO clones.

The same procedure was followed for the generation of the **double KOs** with *ABCB1* and *MCL1* in *FBXW7* WT and KO DLD1 cells. For *B-RAF, A-RAF, C-RAF, FYN* and *CSK* double KO experiments, a *FBXW7* WT-eGFP+ and KO-Ruby3+ DLD1 defined cell mixture was infected every 7 days with the different lentiviral supernatants encoding the sgRNAs targeting those genes, as well as the empty vector control. The vector used in this case was pLentiCRISPR v2 blasticidin (Addgene, 98293).

Table 2: List of sgRNAs oligonucleotide sequences to be cloned into pLentiCRISPR v2 or pLentiCRISPR v2 blasticidin. Oligonucleotide name and sequence 5' to 3' is indicated.

Oligonucleotide sequences of sgRNAs	
Oligonucleotide name	**Sequence (5' to 3')**
sgRNA-*Ptpn2*-F1	CACCGCACTCTATGAGGATAGTCAT
sgRNA-*Ptpn2*-R1	AAACATGACTATCCTCATAGAGTGC
sgRNA-*Ptpn2*-F2	CACCGCCATTTCTGGCTCATGGTG
sgRNA-*Ptpn2*-R2	AAACCACCATGAGCCAGAAATGGC
sgRNA-*Fbxw7*-F1	CACCGCTCAGGTCCCCAAAAGTTGT
sgRNA-*Fbxw7*-R1	AAACACAACTTTTGGGGACCTGAGC
sgRNA-*Fbxw7*-F2	CACCGCAAAGTCTCAGATTATACC
sgRNA-*Fbxw7*-R2	AAACGGTATAATCTGAGACTTTGC
sgRNA-*FBXW7*-F1	CACCGATGAAGTCTCGTTGAAACTG
sgRNA-*FBXW7*-R1	AAACCAGTTTCAACGAGACTTCATC
sgRNA-*FBXW7*-F2	CACCGTCAGAGCAGCCAATGGCCAA
sgRNA-*FBXW7*-R2	AAACTTGGCCATTGGCTGCTCTGAC
sgRNA-*MCL1*-F1	CACCGTCGGACTCAACCTCTACTGT
sgRNA-*MCL1*-R1	AAACACAGTAGAGGTTGAGTCCGAC
sgRNA-*ABCB1*-F1	CACCGTCTTCTTTGCTCCTCCATTG
sgRNA-*ABCB1*-R1	AAACCAATGGAGGAGCAAAGAAGAC
sgRNA-*BRAF*-F1	CACCGGGCCAGGCTCTGTTCAACG
sgRNA-*BRAF*-R1	AAACCGTTGAACAGAGCCTGGCCC
sgRNA-*BRAF*-F2	CACCGTGTCCCCGTTGAACAGAGCC
sgRNA-*BRAF*-R2	AAACGGCTCTGTTCAACGGGGACAC
sgRNA-*ARAF*-F1	CACCGACAAGGCCCTGAAGGTGCG
sgRNA-*ARAF*-R1	AAACCGCACCTTCAGGGCCTTGTC
sgRNA-*CRAF*-F1	CACCGCCCAACGTCCTGTCGTTCGG
sgRNA-*CRAF*-R1	AAACCCGAACGACAGGACGTTGGGC
sgRNA-*FYN*-F1	CACCGAACAACTTCCACGCAGCCGG
sgRNA-*FYN*-R1	AAACCCGGCTGCGTGGAAGTTGTTC
sgRNA-*FYN*-F2	CACCGTGGAGGTCACACCGAAGCTG
sgRNA-*FYN*-R2	AAACCAGCTTCGGTGTGACCTCCAC
sgRNA-*CSK*-F1	CACCGCTGGTACAAAGCCAAAAACA
sgRNA-*CSK*-R1	AAACTGTTTTTGGCTTTGTACCAGC
sgRNA-*CSK*-F2	CACCGCTCCCGCTTCTGGACGTAGT
sgRNA-*CSK*-R2	AAACACTACGTCCAGAAGCGGGAGC

1.2.3. Generation of cell lines expressing fluorescent proteins

The lentiviral plasmid **FUGW-eGFP** (Addgene, 14883) was used to constitutively express green fluorescent proteins (GFP). For **Ruby3** red fluorescent protein lentiviral vector generation, the eGFP sequence of the FUGW-eGFP vector was replaced with the Ruby3 sequence (Bajar et al., 2016).

Lentiviral supernatants encoding for the fluorescent proteins were subsequently used to infect the corresponding cells: *Fbxw7/FBXW7* WT cells with eGFP, *Fbxw7/FBXW7* KO cells with Ruby3. After 3 days, GFP+ and Ruby3+ fluorescent cell populations were FACS sorted using a BD Influx™ cell sorter (BD Biosciences).

1.2.4. Knockdown experiments

Exponentially growing cells were trypsinised and **transfected in suspension** with 50nM of control siRNAs or human siRNAs targeting C-MYC (Horizon Discovery Biosciences, ON-TARGETplus siRNAs), following manufacturer´s instructions and using Lipofectamine RNAiMAX reagent (Thermo Fisher Scientific) and OPTIMEM medium (Life Technologies). For the esiRNA libraries (Sigma, MISSION® esiRNA, **Table 3**), the same protocol was followed with 20nM of esiRNA and in a 96-well-plate format.

Table 3: Sequences from the esiRNA library. Target and sequence of the esiRNA is indicated.

esiRNA library sequences	
Target	**Sequence**
RLUC	ATTCATTTATTAATTATTATGATTCAGAAAAACATGCAGAAAATGCTGTTAT
TUFM	CATTGAAAAATTTGAGAAGGAGGCTGCTGAGATGGGAAAGGGCTCCTTCA
POLRMT	GACGGTGGTGTACGGGGTCACGCGCTATGGCGGGCGCCTGCAGATTGAG
PTCD3	TCTGAAATGTCTCCGAAGATTTCATGTGTTTGCAAGATCGCCAGCCTTACAG
MRPS27	ATATACCCTTGTAAATAAGGTTCAATATGGAATTTTTCCAGATAACTTTACA
UQCRC1	GGTGACATTGTGCAGAACTGTAGTCTGGAAGACTCACAGATTGATTGAGAAGG

1.3. CRISPR-Cas9 screens

The generation of doxycycline-inducible mESCs Cas9 cells and the **mES Cas9 loss-of-function libraries** was previously described (Ruiz et al., 2016). For each of the screens, $5 \cdot 10^6$ cells (50X library coverage) from the mESCs KO libraries (each coming from a different mES^{Cas9} clone) were plated on gelatin. The cells were treated for approximately 10 days with the different compounds at previously tested doses (indicated in the text) at which no WT mESCs Cas9 cell survives. In the case of the UV-light screen, a single UV-light (254-nm UV-C) exposure was performed using a UVC 500 UV Crosslinker (Hoefer).

Once there were **less than 100 resistant clones**, these were picked, isolated, and expanded. The resistance of individual clones was validated with the corresponding compound before following to the sequencing step. When the number of resistant clones **exceeded 100**, a pool of cells was grown, its resistance validated, and sequenced.

1.4. Compounds

The following **compounds** were used to treat the cells at the dose indicated in the text. All compounds were dissolved in Dimethyl sulfoxide (DMSO) except from cisplatin and oxaliplatin, which were dissolved in Dimethyl sulfoxide (DMF); rapamycin and chloramphenicol, dissolved in ethanol (EtOH); and doxycycline and minocycline, dissolved in sterile water. The references for all compounds used can be seen in **Table 4**. The FDA-approved drug library of 114 antitumoural compounds was obtained from the CNIO Experimental Therapeutics Programme (**Table 5**).

Table 4: List of the compounds used for the different experiments. Compound name and vendor reference is indicated. For paclitaxel and tigecycline it is specified if its intended use is *in vitro* or *in vivo*.

Compounds		
Compound	**Reference**	
10-Desacetylbaccatin-III (DAB-III)	Selleckchem	S2409
5-fluorouracil (5-FU)	Selleckchem	S1209
BI2536 (PLKi)	Kind gift from Marcos Malumbres (CNIO, Spain)	
CAY10576	Santa Cruz Biotechnology	862812-98-4
Chloramphenicol	Roche	634 433
Cisplatin	Sigma	P4394
CSCi	Kind gift from Manuel Serrano (IRB, Spain)	
Dabrafenib	Synthesized by CNIO ETP Unit	
Dasatinib	Selleckchem	S1021
Doxorubicin	Sigma	D1515
Doxycycline	Pancreac Applichem	D9891
Erlotinib	Selleckchem	S7786
Gefitinib	Selleckchem	S1025
Gemcitabine	Sigma	G6423
GSK2606414 (PERKi)	Sigma	516535
Hydroxyurea (HU)	Sigma	H8627
IACS-10759	Axon Medchem	2909
Ifosfamide	Selleckchem	S1302
ISRIB	Sigma	SML0843
Minocycline	Sigma	M9511
ML334	Tocris	5625
NCS30930	Alichem	6640-09-1
Oligomycin	Sigma	495455
Oxaliplatin	Sigma	O9512
Paclitaxel (*in vitro* and *in vivo*)	Sigma	T7402
Pevonedistat (MLN4924)	Quimigen	A11260-10
PLX-4720	Selleckchem	S1152
Rapamycin	Alfa Aesar	J62473
Rigosertib	Selleckchem	S1362
Sorafenib	Selleckchem	S7397
Tedizolid	Selleckchem	S4641
Tigecycline (*in vitro*)	Sigma	Y0001961
Tigecycline (*in vivo*)	Carbosynth	AT10818
Trametinib	Selleckchem	S2673
Tunicamycin	Sigma	T7765
VAF-347	Sigma	182690
Vemurafenib	Selleckchem	S1267
Vincristine	Selleckchem	S1241
ZM-336372	Synthesized by CNIO ETP Unit	

Table 5: List of the compounds included in the FDA-approved drug library. Compound name is indicated. Compounds are ordered by alphabetical order.

Compounds – FDA-approved library		
4-PB	EX-527	Pazopanib
5-Fluoracil (5-FU)	Finasteride	PD-0325901
Abiraterone	Flavopiridol	Pemetrexed
AICAR	Fulvestrant	Perifosine
Alisertib	Galunisertib	PF 4708671
AT7519	GDC-0941	PI3K-CNIO
AZ ATR inhibitor	GDC-0994	Pilaralisib
AZD5363	Gedatolisib	PX-478
Bardoxolone methyl	Gefitinib	Quizartinib
BAY 61-3606	Geldanamycin	Rapamycin
BAY 87-2243	Gemcitabine	Ricolinostat
BEZ-235	Genistein	Roscovitine
BKM120	Gleevec-imatinib	S7289, PFK15
Bortezomib	GSK2126458 CNIO	SB 203580
BYL-719	GSK2636771	SB 505124
Carfilzomib	GSK461364	SCH772984
Cdk4/6 inhibitor	Idelalisib	Selumetinib
Cisplatin	Irinotecan	Semagacestat
CNIO-ATR inhibitor	Ixazomib	Silmitasertib
CNIO-DUAL	Ketoconazole	SN-38
CNIO-PIM	KU-0063794	SNS-314 mesylate
CNIO-TRIPLE	KU-57788	Sorafenib
Crizotinib	Lapatinib	S-Ruxolitinib
CUDC-101	Letrozole	Suramin
CUDC-907	Linifanib	Tamoxifen
Cyclophosphamide monohydrate	Lomustine	Tanzisertib
Dabrafenib	LY2801653	Temozolomide
Dasatinib	Metformin	Tempol
Deshydroxy LY-411575	Mifepristone	TGX-221
Disulfiram	Mitomycin C	Tozasertib
Docetaxel	MK-2206	Trametinib
Doramapimod	NVP-BGJ398	TX-1123
Dovitinib	Olaparib	Valproic acid sodium salt
Doxorubicin	OSI-906	Vincristine
Eflornithine	Oxaliplatin	Vismodegib
Elesclomol	P-0956-Vemurafenib	Vorinostat
Erlotinib	Paclitaxel	Zileuton
Etoposide	Panobinostat	ZSTK474

1.5. Flow cytometry and Flow Activated Cell Sorting (FACS)

1.5.1. Flow cytometry and High-Throughput flow cytometry for competition-two-colour assays

In order to analyse the **proportion of each cell population** (eGFP and Ruby3) in a mixed culture, 70.000 cells at the corresponding mixture ratios were plated in 6-well tissue culture plates. If performing High-Throughput flow cytometry, 4.000 cells were plated in µCLEAR bottom 96-well plates (Greiner Bio-One). The following day (or 8h after plating for mESCs) cells were treated with the indicated concentrations of drugs for 72 h (unless specified) and then analysed by Flow cytometry and High-Throughput flow cytometry.

Same procedure was done in the case of *B-RAF, A-RAF, C-RAF, FYN* and *CSK* **double KO experiments**, but infecting the cell population mixture with the lentiviral supernatants encoding for the different sgRNAs one day after plating the cells. Cells were split every 3-4 days, and every 7 days, part of the cells was analysed by flow cytometry and the rest was split and re-infected with the lentiviral supernatants.

For **esiRNAs library transfection** experiments, 4.000 cells from each mixed population were transfected and grown in µCLEAR bottom 96-well plates (Greiner Bio-One). Every 3-4 days, a part of the cells was analysed by flow cytometry, while splitting and re-transfecting the rest with the esiRNAs.

For **flow cytometry analysis** of the cell mixtures under different conditions, cells were trypsinised, centrifuged and resuspended in PBS. For staining of viable cells, cells were incubated with DAPI for 10 minutes and subsequently analysed the different cell populations using a flow cytometer BD Fortessa™ (BD Biosciences). For high-throughput flow cytometry, the mixture of cells was trypsinised and directly inactivated trypsin with the corresponding medium. After staining with DAPI, we analysed the expression of the different fluorescent markers by high throughput flow cytometry (BD FACS Canto II™, BD Biosciences). Data was processed with the Flow Jo 10™ software to represent each cell population percentage.

1.5.2. Flow Activated Cell Sorting (FACS) of fluorescent-proteins-expressing cells

Around 3 days after infection with lentiviral supernatants encoding for the fluorescent proteins, cells were trypsinised, centrifuged, and resuspended in their corresponding media containing 2% FBS, 2% penicillin/streptomycin, and 0.2% gentamycin (Life Technologies). For **GFP+ and Ruby3+ fluorescent cell populations**, a BD InfluxTM cell sorter (BD Biosciences) was used. Mid-high fluorescence-expressing populations were sorted, and then resuspended in their corresponding media supplemented with 10% FBS and 2% penicillin/streptomycin and 0.2% gentamycin. The following day, the media was replaced with the normal corresponding media. The purity of the sorted cells was checked after each sorting by flow cytometry.

1.6. Cell viability assays

1.6.1. Clonogenic assays

2.000 cells were plated in 6-well tissue culture plates in the corresponding culture medium. For the testing of the toxic dose in mESCs clones, 70.000 cells were plated in 6-well tissue culture plates, corresponding the cell density to the one used in the actual screen, despite not being a standard clonogenic assay. The following day, cells were incubated with the corresponding drugs, changing the medium every 2-3 days. Cells were maintained with the drug for 10 days, and then they were fixed and stained with 0.4% **methylene blue in methanol** for 30 min.

1.6.2. Cell-Titer Glo assays

10.000 cells were plated in µCLEAR bottom 96-well plates (Greiner Bio-One) and treated with the indicated concentrations of drugs the following day. 48 h later, cell viability was measured **by luminescence using the Cell-Titer Glo kit** (Promega), following manufacturer's guidelines. Cell viability measure was plotted as a percentage compared to DMSO-treated controls.

1.6.3. Cell viability measurement by High Throughput Microscopy

For **FBXW7 experiments**, cell viability was measured by High Throughput Microscopy. In brief, 3.000 cells were seeded per well in µCLEAR bottom 96-well plates (Greiner Bio-One) and treated with the indicated concentrations of drugs the following day. 72 h later, cells were fixed with 4% Paraformaldehyde (PFA) and permeabilised with 0.5% Triton X-100, following standard procedures. Plates were stained with DAPI and images were automatically acquired from each well using an Opera High-Content Screening System (Perkin Elmer) or a ImageXpress Pico Automated Cell Imaging System (Molecular Devices). A 20x or 10x magnification lenses were used indifferently and images were taken at non-saturating conditions. Images were segmented using **DAPI signals to generate masks matching cell nuclei** and, thus, the number of nuclei was calculated, and used as the measure of cell viability, which was plotted as a percentage compared to DMSO-treated controls.

1.7. Immunofluorescence stainings

1.7.1. ATF4 nuclear localisation by High Throughput Microscopy

8.000 cells were seeded per well in µCLEAR bottom 96-well plates (Greiner Bio-One). The following day, cells were **pre-treated** for 1 h with 50nM of ISRIB or 500nM PERK inhibitor and then treated with the indicated concentrations of drugs for 3 h. Then, cells were fixed with 4% PFA and permeabilised with 0.5% Triton X-100, following standard procedures. After blocking (3% BSA and 0.1% Tween-20 in Phosphate-buffered saline (PBS)) for 30 min, we stained with ATF4 primary antibody overnight (**Table 6**). Anti-rabbit IgG-488 secondary antibody (Invitrogen, A21441) was added at 1:200 for 1 h at room temperature (RT) the following day. Plates were then stained with DAPI and images were automatically acquired from each well using an Opera High-Content Screening System (Perkin Elmer). A 20x magnification lens was used and images were taken at non-saturating conditions. Images were segmented using DAPI signals to generate masks matching cell nuclei, and **nuclear ATF4 intensity per cell was measured** and directly plotted.

1.7.2. Mitochondrial staining by Confocal Microscopy

8.000 cells were seeded per well in µ-slide 8-well plate (Ibidi). The following day, cells were fixed with 4% PFA and permeabilised with 0.5% Triton X-100, following standard procedures. After blocking (3% BSA and 0.1% Tween-20 in PBS) for 30 min, we stained with **citrate synthetase (CS)** primary antibody for 30 min at 37ºC (**Table 6**), and then with anti-rabbit IgG-488 secondary antibody (Invitrogen, A21441) at 1:200 for another 30 min at 37ºC. Plates were then stained with DAPI and images were acquired using a LEICA SP5 WLL confocal microscope. A 63x magnification lens was used and images were taken at non-saturating conditions. Images were segmented using DAPI and 488 signals to generate masks matching cell nuclei and mitochondria, respectively, to obtain the **number of cells and values of different mitochondrial features**.

2. MOLECULAR BIOLOGY

2.1. CRISPR-Cas9 screens sgRNA sequencing

To identify the **sgRNA sequences inserted in the single-isolated resistant** clones, the DNA was extracted by standard methods and the fragment flanking the U6-sgRNA cassette from the lentiviral vector was amplified by PCR. Once purified from an agarose gel, the PCR product was subcloned into a TOPO-TA vector (Invitrogen, 45-0030) and sequenced by Sanger sequencing.

To identify the **sgRNAs present in a pool of cells**, we extracted DNA using a Gentra Puregene Blood Kit (Quiagen, 158445), following the manufacturer's instructions. The U6-sgRNA cassette was then amplified by PCR using the KAPA HIFI Hot Start PCR kit (Roche, KK2502) and different tagged primers required for the subsequent Illumina sequencing. The PCR product was precipitated with sodium acetate 3M in EtOH 100% at -80ºC for at least 20 min, pelleted and resuspended in water prior purification in agarose gel. Following a purity check of the PCR product, samples were sent for Illumina

sequencing. The sgRNA sequences were obtained from the fastq file using Galaxy (https://usegalaxy.org/) (see **Material and Methods 4.1.**).

2.2. Western Blot

Cell pellets were obtained after cell trypsinization and a washing step with cold PBS. They were then lysed in 50mM Tris pH 7.9, 8M Urea and 1% Chaps followed by 30 min incubation with shaking at 4°C. For FBXW7 detection, pellets were lysed in 20mM HEPES pH 7.9, 0.4M NaCl, 1mM EDTA and protease inhibitors, followed by sonication and a 30 min incubation with shaking at 4°C. After lysis, soluble protein extracts supernatants were obtained by centrifugation, and protein concentration was determined using the Bio-Rad Protein Assay (BIO-RAD). NuPAGE LDS (Life Technologies) with 10 mM dithiothreitol (DTT) (Sigma) loading buffer was added to **20-30 µg of protein extracts**, and samples were denatured for 10 min at 70 ºC. For OXPHOS complexes detection, the denaturing step had to be performed at 50ºC for 1h, due to COX1 sensitivity to heating. Samples were run in precast gels and transferred for protein detection, following standard Western Blot techniques. A list of the primary antibodies used can be seen in **Table 6**. Horseradish peroxidase (HRP)-conjugated secondary antibodies (ThermoFisher, mouse 31430 and rabbit 31460) were **used for detection** with the SuperSignal™ West Pico PLUS Chemiluminescent Substrate (ThermoFisher, 34580) in a ChemiDoc MP Imagine System (BIO-RAD, 1708280). Western Blot quantification was performed using Image J.

Table 6: List of primary antibodies used for immunofluorescence and Western Blot. Antibody target, vendor reference, host species, usage and dilution used is indicated. For usage: Western Blot (WB) or immunofluorescence (IF) is indicated.

Primary antibodies					
Antibody	**Reference**		**Host species**	**Use**	**Dilution**
ABCB1	Santa Cruz	SC-55510	Mouse	WB	1:500
ACTIN	Sigma	A5441	Mouse	WB	1:5000
ATF4	Cell Signalling	11815S	Rabbit	IF	1:200
CDK2	Santa Cruz	SC-163	Rabbit	WB	1:250
CHOP	Cell Signalling	2895T	Mouse	WB	1:1000
C-MYC	Santa Cruz	SC-40	Mouse	WB	1:250
CS	Abcam	ab96600	Rabbit	WB, IF	1:1000, 1:500
FBXW7	Bethyl	A301-720A	Rabbit	WB	1:1000
GAPDH	Cell Signalling	2118	Rabbit	WB	1:1000
GCN2	Santa Cruz	SC-374609	Mouse	WB	1:500
HRI	MyBioSource	MBS2538144	Rabbit	WB	1:1000
MCL1	Cell Signalling	94296	Rabbit	WB	1:1000
MCM7	LSBio	LS-C331288	Rabbit	WB	1:1000
MRPL12	Santa Cruz	SC-100839	Mouse	WB	1:500
OXPHOS	Abcam	ab110413	Mouse	WB	1:500
PERK	Santa Cruz	SC-377400	Mouse	WB	1:500
PKR	Santa Cruz	SC-6282	Mouse	WB	1:500
POLRMT	Abcam	ab32988	Rabbit	WB	1:500
PTPN2	R&D Systems	MAB1930	Mouse	WB	1:1500
TUBULIN	Sigma	T9026	Mouse	WB	1:5000
TUFM	Santa Cruz	SC-393924	Mouse	WB	1:500

2.3. Mass spectrometry

2.3.1. Samples preparation

Cells pellets were obtained after cell trypsinization and two washing steps with cold PBS. **Samples were then solubilised** for 10 minutes at 95°C in 5% SDS, 50mM TEAB, and pH 7.55. After cooling, DNA was sheared by 10 min of sonication. Protein concentration was determined using micro BCA and BSA as a standard. Then, 200 µg of each sample were digested by using the Protifi™ S-Trap™ Mini Spin Column Digestion Protocol. Briefly, proteins were reduced and alkylated (15mM TCEP, 25mM CAA) 1 h at 45 °C in the dark. SDS was removed from samples in the S-Trap column using 90% methanol in 100mM TEAB and proteins were digested with trypsin (Promega) (protein:enzyme ratio 1:100, 1 h at 47 °C).

Next, samples (100µg of peptides) were **labelled using TMT® reagent 11-plex** following manufacturer's instructions. Labelling scheme for mESCs was as follows: WT rep1 (126), WT rep2 (127N), WT rep3 (127C), WT rep4 (128N and 130C), *Fbxw7* KO clone 1 rep1 (129C), *Fbxw7* KO clone 1 rep2 (130N and 131C), *Fbxw7* KO clone 2 rep1 (128C), *Fbxw7* KO clone 2 rep2 (129N and 131). Labelling scheme for DLD1 human cell lines was as follows: WT rep1 (129C), WT rep2 (130N), *FBXW7* KO clone 1 rep1 (130C), *FBXW7* KO clone 1 rep2 (131), *FBXW7* KO clone 2 rep1 (131C). Samples were mixed in 1:1 ratios based on total peptide amount. The final mixture was finally desalted using a Sep-Pak C18 cartridge (Waters) and dried prior high pH reverse phase HPLC pre-fractionation.

2.3.2. High pH reverse phase chromatography

Peptides were pre-fractionated offline by means of high pH reverse phase chromatography, using an Ultimate 3000 HPLC system equipped with a sample collector. Briefly, peptides were dissolved in 100µl of phase A (10mM NH4OH) and loaded onto a XBridge BEH130 C18 column (3.5µm, 150mm length and 2.1mm ID) (Waters). Phase B was 10mM NH4OH in 90% CH3CN. The following gradient (flow rate of 100µL/min) was used: 0-55 min 0-45% B, 55-65 min 45-65% B, 65-65.5 min 66-95% B. Fractions were collected at 1 minute intervals. 36 fractions were speed-vac dried and re-dissolved in 2% formic acid.

2.3.3. Liquid Chromatography with tandem mass spectrometry (LC-MS/MS)

LC-MS/MS was done by **coupling an UltiMate 3000 RSLCnano LC system to a Q Exactive Plus mass spectrometer** (Thermo Fisher Scientific). Peptides were loaded into a trap column (Acclaim™ PepMap™ 100 C18 LC Columns 5µm, 20mm length) for 3 min at a flow rate of 10µl/min in 0.1% formic acid. Then, peptides were transferred to an EASY-Spray PepMap RSLC C18 column (Thermo) (2µm, 75µm x 50cm) operated at 45 °C and separated using a 60 min effective gradient (buffer A: 0.1% FA; buffer B: 100% ACN, 0.1% FA) at a flow rate of 250nL/min. The gradient used was: from 4% to 6% B in 2 min, from 6% to 33% B in 58 minutes, plus 10 additional minutes at 98% B. Peptides were sprayed at 1.7kV into the mass spectrometer via the EASY-Spray source. The capillary temperature was set to 300°C.

The **mass spectrometer was operated** in a data-dependent mode, with an automatic switch between MS and MS/MS scans using a top 15 method (intensity threshold ≥ 3.3e4, dynamic exclusion of 25 secs and excluding charges unassigned, +1 and > +6). MS spectra were acquired from 350 to 1500m/z with a resolution of 70,000 FWHM (200m/z). Ion peptides were isolated using a 1.4 Th window and fragmented using higher-energy collisional dissociation (HCD) with a normalized collision energy of 33. MS/MS spectra were acquired with a fixed first mass of 100 m/z and a resolution of 35,000 (200m/z). The ion target values were 3e6 for MS (maximum IT of 25 ms) and 1e5 for MS/MS (maximum IT of 110 msec for DLD1 cells and 90 msec for mESCs).

2.4. Quantitative RT-PCR

Total RNA was extracted using the Agilent Absolutely RNA Miniprep Kit following the manufacturer's instructions. mRNA levels were measured by real-time quantitative PCR after reverse

transcription of RNA, using for both the Invitrogen SuperScript III Platinum SYBR Green One-Step qRT-PCR Kit with ROX. **Quantitative RT-PCR was performed** on an Applied Biosystems QuantStudio 6 Flex Real-Time PCR System. We used the following primer sequences: GAPDH (GGACTCATGACCACAGTCCATGCC, TCAGGGATGACCTTGCCCACAG) and ND1 (CCCTAAAACCCGCCACATCT, GAGCGATGGTGAGAGCTAAGGT) (Skrtic et al., 2011). The levels of GAPDH mRNA were used as control to normalize expression values.

3. MOUSE BIOLOGY

3.1. Xenograft experiments

Athymic Nude-Foxn1nu 6-week female mice were acquired from Charles Rivers. $5{\cdot}10^6$ exponentially-growing DLD1 *FBXW7* KO and WT cells were trypsinised and resuspended in PBS for injection in the flank of 8-week mice. 6 days after, mice were randomized into three groups per genotype (six groups in total, 10 mice per group) and **treatment was started** with 1,5mg/kg paclitaxel (*in vivo* reference in **Table 4**), 50mg/kg of tigecycline (*in vivo* reference in **Table 4**) or vehicle via intraperitoneal (i.p.) injection, on a three times per week schedule. Tumours were measured every 2-3 days, and once they reached 1600 mm^3 (measures were calculated using the standard formula length x width x 0.5), the mice were sacrificed and their tumours were extracted. Health status of mice was monitored daily. Mice were maintained under standard housing conditions with free access to chow diet and water, as recommended by the Federation of European Laboratory Animal Science Association. All mice work was performed in accordance with the Guidelines for Humane Endpoints for Animals Used in Biomedical Research, and under the supervision of the Ethics Committee for Animal Research of the "Instituto de Salud Carlos III".

4. BIOINFORMATICS, DATA ANALYSIS AND REPRESENTATION

4.1. Identification of CRISPR-Cas9 screens sgRNA sequences using Galaxy

The sgRNA sequences were **obtained from the fastq file using Galaxy** (https://usegalaxy.org/). In brief, fastq files were uploaded using get data option and converted to FASTA format with the tool convert formats. Next, clip adapter sequences were selected (NGS: QC and manipulation options, entering this custom sequence AGAGCTAGGCCAACATGAGGATGAT, minimum length 10, not discarding sequences with unknown (N) bases, and generating both clipped and non-clipped outputs). After that, delimiters were converted to TAB and the columns were trimmed so that we only had the actual sgRNA sequences (Trim leading or trailing characters, options: Trim this column only (1), Trim from the beginning up to this position (2), Remove everything from this position to the end (21), Ignore lines beginning with these characters (select all)). Then, the sgRNAs were grouped by the sum up of the values. Finally, the samples were sorted based on the values of column 2, resulting in a file ordered by the number of reads.

4.2. *FBXW7* mutations/expression and drug response analysis

4.2.1. Representation of the most *FBXW7*-mutated cancer types

In order to represent the **most *FBXW7*-mutated cancer types and distribution** of *FBXW7* mutations along the protein sequence in the genome of cancer patients, CBioPortal (Cerami et al., 2012, Gao et al., 2013) (https://www.cbioportal.org/) was employed. For *FBXW7* mutation frequency in different human cancer types, the curated set of non-redundant studies was explored, and cancer types which included a minimum 40 total cases and minimum 5.5% of alterations were chosen as parameters to obtain and represent the data.

4.2.2. Analysis of the multi-drug resistance phenotype of *FBXW7* mutated cancer cells

For the analysis of the multi-drug resistance phenotype of *FBXW7*-mutant cancer cells, the **profile of drug response of all the available *FBXW7*-mutant** cancer cell lines from the US National Cancer Institute 60 human tumour cell line anticancer drug screen (NCI60) and the Cancer Cell Line

Encyclopaedia (CCLE) was analysed and downloaded using the Genomics and Drugs integrated Analysis (GDA) (http://gda.unimore.it/) portal. The same analysis was performed for *ABCB1*-mutant cell lines of the NCI60 (there was no data available in the CCLE).

The **lineal model analysis between *FBXW7* expression and the Area Under the Curve** (AUC) of multiple therapeutic compounds was performed using the Cancer Therapeutics Response Portal database (CTRP) (https://portals.broadinstitute.org/ctrp.v2.1/). Then, the coefficient of the compounds which reached statistical significance was plotted. A R version compatible with version 3.6.3 was employed for analysis and representation of data.

4.2.3. Patients' survival, drug treatment, and *FBXW7* gene expression correlation

The UCSC XenaBrowser (https://xenabrowser.net/) was used to explore the **GDC Pan-Cancer database containing patients' survival**, drug treatment and *FBXW7* gene expression in the tumour. The data was downloaded, and then separated into two datasets: one containing data from patients under treatment and the other from patients without drug treatment information. For each of those datasets, patient's data was stratified into two groups according to the mean of *FBXW7* expression, and survival data from each group was plotted. A Cox regression, including tumour type as co-variable, was also performed. R version compatible with version 3.6.3 was employed for analysis and representation of data.

4.3. Proteomics data analysis

4.3.1. Mass spectrometry data analysis

Raw files were **processed with MaxQuant** (v1.6.0.16) using the standard settings against either mouse (UniProtKB/TrEMBL, 53,449 sequences) or human (UniProtKB/Swiss-Prot, 20,373 sequences) protein databases supplemented with contaminants. Reporter ion MS2-based quantification was enabled for TMT 11-plex. Carbamidomethylation of cysteines was set as a fixed modification, whereas oxidation of methionines, deamidation of asparagines (only for DLD1 cells) and protein N-term acetylation was set as variable modifications. Minimal peptide length was set to 7 amino acids and a maximum of two tryptic missed-cleavages were allowed. Results were filtered at 0.01 FDR (peptide and protein level). Afterwards, the file was loaded in Prostar (Wieczorek et al., 2017) using the intensity values for further statistical analysis. Briefly, a global normalization of log2-transformed intensities across samples was performed using the LOESS function.

Differential expression analysis was done using the empirical Bayes statistics limma. Proteins with a p-value < 0.05 and a $\log_2$ ratio higher than 0.27 (mESCs) or 0.3 (DLD1 cells) were defined as regulated. The FDR was estimated to be below 2% by Pounds.

For the **Gene Set Enrichment Analysis** (GSEA) of the proteomics differential expression analysis results, the GSEA programme (v2.2.4.) was used. Pre-ranked Fold Change values list was used as an input.

4.3.2. Cancer Cell Line Encyclopaedia (CCLE) proteomics analysis

For the Cancer Cell Line Encyclopaedia (CCLE) proteomics analysis, **data was extracted** from the recently published work (Nusinow et al., 2020). 388 cancer cell lines were classified according to *FBXW7* mutational and copy number variation status. Only cell lines harbouring coding, damaging, or non-conserving alterations in *FBXW7* were labelled as mutated. Cell lines with an absolute copy number score of 0 for *FBXW7* were also included. **Differential expression analysis** was carried out using limma (Ritchie et al., 2015) on normalized expression levels between mutated and WT cancer cell lines. Differentially expressed proteins were mapped to gene symbols by the Broad Institute. For analysis and representation, R version 3.6.1 was used.

4.4. Connectivity Map (CMap) analysis

4.4.1. CMap data analysis

The **CMap Touchstone clue.io tool** (https://clue.io/) was used to extract perturbagens (compounds, CMap classes and the over-expression or knock-down of genes) with signatures to the PLX-4720 signature from the CMap data (Subramanian et al., 2017). Similarity scores were downloaded and results were sorted based on their scores and the type of perturbagen.

4.4.2. Drug "Gene Set Enrichment Analysis" (GSEA)

Gene Set Enrichment Analysis **(GSEA) was adapted to enable enrichment analyses of "drug classes"** based on their mechanism of action (MOA), for which the GSEA method implemented in the R package fgsea (Korotkevich et al., 2019) was used, adapted from two manuscripts (Sinha et al., 2020, Sanchez-Burgos et al., 2020). In brief, the similarity scores from the signatures associated to all the compounds were ranked, and the GSEA method was applied to the ranked list with "gene sets" for GSEA analysis, the "gene sets" being the sets of drugs of each class. The drug classes were based on the mechanisms of action (MOA), which was available in the annotation data included in CMap analysis in the "description" field. For the computational analysis, R version 3.6.3 was used, and a sample of the code used for a similar analysis can be obtained from https://github.com/Genomic-Instability-Lab/An-in-silico-analysis-of-drugs-potentially-modulating-the-cytokine-storm-triggered-by-SARS-CoV-2-inf.

4.5. Other graphical representations and statistical analyses

For the rest of the **graphical representations and statistical analyses** GraphPad Prism version 7.04 was used, using the statistical comparisons indicated in the corresponding Figure Legends.

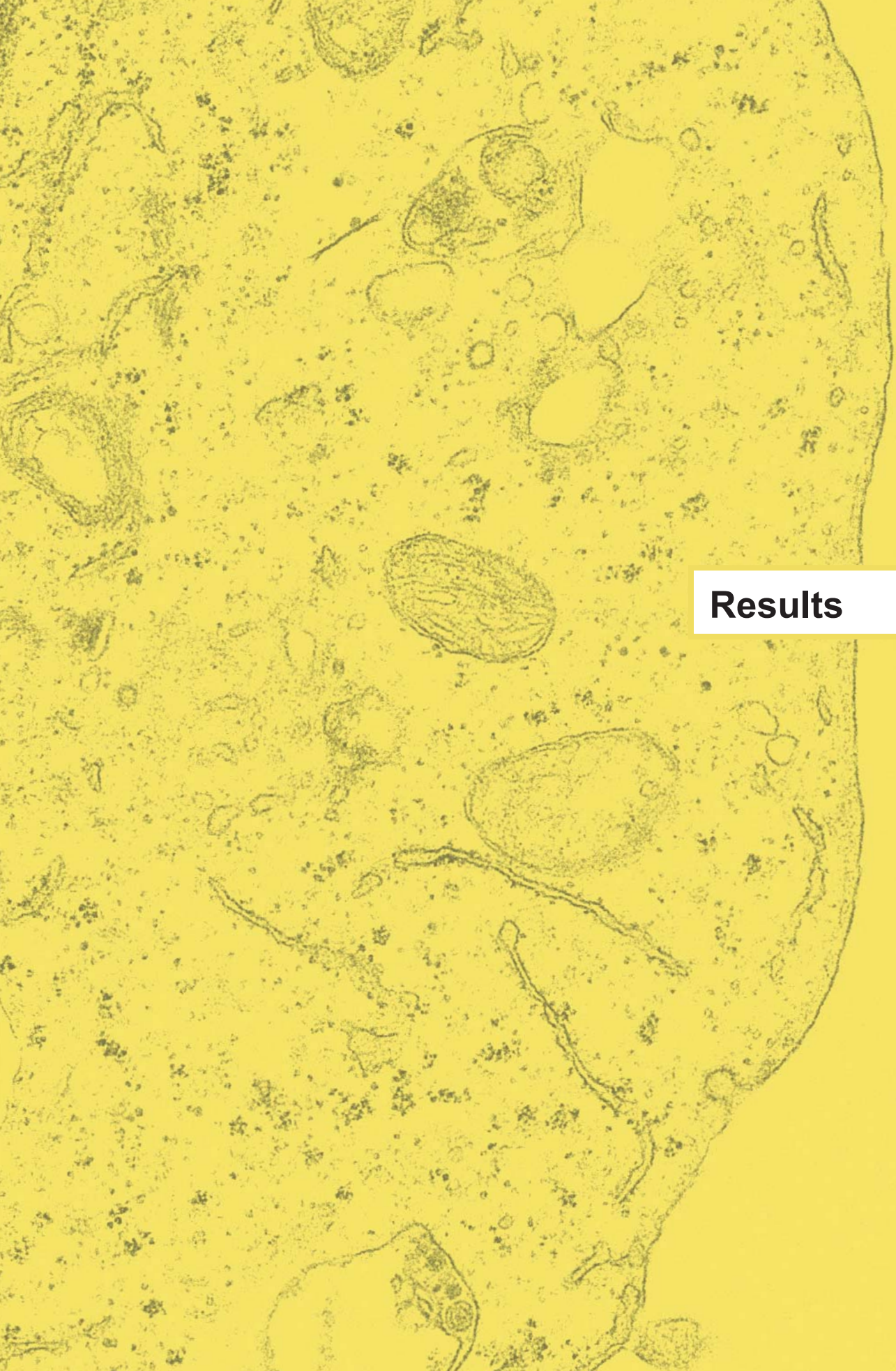

Results

1. IDENTIFICATION OF NOVEL MECHANISMS OF RESISTANCE TO GENOTOXIC THERAPIES THROUGH CRISPR-CAS9 SCREENS

The first goal of this Thesis was to **conduct CRISPR-Cas9 genome-wide genetic screens**, to explore resistance to two of the most widely used genotoxic agents; the nuclear DNA damaging agent cisplatin, and high-dose UV light. To this end, we employed loss-of-function libraries previously developed in mESCs (Ruiz et al., 2016). In brief (**Figure 13**), the mESCs-KO libraries were generated by infecting mESCs carrying a doxycycline-inducible Cas9 cells with a sgRNA-BFP library that contains 87.897 sgRNAs targeting 20.000 murine genes (Koike-Yusa et al., 2014). After sorting for BFP+, cells were next treated for 10 days with doxycycline to induce Cas9-mediated mutations. These loss-of-function libraries were used for the subsequent genome-wide screens, and some of the hits obtained from the cisplatin and UV screens, as well as other screens performed by other members of the lab for other antitumoural compounds, were further validated.

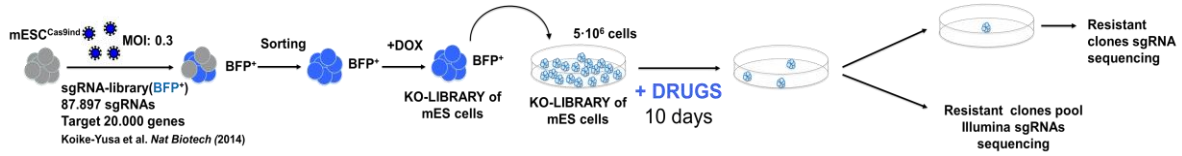

Figure 13: Pipeline of CRISPR-Cas9 screens. Briefly, doxycycline-inducible mESCs^{Cas9} were infected at a low multiplicity of infection (MOI 0.3) with a mouse library of sgRNAs (Koike-Yusa et al., 2014). The BFP of the lentiviruses that contain the library, enabled FACS sorting of the correctly infected cells. Doxycycline 2µg/ml was added for 10 days to induce Cas9 expression and generate mutant cells. The generated libraries (coming from two different mES clones) were used for the corresponding screens. $5{\cdot}10^6$ cells were used per screen (50X library coverage) and exposed for around 10 days to test compounds at a dose at which no WT cell is able to survive. The resistant clones, if any, were then isolated and expanded, and the DNA fragments containing sgRNA sequences, were amplified by PCR and identified by Sanger sequencing. If more than 100 clones appeared, a pool of those resistant cells was taken and, following PCR amplification, sent for Illumina sequencing.

1.1. CRISPR-Cas9 screens for mediators of cisplatin-resistance

Cisplatin, serendipitously discovered as an antibacterial agent (Rosenberg et al., 1965, Rosenberg et al., 1969), is still one of the most routinely used chemotherapies in the clinic, approved for the treatment of a wide spectrum of solid tumours (Prestayko et al., 1979, Galluzzi et al., 2014). Yet, as for other chemotherapeutic agents, drug resistance prevents achieving curative responses. Many mechanisms of resistance to cisplatin are already known and include an increased DNA repair or tolerance to the drug-produced DNA lesions (mutations for example in *ERCC1, MSH2, MLH1*), defective execution of the cell death programme (mutations in *TP53* or pro/anti-apoptotic genes); or others related to the drug influx/efflux, its metabolic inactivation or off-target effects (Galluzzi et al., 2012, Galluzzi et al., 2014). Nevertheless, a complete understanding of all the mediators in cisplatin resistance is still lacking.

Previous genome-wide screens in yeast (Burger et al., 2000, Wu et al., 2004, Lum et al., 2004) or in mammalian cells using RNAi (Nijwening et al., 2011, Jin et al., 2018, Pan et al., 2019) helped to unravel novel cisplatin-resistance genes. Nonetheless, by the time we started the project, there were no reports of cisplatin-resistance CRISPR-Cas9 screens (although several papers were published later using this technology (Ko and Li, 2019, Ouyang et al., 2019, Stover et al., 2019, Goodspeed et al., 2019, Xu et al., 2020, Olivieri et al., 2020, Hundley et al., 2021)). Hence, we aimed to characterise novel mutations involved in the resistance to this relevant antitumoural agent using our mESCs loss-of-function libraries.

We first defined the **toxic dose** of cisplatin in the doxycycline-inducible mES Cas9 clones by performing a clonogenic assay. We observed complete death of the cells at 1.5µM in one mutant library and at 1µM in an independent one (**Annex Figure 1A**). Nevertheless, we performed both screens at the same dose, 1.5µM, and, as there were more than 100 resistant clones, we expanded the **pool of cells** and identified their sgRNAs by Illumina sequencing. The top hit in the first library was *Fbxw7*, for which we also identified two different sgRNAs in the other library (**Annex Table 6**). The other genes that were identified in both libraries include *Myh9*, *Fam115c, Bicd1* and *Mlf1* (**Annex Table 6**). The top

hits in the other library were *Gpr176, Pdcl* and *Tsc2* (**Annex Table 6**). Of note, we did not find any of previously-known cisplatin-resistant mediators, which we think that could be related to the cell line or dose of choice.

As the first screen dose was not extremely restrictive, we conducted a **second screen** by using higher doses of cisplatin. This time, there were only 11 resistant clones per library, which allowed us to identify the sgRNAs per clone without next-generation sequencing. In the first library, we found only three sgRNAs, which were also found in the previous sub-lethal dose screen: *Fbxw7, Myh9* and *Ptpn2* (**Annex Table 7**). In the other library we identified completely different hits (like *Tbck, Ptgs1* or *Glod4*) except from *Fbxw7*, which was also present (**Annex Table 7**). Of note, in most cases, clones contained a combination of sgRNAs (**Annex Table 7**), difficulting the identification of the resistance-driving mutations.

1.2. CRISPR-Cas9 screens for modulators of UV-light sensitivity

The relationship between solar **ultraviolet (UV)** irradiation and skin cancers and ageing has been largely known (Epstein, 1983, IARC, 1992, Ley, 1993, de Gruijl and Forbes, 1995, Kraemer, 1997, Berwick et al., 2008, Weinberg, 2014, Leiter et al., 2020). UV-C (180–280nm) and UV-B (280–320nm) radiations, although almost completely absorbed by the atmosphere ozone layer, are highly mutagenic and can induce two of the most abundant DNA lesions: cyclobutyl pyrimidine dimers and 6–4 photoproducts (Clingen et al., 1995, Yoon et al., 2000, Errol et al., 2006, Pfeifer et al., 2005). Nevertheless, a number of repair/tolerance mechanisms emerged during evolution to cope with this DNA damage. Indeed, photoreactivation, the process of repair of cyclobutyl pyrimidine dimers, is believed to be the first DNA repair mechanism that evolved in nature (Friedberg, 2008), being also the first to be discovered (Kelner, 1949, Dulbecco, 1949).

The **main components** of the repair (nucleotide excision repair (NER) pathway) or signalling (ATR and CHK1) of UV lesions have already been vastly studied (Sinha and Häder, 2002, Errol et al., 2006, Marteijn et al., 2014). However, more elements and pathways have been more recently related to UV responses such as NFκ-B, STAT3, AKT/mTOR, p38, MAPK, JNK, ERK, or ATM kinases (Lopez-Camarillo et al., 2012, Strozyk and Kulms, 2013). In order to identify more factors of the UV-light response pathway, and maybe establish a link with cancer initiation or promotion, we performed an UV-resistance CRISPR-Cas9 screen.

Again, we took advantage of the loss-of-function libraries in mESCs. We established 25J/m^2 of UV-C light as the **lethal dose** for both libraries (**Annex Figure 1B**). In this case, we sequenced the pool of one library resistant colonies, as there were more than 100; and we isolated and sequenced 25 individual resistant clones from the other library. From both libraries the **most relevant hits** were *Fbxw7* and *Ptpn2*, as we identified 4 independent sgRNAs from each of them in both libraries (**Annex Table 8**). There were some hits that we had identified also in the cisplatin screen (*Ptgs1, Fam115c, Glod4, Myh9* or *Tbck*), but many were specific to the UV screen, like *Apc, Gas6* or *Ttc3* (**Annex Table 8**). We acknowledge that one of the drawbacks of this screen was the fact that we couldn't discard that the resistant clones' resistance aroused from mutations generated by UV-light itself. Therefore, we next aimed to validate the resistance of the two most interesting hits: *Fbxw7* **Results 1.4. and 2.1.**) and *Ptpn2* (**Results 1.3.**).

1.3. Validation of CRISPR-Cas9 screens hits: *Ptpn2*

For the **validation of *Ptpn2* resistance** to UV-light, we generated *de novo* knock-out (KO) clones in another mESC line (R1 cells) (**Figure 14A**) and exposed the cells to UV radiation. Three different *Ptpn2* KO clones proved to be resistant to UV (**Figure 14B**). We also confirmed that they were moderately resistant to cisplatin (**Figure 14C**), as it was also a hit in that screen. Nevertheless, we did not explore further, as the role of T-cell protein tyrosine phosphatase (TC-PTP) (encoded by *Ptpn2*) in UV-light signalling pathways and cancer initiation and promotion, through negative regulation of STAT3 and AKT, has already been deeply studied (Kim et al., 2010, Kim et al., 2017b, Lee et al., 2015, Lee et al., 2017a).

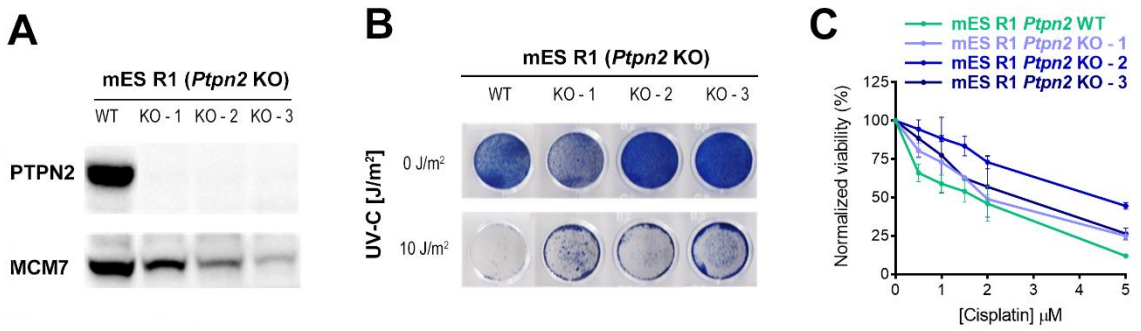

Figure 14: Validation of *Ptpn2* KO in resistance to UV. (**A**) Western Blot illustrating *Ptpn2* KO in R1 mESCs generated using CRISPR-Cas9. MCM7 levels are shown as a loading control. (**B**) Clonogenic assay of R1 mESCs WT or KO for *Ptpn2* cells exposed to 0 or 10 J/m^2 UV-C. Experiment was repeated three times, and a representative example is shown. (**C**) Normalized viability of R1 mES WT (in green) and R1 mES *Ptpn2* KO clones (in blue) upon cisplatin treatment. Cell viability was measured using CellTiter-Glo® Luminescent Cell Viability Assay. Error bars indicate SD (two technical replicates).

1.4. Identification of *Fbxw7* as a recurrent hit in CRISPR-Cas9 screens

Besides the cisplatin and UV-light screens performed by me, other members of the lab performed **additional screens for resistance** to another three cytotoxic compounds: the precursor of the microtubule poison paclitaxel, 10-Desacetylbaccatin III (DAB-III); another microtubule destabilizing agent with indirect actions in RAS signalling (Ritt et al., 2016, Jost et al., 2020), rigosertib; and an unpublished cancer stem cell inhibitor (CSCi). Surprisingly, we observed that ***Fbxw7***, a substrate recognition component of an E3 ubiquitin-protein ligase complex, was a recurrent and frequent hit in all of these CRISPR-screens (**Figure 15**). For example, in one of our cisplatin screens, 8 out of 11 clones were carrying one independent *Fbxw7*-targeting sgRNAs (**Figure 15A**), and from one to four independent *Fbxw7*-targeting sgRNAs appeared at high rates in the other screens (**Figure 15A-B**).

At first, we considered the possibility of having a contamination of the *Fbxw7* sgRNA DNA in the lab. Nevertheless, we discarded that option, as Fbxw7 targeting sgRNAs were not detected in gain-of-function genetic screens that were performed in the lab at the same time (data not shown). *Fbxw7* was therefore a **bona-fide specific hit of loss-of-function screens**. That, together with the known role of *FBXW7* deletions in cancer as a tumour suppressor and drug resistance to several individual compounds (**Figure 8** and **Annex Table 4**), led us to hypothesise that *FBXW7* mutations could be a multi-drug resistance related event. Thus, we next centred our efforts in testing that hypothesis and trying to understand the role of *FBXW7* mutations in multi-drug resistance.

A

Clones carrying *Fbxw7*-targeting sgRNAs

	Library 1	Library 2
CISPLATIN	**8/11** (1 sgRNA (1))	**1/11** (1 sgRNA (1))
DAB-III	**9/15** (1 sgRNA (1))	
RIGOSERTIB	**5/8** (1 sgRNA (1))	**0/1**
CSCi		**5/20** (2 sgRNAs (1&2))
UV		**5/25** (2 sgRNAs (1&2))

B

Illumina pool sequencing - *Fbxw7*-targeting sgRNAs

	sgRNA sequence	Pos.	Nº reads
CISPLATIN LIBRARY 1	*Fbxw7* sgRNA (1)	1	362449
CISPLATIN LIBRARY 2	*Fbxw7* sgRNA (1)	20	1465
	Fbxw7 sgRNA (2)	44	178
UV LIBRARY 1	*Fbxw7* sgRNA (1)	7	38937
	Fbxw7 sgRNA (2)	32	5733
	Fbxw7 sgRNA (3)	9	35081
	Fbxw7 sgRNA (4)	204	340

* **sgRNA sequences**

Fbxw7 sgRNA (1) - AGTGTCTGAGAACGTTAGTG
Fbxw7 sgRNA (2) - GTGGCAACCGCATAGTTAGG
Fbxw7 sgRNA (3) - TGGTCAGCGGTCACGGGCAG
Fbxw7 sgRNA (4) - GGCTCAGACTTGTCGATACG

Figure 15: *Fbxw7* as a recurrent hit in CRISPR-Cas9 screens. (**A**) Number of clones carrying *Fbxw7*-targeting sgRNAs in cisplatin, DAB-III, rigosertib, CSCi and UV screens per library. Number of clones carrying *Fbxw7*-targeting sgRNAs is indicated per library and compound screen. The number of different *Fbxw7*-sgRNAs found in the screen is indicated inside parentheses. (**B**) *Fbxw7*-targeting sgRNAs identified by Illumina sequencing of the pool of cells from cisplatin libraries and from one of the UV screen libraries. The number of the different *Fbxw7*-sgRNAs found in the screens are indicated inside parentheses as well as the number of reads and the position that the sgRNAs occupied in the rank of the screen. * *Fbxw7*-sgRNA sequences are indicated.

2. FBXW7 DEFICIENCY AS A MULTI-DRUG RESISTANCE AND POOR PROGNOSIS MARKER IN CANCER

2.1. *Fbxw7* deletion is associated with multi-drug resistance

FBXW7 is among the **top 10 most mutated** genes in cancer (Lawrence et al., 2013). Surprisingly, it has never been studied as deeply as other relevant genes like *TP53, RAS* or *MYC*. What is more, even if there has been multiple reports linking *FBXW7* mutations to resistance to several anticancer compounds (**Figure 8** and **Annex Table 4**), their potential impact in multi-drug resistance has never been specifically examined.

2.1.1. Loss of *Fbxw7* is associated to multi-drug resistance in mESCs

To validate our hypothesis that *Fbxw7* deficiency leads to resistance to multiple compounds, we generated *de novo Fbxw7* knock-out (KO) clones in a mESCs line (R1 cells) using CRISPR-sgRNAs (**Figure 16A**) and **compared the resistance** of these cells to several drugs to wild-type (WT) cells infected with an empty vector. For a better comparison of drug response, *Fbxw7* WT and KO cells were infected with lentiviruses encoding for enhanced green fluorescent protein (eGFP) and Ruby3 red fluorescent protein, respectively. This **two-colour cell-labelling approach**, used by other authors (Vanneste et al., 2019, Olbrich et al., 2019), despite not providing a numeric measure of viability for each compound, allows to rapidly explore survival of specific resistant populations by flow cytometry. Alongside, WT^{eGFP} and Fbxw7-KO^{Ruby3} cells were mixed together at a ratio around 3:1 and treated with nearly-toxic doses of different drugs already described to generate resistance in *FBXW7* KO cells: paclitaxel (Wertz et al., 2011, Inuzuka et al., 2011, Yokobori et al., 2014, Gasca et al., 2016, Ishii et al., 2017), oxaliplatin (Li et al., 2015b, Fang et al., 2015), 5-FU (Li et al., 2019, Lorenzi et al., 2016), and doxorubicin (Yu et al., 2014, Li et al., 2016, Ding et al., 2018) (**Figure 16B**).

Consistent with the previous reports, flow cytometry analyses of these cultures after 48h revealed a significant **increase in the percentage of Fbxw7-KO^{Ruby3} cells** treated with the drugs (**Figure 16C**). In contrast, GFP-Ruby3 ratios remained unaltered in DMSO treated cultures (**Figure 16C**).

To get a better idea of the extent of the potential multi-drug resistance in *Fbxw7*-KO cells, we further tested a **FDA-approved drug library** of 114 antitumoural compounds and analysed the cell population percentage changes by high-throughput flow cytometry after 48h. At the dose tested (5µM), only some drugs presented a substantial decrease in viability (**Figure 16D**). Interestingly, compounds to which *Fbxw7* KO were significantly more resistant than the WT cells (**Figure 16E**), corresponded to the drugs that had the bigger impact in cell viability (**Figure 16D**), meaning that depletion of *Fbxw7* provided resistance to all antitumoural agents that have a toxic effect in mESCs.

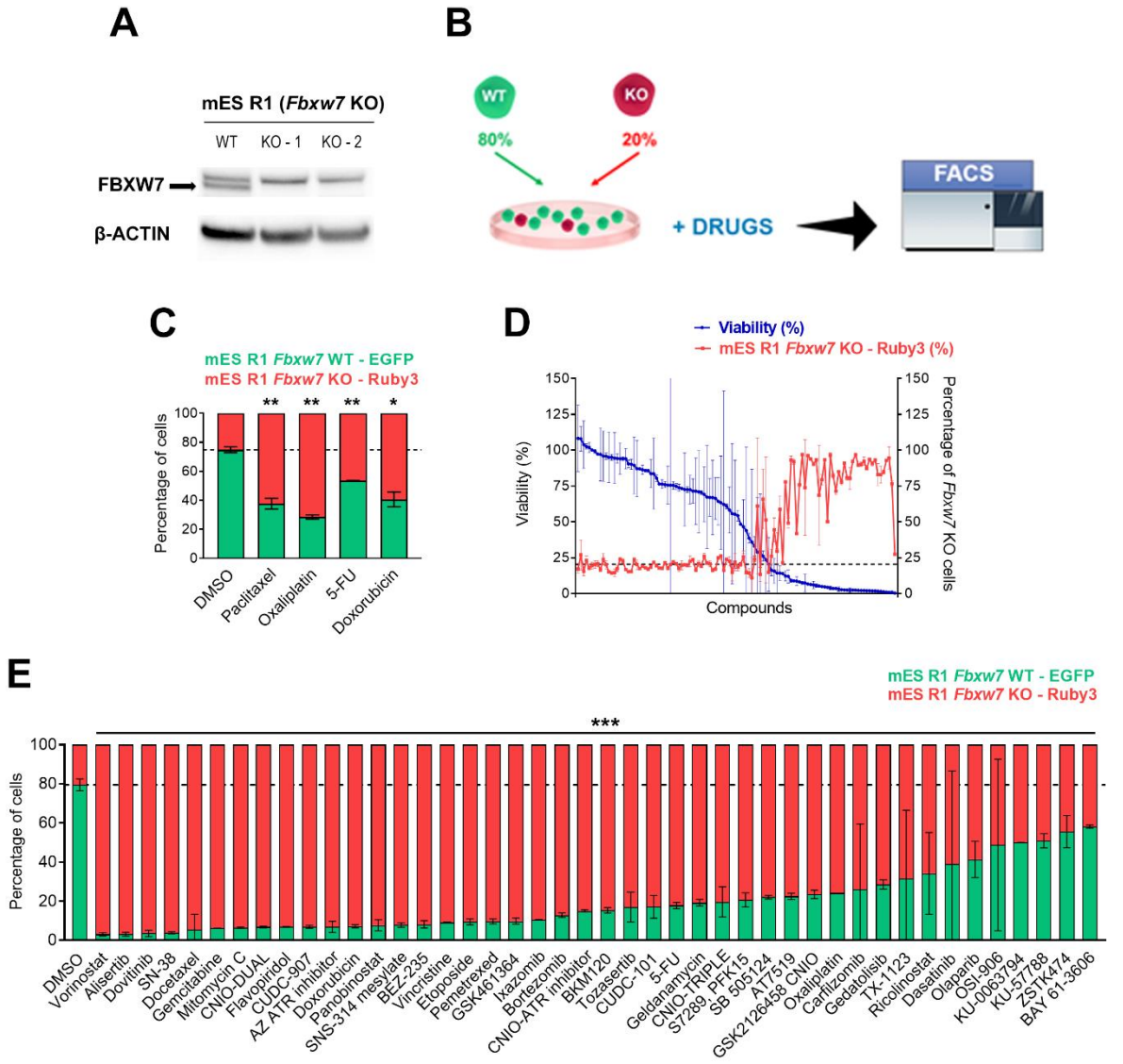

Figure 16: Fbxw7 deficiency generates multi-drug resistance in mESCs. (**A**) Western Blot illustrating the KO of *Fbxw7* in R1 mESCs generated using CRISPR-Cas9. ß-ACTIN levels are shown as a loading control. (**B**) Two-colour experiment flowchart. *Fbxw7* WT and KO cells were infected with lentiviruses encoding for enhanced green fluorescent protein (eGFP) and Ruby3 red fluorescent protein, respectively, and mixed together at a ratio around 3:1 and treated with nearly-toxic doses of different drugs. After several days, FACS analyses of these cultures were performed. (**C**) Cell percentages of eGFP+ R1 WT cells and Ruby3+ R1 *Fbxw7* KO cells after 48h treated with DMSO (control), paclitaxel (30nM), oxaliplatin (750nM), 5-FU (2µM) and doxorubicin (25nM). The culture started with 3:1 ratio of WT^{eGFP} and Fbxw7-KO^{Ruby3} respectively. The experiment was repeated three times and a representative example is shown. Error bars indicate SD (two technical replicates). n.s. p>0.05, *p<0.05, **p<0.01, ***p<0.001 (t-test). (**D**) Representation of the percentage of cell viability versus cell percentage of Ruby3+ R1 *Fbxw7* KO cells after 48h treated with 5 µM of a FDA-approved drug library of 114 antitumoural compounds. DMSO was used a control. The culture started with 3:1 ratio of WT^{eGFP} and *Fbxw7*-KO^{Ruby3} respectively. Error bars indicate SD (two technical replicates). (**E**) Cell percentages of eGFP+ R1 WT cells and Ruby3+ R1 *Fbxw7* KO cells from the experiment in (D). Only the 44 significative compounds are displayed. DMSO was used as control. Error bars indicate SD (two technical replicates, except for DMSO with more technical replicates). n.s. p>0.05, *p<0.05, **p<0.01, ***p<0.001 (t-test).

2.1.2. FBXW7 deficiency is associated with multi-drug resistance in human cancer cell lines

Given the impact of *Fbxw7* deletion in mESCs, we next evaluated whether **FBXW7-deficient human cancer cells** presented a similar phenotype. To this end, we generated *FBXW7* knock-out (KO) cells in DLD1 colorectal cancer cell line (**Figure 17A**), as this is one of the cancer types where *FBXW7* is most frequently mutated (**Figure 6**), and DLD1 cell line has been largely used to explore FBXW7 biology (Wertz et al., 2011, Davis et al., 2018, Li et al., 2019). *FBXW7* WT and KO clones were exposed to several drugs with different mechanisms of action: microtubule poisons (paclitaxel and vincristine), a DNA intercalating agent (doxorubicin), different nucleotide synthesis inhibitors or antimetabolites (hydroxyurea (HU), gemcitabine and Fluorouracil (5-FU)), and inhibitors of MEK1/2 (trametinib), Polo-like kinase 1 (PLK1i BI2536), NEDD8-ubiquination (pevonedistat or MLN4924), and mTOR (rapamycin). After 72h, we quantified cell viability by counting nuclei by High Throughput Microscopy. Both *FBXW7* KO clones presented significant resistance to all the tested compounds (**Figure 17B**). Hence, FBXW7 deficiency is associated with a multi-drug resistance phenotype in the colorectal human cancer cell line DLD1.

Next, we explored different **publicly available bioinformatics resources** to gain more insights into the extent of the multi-drug resistance phenotype of FBXW7-deficient cancer cells. First, we analysed the profile of drug responses of *FBXW7*-mutant cancer cell lines using data coming from the US National Cancer Institute 60 human tumour cell line anticancer drug screen (NCI60) and the Cancer Cell Line Encyclopaedia (CCLE). These databases were constructed by exposing hundreds of human cancer cell lines to large collections of compounds and combining that information with the cell lines mutational data (Alley et al., 1988, Barretina et al., 2012). More recently, additional layers of information such as transcriptomics, proteomics or metabolomics of these cell lines have been added to these efforts to elaborate a bigger picture of genetic variants, candidate targets, potential therapeutics, and new cancer dependencies (Su et al., 2011, Ghandi et al., 2019, Nusinow et al., 2020). Analysing these datasets for the drug response of *FBXW7*-mutant cells, we found that *FBXW7*-mutant cell lines displayed drug resistance for most of the drugs (**Figure 17C-D**). Noteworthy, the multi-drug resistance phenotype of *FBXW7*-mutant cells was even more pronounced that the one associated with the canonical multi-drug resistance gene *ABCB1* (**Figure 17C**).

In an **independent approach**, we also took advantage of the Cancer Therapeutics Response Portal (CTRP) data. Similar to the previous datasets, this portal links different cellular features like gene expression of cancer cell lines to drug sensitivity (Basu et al., 2013, Seashore-Ludlow et al., 2015, Rees et al., 2016). Drug response is represented in this case by its Area Under the Curve (AUC), which is positively correlated with the IC_{50} of the drug and inversely related to the response. The lineal model analysis between *FBXW7* expression and the AUC of hundreds of therapeutic compounds revealed a significant negative correlation for most of the drugs (**Figure 17E**). That implied that for the 379 compounds with negative coefficient, the lower the expression of *FBXW7*, the higher the AUC and the resistance to the compound was (**Figure 17E**). Only 14 compounds showed an opposite effect, in which low levels of FBXW7 correlated with sensitivity (**Figure 17E**). In conclusion, the use of three different human cancer cell line databases revealed the existence of a correlation between *FBXW7* mutations and multi-drug resistance in cancer.

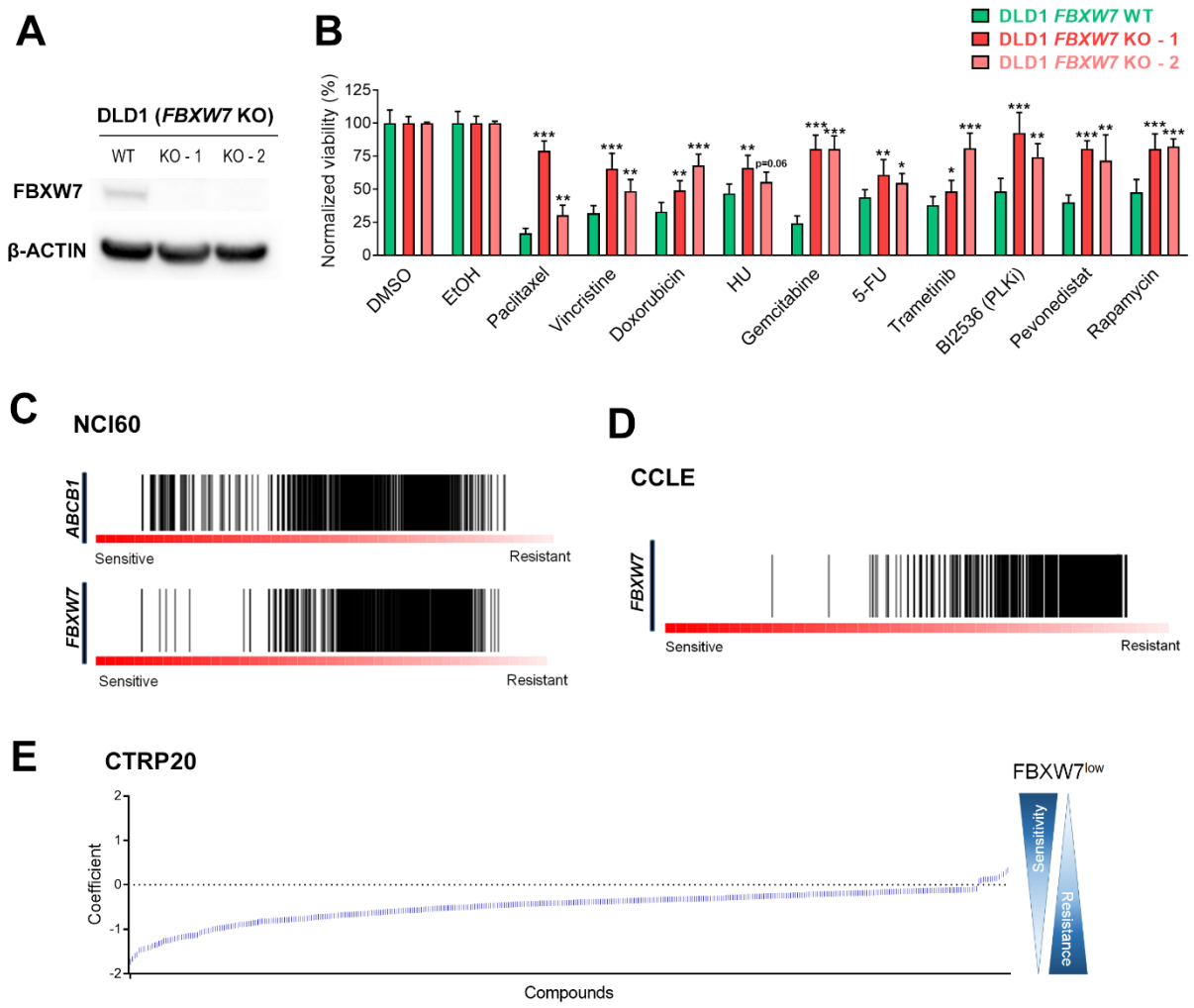

Figure 17: *FBXW7* deficiency is associated with multi-drug resistance in human cancer cell lines. (**A**) Western Blot illustrating the KO of *FBXW7* in DLD1 cells generated using CRISPR-Cas9. ß-ACTIN levels are shown as a loading control. (**B**) Normalized viability of DLD1 WT (in green) and DLD1 *FBXW7* KO clones (in red) upon different drug treatments: DMSO (control), EtOH (control for rapamycin), paclitaxel (40nM), vincristine (10nM), doxorubicin (25nM), hydroxyurea (HU, 75µM), gemcitabine (10nM), Fluorouracil (5-FU, 10µM), trametinib (5µM), BI2536 (PLK1i, 10nM), pevonedistat (200nM) and rapamycin (10µM). DAPI staining was performed to count nuclei by high-throughput microscopy. Error bars indicate SD (n=3, three independent experiments, with two technical replicates per experiment). n.s. $p>0.05$, *$p<0.05$, **$p<0.01$, ***$p<0.001$ (t-test). (**C**) Profile of the drug response of *FBXW7* and *ABCB1*-mutant cancer cell lines from the NCI60. Each line represents a compound. (**D**) Profile of the drug response of *FBXW7*-mutant cancer cell lines from the CCLE. Each line represents a compound. (**E**) Representation of the coefficients resulting from the lineal model analysis between FBXW7 expression and the AUC of multiple therapeutic compounds in cell lines of the CTRP. Each line represents a compound. Positive coefficients relate to sensitivity of $FBXW7^{low}$ cells to the compound; negative, to resistance to the compound.

2.1.3. FBXW7 deficiency is associated with poor therapy response in cancer patients

Additionally, we investigated if the resistance to therapies caused by FBXW7 deficiency could have some **relevance in cancer patients**. To address this question, we mined the UCSC XenaBrowser (https://xenabrowser.net/) GDC Pan-Cancer database, which contains patients' survival data, treatment information, and their tumours' gene expression values. These data were first stratified by treatment (patients under treatment and patients without drug treatment information) and, then, according to their *FBXW7* expression's mean to finally plot survival data. The analysis revealed that for patients for whom there was not drug information, prognosis was independent of *FBXW7* levels (**Figure 18A**). However, for patients under any type of therapy, there was a significative reduction of survival when *FBXW7* tumour levels were low (**Figure 18B**). Altogether, we propose that FBXW7 deficiency could be used in medical practice as a biomarker of therapy response in cancer patients.

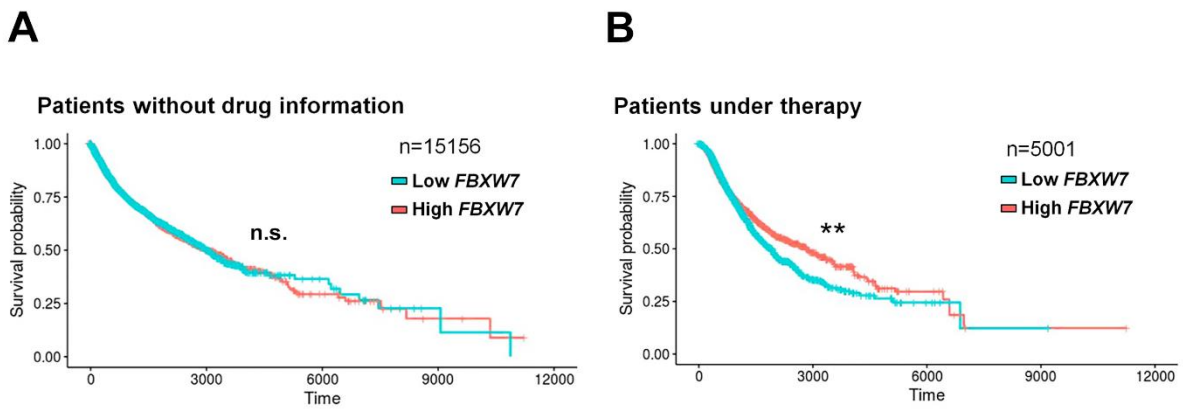

Figure 18: FBXW7 deficiency is a poor prognosis marker in cancer. (**A,B**) Patient survival probability of cancer patients without drug information (A) and under any therapy (B), stratified by *FBXW7* mRNA levels (low in blue, high in red). Data comes from GDC Pan-Cancer study available at Xenabrowser. N indicates number of patients. n.s. p>0.05, *p<0.05, **p<0.01, ***p<0.001. After Cox regression taking tumoural type as covariable, coef = -1.22 and p = 0.0508 for (B).

2.2. Mechanisms of therapy resistance driven by FBXW7-deficiency

2.2.1. MCL1

Previous works indicated that the accumulation of the **anti-apoptotic factor MCL1** was responsible for the resistance of FBXW7-deficient cells to certain agents like vincristine, taxol, nocodazole, etoposide, and the BCL2 inhibitor ABT-737 (Wertz et al., 2011, Inuzuka et al., 2011), and later expanded to many other compounds (**Figure 8** and **Annex Table 4**). In this context, we wondered if the accumulation of MCL1 was behind the multi-drug resistance phenotype unravelled by this work. However, deletion of *MCL1* in FBXW7-deficient DLD1 cells (**Figure 19A**) was not sufficient to rescue their resistance to several compounds (**Figure 19B**). For instance, the resistance to HU, gemcitabine, 5-FU, trametinib, PLKi and rapamycin resistance were MCL1-independent (**Figure 19B**). On the other hand, the resistance of FBXW7-deficient DLD1 cells to paclitaxel, vincristine, doxorubicin and pevonedistat was significantly reduced upon *MCL1* deletion (**Figure 19B**). Indeed, the resistance phenotype to clinically relevant agents like doxorubicin was completely ablated in MCL1-deficient cells (**Figure 19B**). Of note, WT cells depleted for MCL1 also displayed a significantly reduced viability to paclitaxel, vincristine, doxorubicin and pevonedistat, arguing that this sensitization phenomenon is independent of *FBXW7* (**Figure 19C**).

2.2.2. ABCB1

We next wondered whether the multi-drug resistance phenotype of FBXW7-deficient cells was caused by the upregulation of an already described multi-drug resistance mechanism such as the **increased expression or activity of ABCB1** (Kartner et al., 1983a, Kartner et al., 1983b), which promotes the expulsion out of the cell of various hydrophobic compounds, including major cancer chemotherapeutics such as taxanes, topoisomerase inhibitors and antimetabolites (Hodges et al., 2011, Wolking et al., 2015). Moreover, ABCB1 was described to be upregulated in *FBXW7*-mutant cells in a very recent report (Mun et al., 2020).

Consistent with the recent report, DLD1 *FBXW7*-depleted cells **upregulated ABCB1** (**Figure 20A**). Moreover, *ABCB1* deletion completely rescued the resistant phenotype of *FBXW7*-deficient cells to paclitaxel, vincristine, doxorubicin, PLK1i and pevonedistat (**Figure 20B**), reducing viability even more than that of WT cells. As a matter of fact, *ABCB1* deletion was *per se* a sensitiser to these compounds, regardless of the *FBXW7* mutational status (**Figure 20C**). Interestingly, there was a reduction in viability upon rapamycin treatment in double *FBXW7 ABCB1* KO cells (**Figure 20B**), that was not seen in *FBXW7* WT *ABCB1* KO cells (**Figure 20C**). For the rest of the tested compounds, the resistance was ABCB1-independent (**Figure 20B**). These results are concordant to what we reported

previously in **Figure 17**. Namely, that the resistance profile of *FBXW7*-mutant cells is even more profound than that of *ABCB1*-mutant tumours. That is explained by the fact that, in addition to upregulating ABCB1, *FBXW7*-mutant cells present additional mechanisms that further increase their resistance to anticancer agents.

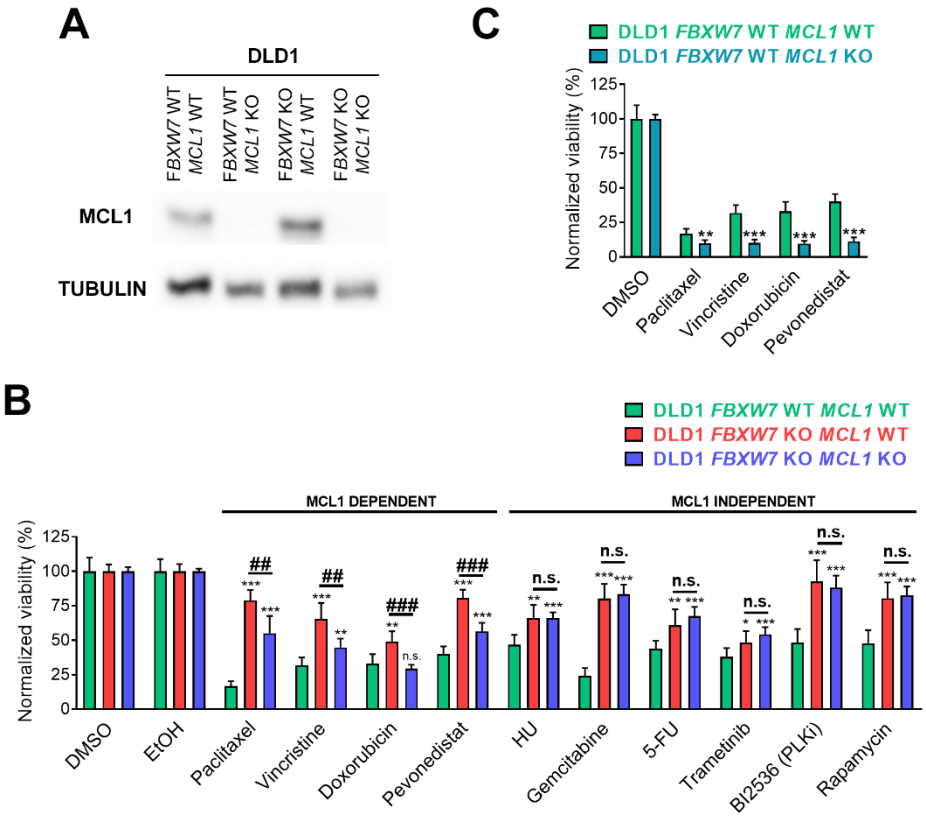

Figure 19: *MCL1* deletion overcomes the resistance of *FBXW7* KO cells to some, but not all, compounds. (**A**) Western Blot illustrating the KO of *MCL1* in DLD1 *FBXW7* WT and KO cells generated using CRISPR-Cas9. TUBULIN levels are shown as a loading control. (**B**) Normalized viability of DLD1 WT (in green), DLD1 *FBXW7* KO (in red) and DLD1 *FBXW7 MCL1* KO (in blue) cells upon different drug treatments: DMSO (control), EtOH (control for rapamycin), paclitaxel (40nM), vincristine (10nM), doxorubicin (25nM), hydroxyurea (HU, 75μM), gemcitabine (10nM), Fluorouracil (5-FU, 10μM), trametinib (5μM), BI2536 (PLK1i, 10nM), pevonedistat (200nM) and rapamycin (10μM). DAPI staining was performed to count nuclei by high-throughput microscopy. Error bars indicate SD (n=3, three independent experiments, with two technical replicates per experiment). The experiment was performed in another DLD1 *FBXW7 MCL1* KO clone with similar results. T-test comparisons for each drug versus DLD1 WT: n.s. p>0.05, *p<0.05, **p<0.01, ***p<0.001. T-test comparisons for each drug of DLD1 *FBXW7* KO and DLD1 *FBXW7 MCL1* KOs: n.s. p>0.05, #p<0.05, ##p<0.01, ###p<0.001. (**C**) Normalized viability of DLD1 WT (in green) and DLD1 *MCL1* KO (in blue) cells upon different drug treatments: DMSO (control), paclitaxel (40nM), vincristine (10nM), doxorubicin (25nM) and pevonedistat (200nM). DAPI staining was performed to count nuclei by high-throughput microscopy. Error bars indicate SD (n=3, three independent experiments, with two technical replicates per experiment). The experiment was performed in another DLD1 *MCL1* KO clone with similar results. n.s. p>0.05, *p<0.05, **p<0.01, ***p<0.001 (t-test).

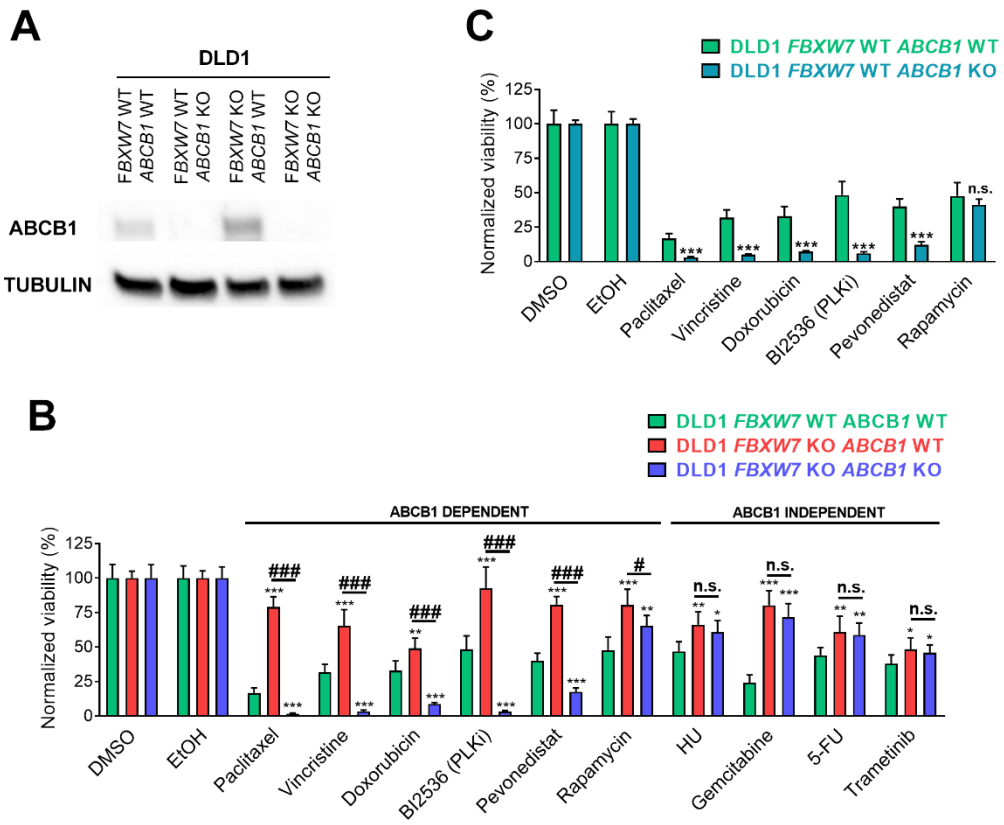

Figure 20: *ABCB1* deletion overcomes the resistance of *FBXW7* KO cells to some, but not all, compounds. (**A**) Western Blot illustrating the KO of *ABCB1* in DLD1 *FBXW7* WT and KO cells generated using CRISPR-Cas9. TUBULIN levels are shown as a loading control. (**B**) Normalized viability of DLD1 WT (in green), DLD1 *FBXW7* KO (in red) and DLD1 *FBXW7 ABCB1* KO (in blue) cells upon different drug treatments: DMSO (control), EtOH (control for rapamycin), paclitaxel (40nM), vincristine (10nM), doxorubicin (25nM), hydroxyurea (HU, 75µM), gemcitabine (10nM), Fluorouracil (5-FU, 10µM), trametinib (5µM), BI2536 (PLK1i, 10nM), pevonedistat (200nM) and rapamycin (10µM). DAPI staining was performed to count nuclei by high-throughput microscopy. Error bars indicate SD (n=3, three independent experiments, with two technical replicates per experiment). The experiment was performed in another DLD1 *FBXW7 ABCB1* KO clone with similar results. T-test comparisons for each drug versus DLD1 WT: n.s. p>0.05, *p<0.05, **p<0.01, ***p<0.001. T-test comparisons for each drug of DLD1 *FBXW7* KO and DLD1 *FBXW7 ABCB1* KOs: n.s. p>0.05, #p<0.05, ##p<0.01, ###p<0.001. (**C**) Normalized viability of DLD1 WT (in green) and DLD1 *ABCB1* KO (in blue) cells upon different drug treatments: DMSO (control), EtOH (control for rapamycin), paclitaxel (40nM), vincristine (10nM), doxorubicin (25nM), BI2536 (PLK1i, 10nM), pevonedistat (200nM) and rapamycin (10µM). DAPI staining was performed to count nuclei by high-throughput microscopy. Error bars indicate SD (n=3, three independent experiments, with two technical replicates per experiment). n.s. p>0.05, *p<0.05, **p<0.01, ***p<0.001 (t-test).

Given that **neither MCL1 or ABCB1 dysregulation can explain the MDR** phenotype of FBXW7-deficient cells, we next decided to investigate into more general potential phenotypes that could explain this phenomenon and, hopefully, to offer additional opportunities for selectively targeting FBXW7-deficient cells.

3. PROTEOMIC APPROACHES IDENTIFIED MITOCHONDRIAL TRANSLATION AND OTHER MITOCHONDRIAL PROCESSES AS A VULNERABILITY FOR FBXW7-DEFICIENT CELLS

3.1. Proteomic comparison between *FBXW7*-mutated and WT cells revealed an upregulation of mitochondrial processes in FBXW7-deficient cells

In order to have an overview of the **pathways that are dysregulated** in FBXW7-deficient cells, we performed proteomic comparisons between *FBXW7* WT and KO DLD1 and mESCs.

First, we had a general overview of the proteomic analysis of DLD1 cells, which showed significant differences in 731 and 371 proteins that were down or upregulated, respectively (**Figure 21A**, **Annex Table 9**). As expected, we observed multiple known **substrates of FBXW7** to be upregulated in *FBXW7* KO DLD1 cells including DAB2IP, CCNE1, MYC, TGIF1, KLF13, KLF10, KLF5, or MED13 (**Figure 21B**, **Annex Table 9**, **Annex Table 3**).

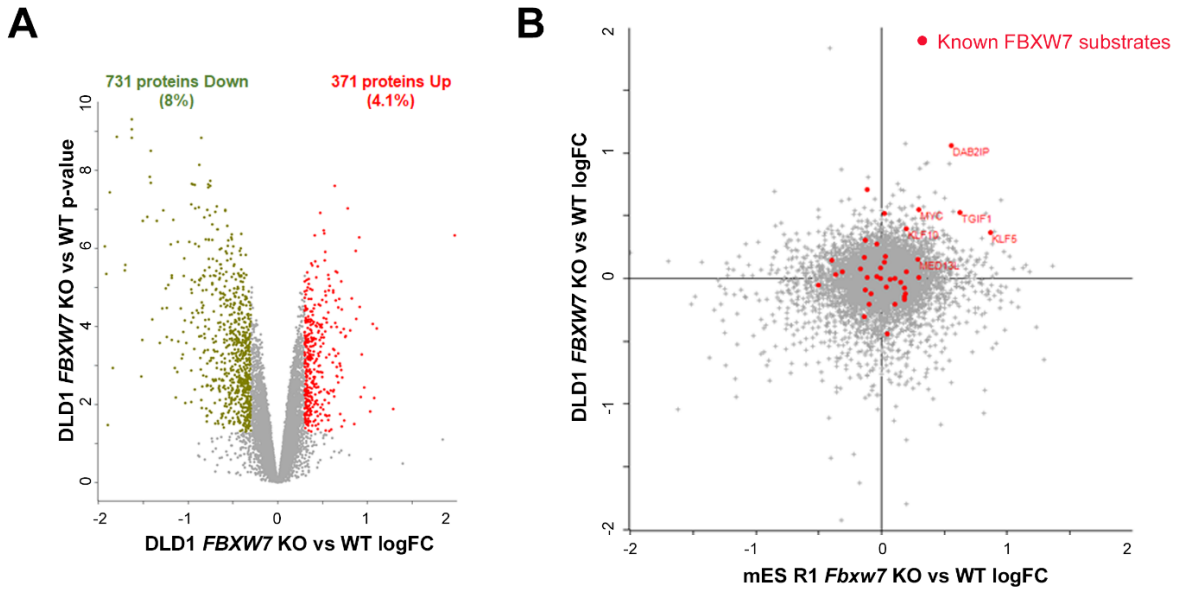

Figure 21: A proteomic comparison between *FBXW7* KO and WT cells revealed an upregulation of known FBXW7 substrates. (**A**) Vulcano plot representing the number in proteins downregulated (731, 8%, in green) and upregulated (371, 4.1%, in red) in DLD1 *FBXW7* KO versus WT cells. A protein was considered downregulated or upregulated if p-value<0.05 (FDR<5%) and log_2FC>0.3 or <-0.3. (**B**) Representation of the log_2FC values of the proteomic comparisons between *Fbxw7*/*FBXW7* KO and WT mES R1 and DLD1 cells. Known FBXW7 substrates are marked in red.

A

GSEA TOP ENRICHED PROCESSES in DLD1 *FBXW7* KO

GO TERM	NES	FDR q-val
Mitochondrial translation	2,98	0
Mitochondrial respiratory chain complex assembly	2,95	0
Mitochondrial gene expression	2,93	0
Mitochondrial translation termination	2,77	0
Translational termination	2,76	0
NADH dehydrogenase complex assembly	2,76	0
Oxidative phosphorylation	2,74	0
Cellular respiration	2,68	0
ATP synthesis coupled electron transport	2,65	0
Translational elongation	2,62	0
Respiratory electron transport chain	2,59	0
Aerobic respiration	2,45	0
Mitochondrial electron trans. NADH to ubiquinone	2,28	0

B

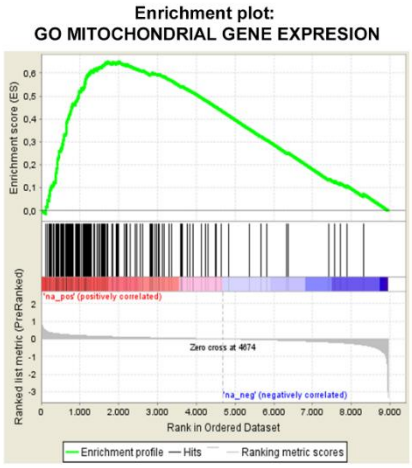

C

GSEA TOP ENRICHED PROCESSES in mES R1 *Fbxw7* KO

REACTOME TERM	NES	FDR q-val
Respiratory electron transport	2,43	0
Respiratory electron transport – ATP synthesis	2,32	0
TCA cycle and respiratory electron transport	2,03	0,006
HALLMARK TERM	**NES**	**FDR q-val**
Oxidative phosphorylation	1,79	0,02

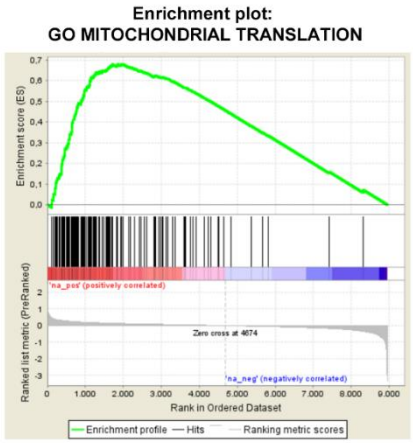

D

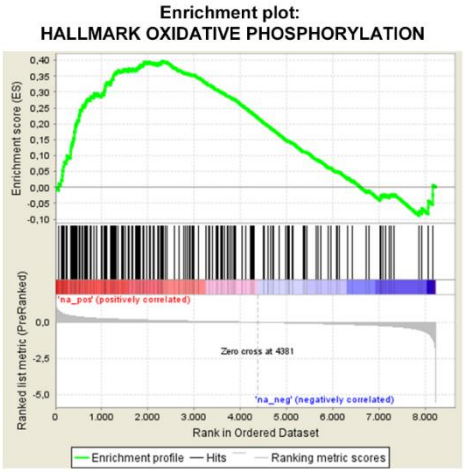

E

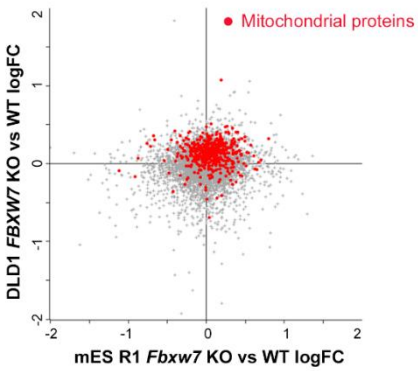

Figure 22: A proteomic comparison between *FBXW7* KO and WT cells revealed an upregulation mitochondrial processes. (**A**) GSEA top enriched processes in DLD1 *FBXW7* KO cells. Gene ontology (GO) terms; normalized enrichment score (NES); and False discovery rate (FDR) q-value are shown. Mitochondrial specific processes are highlighted in yellow, mitochondrial and cytosolic processes in green. Analysis performed using the data coming from the proteomic comparison between DLD1 *FBXW7* KO and DLD1 WT cells. (**B**) Enrichment plots of the gene ontology terms mitochondrial gene expression and mitochondrial translation from (A). (**C**) GSEA top enriched processes in mESCs R1 *Fbxw7* KO cells. Reactome and Hallmark terms; normalized enrichment score (NES); and False discovery rate (FDR) q-value are shown. Mitochondrial specific processes are highlighted in yellow. Analysis performed using the data coming from the proteomic comparison between mESCs R1 *Fbxw7* KO and mES R1 WT cells. (**D**) Enrichment plot of the Hallmark term oxidative phosphorylation from (C). (**E**) Representation of the log_2FC values of the proteomic comparisons between *Fbxw7/FBXW7* KO and WT mESCs R1 and DLD1 cells. Mitochondrial proteins are marked in red.

Nevertheless, and besides effects in specific genes, we were more interested in performing more **general pathway analyses of the proteomics** comparisons. Interestingly, Gene Set Enrichment Analysis (GSEA) analysis of the data revealed that most of the pathways enriched in DLD1 *FBXW7* KO cells were related to mitochondria processes, such as mitochondrial translation and gene expression, or the assembly of respiratory complexes, among others (**Figure 22A-B**). Similarly, *Fbxw7* KO mESC were also found to be enriched in mitochondrial processes, such as oxidative phosphorylation or respiratory electron chain (**Figure 22C-D**). Of note, the enrichment for mitochondrial processes in mESC was not as dramatic as in DLD1 cells, where almost all mitochondrial proteins were found to be upregulated in *FBXW7* KO cells (**Figure 22E**).

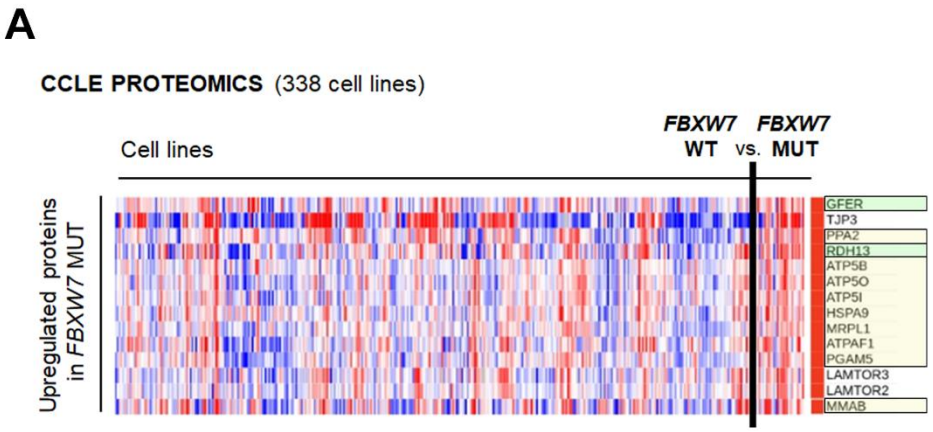

Figure 23: A proteomic comparison between *FBXW7*-mutant and WT cells across CCLE 338 cancer cell lines revealed an upregulation of mitochondrial proteins. (**A**) Differential expression analysis between *FBXW7*-mutated and WT cancer cell lines from the Cancer Cell Line Encyclopaedia (CCLE, 338 cell lines). Upregulated proteins in *FBXW7* mutated cell lines are displayed. Mitochondrial specific proteins are highlighted in yellow, proteins with both mitochondrial and cytosolic localisation, in green. Cell lines were ordered by mutational status and also for lineage.

To perform a more comprehensive analysis of the potential proteomic alterations that might exist in FBXW7-deficient tumours we next performed a **meta-analysis of proteomic data** from the Cancer Cell Line Encyclopaedia (CCLE), which contains proteomic data from 338 cancer cell lines (Nusinow et al., 2020). Differential expression analysis between *FBXW7*-mutant and WT cell lines revealed that most of the upregulated proteins in mutant cells were related to energetic metabolism and mitochondrial protein import (**Figure 23A**). Among the upregulated proteins we found ATP5I, ATP5O and ATPAF1 (**Figure 23A**), part of the mitochondrial complex V, and which were also upregulated in our proteomics, as well as MRPL1. In conclusion, all of our proteomic analyses converge in identifying an upregulation of mitochondrial processes as a common feature of *FBXW7*-mutant cells.

3.2. Mitochondrial translation and other mitochondrial processes are upregulated in FBXW7-deficient cells

Next, we aimed to **validate the upregulation of mitochondrial translation proteins** seen in the proteomic analyses. Western blot analysis revealed that DLD1 *FBXW7* KO cells presented higher levels of POLMRT, the mitochondrial RNA polymerase, and MRPL12, a mitochondrial ribosomal protein, compared to their WT counterparts (**Figure 24A**). Similar results were obtained for OXPHOS complexes, particularly for complex II and IV (**Figure 24B**).

We then questioned if the upregulation on mitochondrial proteins was due to an increment on the **mitochondrial mass**. The most usual way to quantify mitochondrial mass is to stain cells with mitochondrial dyes such as Mitotrackers. Unfortunately, cells overexpressing ABCB1 are known to expulse mitochondrial dyes (Marques-Santos et al., 2003), and since ABCB1 is upregulated in *FBXW7* KO cells, we switched to a different methodology. qPCR measurement of mtDNA-encoded genes revealed similar amounts between *FBXW7* WT and KO cells (**Figure 25A**). Additionally, the use of a stable marker of mitochondria as the citrate synthetase, revealed similar amount of this protein by

Western Blot analyses (**Figure 25B**). Immunostainings of mitochondria with the same antibody revealed a slight reduction in the number of mitochondria in DLD1 FBXW7-deficient cells (**Figure 25C**). In contrast, *FBXW7* loss was associated with an increase of the mitochondrial volume, which was due to a higher frequency of mitochondrial fusion events (**Figure 25D-E**).

Among the factors that may be involved in the increase of mitochondrial activity of tumours cells, **C-MYC overexpression** has emerged as one of the main regulators (Morrish and Hockenbery, 2014). The transcription factor C-MYC stimulates nuclearly encoded mitochondrial genes and mitochondrial biogenesis (Li et al., 2005), triggering the activation of a general mitochondrial programme in the cell. Noteworthy, C-MYC was one of the main upregulated proteins in both of our proteomic analyses of FBXW7-deficient mESC and DLD1 cells, consistent which its description as a FBXW7 target (Welcker et al., 2004b, Yada et al., 2004) (**Figure 21B**, **Annex Table 3**). Western Blot analyses validated the observation that C-MYC was overexpressed in DLD1 FBXW7-deficient cells (**Figure 26A**). Moreover, C-MYC downregulation with siRNAs in *FBXW7* KO DLD1 cells (**Figure 26B**), led to the downregulation of several mitochondrial translation factors that were overexpressed in *FBXW7* KO cells (POLRMT, TUFM elongation factor, and MRPL12) (**Figure 26C**).

Together, these results indicate that FBXW7-deficient cells present a general increase in mitochondrial translation, which is due to a large extent dependent on the accumulation of C-MYC.

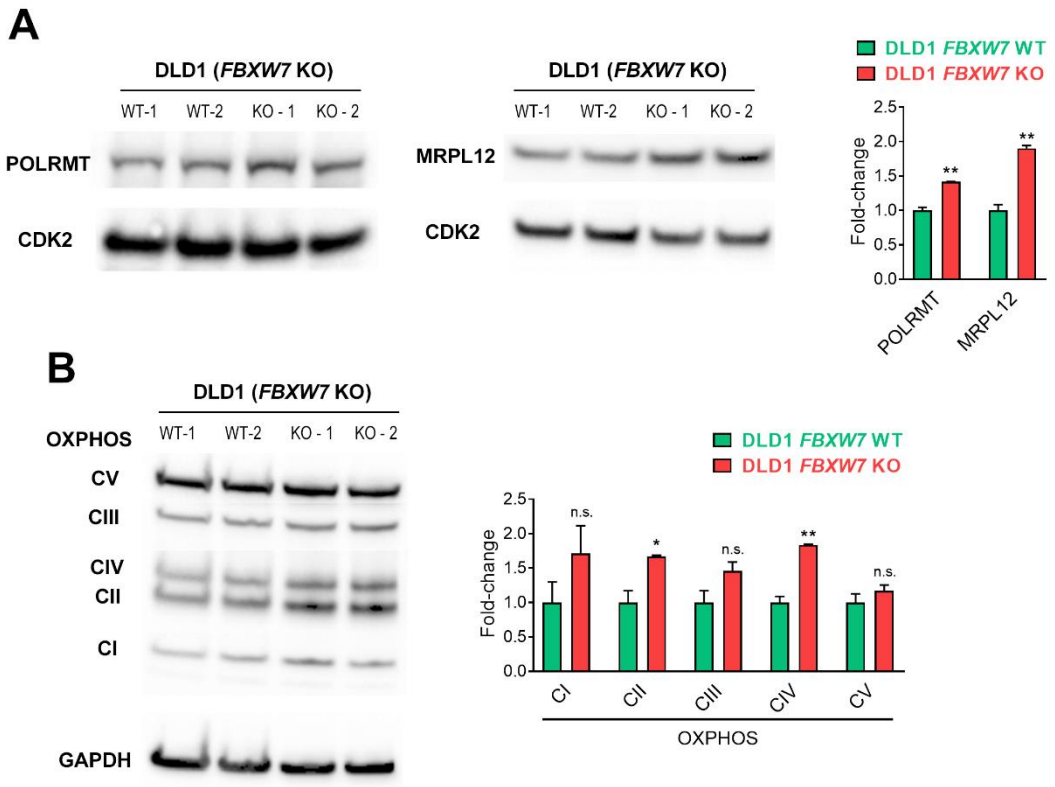

Figure 24: *FBXW7*-deleted cells present an upregulation of mitochondrial translation and OXPHOS complexes proteins. (**A,B**) Western Blot showing (A) POLRMT and MRPL12 protein levels, and (B) OXPHOS complexes protein levels in DLD1 WT and *FBXW7* KO cells and its quantification. CDK2 and GAPDH levels are shown as loading controls. Error bars indicate SD (n=2, two biological replicates). n.s. p>0.05, *p<0.05, **p<0.01, ***p<0.001 (t-test).

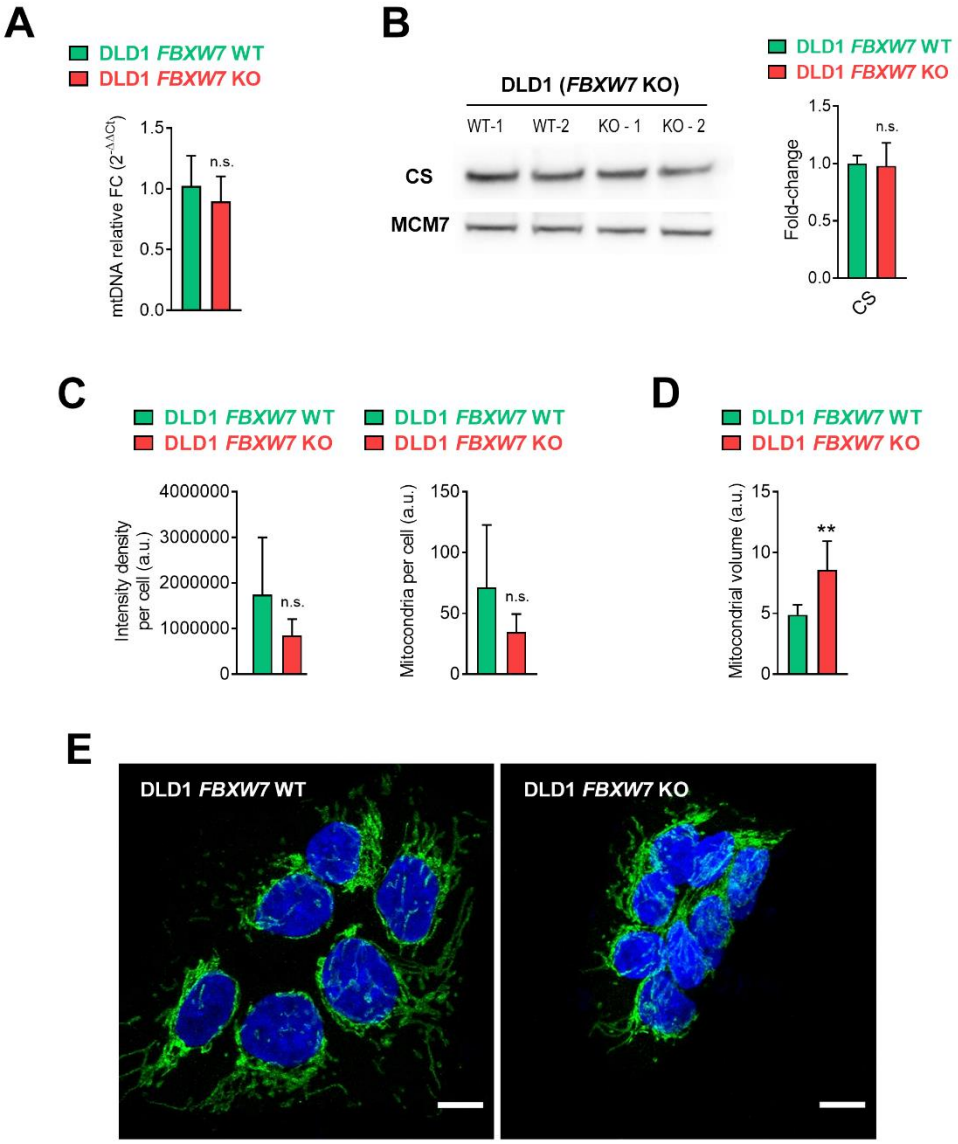

Figure 25: Mitochondrial mass is independent of *FBXW7* status, but *FBXW7*-deleted cells present more fusion events. (**A**) Mitochondrial DNA relative fold-change in DLD1 WT and *FBXW7* KO cells. *ND1* mitochondrial-expressed gene levels were measured by qPCR, and were normalized against the levels of *GAPDH* nuclearly-encoded gene (2^-ΔΔCt (FC)). Error bars indicate SD (n=3, three independent experiments, with three technical replicates per experiment). n.s. p>0.05, *p<0.05, **p<0.01, ***p<0.001 (t-test). (**B**) Western Blot showing CS protein levels in DLD1 WT and *FBXW7* KO cells and its quantification. MCM7 levels are shown as a loading control. Error bars indicate SD (n=2, two biological replicates). n.s. p>0.05, *p<0.05, **p<0.01, ***p<0.001 (t-test). (**C**) Intensity density and mitochondrial mass per cell in DLD1 WT and *FBXW7* KO cells. DAPI staining was performed to count nuclei, and CS to mark and quantify mitochondrial features by confocal microscopy. Error bars indicate SD (six technical replicates). n.s. p>0.05, *p<0.05, **p<0.01, ***p<0.001 (t-test). Arbitrary units (a.u.) (**D**) Mitochondrial volume in DLD1 WT and DLD1 *FBXW7* KO cells. DAPI staining was performed to count nuclei, and CS to mark and quantify mitochondrial features by confocal microscopy. Error bars indicate SD (six technical replicates). n.s. p>0.05, *p<0.05, **p<0.01, ***p<0.001 (t-test). Arbitrary units (a.u.). (**E**) Representative images from (C) and (D), DLD1 WT and DLD1 *FBXW7* KO cells. DAPI staining was performed to count nuclei, and CS to mark and quantify mitochondrial features by confocal microscopy. Scale bar = 10μm.

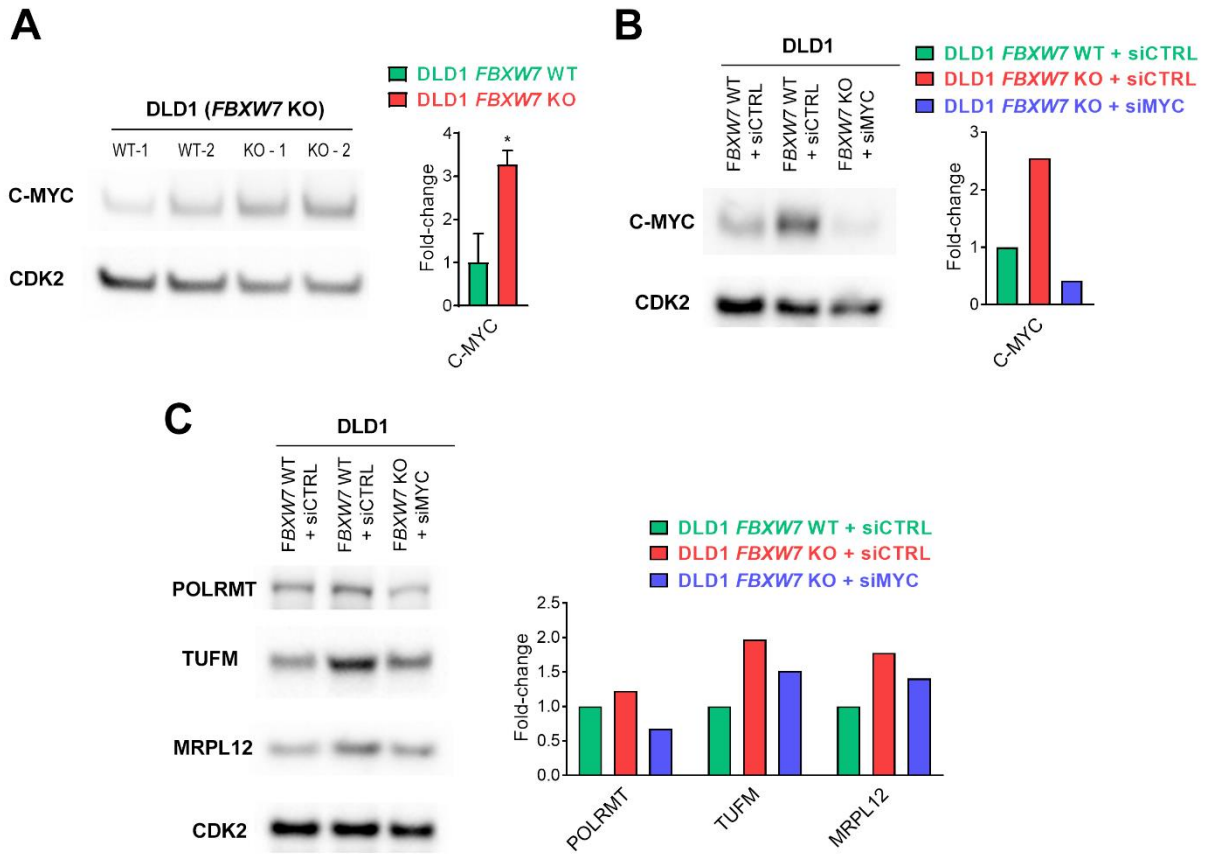

Figure 26: C-MYC overexpression is involved in the upregulation of mitochondrial translation in *FBXW7* KO cells. (**A**) Western Blot showing C-MYC protein levels in DLD1 WT and *FBXW7* KO cells and its quantification. CDK2 levels are shown as a loading control. Error bars indicate SD (n=2, two biological replicates). n.s. p>0.05, *p<0.05, **p<0.01, ***p<0.001 (t-test). (**B**) Western Blot showing C-MYC protein levels in DLD1 WT, *FBXW7* KO and *FBXW7* KO + siMYC cells, and its quantification. CDK2 levels are shown as a loading control. (**C**) Western Blot showing POLRMT, TUFM, and MRPL12 protein levels in DLD1 WT, *FBXW7* KO and *FBXW7* KO + siMYC cells and its quantification. CDK2 levels are shown as a loading control.

3.3. Targeting mitochondrial activity is selectively toxic for FBXW7-deficient cells

3.3.1. Genetic and pharmacological inhibition of mitochondrial activity

The **mitochondrial ribosome** has emerged as a promising vulnerability in C-MYC-overexpressing tumours (D'Andrea et al., 2016, Oran et al., 2016, Ravà et al., 2018). Given the role of C-MYC overexpression and its associated increase in mitochondrial translation in *FBXW7*-deficient cells (**Figure 26**), we reasoned that, similarly to what is seen in MYC-overexpressing tumours, FBXW7-deficient tumours may also be sensitive to mitochondrial translation inhibition. In this regard, antibiotics that interfere with bacterial protein synthesis have the potential to inhibit mitochondrial translation due to conserved evolutionary similarities between bacterial and mitochondrial ribosomes. Consistently, previous work from several groups has opened the window to **repurpose certain antibiotic families** targeting the bacterial ribosomes such as tetracyclines, glycylcyclines, oxazolidinones and chloramphenicol for cancer therapy (D'Andrea et al., 2016, Oran et al., 2016, Ravà et al., 2018, Sheth et al., 2014, Jia et al., 2016, Lamb et al., 2015, Sharon et al., 2019, Skrtic et al., 2011).

In this context, we decided to evaluate the **sensitivity of FBXW7-deficient cells to several antibiotics** including two tetracyclines (doxycycline and minocycline), chloramphenicol, one oxazolidinone (tedizolid), and one glycylcycline (tigecycline). Among the different antibiotics tested to abrogate mitochondrial translation, the use of the glycylglycine antibiotic tigecycline proved to be the most efficient, as other authors had also previously reported (D'Andrea et al., 2016, Skrtic et al., 2011). Flow cytometry analysis of cell mixtures of DLD1 WT^{eGFP} and *FBXW7*-KO^{Ruby3} mixed at 1:3 ratios showed a significant decrease of the *FBXW7*-KO^{Ruby3} cell percentage after 72 hours of tigecycline

treatment, even at low doses (**Figure 27A-B**). A milder, but significant, decrease in the population of FBXW7-deficient cells was also observed with the other antibiotics (**Figure 27A-B**), an effect that became significant at high doses and longer times for chloramphenicol and tedizolid (**Figure 27C**). An independent evaluation of the effect of the antibiotics on FBXW7-deficient cells made by quantifying nuclei counts by high-content microscopy yielded similar results. Once again, tigecycline showed to have a dose-dependent selective toxicity for DLD1 *FBXW7* KO cells (**Figure 27D**). Furthermore, tigecycline was also preferentially toxic for FBXW7-deficient cells in clonogenic survival assays (**Figure 27E**).

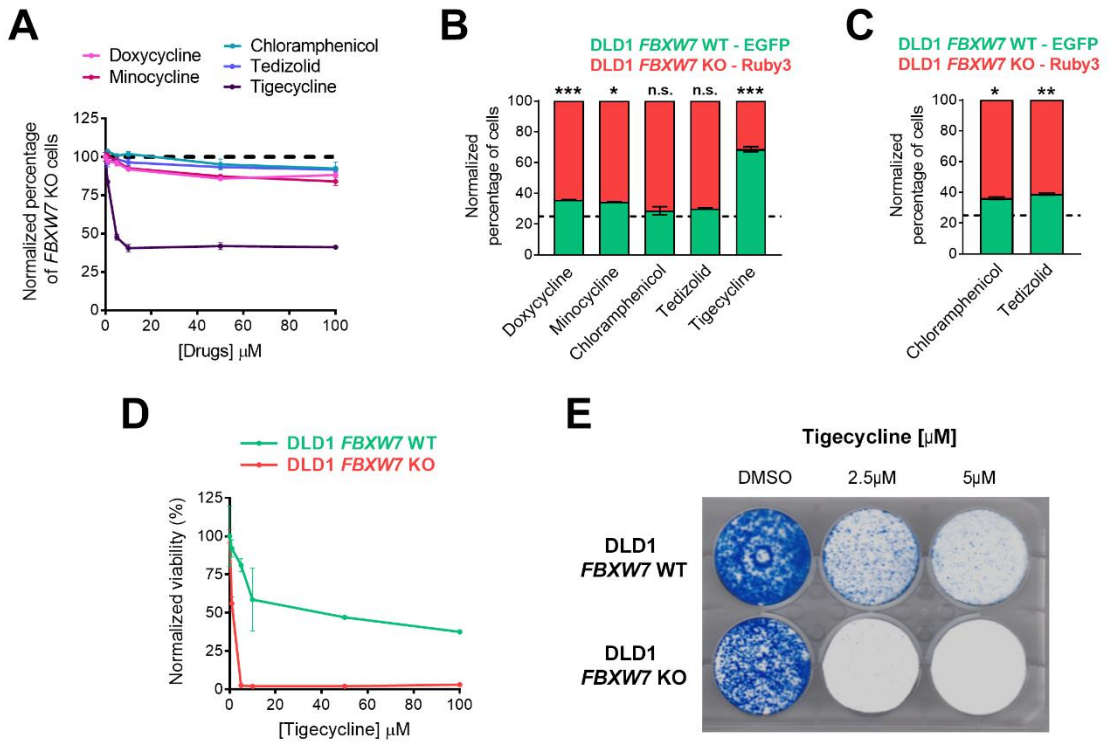

Figure 27: Interference of mitochondrial translation with tigecycline and other compounds is selectively lethal in *FBXW7*-deleted cells. (**A**) Normalized cell percentages of Ruby3+ DLD1 *FBXW7* KO cells after 72h treatment with different doses of doxycycline, minocycline, chloramphenicol, tedizolid and tigecycline. Each compound percentages were normalized to its control: water (doxycycline, minocycline), ethanol (chloramphenicol) and DMSO (tedizolid and tigecycline). Control is represented as a dotted line, equal for all compounds after the normalization. The culture started with 1:3 ratios of WT^{eGFP} and *FBXW7*-KO^{Ruby3} respectively. The experiment was repeated three times and in another DLD1 *FBXW7* KO clone, and a representative example is shown. Error bars indicate SD (two technical replicates). (**B**) Normalized cell percentages of eGFP+ DLD1 WT cells and Ruby3+ DLD1 *FBXW7* KO cells from (A) treated with 50µM of each compound. Error bars indicate SD (two technical replicates). n.s. $p>0.05$, *$p<0.05$, **$p<0.01$, ***$p<0.001$ (t-test). (**C**) Normalized cell percentages of eGFP+ DLD1 WT cells and Ruby3+ DLD1 *FBXW7* KO cells after treatment for 7 days with chloramphenicol (500µM) and tedizolid (25µM). Each compound percentages were normalized to its control: ethanol (chloramphenicol) and DMSO (tedizolid). Control is represented as dotted line equal for all compounds after the normalization. The culture started with 1:3 ratios of WT^{eGFP} and *FBXW7*-KO^{Ruby3} respectively. The experiment was repeated two times, and a representative example is shown. Error bars indicate SD (two technical replicates). n.s. $p>0.05$, *$p<0.05$, **$p<0.01$, ***$p<0.001$ (t-test). (**D**) Normalized viability of DLD1 WT (in green) and DLD1 *FBXW7* KO cells (in red) upon different doses of tigecycline. DAPI staining was performed to count nuclei by high-throughput microscopy. The experiment was repeated three times and in another DLD1 *FBXW7* KO clone, and a representative example is shown. Error bars indicate SD (two technical replicates). (**E**) Clonogenic assay of DLD1 *FBXW7* WT cells (above) and DLD1 *FBXW7* KO cells (below) treated with different doses of tigecycline or a DMSO control. Experiment was performed in triplicate, and a representative example is shown.

Next, we validated the **effect of tigecycline in two additional cell lines**: cervical cancer HeLa cells and ovarian cancer A2780 cells (**Figure 28A**). In all cases, FBXW7-deficient cells presented a marked sensitivity to tigecycline when compared to their WT counterparts (**Figure 28B**), indicating that this phenomenon could be extensive for multiple cancer cell types.

Finally, we determined whether we could reproduce our above findings by a **genetic perturbation of mitochondrial translation and other mitochondrial processes**. To this end, we performed, once again, competition experiments mixing WT^{eGFP} and *FBXW7*-KO^{Ruby3} DLD1 cells at a ratio of around 1:3. Cell mixes where then transfected with esiRNAs targeting the mitochondrial transcription polymerase (POLRMT), an elongation factor (TUFM), an essential translation factor (PTCD3), a mitoribosomal protein (MRPS27), and an OXPHOS protein (UQCRC1). Population percentages were subsequently analysed by FACS at days 3 and 7 of the experiment, transfecting again the esiRNAs on day 3 to maintain the downregulation at longer time points. In general, the downregulation of mitochondrial proteins supposed a significant reduction in the percentage of *FBXW7*-KO^{Ruby3} cells (**Figure 28C**). Besides this genetic approach, we also confirmed that inhibition of mitochondrial electron chain activity by two different complex inhibitors (IACS-10759 complex I inhibitor and oligomycin complex V inhibitor) was preferentially lethal for *FBXW7* KO cells (**Figure 28D**).

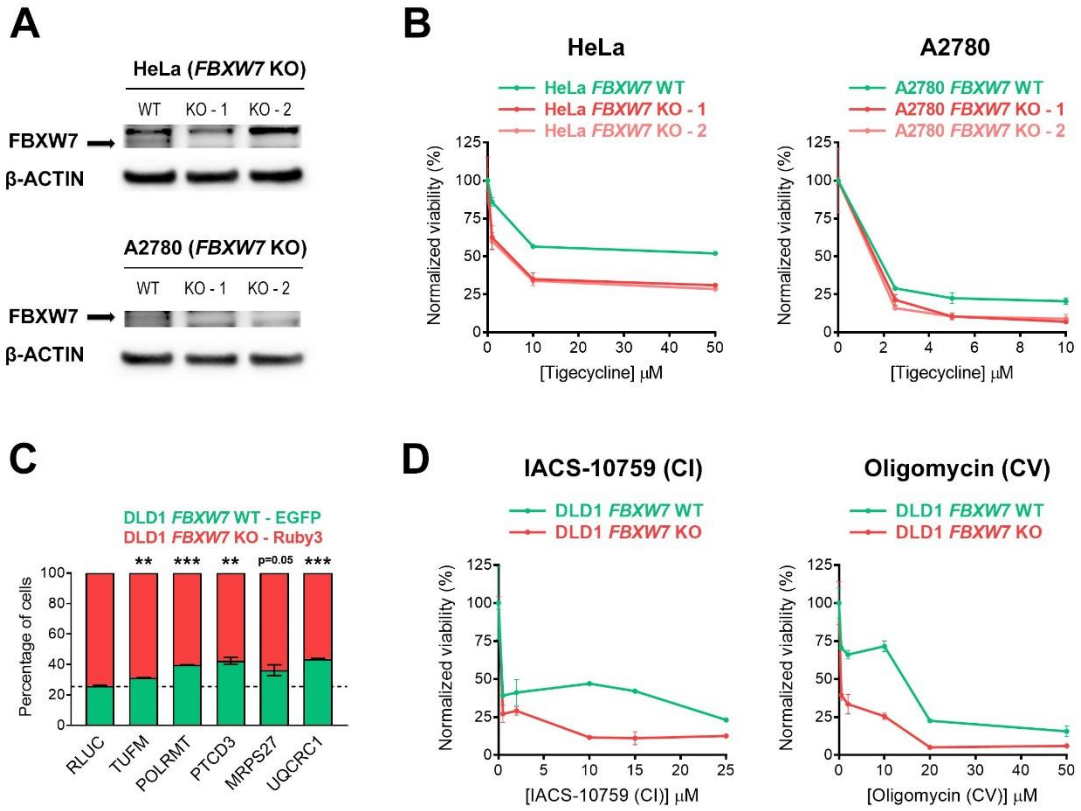

Figure 28: Interference of mitochondrial translation with tigecycline in other cellular models, and of other mitochondrial processes by genetic or pharmacological approaches, is selectively lethal in *FBXW7*-deleted cells. (**A**) Western Blot illustrating the KO of *FBXW7* in HeLa and A2780 cells generated using CRISPR-Cas9. ß-ACTIN levels are shown as a loading control. (**B**) Normalized viability of WT (in green) and *FBXW7* KO clones (in red) upon different doses of tigecycline in HeLa and A2780 human cancer cell lines. DAPI staining was performed to count nuclei by high-throughput microscopy. The experiment was repeated three times, and a representative example is shown. Error bars indicate SD (two technical replicates). (**C**) Cell percentages of eGFP+ DLD1 WT cells and Ruby3+ DLD1 *FBXW7* KO cells after transfecting twice (at day 0 and day 3) with a esiRNA library of mitochondrial related genes and the RLUC control. Analysis was performed at day 3 and 7 by flow cytometry, here represented day 7 data. The culture started with 1:3 ratios of WT^{eGFP} and *FBXW7*-KO^{Ruby3} respectively. The experiment was repeated three times and a representative example is shown. Error bars indicate SD (two technical replicates). n.s. $p>0.05$, *$p<0.05$, **$p<0.01$, ***$p<0.001$ (t-test). (**D**) Normalized viability of DLD1 WT (in green) and DLD1 *FBXW7* KO (in red) upon IACS-10759 and oligomycin mitochondrial electron chain inhibitors treatment. DAPI staining was performed to count nuclei by high-throughput microscopy. The experiment was repeated three times and in another DLD1 *FBXW7* KO clone, and a representative example is shown. Error bars indicate SD (two technical replicates).

3.3.2. Mechanism of action of the sensitivity to mitochondrial poisons: MYC and the ISR

Following our previous results, we next explored if the effect of tigecycline on FBXW7-deficient cells was **dependent on C-MYC overexpression**. Indeed, cell viability assays showed that C-MYC downregulation (**Figure 26B**) was able to partially rescue the differential sensitivity to tigecycline-induced cell death of *FBXW7* KO cells (**Figure 29A**).

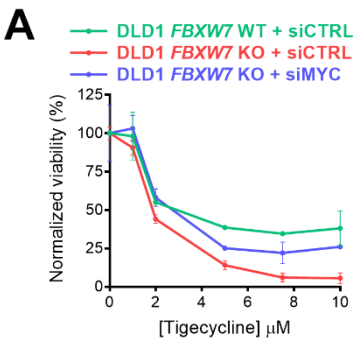

Figure 29: C-MYC is involved in the sensitivity of *FBXW7*-deficient cells to tigecycline. (**A**) Normalized viability of DLD1 WT cells with siCTRL (in green), DLD1 *FBXW7* KO with siCTRL cells (in red) and DLD1 *FBXW7* KO cells downregulated for C-MYC using siRNAs (in blue) upon tigecycline treatment. DAPI staining was performed to count nuclei by high-throughput microscopy. The experiment was repeated three times and in another DLD1 *FBXW7* KO clone, and a representative example is shown. Error bars indicate SD (two technical replicates).

The mechanisms by which this antibiotic present antitumoural properties remain uncharacterised. As tedizolid was recently shown to activate the ISR (Sharon et al., 2019), we speculated whether that was also the case for tigecycline. To test this possibility, we **evaluated the activation of the ISR** by high-content microscopy through quantifying the nuclear translocation of ATF4. Interestingly, we noticed that *FBXW7* KO cells presented a basal activation of the ISR, which might contribute to the further ISR activation that is observed in these cells upon tigecycline treatment (**Figure 30A-B**). Moreover, the translocation of ATF4 induced by tigecycline could be reversed by an inhibitor of the ISR, ISRIB (Sidrauski et al., 2013, Sidrauski et al., 2015) (**Figure 30A-B**). Importantly, ISRIB rescued the toxicity of tigecycline in both WT and *FBXW7* KO cells (**Figure 30C-D**), implying that the ISR plays a determinant role in the cytotoxic effects of this antibiotic in cancer cells.

Collectively, these results support that **targeting mitochondrial translation through the use of tigecycline** or other genetic and pharmacological approaches is an effective way to preferentially eliminate FBXW7-deficient cancer cells, in a C-MYC- and ISR-dependent manner.

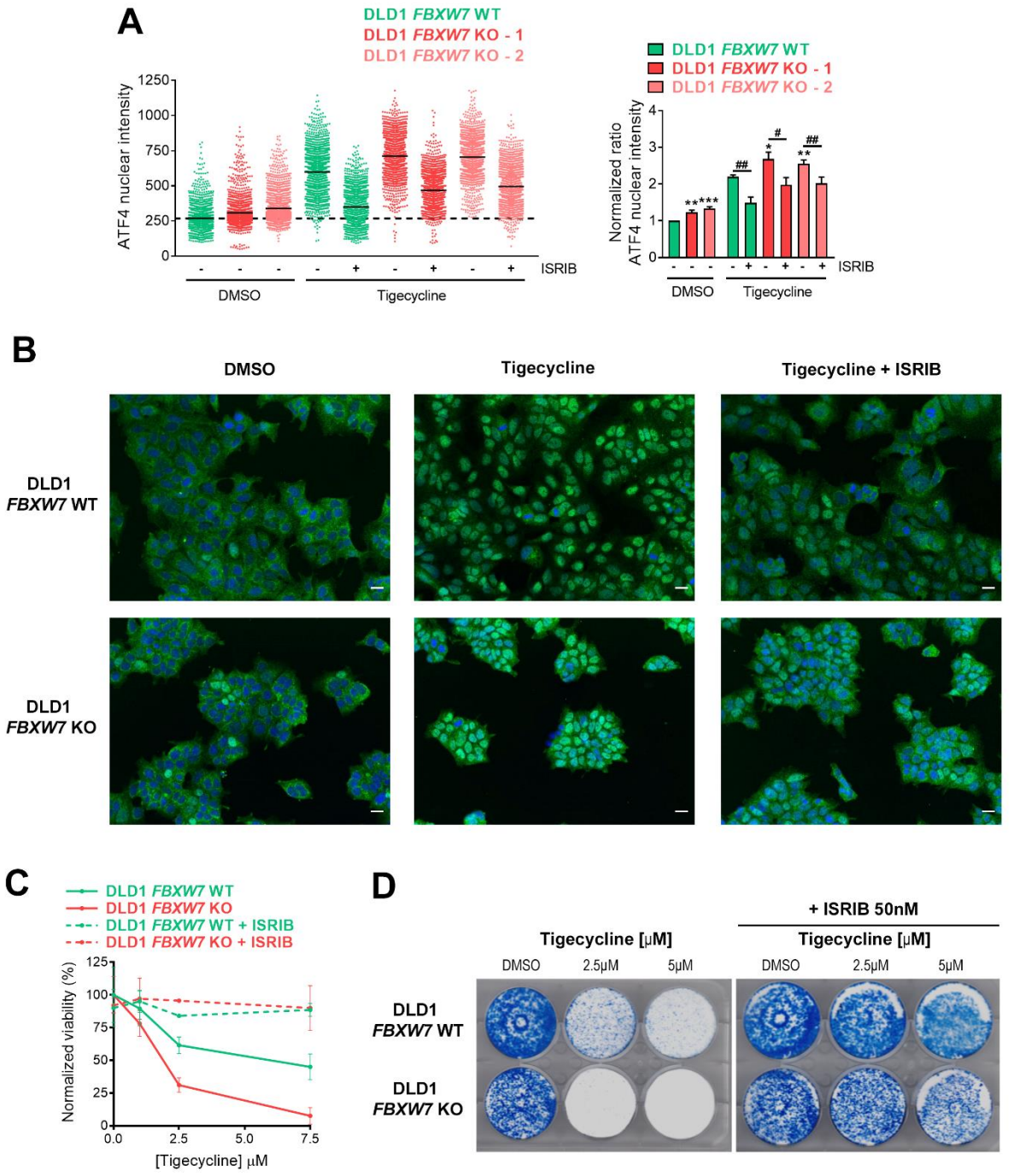

Figure 30: Activation of the integrated stress response (ISR) is involved in the mechanism of action of tigecycline. (**A**) Nuclear ATF4 intensity measured by high-throughput microscopy in DLD1 WT (in green) and DLD1 *FBXW7* KO clones (in red) upon DMSO or tigecycline (10µM) treatment with or without an ISR inhibitor (ISRIB, 50nM). The experiment was repeated three times and a representative example is shown (left). The average of the three experiments was represented (right), with error bars indicating their SD. T-test comparisons between DLD1 WT and DLD1 *FBXW7* KO clones: n.s. p>0.05, *p<0.05, **p<0.01, ***p<0.001. T-test comparisons for each cell type to calculate the effect of ISRIB treatment: n.s. p>0.05, #p<0.05, ##p<0.01, ###p<0.001. T-test comparisons between with or without tigecycline for each cell type were significant with ***p<0.001. (**B**) Representative images from (A). *FBXW7* WT and KO treated with DMSO, or tigecycline (10µM) treatment with or without an ISR inhibitor (ISRIB, 50nM). Scale bar = 20µm. (**C**) Normalized viability of DLD1 WT (in green) and DLD1 *FBXW7* KO (in red) upon tigecycline treatment, with (dotted lines) or without ISRIB (50nM). DAPI staining was performed to count nuclei by high-throughput microscopy. The experiment was repeated three times and in another DLD1 *FBXW7* KO clone, and a representative example is shown. Error bars indicate SD (two technical replicates). (**D**) Clonogenic assay of DLD1 *FBXW7* WT cells (above) and DLD1 *FBXW7* KO cells (below) treated with different doses of tigecycline or a DMSO control, and then of DMSO or 50nM ISRIB. Experiment was performed in triplicate, and a representative example is shown.

3.4. Efficacy of tigecycline in preclinical models of FBXW7-deficient tumours

To address the **significance of our results in an *in vivo* setting**, we tested the efficacy of tigecycline to selectively kill *FBXW7* KO DLD1 xenografts. For this, $5{\cdot}10^6$ DLD1 *FBXW7* KO and WT cells were injected in the flanks of nude/SCID mice (**Figure 31A**). 6 days after, mice were randomized into three groups per genotype (six groups in total, 10 mice per group) and we started treating them intraperitoneally (i.p) with vehicle, 1,5mg/kg paclitaxel or 50mg/kg of tigecycline three times per week (**Figure 31A**). Consistent with the role of *FBXW7* as a tumour suppressor, *FBXW7* KO tumours grew significantly faster than WT DLD1 tumours (**Figure 31B-D**). Moreover, *FBXW7* KO failed to respond to paclitaxel treatment, supporting that FBXW7 deficiency confers resistance to cancer therapies (**Figure 31B-D**). Importantly, while the treatment with tigecycline had almost no effect on WT tumours, it significantly reduced tumour growth of *FBXW7* KO tumours (**Figure 31B-D**). These data provide initial indications of the potential use of strategies targeting mitochondrial function to target *FBXW7* mutant tumours that might otherwise be resistant to the vast majority of available cancer therapies.

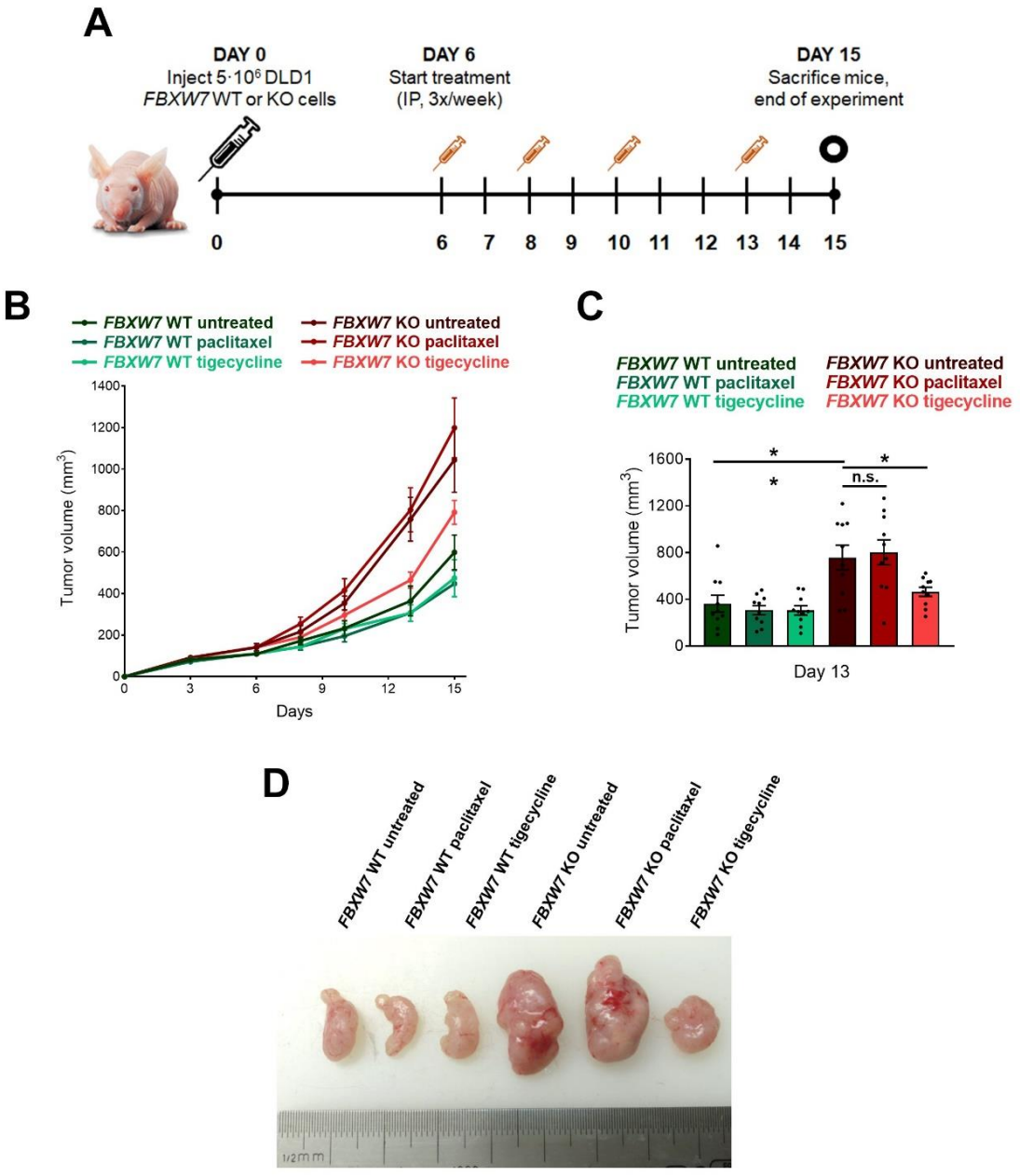

Figure 31: Interference of mitochondrial translation with tigecycline is selectively lethal in *FBXW7*-depleted tumours *in vivo*. (**A**) Schematic representation of the xenograft experiment. $5{\cdot}10^6$ DLD1 *FBXW7* KO and WT cells were injected in the flank

of nude/SCID mice. 6 days after, mice were randomized into three groups per genotype: six groups in total, 10 mice per group. Intraperitoneal injection (i.p.) with either vehicle, paclitaxel (1,5mg/kg) or tigecycline (50mg/kg) was started at day 6 post-tumour-injection, following a scheme of treatment of three times per week (at days 6, 8, 10, 13). Tumours were measured every 2-3 days, and when they reached 1600mm^3 (measures were calculated using the standard formula length x width x 0.5), mice were sacrificed and their tumours extracted. (**B**) Tumour growth (in mm^3) during the 15 days of the xenograft experiment, following DLD1 WT and *FBXW7* KO cells injection into nude mice. Error bars indicate SEM (n=10). (**C**) Tumour growth (in mm^3) at day 13 of the xenograft experiment after tumour inoculation. Error bars indicate SEM (n=10). n.s. p>0.05, *p<0.05, **p<0.01, ***p<0.001 (t-test). (**D**) Representative images of the xenograft experiment. DLD1 WT and FBXW7 KO tumours extracted from mice untreated or treated with paclitaxel or tigecycline are displayed here. Tumours were extracted 15 days after cells were injected.

4. DISCOVERY OF ADDITIONAL COMPOUNDS SELECTIVELY KILLING *FBXW7*-DEFICIENT CELLS

4.1. A focused chemical screen identifies the B-RAF inhibitor PLX-4720 as a compound selectively killing *FBXW7* KO cells

Chemical screens looking for compounds selectively killing cells presenting specific tumourigenic or resistance mutations is one of the main approaches used to identify synthetic lethalities (Miller et al., 2016, Hangauer et al., 2017, Liu et al., 2019, Mariniello et al., 2020). Our previous approach to identify compounds targeting FBXW7-deficient cells was based on the characterization of pathways that might be altered in these cells in order to look for potential vulnerabilities. Independently, we decided to explore a more agnostic approach, by conducting a small and focused chemical screen with the aim of discovering more compounds able to selectively kill *FBXW7* KO cells.

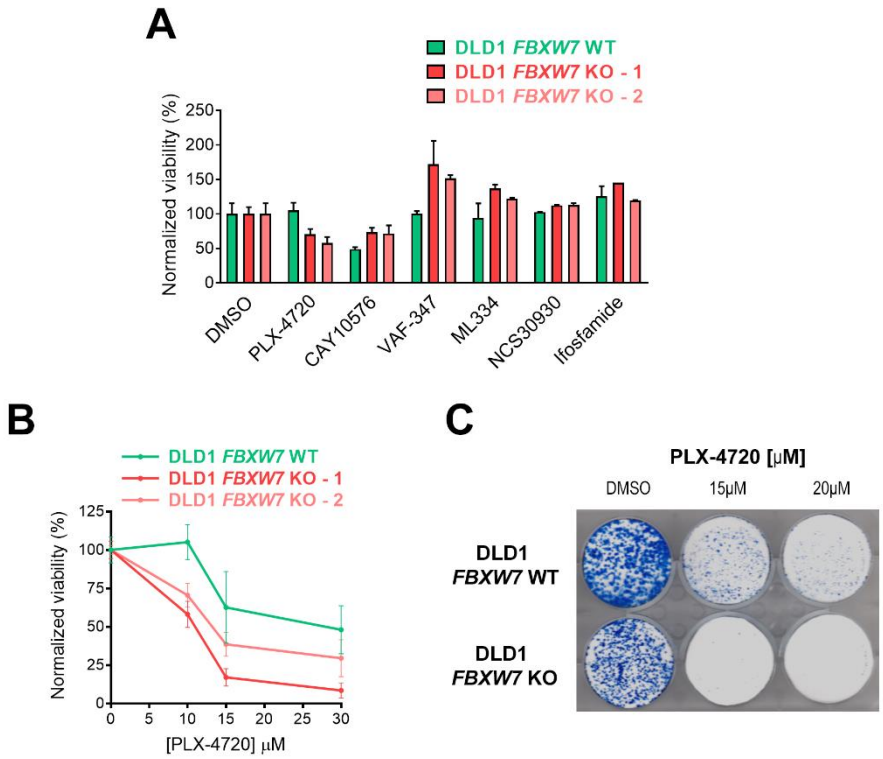

Figure 32: Identification of PLX-4720 in a focused chemical screen for compounds selectively toxic for *FBXW7* KO tumours. (**A**) Normalized viability of DLD1 WT (in green) and DLD1 *FBXW7* KO clones (in red) upon treatment with 10µM of PLX-4720, CAY10576, VAF-347, ML334 and NCS30930, and 50µM of ifosfamide. DAPI staining was performed to count nuclei by high-throughput microscopy. Error bars indicate SD (two technical replicates). (**B**) Normalized viability of DLD1 WT (in green) and DLD1 *FBXW7* KO clones (in red) upon treatment with PLX-4720. Error bars indicate SD (two technical replicates). (**C**) Clonogenic assay of DLD1 *FBXW7* WT cells (above) and DLD1 *FBXW7* KO cells (below) treated with different doses of PLX-4720. Experiment was performed in duplicate, and a representative example is shown.

The screen was focused as we selected compounds **based on our previous meta-analysis** of CTRP data, which suggested a potential action for certain drugs to be toxic for cells with low FBXW7 levels (**Figure 17E**). Six compounds were evaluated: PLX-4720, CAY10576, VAF-347, ML334, NSC30930, and ifosfamide. Of these compounds, only PLX-4720 displayed a selective toxicity towards DLD1 *FBXW7* KO cells (**Figure 32A**). For CAY10576, VAF-347, and ML334, *FBXW7*-deficient cells were even more resistant, and NSC30930 and ifosfamide did not yield any toxicity even at high doses (**Figure 32A**). PLX-4720 proved to be preferentially toxic for *FBXW7* KO cells in short and long-term experiments (**Figure 32B-C**), and we decided to further characterise this compound and its mechanism of action.

4.2. Connectivity Map (CMap) tool identified more compounds similar to PLX-4720 in the ability to selectively kill *FBXW7* KO cells

PLX-4720 is a 7-azaindole derivative that inhibits B-RAF^{V600E} with an IC_{50} of 13 nM (Tsai et al., 2008). However, our DLD1 cells do not present the *B-RAF^{V600E}* mutation, therefore the effect we see on selectively killing FBXW7-deficient cells must be due to another target. PLX-4720 displays more than 10 times selectivity against WT B-RAF or C-RAF (Tsai et al., 2008), and more than 100 times selectivity over other kinases with IC_{50} of 1-3μM (PLX-4720 Kinome Scan, **Annex Table 10**). Nevertheless, deletion of B-RAF, C-RAF, A-RAF or two kinases with low IC_{50} in WT^{eGFP} and *FBXW7*-KO^{Ruby3} cell mixtures, did not result in any significant selective death of the latter (**Figure 33A**). Moreover, from another three independent B-RAF^{V600E} or B-RAF/C-RAF inhibitors, only vemurafenib showed a similar effect to PLX-4720 in sensitising FBXW7-deficient cells (**Figure 33B**). These observations, together with the fact that the effect on FBXW7 cells demands doses as high as 10-20μM, further supports that this phenomenon is due to an off-target effect.

The list of possible kinases that PLX-4720 could be targeting at 10μM is very large (PLX-4720 Kinome Scan, **Annex Table 10**), making it unrealistic for us to test them one by one as mediators of our observations. Therefore, we first aimed to identify compounds that may be producing a similar cellular effect as PLX-4720. The development of **databases containing transcriptional signatures** of human cancer cell lines exposed to a specific perturbation such as pharmacological or genetic manipulations have brought an excellent platform for drug repurposing or to better understand the mechanism of action of compounds (Wang et al., 2016c, Keenan et al., 2018, Papatheodorou et al., 2018).

For this last purpose, we used the **Connectivity Map (CMap)** from the Broad Institute at MIT, which stores over 1,5M signatures from human cancer cell lines exposed to around 5,000 drugs and 3,000 genetic perturbations (overexpression or shRNA-mediated depletion) (https://www.broadinstitute.org/connectivity-map-cmap) (Lamb et al., 2006, Subramanian et al., 2017), trying to identify compounds triggering a similar transcriptional signature to PLX-4720. Supporting the usefulness of this approach, if the transcriptional signature of PLX-4720 is used as an input, we can find vemurafenib as the 4th most similar compound, as well as multiple RAF/MAPK and EGFR inhibitors among the first positions (**Figure 33C**, **Annex Table 11**). Interestingly, the 3rd compound from this similarity list was oligomycin, the mitochondrial complex V inhibitor which we already found to selectively kill *FBXW7* KO cells (**Figure 28C**).

We then decided to **test the effects of some of these compounds** including the two B-RAF inhibitors (PLX-4720 and vemurafenib), the FLT3 inhibitor sorafenib (ranked 2nd), the BCR-ABL kinase inhibitor dasatinib (6th) and two EGFR inhibitors (erlotinib (10th) and gefinitib (even though it ranked 22nd, it still had a similarity score above 99%)). Both competition experiments measured by flow cytometry (**Figure 33D**) and cell viability measurements by high-content microscopy (**Figure 33E**) revealed a significant effect of the 6 different compounds in selectively targeting *FBXW7* KO cells. While dasatinib and erlotinib had the biggest effect, they were also very toxic for WT cells (**Figure 33E**). In any case, these data support that our approach was a valid strategy to identify drugs selectively toxic for FBXW7-deficient cells.

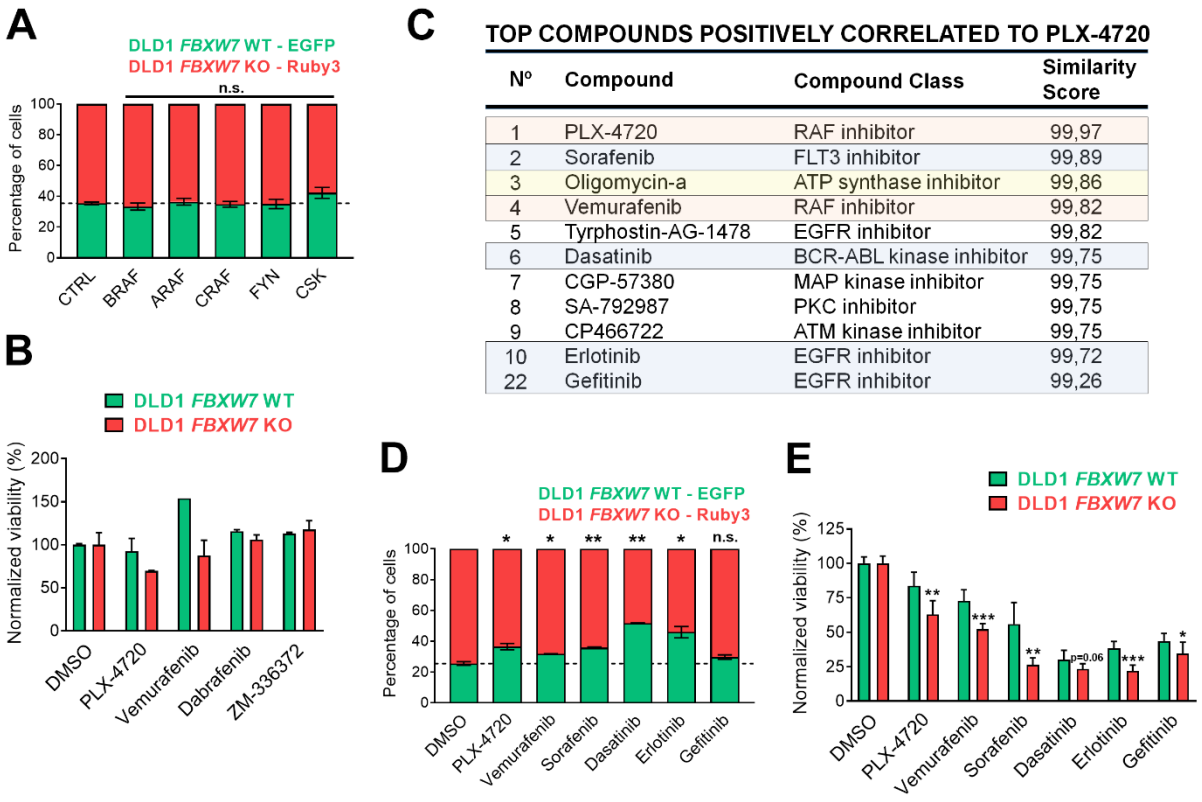

Nº	Compound	Compound Class	Similarity Score
1	PLX-4720	RAF inhibitor	99,97
2	Sorafenib	FLT3 inhibitor	99,89
3	Oligomycin-a	ATP synthase inhibitor	99,86
4	Vemurafenib	RAF inhibitor	99,82
5	Tyrphostin-AG-1478	EGFR inhibitor	99,82
6	Dasatinib	BCR-ABL kinase inhibitor	99,75
7	CGP-57380	MAP kinase inhibitor	99,75
8	SA-792987	PKC inhibitor	99,75
9	CP466722	ATM kinase inhibitor	99,75
10	Erlotinib	EGFR inhibitor	99,72
22	Gefitinib	EGFR inhibitor	99,26

Figure 33: Identification of compounds transcriptionally similar to PLX-4720 in the ability to selectively kill *FBXW7* KO cells. (**A**) Cell percentages of eGFP+ DLD1 WT cells and Ruby3+ DLD1 *FBXW7* KO cells after infecting them every 7 days with lentiviral supernatants encoding for sgRNAs against *BRAF, CRAF, ARAF, FYN* or *CSK*. Analysis was performed at day 19 by flow cytometry. The culture started with 1:3 ratios of WT^{eGFP} and *FBXW7*-KO^{Ruby3} respectively. Error bars indicate SD (two technical replicates). n.s. p>0.05, *p<0.05, **p<0.01, ***p<0.001 (t-test). (**B**) Normalized viability of DLD1 WT (in green) and DLD1 *FBXW7* KO cells (in red) upon treatment with 20μM of PLX-4720, vemurafenib, dabrafenib and ZM-336372. DAPI staining was performed to count nuclei by high-throughput microscopy. Error bars indicate SD (two technical replicates). (**C**) Similarity scores of the top compounds with a transcriptional signature similar to the PLX-4720 signature, identified by using CMap tool. Compounds already identified as similar are highlighted in orange, in yellow a mitochondrial poison already proven to work against *FBXW7* KO tumours, and in blue the compounds selected for further analysis. (**D**) Cell percentages of eGFP+ DLD1 WT cells and Ruby3+ DLD1 *FBXW7* KO cells after 72h treatment with 15μM of PLX-4720, vemurafenib, sorafenib, dasatinib, erlotinib and gefitinib. The culture started with 1:3 ratios of WT^{eGFP} and *FBXW7*-KO^{Ruby3} respectively. The experiment was repeated three times and a representative example is shown. Error bars indicate SD (two technical replicates). n.s. p>0.05, *p<0.05, **p<0.01, ***p<0.001 (t-test). (**E**) Normalized viability of DLD1 WT (in green) and DLD1 *FBXW7* KO cells (in red) upon treatment with 10μM of PLX-4720, vemurafenib, erlotinib and gefitinib, and 5μM of sorafenib and dasatinib. DAPI staining was performed to count nuclei by high-throughput microscopy. Experiments were performed also in another DLD1 *FBXW7* KO clone, with similar results. Error bars indicate SD (n=3, three independent experiments, with two technical replicates per experiment). n.s. p>0.05, *p<0.05, **p<0.01, ***p<0.001 (t-test).

4.3. Compounds preferentially toxic for FBXW7-deficient cells activate the ISR

In order to **understand the possible mechanism of action** that explains the preferential toxicity of these compounds for FXW7 cells, we further used CMap to explore “pathways” -rather than other drugs- that could be related to the effects of PLX-4720. First, we adapted Gene Set Enrichment Analyses (GSEA) to conduct a "drug GSEA", to identify positively enriched “compound classes” similar to PLX-4720 (Korotkevich et al., 2019, Sinha et al., 2020, Sanchez-Burgos et al., 2020). Besides EGFR or RAF inhibitors, this analysis showed an enrichment of mitochondrial oxidative phosphorylation uncouplers as most similar to the effects of PLX-4720 (**Figure 34A**). In addition, CMap contains data from different pathways in a pertubagen called CMap classes. Among the CMap classes with a similarity score most similar to PLX-4720, we once again found VEGFR, EGFR, or RAF inhibition, but also ATP synthase inhibitors (**Figure 34B**, **Annex Table 11**). In fact, and as previously mentioned, oligomycin had ranked 3rd among the individual compounds that positively correlated to PLX-4720 (**Figure 33C**).

Together, these pathway analyses indicated a possible similarity of the drugs that we found to selectively kill FBXW7-deficient cells as PLX-4720, and mitochondrial poisons.

Given that the toxicity of tigecycline was due to an effect of the drug in activating the ISR, we next checked if the mechanism of action of this new set of drugs that selectively killed FBXW7-deficient cells and were related to mitochondrial poisons, was also **associated to the ISR**. In fact, the 6 new compounds related to PLX-4720 activated the ISR in both *FBXW7* WT and KO cells, producing a higher induction in FBXW7-deficient cells (**Figure 35A,C**). Furthermore, this induction was reversed by ISRIB (**Figure 35A,C**). Of note, the activation of the ISR is not just a consequence of using too high doses of a drug, as we could not observe similar effects with other common anticancer drugs such as paclitaxel or trametinib (**Figure 35B-C**). Finally, we confirmed the relevance of the ISR in mediating the toxicity of this new set of compounds, as this was rescued by co-treating the cultures with ISRIB (**Figure 35D**).

In conclusion, based on a focused chemical screen and comparison of publicly available transcriptional signatures of anticancer drugs we have identified **6 additional compounds that selectively kill *FBXW7* KO cells**. Once again, this phenomenon was related to an effect of the drugs in activating the ISR. Together with our previous findings with tigecycline, we finally investigated if the activation of the ISR is a general vulnerability of FBXW7-deficient tumours.

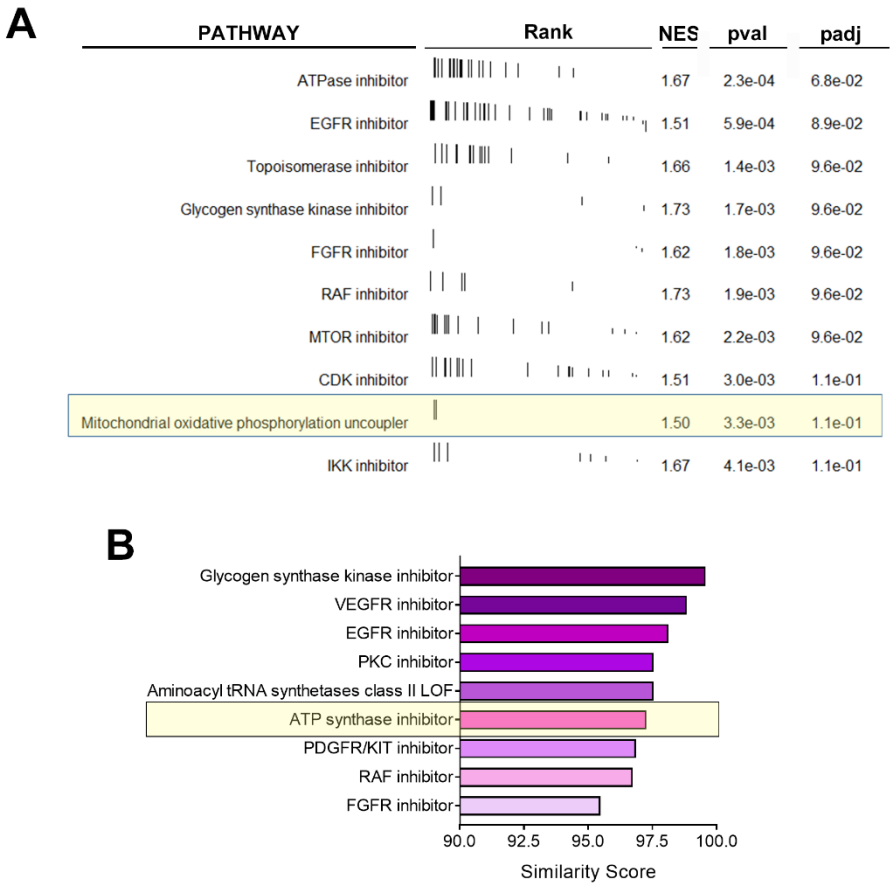

Figure 34: CMap pathway analysis revealed a relationship between PLX-4720 and mitochondrial poisons. (**A**) Drug GSEA analysis of compounds with a transcriptional signature that positively correlates to PLX-4720. Enriched pathways with padj value <0.05 are shown, as well as their gene ranks, Normalized Enrichment Scores (NES), p-value (pval), and adjusted p-value (padj). Mitochondrial poisons are highlighted in yellow. (**B**) Similarity scores of the top CMap classes with a transcriptional signature that positively correlates to PLX-4720. Mitochondrial poisons are highlighted in yellow.

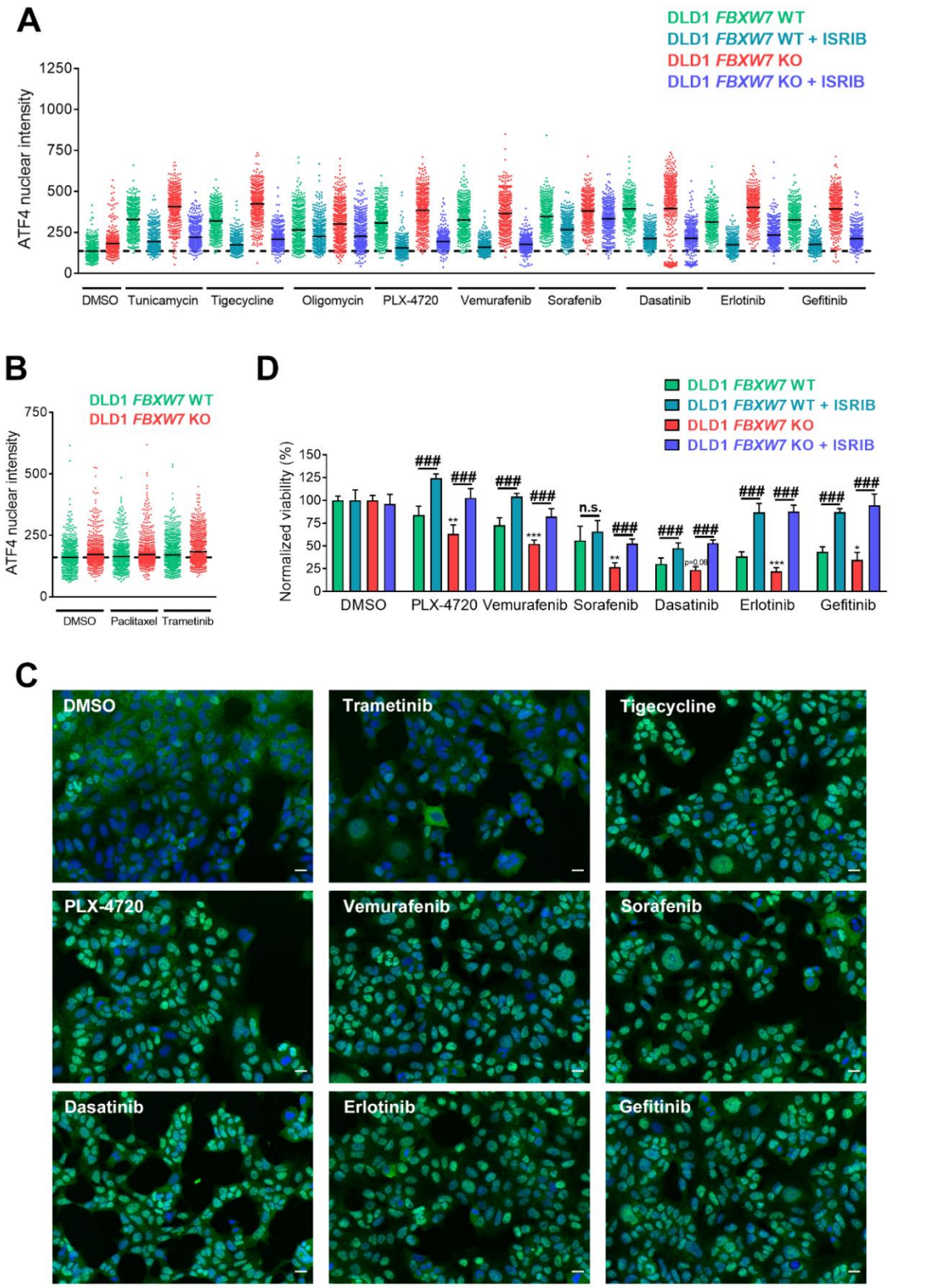

Figure 35: The mechanism of action of PLX-4720 and similar set of compounds involves the activation of the ISR. (**A**,**B**) Nuclear ATF4 intensity measured by high-throughput microscopy in DLD1 WT and DLD1 *FBXW7* KO cells upon treatment with different compounds in the presence or absence of an ISR inhibitor (ISRIB, 50nM): DMSO, paclitaxel (250nM), tunicamycin (1μM) and 10μM of trametinib, tigecycline, oligomycin, PLX-4720, vemurafenib, sorafenib, dasatinib, erlotinib and gefitinib. The experiment was repeated three times and a representative example is shown. (**C**) Representative images from (A,B) DLD1 *FBXW7* WT cells. Scale bar = 20μm. (**D**) Normalized viability of DLD1 WT (in green) and DLD1 *FBXW7* KO cells (in red) upon treatment for 72h with 10μM of PLX-4720, vemurafenib, erlotinib and gefitinib, and 5μM of sorafenib and dasatinib; in the presence or absence of ISRIB (50nM). DAPI staining was performed to count nuclei by high-throughput microscopy. Experiments were performed also in another DLD1 *FBXW7* KO clone, with similar results. Error bars indicate SD (n=3, three independent experiments, with two technical replicates per experiment). n.s. p>0.05, *p<0.05, **p<0.01, ***p<0.001 (t-test).

4.4. Activating the ISR as a general strategy to target FBXW7-deficient tumours

C-MYC overexpressing cells have been reported to have an enhanced ISR (Tameire et al., 2019). Hence, our first question was to address the role of **C-MYC in the higher activation of the ISR** observed in the context of *FBXW7* mutations. Indeed, downregulation of C-MYC reduced the basal levels of nuclear ATF4 in FBXW7-deficient cells and had also a partial effect in reducing the hyperactivation of the ISR induced by tigecycline (**Figure 36A**). The enhanced ISR in C-MYC overexpressing cells is known to be due to ER stress (Tameire et al., 2019). However, inhibition of the PERK kinase, the main mediator of activating the ISR in response to ER stress, did not rescue the basal hyperactivation of the ISR FBXW7-deficient cells (**Figure 36B**), implying that additional MYC-dependent stresses might promote the activation of the ISR in these cells. In contrast, and as previously shown, the use of ISRIB, which inhibits the ISR downstream of the activating kinases, rescued the activation of the ISR in FBXW7-deficient cells (**Figure 36B**).

Furthermore, none of our non-antibiotic additional set of compounds that preferentially killed FBXW7-deficient cells activated the ISR in a PERK-dependent manner (**Figure 36C**). These studies indicate that FBXW7-deficient cells present an enhanced activity of the ISR, produced by **stressors different or additional to ER stress**. In any case, we were able to see also selective killing of *FBXW7* KO tumours with the ER-stressor tunicamycin (**Figure 36D**), implying that any drug that activates the ISR would selectively target FBXW7-deficient cells.

We then evaluated the effect of the compounds selectively targeting FBXW7-deficient cells in **inducing the levels of CHOP**, which is a key mediator of cell death upon activation of the ISR. Notably, all the compounds that were preferentially toxic for FBXW7-deficient cells induced CHOP expression, an effect that was not seen with paclitaxel and trametinib (**Figure 37A**). Moreover, the induction of CHOP was even more pronounced in FBXW7-deficient cells (**Figure 37A**), further indicating that the toxic effects of these compounds are mediated by their induction of the ISR.

As to **which branch of the ISR** is mediating the toxic effects of the compounds that are selectively toxic for FBXW7-deficient cells, it is worth mentioning that besides ER stress, mitochondrial stress has recently emerged as another powerful branch that activates the ISR (Pakos-Zebrucka et al., 2016, Guo et al., 2020a, Fessler et al., 2020). This branch of the ISR is PERK independent and instead signalled through the HRI kinase. Importantly, HRI and GCN2 levels were upregulated in FBXW7-deficient DLD1 cells, while the levels of the remaining ISR kinases (PERK and PKR) were not substantially altered (**Figure 37B**). Together with our previous data, these results collectively support the potential of targeting mitochondrial activity for the selective elimination of FBXW7-deficient cells.

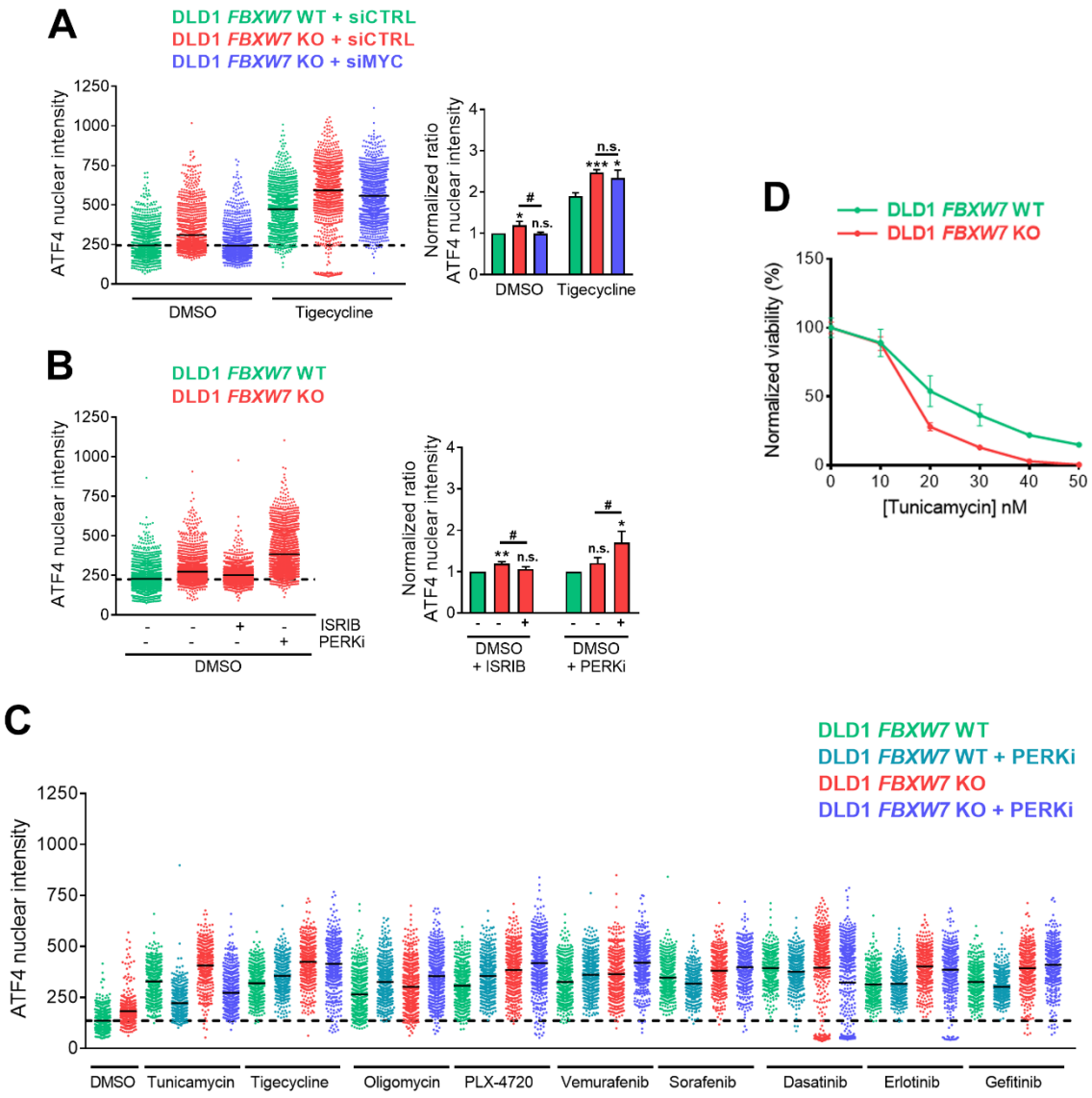

Figure 36: ER stress induction selectively kills *FBXW7* KO tumours, while it is not implicated in the other compounds and the basal ISR activation. (**A**) Nuclear ATF4 intensity measured by high-throughput microscopy in DLD1 WT cells with siCTRL (in green), DLD1 *FBXW7* KO cells with siCTRL (in red) and DLD1 *FBXW7* KO cells downregulated for C-MYC using siRNAs (in blue) upon DMSO or tigecycline (10µM). The experiment was repeated three times and a representative example is shown (left). The average of the three experiments was represented (right), with error bars indicating their SD. T-test comparisons between DLD1 WT and DLD1 *FBXW7* KO (siCTRL or siMYC) cells: n.s. p>0.05, *p<0.05, **p<0.01, ***p<0.001. T-test comparisons between DLD1 *FBXW7* KO siCTRL and siMYC cells: n.s. p>0.05, #p<0.05, ##p<0.01, ###p<0.001. T-test comparisons between with or without tigecycline for each cell type were significant with ***p<0.001. (**B**) Nuclear basal ATF4 intensity measured by high-throughput microscopy in DLD1 WT (green) and DLD1 *FBXW7* KO cells (red) with or without an ISRIB (50nM) and PERKi (500nM). The experiment was repeated three times and a representative example is shown (left). The average of the experiments was represented (right), with error bars indicating their SD. T-test comparisons between DLD1 WT and DLD1 *FBXW7* KO cells: n.s. p>0.05, *p<0.05, **p<0.01, ***p<0.001. T-test comparisons between DLD1 *FBXW7* KO with or without the ISRIB and PERKi: n.s. p>0.05, #p<0.05, ##p<0.01, ###p<0.001. (**C**) Nuclear ATF4 intensity measured by high-throughput microscopy in DLD1 WT and DLD1 *FBXW7* KO cells upon treatment with different compounds in the presence or absence of a PERKi (500nM): DMSO, tunicamycin (1µM) and 10µM of tigecycline, oligomycin, PLX-4720, vemurafenib, sorafenib, dasatinib, erlotinib and gefitinib. The experiment was repeated three times and a representative example is shown. (**D**) Normalized viability of DLD1 WT (in green) and DLD1 *FBXW7* KO (in red) upon tunicamycin treatment. DAPI staining was performed to count nuclei by high-throughput microscopy. The experiment was repeated three times and a representative example is shown. Error bars indicate SD (two technical replicates).

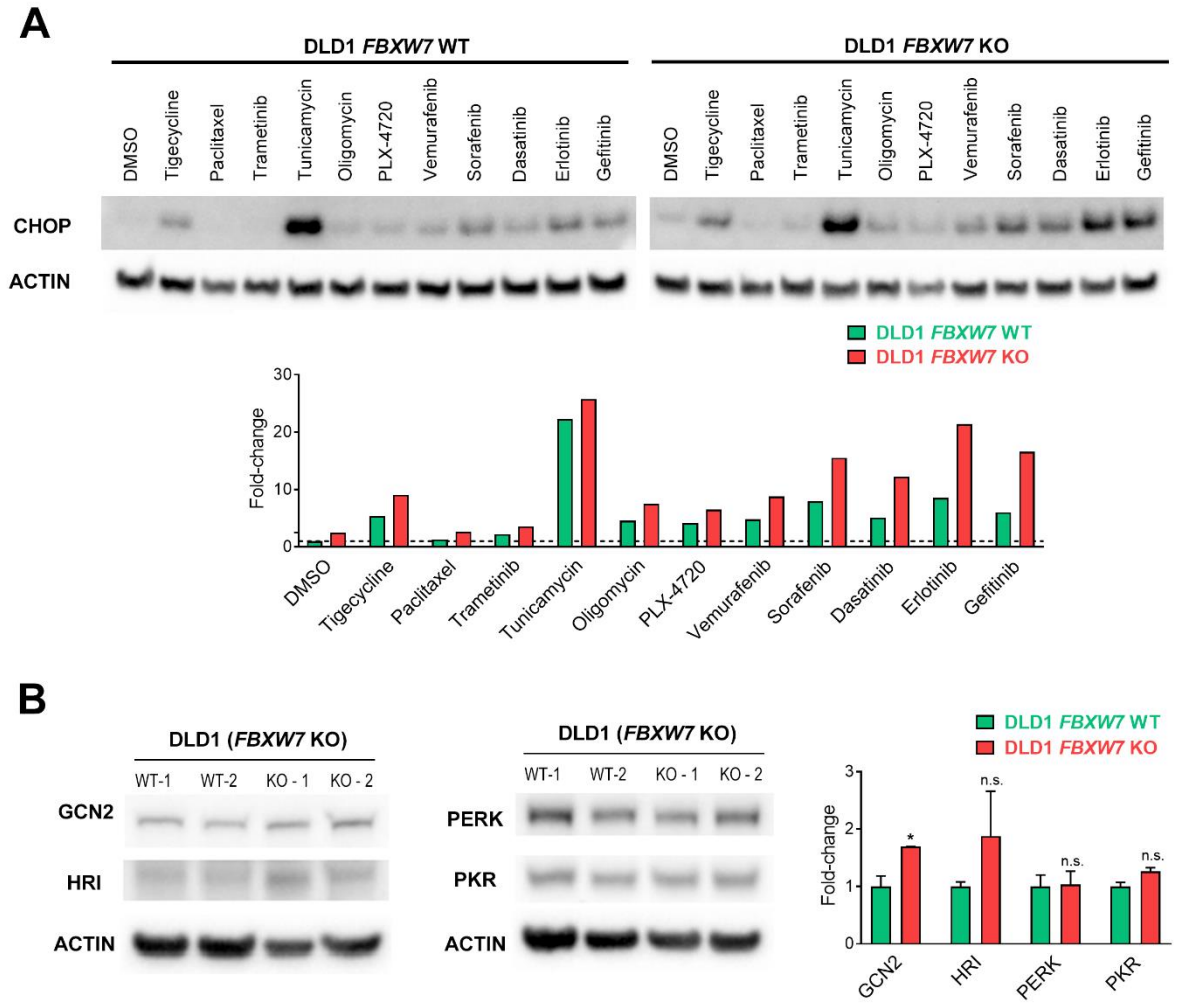

Figure 37*: FBXW7* KO tumours present an upregulation of the downstream effector CHOP and the upstream ISR kinases. (**A,B**) Western Blot showing (A) CHOP protein levels and (B) GCN2, HRI, PERK, and PKR protein levels in DLD1 WT and *FBXW7* KO cells and its quantification. ACTIN levels are shown as loading controls. For (B) Error bars indicate SD (two biological replicates). n.s. p>0.05, *p<0.05, **p<0.01, ***p<0.001 (t-test).

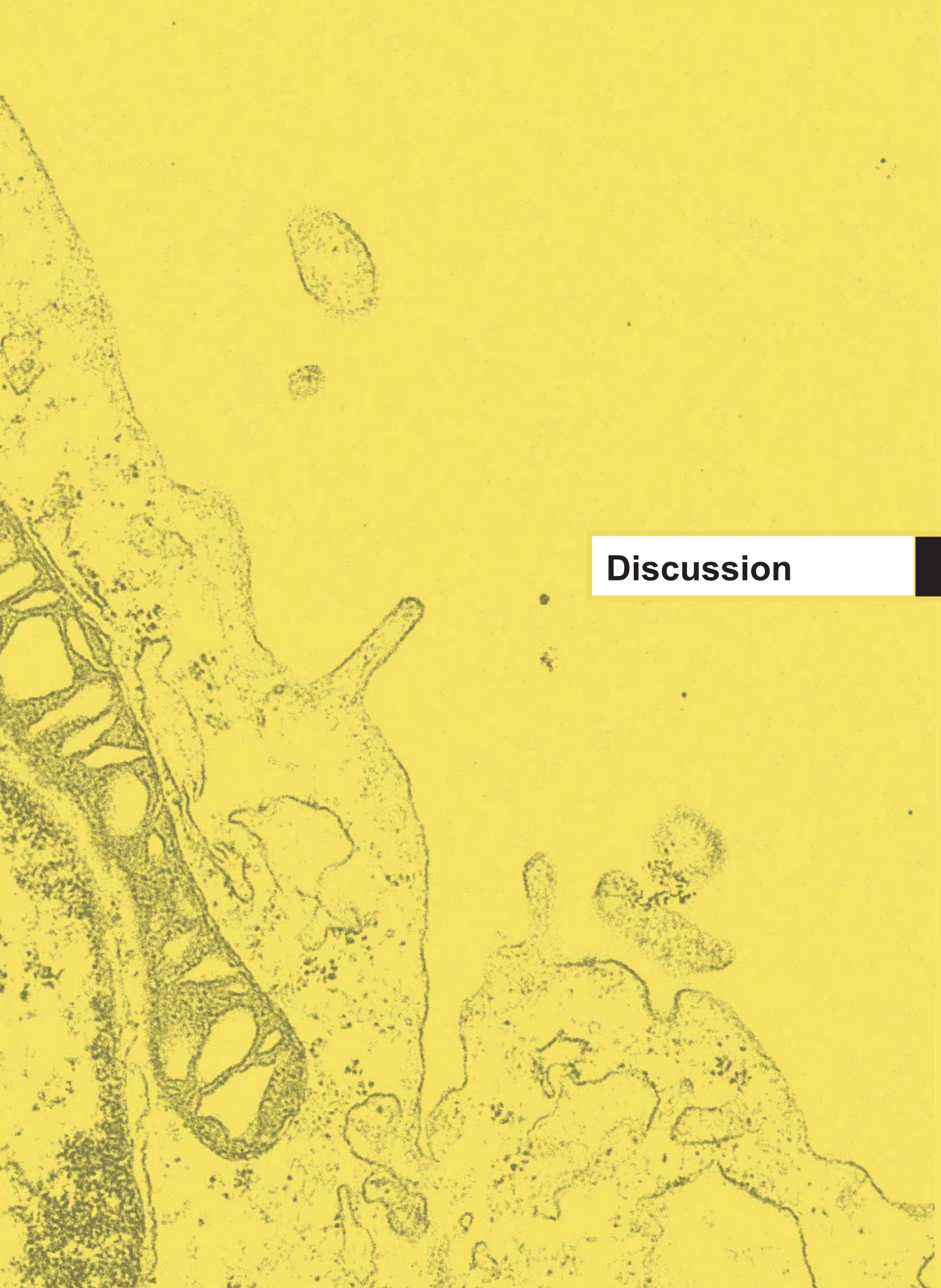

Discussion

1. SHEDDING LIGHT ON THE MECHANISMS BEHIND DRUG RESISTANCE IN CANCER

1.1. Studying the mechanisms of cancer drug resistance

Unfortunately, tackling drug resistance in cancer therapy is like battling with the multi-headed Hydra beast: the initial success of every antitumoural agent in reducing tumour growth has always been quickly tempered by the **appearance of resistance** (Vasan et al., 2019).

Due to the high complexity and heterogeneity of tumours, identifying the **best strategy to overcome drug resistance** is extremely challenging. Nowadays, a personalised treatment of cancer patients is regarded as the future of clinical oncology, and decisions on which treatment to be administered will be based on the knowledge on tumour mutations and their vulnerabilities. Thus, tumours will be treated according not only to their type but also their molecular hallmarks. Moreover, the development and improvement of other aspects of cancer therapy, such as earlier treatments, improvement of the compounds' efficacies, monitoring drug responses, and improving the delivery and regimen strategies, will also contribute to achieve better responses in patients. For instance, new treatment strategies, such as the permutations of on-off or high dose-low dose regimens, result in longer survival and delayed drug resistance for some cancers (Kaiser, 2017, Moriceau et al., 2015, Sale et al., 2019). However, these new strategies are not universal and might depend on the specific mutations of the tumour, therefore, more research on the mechanisms of resistance for each treatment and cancer is required.

In this context, a complete **understanding of the mechanisms that mediate drug resistance** is the first step to circumvent clinical resistance, and effectively cure cancer patients. The molecular mechanisms of anticancer drug resistance have been studied since the 1960s (Brockman, 1963), leading to the identification of some of the mutations involved in drug resistance to single-agents, or even to multiple drugs (Shoemaker, Curt, and Carney 1983). More recently, the development of high-throughput cancer genomics, proteomics, and other OMICS analyses, have facilitated the identification of the driver genes and the principal modules that contribute to the drug resistance at any stage of tumourigenesis. Equally powerful are the more recently developed technologies for systematic gain-of-function or loss-of-function genetic screens, that allow the selection of individual cells with a therapy-resistant phenotype within a mutagenised population. While their initial main drawbacks were their limited resemblance to relevant biological situations and that they are only able to generate single-mutations, not very common in tumours, this technology is gaining power by the expansion of the editing toolbox and the use of combinatorial and *in vivo* screens. During the last years, the contributions from computational biology to the development of databases encompassing data from large chemical and genetic screens and cancer OMICS have greatly facilitated the discovery of many mutations related to the sensitivity and/or resistance to cancer therapies, and it is expected to become a future reference technology to fully understand and circumvent drug resistance.

1.2. CRISPR-Cas9 screens as a powerful technique to discover novel resistance-related genes

The advent of CRISPR-Cas9 technology, with sgRNA libraries that target thousands of genes, have allowed the exhaustive study and identification of novel genes and/or mutations related to resistance to cancer therapies (Wang et al., 2014b, Shalem et al., 2014, Koike-Yusa et al., 2014, Konermann et al., 2015). Here, we exploited this powerful technique to identify novel mediators of drug resistance. Specifically, we used **loss-of-function CRISPR-Cas9 libraries generated in mESCs** (Ruiz et al., 2016) to identify mutations that confer resistance to two of the most widely studied genotoxic agents: cisplatin and UV-radiation.

To perform our screens, we choose **toxic concentrations** of both genotoxics and sequenced only individual clones where we could confirm substantial resistance. This approach contrasts with the general tendency of other CRISPR-Cas9 screens that use sub-lethal doses (Wang et al., 2014b, Shalem et al., 2014, Koike-Yusa et al., 2014, Olivieri et al., 2020), allowing the identification of more hits and biological pathways. However, we preferred to focus on identifying specific mutations that give notable resistance (Ruiz et al., 2016). This focused and low-throughput approach may explain why we

did not find any of the mutations known to mediate resistance to cisplatin and UV. In a very recent report (Olivieri et al., 2020), CRISPR-Cas9 screens against 27 genotoxic agents were performed with the aim to find novel DNA repair genes and drug response modifiers. These screens included UV-C radiation and cisplatin at sub-lethal doses, and were able to identify numerous relevant repair pathways for both agents. In contrast, from the other many recent reports of CRISPR-Cas9 screens to identify mediators of cisplatin resistance (Ko and Li, 2019, Ouyang et al., 2019, Stover et al., 2019, Goodspeed et al., 2019, Xu et al., 2020, Hundley et al., 2021), only one was able to identify a known resistance hit (*MSH2*) among their top hits (Goodspeed et al., 2019).

Besides the limited throughput of our approach, another possibility to explain why we failed to detect previously reported mediators of resistance to cisplatin and UV may be the **cell line of choice**. Certainly, we are aware that one of the caveats of our approach is that we may find hits that are only relevant for mESCs. In fact, hits related to pluripotency related pathways (e.g. WNT) are frequent in our screens. In addition, we found cases where a specific mutation (e.g. *Rock2* deletion) confers resistance to a specific agent in mESCs, but not in human cancer cell lines (data not shown). Moreover, mutations in *Ptgs1, Glod4, Fam115c, Myh9*, *Tbck*, *Ptpn2* and *Fbxw7* were abundant in our screens (**Annex Table 6-8**). We hypothesised four possible non-exclusive explanations for this observation: (**1**) these mutations confer a general fitness advantage for mESCs; (**2**) they are truly involved in pathways that are common for UV-cisplatin signalling (Olivieri et al., 2020); (**3**) they are bona-fide MDR-related genes; or (**4**) they were artefacts carried together with another sgRNA driving-resistance in the same cell. For instance, *Myh9*-sgRNAs came always together in mixed clones with *Fbxw7*-sgRNA (**Annex Table 7**), which we later showed to be a MDR-driver hit. Nevertheless, *MYH9* deletion alone was identified as a tumourigenic gene driver and a FGFR inhibitor-resistance related mutation in different genetic screens (Schramek et al., 2014, Kas et al., 2017, Kas et al., 2018). Whether it was just an accompanying sgRNA, or it was also cooperating to the resistance phenotype of the surviving cells, is yet to be determined.

Noteworthy, the loss of *Fbxw7* and *Ptpn2* has been related to a **naïve state** of pluripotency and impaired differentiation in ESCs (Buckley et al., 2012, Zhang et al., 2018a). While in cancer stemness is related to chemoresistance (Dean et al., 2005, Nunes et al., 2018, Hepburn et al., 2019, Lettnin et al., 2019), the opposite was recently reported to occur in human ESCs (Panina et al., 2021). Still, differences between human and mouse ESCs could exist and, thus, the relationship between the pluripotent state of the mESCs and drug response could be an interesting field to explore. The results of those experiments could be relevant for the platforms that aim to replace compound toxicity testing in animals with *in vitro* assays in ESCs (Adler et al., 2008, Tandon and Jyoti, 2012, Liu et al., 2017), as dosages and responses could not be as easily extrapolated if these are significantly affected by the pluripotent state of the cells.

Even if we focused our study on FBXW7, another of our frequent hits, TC-PTP (encoded by ***Ptpn2***), is a known negative regulator of pro-survival pathways involving factors such as STAT3 and AKT (Kim et al., 2010). In addition, its activation is a suppressor of survival and proliferation following UV irradiation (Lee et al., 2015, Kim et al., 2017b), being a bona-fide mediator of UV-responses. The role of PTPN2 in cancer initiation and promotion upon gene loss has been studied in animal models of skin carcinogenesis (Lee et al., 2017a). The fact that *Ptpn2*-deficient cells are resistant to cisplatin (**Figure 14**) could be due to the relevance of STAT3 signalling in response to this agent (Sun et al., 2019). Finally, we want to note that *PTPN2* deletions were recently identified in an *in vivo* CRISPR screen related to identify mutations that increase the efficacy of anti-PDL1 immunotherapies (Manguso et al., 2017). Thus, PTPN2 seems to have important pleotropic functions that modulate the response to cancer therapies, which deserve further attention.

As for *Fbxw7*, the impact of its mutations on the **resistance to specific compounds**, such as cisplatin (Yu et al., 2013, Song et al., 2015, Zhou et al., 2015, Xiao et al., 2018a) and its derivatives (Li et al., 2015b, Fang et al., 2015, Gombodorj et al., 2018), UV light (Hong et al., 2016) or paclitaxel and other microtubule poisons (Wertz et al., 2011, Inuzuka et al., 2011, Yokobori et al., 2014, Gasca et al., 2016, Ishii et al., 2017, Gombodorj et al., 2018) has been reported numerous times. Furthermore, *FBXW7* mutations have been identified (even if not validated) as resistance hits in multiple CRISPR-

Cas9 genome-wide genetic screens: JQ1 (Liao et al., 2018), pterostilbene and resveratrol (Benslimane et al., 2020), MNNG and Duocarmycin (Olivieri et al., 2020), erlotinib (Zeng et al., 2019), and to multiple compounds (flavopiridol, palbociclib, rivociclib, pictilisib, pravastatin) (Hundley et al., 2021). Moreover, additional genome-wide genetic resistance screens not based on CRISPR-Cas9 also identified *FBXW7* mutations in response to an FGFR inhibitor (Kas et al., 2018), PARP1 inhibitors (Marzio et al., 2019), and to the microtubule damaging agents docetaxel and vinorelbine (Gerhards et al., 2018). Despite all of these previous works, the impact of FBXW7 deficiency in multidrug resistance had never been systematically addressed before.

Regarding the **effects of FBXW7 deficiency in mESCs**, most reports have focused on its impact to impair differentiation and enhance cellular reprogramming through stabilisation of C-MYC (Buckley et al., 2012). Accordingly, *Fbxw7* ablation increases the efficiency of the generation of induced pluripotent stem cells (Okita et al., 2012, Lu et al., 2012). Here, we have provided proof of the multi-drug resistant nature of FBXW7-deficient mESCs (**Figure 16**). The molecular mechanisms of the resistance to different agents could be mediated by specific FBXW7 substrates, as described in human cancer cells. In a proteomic comparison between *Fbxw7* WT and KO mESCs we found upregulation of many of the known substrates of FBXW7, such as C-MYC or RAS (**Figure 21**). The relationship of C-MYC or RAS with stemness is out of doubt and, as mentioned, the cellular pluripotent state of the cells may be the ultimate cause of resistance, as happens in many tumoural contexts (Dean et al., 2005, Nunes et al., 2018, Hepburn et al., 2019, Lettnin et al., 2019). Unfortunately, the extrapolation of these results to cancer, and more specifically to cancer stem cells, may not be appropriate. For instance, *Fbxw7* loss in non-dividing leukaemia-initiating cells triggers proliferation and their exit from quiescence, enhancing the sensitivity to certain agents (Takeishi et al., 2013), as seen in other cancer stem cell populations (Izumi et al., 2017, Shimizu et al., 2019).

To end this section: besides the hits that were common to both, there were also several that were **specific to each screen** (**Annex Table 6-8**). For example, in the cisplatin screen we found *Bicd1* and *Mlf1* sgRNAs. Interestingly, *MLF1* downregulation has been shown to activate D-cyclins and inhibit cisplatin and hypoxia-induced cell death (Rangrez et al., 2017). For UV, some screen-specific hits were *Gas6* or the E3-ligases *Apc* and *Ttc3,* the latter being related to AKT signalling pathway, one of the key pathways modulating the sensitivity to UV-irradiation (Suizu et al., 2009). Thus, despite the limitations that might be associated to the use of mESCs for screenings related to cancer therapy, we believe that our data support its usefulness as a powerful platform to discover novel mediators of resistance.

1.3. FBXW7 deficiency as a multi-drug resistance mediator

One of the main contributions of this Thesis has been to nominate **FBXW7 deficiency as a novel MDR mediator**. FBXW7 is the substrate recognition component of an E3 ubiquitin-protein ligase complex, and mediates the degradation of multiple oncoproteins by marking them for proteasomal degradation (Winston et al., 1999, Koepp et al., 2001, Moberg et al., 2001, Strohmaier et al., 2001). Thus, *FBXW7* mutations have been associated with increased levels and/or deregulation of important oncoproteins (MYC, CYCLIN E, NOTCH, JUN, MCL1 among many), and therefore with multiple cancer-associated processes (Mao et al., 2004, Akhoondi et al., 2007, Ikenoue et al., 2018, Zhang et al., 2016b, Jiang et al., 2017, Davis et al., 2014a).

Previous knowledge, together with our results in screening campaigns (**Figure 15**), pointed out a possible role of *FBXW7* as a multi-drug resistance-related gene which, surprisingly, had never been specifically addressed. In this Thesis we provide sufficient evidences to propose *FBXW7* deficiency as a multi-drug resistance-related event. This MDR phenotype **is not cell-type specific**, as it is present in mESCs, the colorectal cancer cell line DLD1, and in different human cancer cell lines mutated for *FBXW7*, or presenting low levels of the protein (**Figure 16-17**, **Figure 38**).

Based on our findings, we used publicly available cancer databases to explore the possibility of using FBXW7 levels as a **biomarker of the response to therapy in the clinic** (**Figure 18**). In fact, as previously mentioned, there are multiple reports relating mutations of *FBXW7* to clinical resistance to certain drugs (Arita et al., 2017, Li et al., 2017, Rachiglio et al., 2019). Many of these works require

further efforts to validate the clinical resistance of FBXW7-deficient tumours to each resistance-associated therapy. This could be of a great importance, as *FBXW7* is among the most highly mutated genes in cancer (Lawrence et al., 2013), and a large number of patients harbouring these mutations will be exposed to chemotherapeutic agents with no therapeutic benefit.

Importantly, we reported **previously unknown resistance** of FBXW7-deficient cells to compounds such as the nucleotide synthesis inhibitor HU, the MEK inhibitor trametinib, the PLK1 inhibitor BI2536, the NEDD8-ubiquination inhibitor pevonedistat, and the mTOR inhibitor rapamycin (**Figure 17**, **Figure 38**). Again, the translation of our observation to the clinic could be of relevance, as patients with mutations in *FBXW7* may not respond to these treatments. HU is approved for treating several tumours, while trametinib is approved for treating melanoma and lung cancer in combination with dabrafenib, and is under study in several clinical trials, including colorectal tumours. BI2536 or pevonedistat are still in clinical trials, but other PLK1 and NEDD8 inhibitors have already been approved by the FDA. In the case of rapamycin, our results are in discrepancy with a study in which rapamycin was shown to reverse resistance to gefitinib (Xiao et al., 2018b), and in a bioinformatics analysis this was suggested as a possible sensitiser therapy (https://pandrugs.org/#!/) (Piñeiro-Yáñez et al., 2018). Additionally, rapamycin was shown to inhibit the EMT transition of *FBXW7*-altered colorectal cancer cells (Wang et al., 2013b). Nevertheless, rapamycin could still confer resistance by other mechanisms rather than inducing the EMT. The differences between our work and the previous report (Xiao et al., 2018b) could be due to the different cell types employed (colorectal versus lung), or the mutational status of *FBXW7* (knock-out versus knockdown). In fact, we have frequently observed during our project that downregulation of *FBXW7* using siRNAs is not always sufficient to achieve a resistant phenotype (data not shown), and gene deletion is required. Either way, the effects of rapamycin should be interpreted cautiously as they may be cell-type dependent.

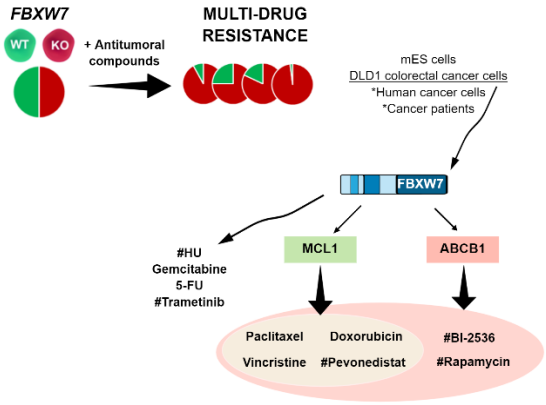

Figure 38: Involvement of FBXW7 in multi-drug resistance. *FBXW7* KO resulted in multi-drug resistance to multiple antitumoural compounds. This was demonstrated in mESCs, DLD1 colorectal cancer cell lines, and other human cancer cells, as well as in cancer patients. (*) indicates bioinformatics analysis. Resistance mediators in DLD1 cells were identified for some compounds: MCL1 and ABCB1. The mediators were drug-dependant, and for some compounds resistance was multi-factorial, while for others the resistance is still unknown. (#) indicates novel resistance to drugs identified in this Thesis.

Despite the lack of novelty of the results regarding the resistance of FBXW7-deficient cells to some other compounds, these data **supported our model of the MDR phenotype**. In the case of paclitaxel, it was rewarding to see that in our model we could reproduce the resistance phenotype observed in most studies (Wertz et al., 2011, Inuzuka et al., 2011, Yokobori et al., 2014, Gasca et al., 2016, Ishii et al., 2017) (**Figure 17**), although there are some cellular models in which the opposite was found (Ding et al., 2017, Shimizu et al., 2019). Again, this may be due to the cellular type (breast cancer disseminated tumour cells (Shimizu et al., 2019)), or to the fact that these studies were only based on correlations to FBXW7 levels (Ding et al., 2017). We also confirmed previous observations with vincristine (Wertz et al., 2011), 5-FU (Li et al., 2019, Lorenzi et al., 2016), and doxorubicin (Yu et al., 2014, Li et al., 2016, Ding et al., 2018), validated also in colorectal cancer cells. Besides, it was noteworthy that the resistance of *FBXW7*-deleted cells for gemcitabine holds in a different cell type apart from pancreatic cancer (Ishii et al., 2017, Hu et al., 2017) (**Figure 17**). All the data presented in this Thesis confirmed the role of FBXW7 deficiency as a MDR factor.

1.4. FBXW7 deficiency mechanism of MDR may be multifactorial and drug-dependent

As to the mechanism of multi-drug resistance, previous work focused on the study of single factors. However, in this Thesis we revealed that MCL1 and ABCB1 upregulation in FBXW7-deficient cells was conferring resistance to some, but not all, compounds. This means that there may be multiple factors contributing to MDR in FBXW7-deficient cells.

1.4.1. MCL1

MCL1 has already been found to **mediate the resistance** of FBXW7-deficient cells to vincristine, paclitaxel, regorafenib, HSP90 inhibitor, BCL2 inhibitor ABT-737, etoposide, camptothecin, nocodazole, gemcitabine, gefitinib, crizotinib, nedaplatin, docetaxel, and radiation (Wertz et al., 2011, Tong et al., 2017a, Tong et al., 2017b, Inuzuka et al., 2011, Ishii et al., 2017, Ye et al., 2017, Gombodorj et al., 2018, Gasca et al., 2016). In these situations, the stabilisation of this anti-apoptotic protein reduces mitochondrial priming and impedes reaching the MOMP and death by apoptosis. We confirmed that loss of MCL1 was able to re-sensitise cells to paclitaxel and vincristine, as already reported (Wertz et al., 2011, Inuzuka et al., 2011, Yokobori et al., 2014, Gasca et al., 2016, Ishii et al., 2017), and to pevonedistat and doxorubicin (**Figure 19**, **Figure 38**). Interestingly, while doxorubicin resistance of FBXW7-deficient cells had been previously linked to an activation of the EMT (Yu et al., 2014, Li et al., 2016, Ding et al., 2018), here we observed that MCL1 could also be contributing to the resistance phenotype. Nevertheless, *MCL1* deletion sensitised to only four compounds out of those tested (**Figure 19**). Therefore, there should be **other resistance mechanisms** in FBXW7-deficient cells apart from MCL1 contributing to MDR.

1.4.2. ABCB1

Besides MCL1, we found that the well-established MDR factor **ABCB1** was upregulated in DLD1 *FBXW7* KO cells (**Figure 20**), in consensus with a recent study in another cell line (Mun et al., 2020). Moreover, ABCB1 deletion re-sensitised *FBXW7* KO cells to some, but not all, treatments (**Figure 20**, **Figure 38**). The role of *ABCB1* mutations in resistance to paclitaxel, vincristine, doxorubicin, and BI2536, due to enhanced expulsion of these substrates is largely known (Hodges et al., 2011, Wolking et al., 2015, Wu et al., 2013). For pevonedistat, it has been only suggested (Ferris et al., 2020), but here we provided proofs that loss of *ABCB1* also sensitises cells to this compound.

It remains to be determined whether ABCB1 **is a substrate** of FBXW7, or if its upregulation following *FBXW7* loss is an indirect effect. In this regard, we searched for potential CPDs in the *ABCB1* sequence, but only found three possible suboptimal CPDs containing at least the Ser or Thr at position 0 and the Pro +1 position (**Annex Figure 2A**). It remains to be tested if these sequences are true CPDs and if ABCB1 is targeted by FBXW7 for its proteasomal degradation.

Importantly, there are many factors for which resistance in FBXW7-deficient cells is independent of ABCB1, such as HU, gemcitabine, 5-FU, or trametinib (**Figure 20**). These results are consistent with our observation that the resistance profile of *FBXW7*-mutant cells is even broader than that of *ABCB1*-mutant tumours (**Figure 17**), as there must be alternative mechanisms of resistance in *FBXW7*-altered cells besides those provoked by ABCB1 upregulation.

1.4.3. Cellular phenotype

Our results, together with previous reports, show that the resistance to therapies observed in FBXW7-deficient cells is **drug-dependent** and that multiple proteins can be contributing towards resistance to the same compound. We cannot exclude the possibility that there are also cell-type or mutational status dependent mechanisms of resistance in FBXW7-deficient cells.

Nevertheless, and besides the impact of specific mutations, our work here reveals that there might be a general phenomenon that increases the overall resistance to toxic therapies in FBXW7-deficient cells, namely, the **upregulation of mitochondrial processes**. Our proteomic analysis revealed that *FBXW7*-deleted cells, in addition to presenting altered levels of specific factors such as

MYC or CCNE1, also present a generalised activation of pathways related to mitochondrial metabolism and translation (**Figure 22**), which may create a pro-survival and pro-growth cellular context that enables cells to survive very different insults. Interestingly, the upregulation of mitochondrial pathways has largely been related to chemoresistance (Vazquez et al., 2013, Farnie et al., 2015, Ippolito et al., 2016, Farge et al., 2017, Xu et al., 2018, Cruz-Bermudez et al., 2019, Hirpara et al., 2019, Chen et al., 2019b, Zhang et al., 2019b, Messner et al., 2020), and even MDR (Roesch et al., 2013, Lee et al., 2017b). Moreover, and specifically, two substrates upregulated in FBXW7-deficient cells, MCL1 and C-MYC, were recently shown to induce chemoresistance via an increase in OXPHOS (Lee et al., 2017b).

All things considered, we propose that, although altered levels of factors such as ABCB1 or MCL1 might contribute to resistance to specific therapies, the MDR phenotype of FBXW7-deficient cells might be mostly related to a generalised increase in mitochondrial translation and metabolism. How this property can be **exploited in cancer therapy** will be next discussed.

2. OVERCOMING RESISTANCE

2.1. General strategies to overcome drug resistance

Once the molecular causes of a resistance to a given compound have been determined, subsequent efforts concentrate on **finding ways to overcome such resistance**. Most often, combinatorial therapies are investigated. However, in some cases, the resistance offers a novel vulnerability that can be targeted by a single targeting agent, as we will discuss later for FBXW7 deficiency.

Strategies to identify compounds that overcome resistance range from knowledge-based targeting to unbiased chemical screens for selective toxicity in resistant cells, as well as CRISPR-Cas9 screens to identify synthetic lethality partners. The field of overcoming drug resistance is rapidly moving towards the latter approaches; accordingly, CRISPR-Cas9 screens have already been performed in thousands of cell lines, and it is expected to accelerate the development of novel precision treatments (Tsherniak et al., 2017, McDonald et al., 2017, Dharia et al., 2021). In conclusion, the identification of dependencies and vulnerabilities in cancer cells that have evolved resistance to therapy is a powerful incipient field that may help to overcome the major problem of drug resistance in cancer patients (Finn et al., 2016).

2.2. Current potential strategies to overcome therapy resistance in FBXW7-deficient cells

Collectively, our work revealed the need for **effective treatments for cancer patients** presenting *FBXW7*-inactivating mutations, as they are resistant to most the current therapies.

Previous works revealed the possibility to overcome the resistance of *FBXW7* KO cells to certain compounds such as regorafenib, gefitinib and taxol, by **combining the treatments** with MCL1 inhibitors, rapamycin, or an HDAC inhibitor (Tong et al., 2017b, Xiao et al., 2018b, Yokobori et al., 2014). Rapamycin, in our hands, instead of overcoming resistance, enhanced it. Nevertheless, our data does support that MCL1 inhibitors would be a good approach to overcome resistance to compounds like microtubule poisons, doxorubicin, or pevonedistat. Besides the previously defined role of MCL1, our work here revealed that the use of ABCB1 inhibitors is also a valid approach to overcome resistance to these compounds, as well as towards PLK1 inhibitors or rapamycin. Inhibiting ABCB1 or targeting the BCL2 pathway is a recurrent approach to overcome drug resistance, and multiple inhibitors have been developed (Cornwell et al., 1987, Starling et al., 1997, Roe et al., 1999, Oltersdorf et al., 2005, van Delft et al., 2006, Souers et al., 2013, Friberg et al., 2013). Unfortunately, this strategy has shown limited results in clinical trials, especially in the case of ABCB1 inhibitors (Baer et al., 2002, Gruber et al., 2003, Pusztai et al., 2005, Fox et al., 2015).

Other authors have reported the action of several **single agents** that seemed to target *FBXW7*-altered cells, but most were in contradiction with other reports (Izumi et al., 2017, Ding et al., 2017, Galindo-Moreno et al., 2019, Honma et al., 2019, Shimizu et al., 2019, Cui et al., 2020) or have been

only shown to work in a specific cellular context (Inuzuka et al., 2011, Takeishi et al., 2013, He et al., 2013, Urick and Bell, 2018, Fiore et al., 2019) or cell line (Davis et al., 2018). Among others, a recent screen identified 11 compounds to which FBXW7-deficient cells could be specifically sensitive (Hundley et al., 2021). However, as mentioned, we know that FBXW7-deficient cells are not sensitive, but rather resistant, at least to PLK1 inhibition. It remains to be explored how FBXW7-deficient cells respond to the rest of the predicted compounds. Furthermore, and as we have seen in this work, these strategies are cell- and treatment-dependent and, thus, their usefulness is limited to very specific contexts. For these reasons, we believe that the identification of a general strategy that exploits the essence of the resistant phenotype and that is able to selectively kill FBXW7-deficient tumours may be a better therapeutic approach than looking for combinatorial treatments that may recurrently face resistance.

2.3. Novel ideas to overcome therapy resistance in FBXW7-deficient cells

Besides combinatorial strategies, several **targeted strategies** have been envisioned as a potential treatment for FBXW7-deficient tumours, and include (1) small-molecule agonists that can increase FBXW7-substrate binding affinity, (2) the targeting of FBXW7 regulators specially FBXW7-related deubiquitylases, (3) the therapeutic targeting of downstream oncoproteins and (4), the discovery of synthetic-lethal strategies (Davis et al., 2014b, Xu et al., 2016) (**Figure 39**).

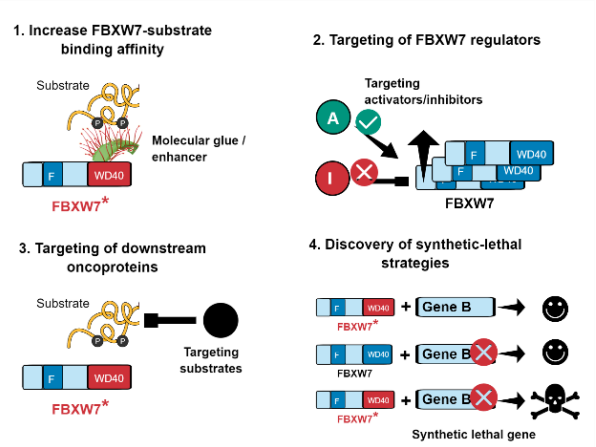

Figure 39: Novel ideas to overcome therapy resistance in FBXW7-deficient cells. Four different strategies to target FBXW7-deficient tumours are (1) molecular glues or enhancers that can increase FBXW7-substrate binding affinity, (2) the targeting of FBXW7 activators (A) or inhibitors (I), (3) the targeting of downstream substrates of FBXW7, and (4) the discovery of synthetic-lethal strategies. FBXW7* (with the WD40 domain in red) indicates that *FBXW7* is mutated or deleted. F-box motif (F), Phosphorylation (P).

2.3.1. Increase FBXW7-substrate binding affinity

Regarding the first approach, some point mutations in the WD substrate-recognition motifs of FBXW7 lead to decreased affinity for substrates. Therefore, tumours carrying these mutations could benefit from the development of small-molecule agonists that increase the binding affinity by acting as a **molecular glue**. In recent years, substantial progress has been made in the field of molecular glues with the development of PROteolysis-Targeting Chimeras (PROTACs) (Sakamoto et al., 2001, Lai and Crews, 2017, Mayor-Ruiz et al., 2020), that in principle could allow the targeting for degradation of any protein of interest, including those traditionally categorised as undruggable. This system is based on bridging two small molecules, one recognising the substrate and another binding to the E3 ubiquitin ligase, thereby bringing the substrate in close proximity with the E3 protein, promoting its ubiquitylation and degradation.

For *FBXW7* mutations, a simpler approach could be used, by using a linker molecule that would act as an **enhancer of the naturally occurring interaction** (**Figure 39**). An example of such agonists can be found in the nature: the plant hormone auxin, which functions as a molecular glue between an F-box protein and its substrates (Gray et al., 2001, Tan et al., 2007). Similarly, enhancers of the interaction between β-catenin and its cognate E3 ligase, $SCF^{\beta\text{-}TrCP}$, were recently developed (Simonetta et al., 2019). Moreover, the discovery of an inhibitor of the yeast orthologue of FBXW7, Cdc4, suggest that the WD40 domain of F-box mammalian proteins may be generally accessible to allosteric modulation by small molecules (Orlicky et al., 2010). Hence, directing drug discovery and development to those classes of molecules represent an attractive strategy for targeting *FBXW7*-mutant tumours.

2.3.2. Targeting of FBXW7 regulators

An alternative approach would be to **stabilise FBXW7** (**Figure 39**), especially for tumours presenting low levels of FBXW7. In principle, this could be achieved by inhibiting the transcriptional inhibitor of FBXW7α (Balamurugan et al., 2010), C/EBPδ. However, as C/EBPδ is also a known tumour suppressor, the global effects of this strategy are unpredictable. Other ways to increase FBXW7 levels could be potentially targeting its epigenetic silencing by inhibiting PRMT5, or decreasing its protein product destabilisation by inhibiting ERK/MAPK kinases (Ji et al., 2015, Zhang et al., 2020a), or by PLK1 (Xiao et al., 2016). Actions of other regulators, such as the deubiquitylase USP28, might be more complicated, as this protein stabilises FBXW7 by reversing its self-ubiquitylation, but simultaneously also reverses FBXW7-dependent substrate ubiquitylation (Popov et al., 2007, Schulein-Volk et al., 2014).

Of note, for the few cases in which decreasing the levels of FBXW7 could be a vulnerability for the tumour, as in the case of non-dividing leukaemia-initiating cells (Takeishi et al., 2013); **enhancing the actions of negative regulators** of FBXW7 may be an interesting possibility. For these cases, a direct protein inhibitor of FBXW7 has been recently described, STYX (Reiterer et al., 2017, Liu et al., 2020), although its potential for cancer therapy remains to be addressed.

2.3.3. Targeting of downstream oncoproteins

Regarding the downstream oncoproteins, we believe that targeting only one substrate may not be enough, due to the alteration of many others, as we have seen in the case of drug resistance. Moreover, most of the more relevant substrates are **difficult to target**. For instance, C-MYC has generally been regarded as undruggable, mainly due to lack of defined pocket domains and a narrow therapeutic window caused by on-target toxicity in normal tissues (McKeown and Bradner, 2014). MYC/MAX heterodimerisation disrupters, while displaying potent anti-tumoural effects, are dependent on MYC degradation for their efficacy (Han et al., 2019). Therefore, *FBXW7*-altered tumours are expected to be refractory to these novel therapeutic inhibitors. The recently discovered synthetic lethality between CCNE1 amplification with PKMYT1 kinase inhibition may be potentially more interesting (Gallo et al., 2021). Given that FBXW7-deficient tumours present high levels of CCNE1, this could render them sensitive to PKMYT1 inhibition.

2.3.4. Discovery of synthetic-lethal strategies

The example of the CCNE1/PKYMT1 interaction adds to the recent interest in the discovery of **synthetic-lethal strategies**, which has been greatly facilitated by the use of CRISPR-Cas9 screens in isogenic cell lines (Mengwasser et al., 2019, DeWeirdt et al., 2020, Gallo et al., 2021). In this regard, a competitive loss-of-function CRISPR screen in the isogenic pair of *FBXW7* KO and WT cells, could allow the identification of mutations that are selectively lethal for *FBXW7* KO cells (**Figure 39**). Moreover, the performance of CRISPR screens in thousands of cancer cell lines have unravelled many tumour dependencies. These types of studies have allowed, for example, the discovery of the Werner syndrome ATP-dependent helicase (WRN), as a synthetic lethal target in tumours with microsatellite instability (Behan et al., 2019). Of note, the same study also identified WRN as a strong Pan-Cancer synthetic lethal target in *FBXW7*-mutant cell lines, together with many other weaker unknown dependencies in colorectal cancer and Pan-Cancer. In addition, many other Big Data computational efforts may be relevant to lead the discovery of novel FBXW7-deficient cells vulnerabilities. One example is the DepMap Consortium (Chan et al., 2019, Dharia et al., 2021), which has merged tumour features, dependencies (based on CRISPR and RNAi screens), and drug sensitivity data, to allow the identification of novel synthetic lethal interactions and faster the development of innovative cancer treatments. According to DepMap (https://depmap.org/portal/), the three top co-dependencies for FBXW7 for all tumour types are C-MYC, MED23 and KLF10, which is consistent with our data on C-MYC and validates the power of this strategy.

2.3.5. This Thesis approach

In this Thesis, we tried to identify single agents that produce selective toxicity in *FBXW7*-depleted cells, for which we used **two independent approaches** (**Figure 40**): (1) proteomics, to identify pathways that are selectively altered in FBXW7-deficient cells, and (2) chemical screens. Interestingly, while the molecules identified in these two approaches did not seem similar at a first glance, further work revealed that they all converged at the ISR, reinforcing the value of these strategies.

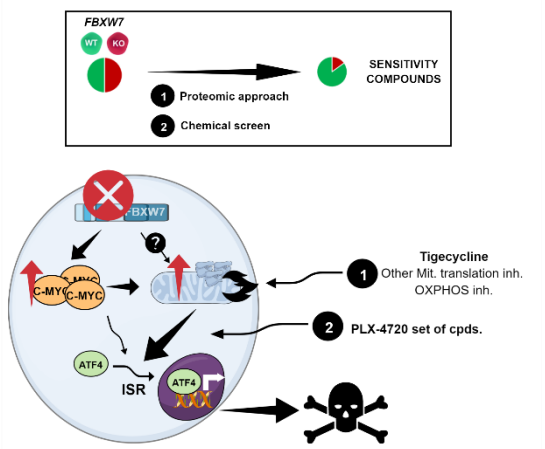

Figure 40: Strategies to selectively kill FBXW7-deficient cells developed in this Thesis. *FBXW7* KO cells were found to overexpress mitochondrial proteins, especially those involved in mitochondrial translation. This effect was dependent on C-MYC (although there may be other factors involved, marked with a "?" sign), as well as a slight activation of the ISR pathway, represented by the translocation of ATF4 to the nucleus. Targeting the mitochondria with (1) tigecycline and other mitochondrial translation and OXPHOS inhibitors generated mitochondrial damage that converged on hyperactivation of the ISR. These compounds were identified by a proteomic approach to selectively kill *FBXW7* KO cells. The use of (2) a set of a PLX-4720 compounds identified by a chemical screen also resulted in the hyperactivation of the ISR. ATF4 translation upon extreme activation of the ISR leads to cell death, specifically in *FBXW7* KO tumours.

2.4. Final considerations to overcome therapy resistance in FBXW7-deficient cells

There are two final considerations regarding any compound with the prospect to target FBXW7-deficient cells. First, the efficacy of compounds with the ability to overcome the resistance of FBXW7-deficient tumours are expected to be also effective in patients presenting tumours with reduced levels of FBXW7 due to **mutations in regulators of FBXW7**.

Secondly, most studies, including ours, are based on *FBXW7*-deletion models. However, data coming from mouse studies indicate that we may expect differences between FBXW7 **deletion and point mutations** (Davis et al., 2014a, Davis et al., 2011). Therefore, it will be interesting to test whether the antitumoural effects of tigecycline, and the other single-agents identified as selectively toxic for *FBXW7*-depleted tumours hold true in *FBXW7*-point-mutation models. This can be achieved by the use of cell lines containing *FBXW7* point-mutations, or by generating knock-in cellular models encompassing the most frequent point-mutations present in cancer patients.

3. TARGETING MITOCHONDRIAL TRANSLATION

3.1. Targeting the mitochondria to overcome resistance in FBXW7-deficient cells

The identification of pathways that could be exploited to kill FBXW7-deficient cells motivated a comparison of WT and *FBXW7* KO proteomes. Interestingly, we found a generalised **upregulation of mitochondrial proteins and processes** in the mutant cells (**Figure 22-24**). Whether this increase in OXPHOS proteins led to a functional increase of mitochondrial respiration is still to be determined. In any case, the presence of more fused mitochondria, as seen in FBXW7-deficient cells (**Figure 25**), has been related to higher dependence on OXPHOS metabolism (Yao et al., 2019, Dai and Jiang, 2019). Of note, the increased number of fused mitochondria has also been observed upon C-MYC overexpression (Graves et al., 2012), which, as previously mentioned, is a hallmark of *FBXW7* depletion. Surprisingly, one manuscript reported lower number of fused mitochondria upon *FBXW7* downregulation by siRNAs (Abbate et al., 2018), although these results are contrary to what we and many others have linked to FBXW7.

In contrast to the roles of FBXW7 in proliferation and differentiation, the links to mitochondrial function have been barely studied. It was only recently revealed that *FBXW7* lead to an enhanced mitochondrial gene transcriptional program in melanoma (Abbate et al., 2018) and in pan-cancer signatures (Davis et al., 2018). However, here we single out the specific significance of **mitochondrial translation** among the many upregulated mitochondrial processes (**Figure 22**). This overexpression of

mitochondrial translation proteins is present in many tumours (Sotgia et al., 2012, Kim et al., 2017a). Moreover, this process has been shown to be driven by several pro-tumoural events such as the loss of *RB1* (Jones et al., 2016), or C-MYC overexpression (Skrtic et al., 2011, D'Andrea et al., 2016). Our results here add FBXW7 deficiency to the list of mutations linked to increased mitochondrial translation and contribute to lengthen the list of evidences that contradict Warburg's original hypothesis (Warburg, 1956), namely the universal downregulation of mitochondrial OXPHOS in tumours.

Interestingly, recent work already indicated mitochondrial hyperactivation in *FBXW7*-mutant melanoma cells, mediated by the upregulation of MITF (Abbate et al., 2018). However, here we found that this response is **mediated by C-MYC** (**Figure 26**). C-MYC coordinates a general mitochondrial transcriptional programme (Li et al., 2005), and is a well-characterised FBXW7 substrate (Yada et al., 2004, Welcker et al., 2004b). Therefore, it was straight-forward to hypothesise that *FBXW7* KO cells could present an accumulation of C-MYC that activates mitochondrial metabolism.

The fact that C-MYC depletion does not fully rescue the toxicity of tigecycline in FBXW7-deficient cells could be related to an incomplete depletion of C-MYC following RNA interference, nevertheless, we cannot discard the **possible contribution of other factors**. For instance, the master regulator of mitochondrial metabolism and global inducer of mitochondrial gene expression PGC1α is an FBXW7 substrate (Olson et al., 2008, Vazquez et al., 2013). In addition, MITF is able to induce PGC1α (Haq et al., 2013) and, hence, the effect could also be related to an upregulation of MITF, as reported in melanoma (Abbate et al., 2018). There are other FBXW7 substrates that are known to regulate mitochondrial gene expression, such as SREBP1 (Sundqvist et al., 2005) and MCL1 (Inuzuka et al., 2011, Wertz et al., 2011). SREBP1 knockdown has been recently shown to decrease OXPHOS (Ruiz et al., 2020); and MCL1, independently of its anti-apoptotic functions, was shown to cooperate with C-MYC to drive OXPHOS upregulation (Lee et al., 2017b). The possible contribution of all of these factors to the sensitivity of FBXW7-deficient cells to tigecycline remains yet to be tested.

Regardless of the mechanism, in this Thesis we proved that the genetic or pharmacological inhibition of mitochondrial translation machinery **preferentially targets FBXW7-deficient cells** (**Figure 27**), as previously shown for MYC-overexpressing tumours (D'Andrea et al., 2016, Oran et al., 2016, Ravà et al., 2018, Sheth et al., 2014). The toxicity was not restricted to mitochondrial translation inhibitors, but was also observed with mitochondrial poisons or by the genetic inhibition of OXPHOS complexes (**Figure 28**). To our knowledge, this is the first time that *FBXW7*-deficient cells have been successfully targeted by using different inhibitors of mitochondrial processes. In agreement with our results, a recent CRISPR-Cas9 screen reported the presence of *FBXW7*-targeting sgRNAs among the sensitising mutations against the mitochondrial electron chain complex II inhibitor, TTFA (Hundley et al., 2021); although this sensitivity was not further validated. Likewise, the upregulation of mitochondrial metabolism found in *FBXW7*-depleted melanoma cells was not further explored as a targeting strategy (Abbate et al., 2018). Instead, the authors suggested using the expression of mitochondrial proteins as biomarkers of prognostic value of *FBXW7*-mutant tumours in melanoma cancer patients. In a related work, the authors reported an overexpression of OXPHOS components in *FBXW7*-mutated cells in all cancer types, although they then only focused on colorectal cancer and did not exploit this property for the targeting of the mutant cells (Davis et al., 2018). Our study is the first in capitalising on this knowledge, and providing proof of principle of the value of targeting mitochondrial metabolism, and more specifically translation, for killing FBXW7-deficient cells.

3.2. Clinical use of tigecycline

Tigecycline was approved for treating bacterial infections in 2005, b, the FDA delivered a black box warning to the use of tigecycline in 2010, due to the increased risk of death compared to other antibiotics (Dixit et al., 2014). As a result, the use of tigecycline is restricted to infections that present resistance to more frequently used antibiotics. Besides its use in microbiology, there is only one **phase I clinical trial** that has examined the efficacy of tigecycline for cancer treatment, specifically in AML. Despite proven to be safe, none of the patients presented a noticeable response to the tigecycline treatment (Reed et al., 2016). This was mostly attributed to the short half-life of the drug, that can now

be solved using a novel formulation that extends its stability from 9.5 hours to a week (Jitkova et al., 2014).

Two other clinical trials will test soon the efficacy of tigecycline in urogenital cancer (NCT03962920) and in CML (NCT02883036). It is yet to be seen whether tigecycline may finally reach phase II and III clinical trials and be approved for clinical practice. We should have in mind that tigecycline exert its effects by targeting the mitochondrial ribosome of all cells, which might complicate its possible clinical use and further studies are needed to identify whether a therapeutic window exists. Our work adds FBXW7-deficient tumours as another type that could **benefit from the clinical use of tigecycline in oncology**. In any case, we are aware that tigecycline is a broad-spectrum approach to target mitochondrial translation and further efforts are needed to develop more selective agents.

3.3. New strategies to target mitochondrial translation

The development of novel compounds, or the improvement of the current antibiotics targeting mitochondrial translation could improve the anticancer effects that have been observed with tigecycline. An interesting candidate would be the recently discovered inhibitors of mitochondrial transcription, IMTs (Bonekamp et al., 2020). Despite these candidates, strategies to **discover novel mitochondrial translation inhibitors** would open up new families in this relatively small chemical class. One such approach could be through conducting unbiased chemical screens using *in situ* imaging of mitochondrial translation as a read-out. Recently, a method to visualise and quantify global mitochondrial translation was developed, using specific labelling of mitochondrial-translated factors with a non-canonical amino acid that is coupled to fluorescent proteins through chemo-selective, bio-orthogonal 'click-it' reactions (Estell et al., 2017). A simpler approach could be to analyse individual mitochondrial-encoded proteins. However, for large screens, tagging these proteins with a fluorescent reporter would be desirable, although it will display extra difficulties, such as the challenge of transporting RNAs and the Cas9 into mitochondria, or the fact that linearized mtDNA is rapidly degraded, occasioning heteroplasmic shifts that favour uncut mtDNA genomes (Gammage et al., 2018, Peeva et al., 2018, Nissanka et al., 2018). Only recently, a method to efficiently generate a knock-in in mtDNA has been reported (Bian et al., 2019), that could be adapted for these purposes.

Another possibility would be to **enhance the efficacy of the currently used agents** by modifications of the compounds that increase their selective binding to mitochondrial ribosomes. Indeed, there are multiple differences between bacterial and mitochondrial ribosomes, which can be exploited for the development of such compounds. A first requirement would be to find the specific sequence that is bound by tigecycline and other antibiotics in the mitochondrial ribosome. While tigecycline is expected to bind similarly to mitoribosomes as to bacterial ribosomes, where it binds to both subunits and impedes the binding of the aminoacyl-tRNA to the acceptor site (Jenner et al., 2013, Schedlbauer et al., 2015), its exact target is unknown.

Finally, besides improving the compounds, it would also be important to do further work in **identifying the mutations that confer sensitivity** to the inhibition of mitochondrial translation. To date, no CRISPR-Cas9 screen has been performed against tigecycline or any of the most commonly repurposed antibiotics. A loss-of-function CRISPR-screen should reveal factors that modulate sensitivity to tigecycline, and, in fact, we are currently working in that direction. Independently, we could use the transcriptional signature derived from cells exposed to tigecycline to query databases of transcriptional signatures such as the Connectivity Map to search for genes and compounds eliciting similar signatures and, therefore, to identify novel strategies to target mitochondrial translation in eukaryotic cells.

4. TARGETING THE ISR

4.1. Role of the ISR in the toxicity of mitochondrial translation inhibitors

Another antibiotic targeting the mitoribosome, tedizolid, was recently proven to kill cells via an **activation of the integrated stress response** (ISR) (Sharon et al., 2019). Here, we presented that

this is also the case for tigecycline. FBXW7-deficient cells tumours had a basal upregulation of the ISR, which becomes exacerbated with tigecycline (**Figure 30**). The ISR senses and tries to mitigate the consequences of different stressors, but an excessive or prolonged ISR activation eventually causes cell death. We propose that an excessive activation ISR underlies the selective sensitivity of FBXW7-deficient cells to agents that target mitochondrial metabolism.

A remaining question is whether targeting mitochondrial metabolism is itself selectively toxic for FBXW7-deficient cells, or **whether this is due to the activation of the ISR**. Our data support the latter. Accordingly, other inducers of the ISR also showed preferential toxicity for FBXW7-deficient cells. One way to discern between both possibilities would be to find a mitochondrial poison that does not activate the ISR, which might be rather complicated to achieve, as, to date, any interference with mitochondrial processes seems to activate the ISR (Sharon et al., 2019, Chen et al., 2019b, Donati et al., 2020, Guo et al., 2020a, Fessler et al., 2020).

4.2. Discovery of novel drugs activating the ISR

During our search of compounds that selectively target FBXW7-deficient cells, we identified **another chemical family** that kills cells by activating the ISR (**Figure 32-37**). Importantly, many of these compounds are in clinical trials, or even approved, and their ability to trigger the ISR, or the consequences that this may have in cancer patients, was unknown. In the case of FBXW7-deficient cells, activation of the ISR is detrimental and, thus, the repurposing of these agents could be an interesting therapeutic approach to follow in clinical practice. However, the effect could be the opposite for other tumours. In fact, activation of the ISR has been generally considered to contribute to tumourigenic processes, due to its cytoprotective effects (Bi et al., 2005, Ye et al., 2010, Avril et al., 2017). For instance, ATF4 can potentially regulate more than 400 genes, many of which promote cell survival (Pakos-Zebrucka et al., 2016). In fact, most of the efforts to target the ISR in cancer have been made towards its inhibition rather than its activation (Foufelle and Fromenty, 2016, Walczak et al., 2019). Therapeutic targeting of the ISR should, therefore, be done with caution, as consequences of targeting ISR are not the same in all cancer types and there may be undesirable side effects (Pakos-Zebrucka et al., 2016). Thus, the clinical use of compounds with the ability to activate the ISR pathway demands a profound understanding of the molecular context.

Classic **ISR inducer agents**, such as the ER stressor tunicamycin are particularly toxic to FBXW7-deficient cells (**Figure 36**). In addition, two other ER stressors, brefeldin-A and BAPTA-AM, were among the 11 compounds that showed preferential toxicity for FBXW7-deficient cells in a recent work based on CRISPR screens (Hundley et al., 2021). Interestingly, the BCL2 inhibitor, venetoclax, was recently reported to activate the ISR and to synergise with tedizolid to kill cancer cells (Sharon et al., 2019). Taking this into account, and the fact that *FBXW7*-sgRNAs were discovered in a screen for sensitisers to venetoclax (Chen et al., 2019b), we speculate that this compound may also act similarly to the compounds defined in our study. Furthermore, we speculate that targeting the ER or any other branch of the ISR may selectively target FBXW7-deficient cells.

ER stress is the most broadly studied branch of the ISR, and there are many compounds known to generate ER stress (Foufelle and Fromenty, 2016, Walczak et al., 2019), which is sensed by PERK and other factors like ATF6 or IRE1α. Interestingly, there are several compounds, such as the sphingosine kinase inhibitors SKI-II and ABC294640, the latter being already in clinical trials, that have recently been shown to exert their toxicity via ER stress-ISR, independently of their predicted targets (Corman et al., 2021). There is also a selective PERK activator that does not elicit ER stress, CCT020312 (Stockwell et al., 2012). We speculate that these compounds might also be efficient in killing FBXW7-deficient cells.

Regardless of ER stress, the activators of the ISR by **mitochondrial stress** have been recently elucidated (Guo et al., 2020a, Fessler et al., 2020). These authors demonstrated that multiple mitochondrial poisons were able to induce the ISR via a mitochondrial stress pathway involving factors, such as OMA1, DELE1, or HRI. Other mitochondrial targeting perturbations, such as the complex I inhibitor IACS-010759 (Donati et al., 2020), depletion of a mitochondrial chaperonin (Chen et al.,

2019b), and, as mentioned, tedizolid (Sharon et al., 2019), are known to act through activation of the ISR. Similarly, despite not being directly linked to the whole ISR, multiple mitochondrial poisons or alterations of mitochondrial homeostasis, such as the overexpression of misfolded proteins in the mitochondrial matrix (known as the mitochondrial unfolded protein response) have been described to produce mitochondrial stress (Zhao et al., 2002, Vogtle, 2021). Importantly, none of the studies explored the specific ISR kinase that is activated. In our case, it remains to be tested if the mitochondrial stress pathway is involved in the excessive ISR activation of FBXW7-deficient cells and in their sensitivity to tigecycline. Of note, the proteolysis of DELE1 upon OMA1 activation, a bona-fide marker of the mitochondrial stress branch of the ISR, could be used to perform chemical screens and to identify selective activators of this pathway. For instance, a reporter cell-line containing a DELE1 construct attached to a fluorescent protein, or a HaloTag (Los et al., 2008) could serve as a reporter for the activation of mitochondrial stress, and its proteolysis and translocation to the cytosol be the read-out for performing chemical screens. This is an emergent field and possibilities for developing new agents are high.

Besides ER and mitochondrial stress, **other stressors that are known to induce the ISR** include amino acid or heme deprivation and viral infections. Potentially, all of these stressors might be relevant in the context of FBXW7 mutations; as well as activators of the kinases that sense those stresses, such as BTdCPU and related N,N'-diarylureas, which are activators of HRI (Chen et al., 2011b); histidinol, halofuginone, asparaginase, and arginine deiminase, which are GCN2 activators (Zhang et al., 2002, Bunpo et al., 2009, Keller et al., 2012, Long et al., 2013); and BEPP monohydrochloride that is a PKR activator (Hu et al., 2009). As for the latter, apart from its role in the context of viral infections, PKR is also known to be activated by siRNAs (Puthenveetil et al., 2006, Han et al., 2011). Interestingly, during our siRNA or esiRNA transfections we repeatedly noticed that in cellular mixtures transfected with control siRNAs, the percentage of *FBXW7* KO cells was diminished in comparison with untransfected cells (data not shown). One interesting possibility is that this is due to an ISR activation, driven by the detection of double-stranded RNAs of the siRNA sequences by PKR. The relationship between FBXW7-deficiency and viral infections remains mostly unexplored. There are only two reports linking FBXW7-deficiency with reduced dsRNA sensors levels and impaired antiviral responses (Song et al., 2017, Gstalder et al., 2020), but whether this relates in any way with the ISR pathway is unknown.

The number of compounds that are capable of inducing the ISR, even as an off-target, remains as a mystery. Here, we have identified some compounds displaying that property, but we believe that a **chemical screen to identify a collection of compounds activating the ISR** could be of great relevance. Firstly, because these compounds can be used or repurposed for treating certain types of malignancies that are sensible to ISR activators, such as FBXW7-deficient tumours. Secondly, because many of these compounds might already be in clinical trials, and could be exerting their antitumoural effects through this unknown response. As mentioned, for the discovery of compounds that activate the mitochondrial branch of the ISR we could use a DELE1-proteolysis-reporter cell line. Similar reporter strategies could be used for the other branches of the ISR, as has been previously done for ER stress inducers (Jeong et al., 2013, Bi et al., 2015). A chemical screen using an ATF4-luciferase reporter identified a novel inducer of the ISR (Sayers et al., 2013). A similar approach could be designed, using high-content microscopy, to detect the nuclear translocation of ATF4 using fluorescent reporters. Once again, we could also mine databases, such as the Connectivity Map (Lamb et al., 2006, Subramanian et al., 2017), to search for compounds able to induce a transcriptional signature similar to that triggered by the expression of bona-fide markers of the ISR response, such as ATF4 or CHOP (Gao et al., 2019).

An important consideration is that, many of these prospected compounds may activate the ISR indirectly, through other cellular stresses. Therefore, the development of **specific activators of the ISR kinases or effectors** may be even more effective in some contexts. We previously mentioned specific activators of the four kinases that phosphorylate eIF2α. Interestingly, eIF2α phosphorylation can also be directly targeted using inhibitors of its de-phosphorylation such as salubrinal, guanabenz, or the derivative sephin1 (Boyce et al., 2005, Das et al., 2015, Tsaytler et al., 2011, Tsaytler and Bertolotti, 2013). Discovery of other compounds presenting similar capabilities to directly activate the ISR could

be of interest for targeting tumours that are especially sensitive to ISR induction, such as those carrying *FBXW7* inactivating-mutations.

4.3. Other tumour types or diseases that may be targeted by activating the ISR

Whether **ISR hyperactivation is a general property of tumours** overexpressing mitochondrial proteins is yet unknown. C-MYC overexpressing tumours (D'Andrea et al., 2016), and RB1-deficient breast cancer (Jones et al., 2016) present an over-activation of mitochondrial translation and are extremely sensitive to tigecycline, as well as *K-RAS* mutant colorectal cancer cells (Martin et al., 2017). For C-MYC overexpression, the involvement of the ISR in sensitivity to mitochondrial targeting compounds has already been described (Sharon et al., 2019, Donati et al., 2020). Several additional cancer-related events such as *H-Ras*^{V12} mutations (Telang et al., 2007, Yao et al., 2019), B-RAF inhibition (Haq et al., 2013), overexpression of PGC1α or MITF (Vazquez et al., 2013), *PTEN* loss (Naguib et al., 2018), or MCL1 overexpression (Lee et al., 2017b) have also been related to mitochondrial metabolism. Exploring whether this property provides a vulnerability that can maximise the efficacy of cancer therapies is an interesting possibility.

Besides their usefulness in cancer, the discovery of novel compounds that activate the ISR may be **beneficial for the treatment of other human diseases**. Specifically, in diseases where protein misfolding plays a role in the pathogenesis, like some degenerative diseases, the activation of the ISR could be essential to allow the cells to slow down translation and recover homeostasis. Consistently, guanabenz, sephin1, or genetic manipulations that activate the ISR, have been shown to wield beneficial effects in animal models of traumatic brain injury (Dash et al., 2015), multiple sclerosis (Way et al., 2015), Charcot–Marie–Tooth syndrome (Das et al., 2015, D'Antonio et al., 2013), or amyotrophic lateral sclerosis (Wang et al., 2014a, Jiang et al., 2014, Das et al., 2015). In diabetes, the consequences of chronic ER stress were attenuated with the use of salubrinal, which protects cells from death (Krokowski et al., 2013). One of the most widely used treatments for diabetes, metformin, was also proposed to exert its beneficial actions, at least partially, by inducing the expression of an anti-obesity and anti-diabetes hormone through an ATF4-dependent mechanism, independently of AMPK (Kim et al., 2013). Hence, the discovery and development of novel ISR activators may have outstanding implications for the treatment of multiple human pathological conditions.

4.4. Dissecting the induction of the ISR in FBXW7-deficient cells

Our data indicate that the basal ISR upregulation found in FBXW7-deficient cells was, to an important extent, dependent on C-MYC (**Figure 36**). This is consistent with the fact that C-MYC-overexpressing cells present an enhanced ISR due to ER stress (Tameire et al., 2019), although surprisingly PERK inhibition did not rescue the phenotype. We had similar observations with the ISR activation upon treatment with tigecycline, oligomycin, and the PLX-4720 set of compounds; the toxicity was likewise not reverted by PERK inhibition (**Figure 36**). This was surprising for sorafenib, as it was previously reported as an ER stressor and activator of PERK (Holz et al., 2013). However, we have not yet identified the **upstream kinase** that mediates the increased activity of the ISR in *FBXW7* KO cells. For oligomycin and tigecycline, it is easy to speculate that this is caused by mitochondrial stress. As for the other compounds, we believe that the most probable branch may also be mitochondrial stress, based on the transcriptional signature similarity to other mitochondrial poisons. The hyperactivation of mitochondrial translation and other mitochondrial processes which are known to produce mitochondrial stress (Zhao et al., 2002, Vogtle, 2021), may be an interesting idea to explain the basal ISR activation in FBXW7-deficient cells.

A recent study showed that **mitochondrial stress** can be detected by OMA1 and signalled to the ISR through activation of the HRI kinase. Noteworthy, we observed that HRI was upregulated in *FBXW7* KO cells (**Figure 37**). While the levels of the phosphorylated protein should provide a better read-out of its activity, the presence of an increased expression of the global protein could be explain by an increased mitochondrial stress signalling in the mutant cells. However, we cannot discard the involvement of other ISR kinases. For instance, previous reports have pointed out at the activation of

the ISR by mitochondrial poisons via GCN2 (Michel et al., 2015, Mick et al., 2020), which is also upregulated in *FBXW7*-deleted cells (**Figure 37**). What is more, the notion of an universal path linking mitochondrial dysfunction to the ISR has been dissipated by evidences pointing out the existence of multiple paths that depend on the nature of the mitochondrial defect and the metabolic state of the cell (Mick et al., 2020). Cell death upon mitochondrial stress was also proposed to occur independently of any of the core ISR kinases, occurring by a direct activation of ATF4 and CHOP, via the mitochondrial unfolded protein response (Munch and Harper, 2016). However, another study clearly demonstrated that even these type of stressors, previously attributed to the mitochondrial unfolded protein response, are inducers of the ATF4 pathway via the activation of the ISR (Quirós et al., 2017). Nevertheless, in that very same study, individual knock-outs of all four eIF2α kinases following mitochondrial inhibition, surprisingly, did not lead to a substantial reduction of eIF2α phosphorylation, suggesting a possible interplay of all of them (Quirós et al., 2017). Therefore, identifying the exact kinase and mechanism triggering mitochondrial stress responses upon different drug treatments may be extremely challenging due to the interconnectivity and overlap of the different branches of the ISR.

We should also bear in mind that some of the **ISR pathway mediators are actually substrates of FBXW7**. For instance, two ER stress sensors, BBF2H7 and OASIS (Yumimoto et al., 2013), are known to be degraded by FBXW7. While the expression of these two proteins remained unaltered in our DLD1 *FBXW7*-depleted (proteomics data), we observed an increased expression of GCN2 and HRI, particularly the latter. Remarkably, we could detect suboptimal CPDs in all four ISR kinases (**Annex Figure 2B-E**). In fact, the first possible CPD sequence found in HRI kinase (“TPEKE”) has been proposed as a new FBXW7 degron in a recent bioinformatic analysis (Martínez-Jiménez et al., 2019). More research in this direction could illuminate if these ISR kinases are true substrates of FBXW7, or their overexpression is indirect. Noteworthy, β-TrCP, another SCF protein, is a known degrader of ATF4 (Lassot et al., 2001). It is thus possible that FBXW7 might also promote the degradation of ATF4 and/or other effectors of the ISR.

Regardless of the role played by the different upstream factors, what seems clear is that the **downstream effector** that mediates the toxic consequences of activating the ISR in FBXW7-deficient cells is most probably CHOP (**Figure 37**). Overexpression of this pro-apoptotic factor upon exposure to tigecycline and to the other inducers of the ISR used in this study, especially in FBXW7-deficient tumours, may reduce the mitochondrial priming threshold and prompt the induction of the MOMP. Indeed, OXPHOS complex I inhibition lowers the apoptotic threshold via ISR-dependent activation of CHOP in MYC-driven lymphomas (Donati et al., 2020). For tedizolid, suppression of glycolytic capacity was reported as the mechanism of cell death (Sharon et al., 2019). Although we did not investigate the possible role of this metabolic shift after ISR activation, we believe that the effect of CHOP induction is substantial enough to support its primary role in mediating the selective death in FBXW7-deficient cells upon ISR activation.

In **summary**, we have here revealed that the inactivation of *FBXW7* provides a multi-drug resistant phenotype that limits the efficacy of the majority of anticancer drugs. We subsequently discovered that the hyper-activation of mitochondrial metabolism leads to an activation of the ISR in FBXW7-deficient cells, which can be exploited for their selective killing. Moreover, we have identified specific novel compounds that are preferentially toxic for FBXW7-deficient cells, which invariably activate the ISR. Based on our findings, we propose that ISR activation emerges as an exciting possibility in cancer therapy, and that this approach can help to overcome the MDR of FBXW7-deficient tumours.

Conclusions / Conclusiones

1. Los cribados genómicos de pérdida de función con CRISPR-Cas9 en mESCs facilitan la identificación de nuevas mutaciones relacionadas con resistencia, como *Ptptn2* y *Fbxw7*, siendo el último un hallazgo recurrente en múltiples cribados.
2. La deleción de *FBXW7* produce resistencia a múltiples fármacos en mESCs y líneas celulares humanas de cáncer.
3. Los niveles bajos de FBXW7 están asociados con una pobre respuesta a terapias en pacientes de cáncer.
4. El mecanismo de resistencia en células deficientes para FBXW7 está mediado por múltiples dianas como MCL1 y ABCB1, y la multi-resistencia no es debida a un único factor.
5. Dos comparaciones independientes de proteómica entre células WT y deficientes para FBXW7 revelaron una sobre-regulación de la traducción mitocondrial y otros procesos mitocondriales en células con alteraciones en *FBXW7*.
6. La inhibición de la traducción mitocondrial con el antibiótico tigeciclina y otras estrategias genéticas y farmacológicas cuya diana es la función mitocondrial, son selectivamente tóxicas para células deficientes para FBXW7.
7. Los xenotransplantes de tumores deficientes para FBXW7 son resistentes al tratamiento con paclitaxel, pero son selectivamente eliminados con tigeciclina.
8. El mecanismo de acción detrás de la citotoxicidad preferencial de la tigeciclina en células deficientes para FBXW7 es dependiente de la sobre-regulación de C-MYC y de la activación de la ISR.
9. Un cribado farmacológico dirigido identificó un grupo de compuestos que eliminaban selectivamente las células deficientes para FBXW7, activando todos la ISR.
10. La híper-activación de la ISR es una vulnerabilidad que puede ser explotada para eliminar selectivamente las células deficientes para FBXW7.

1. Loss-of-function CRISPR-Cas9 genome-wide screens in mESCs enable the identification of novel resistance-related mutations such as the loss of *Ptptn2* or *Fbxw7*, the latter being a recurrent hit in multiple screens.
2. *FBXW7* deletion leads to multi-drug resistance in mESCs and human cancer cell lines.
3. Low levels of FBXW7 are associated with a poor response to therapy in cancer patients.
4. Drug resistance in FBXW7-deficient cells is mediated by multiple targets, such as MCL1 and ABCB1, and the multi-drug resistance is not due to a single factor.
5. Two independent proteomic comparisons between WT and FBXW7-deficient cells revealed a generalised upregulation of mitochondrial translation and other mitochondrial processes in FBXW7-deficient cells.
6. Inhibition of mitochondrial translation, by repurposing the antibiotic tigecycline or targeting mitochondrial function by genetic or pharmacological strategies, is selectively toxic for FBXW7-deficient cells.
7. FBXW7-deficient xenografts are resistant to treatment with paclitaxel, but are selectively targeted by tigecycline.
8. The mechanism of action behind the preferential cytotoxicity of tigecycline for FBXW7-deficient cancer cells depends on the upregulation of C-MYC and on the activation of the ISR.
9. A focused chemical screen identifies additional compounds selectively killing *FBXW7*-deficient cells, all of which activate the ISR.
10. The hyperactivation of the ISR is a vulnerability that can be exploited to selectively target *FBXW7*-deficient cells.

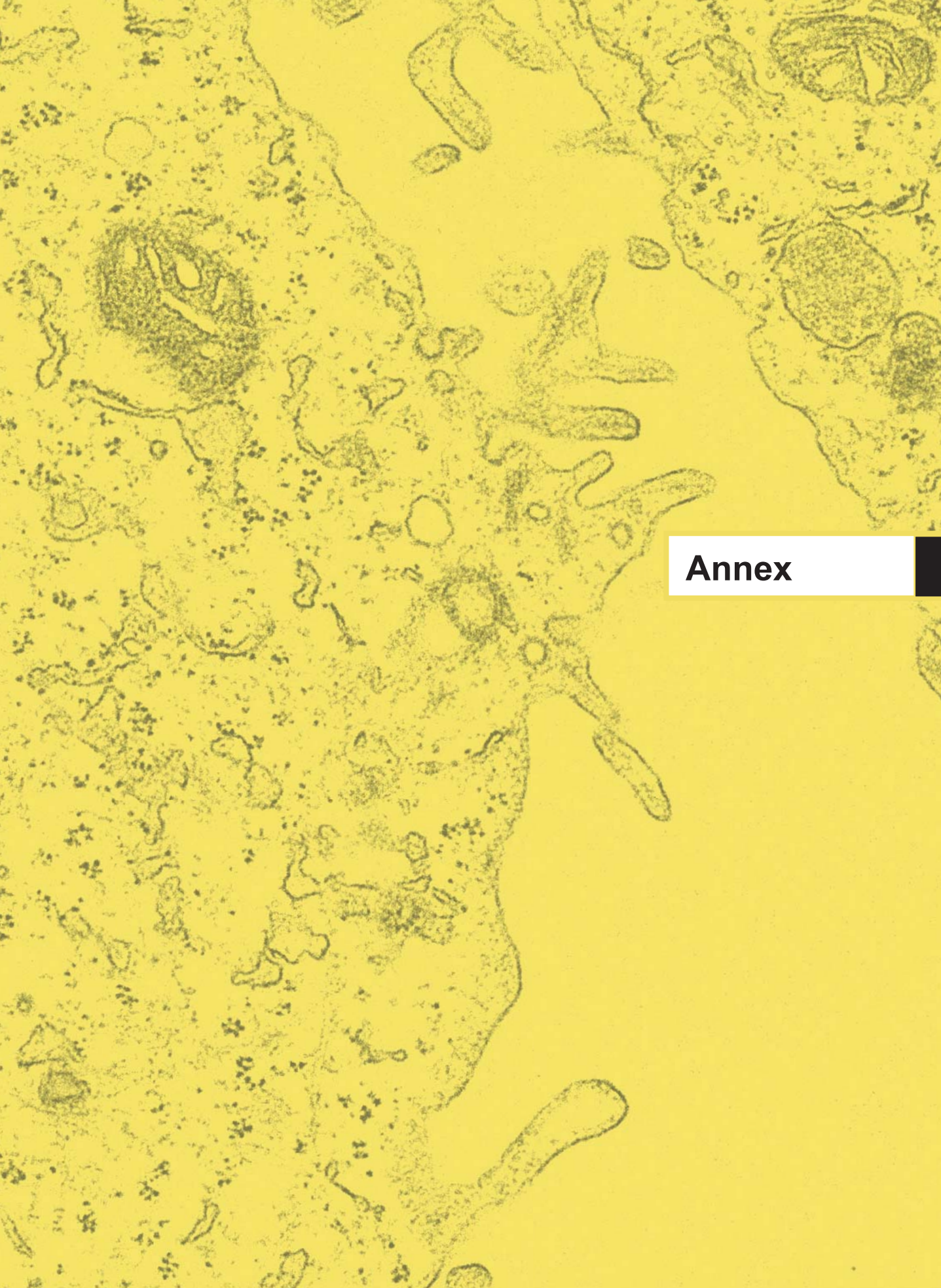

Annex

1. ANNEX FIGURES

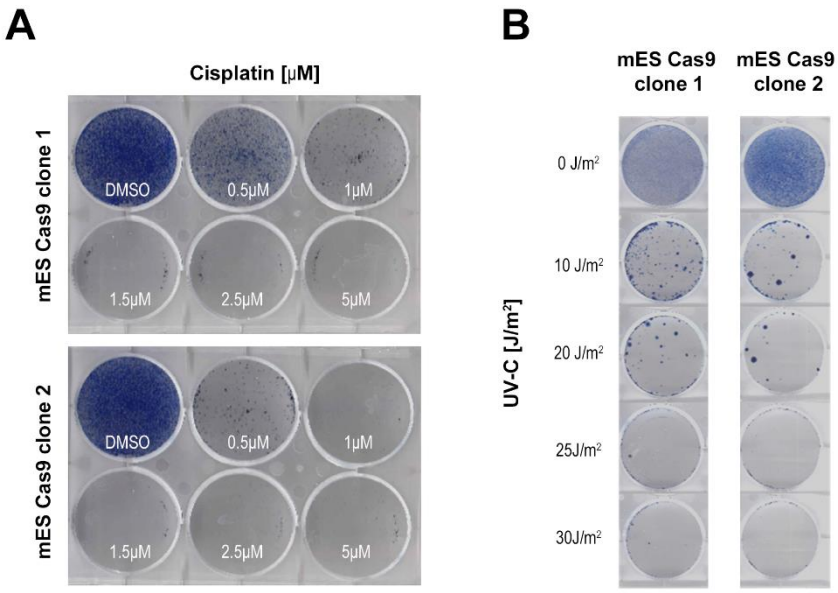

Annex Figure 1: Lethal doses of cisplatin and UV-C light in mES Cas9 clones. (**A**) Clonogenic assay of mES Cas9 clones 1 and 2 exposed to different doses of cisplatin (µM). (**B**) Clonogenic assay of mES Cas9 clones 1 and 2 exposed to different doses of UV-C radiation (J/m^2).

Optimal CPD

φ, X, φ, φ, φ, **T/S**, **P**, P, X, **T/S/D/E**

Positions -5 to +4

A- ABCB1

MDLEGDRNGGAKKKNFFKLNNKSEKDKKEKKPTVSVFSMFRYSNWLDKLYMVVGTLAAIIHGAGLPLMMLVFGEMTDIFANAG
NLEDLMSNITNRSDINDTGFFMNLEEDMTRYAYYYSGIGAGVLVAAYIQVSFWCLAAGRQIHKIRKQFFHAIMRQEIGWFDVHDV
GELNTRLTDDVSKINEGIGDKIGMFFQSMATFFTGFIVGFTRGWKLTLVILAI**SP**VLGLSAAVWAKILSSFTDKELLAYAKAGAVAE
EVLAAIRTVIAFGGQKKELERYNKNLEEAKRIGIKKAITANISIGAAFLLIYASYALAFWYGTTLVLSGEYSIGQVLTVFFSVLIGAFSV
GQA**SP**SIEAFANARGAAYEIFKIIDNKPSIDSYSKSGHKPDNIKGNLEFRNVHFSYPSRKEVKILKGLNLKVQSGQTVALVGNSGC
GKSTTVQLMQRLYDPTEGMVSVDGQDIRTINVRFLREIIGVVSQEPVLFATTIAENIRYGRENVTMDEIEKAVKEANAYDFIMKLPH
KFDTLVGERGAQLSGGQKQRIAIARALVRNPKILLLDEATSALDTESEAVVQVALDKARKGRTTIVIAHRLSTVRNADVIAGFDDG
VIVEKGNHDELMKEKGIYFKLVTMQTAGNEVELENAADESKSEIDALEMSSNDSRSSLIRKRSTRRSVRGSQAQDRKLSTKEALD
ESIPPVSFWRIMKLNLTEWPYFVVGVFCAIINGGLQPAFAIIFSKIIGVFTRIDDPETKRQNSNLFSLLFLALGIISFITFFLQGFTFGKA
GEILTKRLRYMVFRSMLRQDVSWFDDPKNTTGALTTRLANDAAQVKGAIGSRLAVITQNIANLGTGIIISFIYGWQLTLLLLAIVPIIAI
AGVVEMKMLSGQALKDKKELEGSGKIATEAIENFRTVVSLTQEQKFEHMYAQSLQVPYRNSLRKAHIFGITFSFTQAMMYFSYA
GCFRFGAYLVAHKLMSFEDVLLVFSAVVFGAMAVGQVSSFAPDYAKAKISAAHIIMIIEK**TP**LI**D**SYSTEGLMPNTLEGNVTFGEV
VFNYPTRPDIPVLQGLSLEVKKGQTLALVGSSGCGKSTVVQLLERFYDPLAGKVLLDGKEIKRLNVQWLRAHLGIVSQEPILFDCS
IAENIAYGDNSRVVSQEEIVRAAKEANIHAFIESLPNKYSTKVGDKGTQLSGGQKQRIAIARALVRQPHILLLDEATSALDTESEKV
VQEALDKAREGRTCIVIAHRLSTIQNADLIVVFQNGRVKEHGTHQQLLAQKGIYFSMVSVQAGTKRQ

B- GCN2

MAGGRGAPGRGRDEPPESYPQRQDHELQALEAIYGADFQDLRPDACGPVKEPPEINLVLYPQGLTGEEVYVKVDLRVKCPPTY
PDVVPEIELKNAKGLSNESVNLLKSRLEELAKKHCGEVMIFELAYHVQSFLSEHNKPPPKSFHEEMLERRAQEEQQRLLEAKRKE
EQEQREILHEIQRRKEEIKEEKKRKEMAKQERLEIASLSNQDHTSKKDPGGHRTAAILHGG**SP**DFVGNGKHRANSSGRSRRER
QYSVCNSED**SP**TSCEILYFNMG**SP**DQLMVHKGKCIGSDEQLGKLVYNALETATGGFVLLYEWVLQWQKKMGPFLTSQEKEKID
KCKKQIQGTETEFNSLVKLSHPNVVRYLAMNLKEQDDSIVVDILVEHISGVSLAAHLSHSGPIPVHQLRRYTAQLLSGLDYLHSNS
VVHKVLSASNVLVDAEGTVKITDYSISKRLADICKEDVFEQTRVRFSDNALPYKTGKKGDVWRLGLLLLSLSQGQECGEYPVTIPS
DLPADFQDFLKKCVCLDDKERW**SP**QQLLKHSFINPQPKMPLVEQ**SP**EDSEGQDYVETVIPSNRLPSAAFFSETQRQFSRYFIEF
EELQLLGKGAFGAVIKVQNKLDGCCYAVKRIPINPASRQFRRIKGEVTLLSRLHHENIVRYYNAWIERHERPAGPG**TP**PP**D**SGPL
AKDDRAARGQPASDTDGLDSVEAAAPPPILSSSVEWSTSGERSASARFPATGPGSSDDEDDDEDEHGGVFSQSFLPASDSES
DIIFDNEDENSKSQNQDEDCNEKNGCHESEPSVTTEAVHYLYIQMEYCEKSTLRDTIDQGLYRDTVRLWRLFREILDGLAYIHEK
GMIHRDLKPVNIFLDSDDHVKIGDFGLATDHLAFSADSKQDDQTGDLIKSDPSGHLTGMVGTALYV**SP**EVQGSTKSAYNQKVDL
FSLGIIFFEMSYHPMVTASERIFVLNQLRDPT**SP**KFPEDFDDGEHAKQKSVISWLLNHDPAKRPTATELLKSELLPPPQMEESELH
EVLHHTLTNVDGKAYRTMMAQIFSQRI**SP**AI**D**YTYDSDILKGNFSIRTAKMQQHVCETIIRIFKRHGAVQLC**TP**LLLPRNRQIYEHN
EAALFMDHSGMLVMLPFDLRIPFARYVARNNILNLKRYCIERVFRPRKLDRFHPKELLECAFDIVTSTTNSFLPTAEIIYTIYEIIQEF
PALQERNYSIYLNHTMLLKAILLHCGIPEDKLSQVYIILYDAVTEKLTRREVEAKFCNLSLSSNSLCRLYKFIEQKGDLQDLMPTINS
LIKQKTGIAQLVKYGLKDLEEVVGLLKKLGIKLQVLINLGLVYKVQQHNGIIFQFVAFIKRRQRAVPEILAAGGRYDLLIPQFRGPQA
LGPVPTAIGVSIAIDKISAAVLNMEESVTISSCDLLVVSVGQMSMSRAINLTQKLWTAGITAEIMYDWSQSQEELQEYCRHHEITYV
ALVSDKEGSHVKVKSFEKERQTEKRVLETELVDHVLQKLRTKVTDERNGREASDNLAVQNLKGSFSNASGLFEIHGATVVPIVSV
LAPEKLSASTRRRYETQVQTRLQTSLANLHQKSSEIEILAVDLPKETILQFLSLEWDADEQAFNTTVKQLLSRLPKQRYLKLVCDEI
YNIKVEKKVSVLFLYSYRDDYYRILF

C- HRI

MQGGNSGVRKREEEGDGAGAVAAPPAIDFPAEGPDPEYDESDVPAEIQVLKEPLQQPTFPFAVANQLLLVSLLEHLSHVHEPNP
LRSRQVFKLLCQTFIKMGLLSSFTCSDEFSSLRLHHNRAITHLMRSAKERVRQDPCEDISRIQKIRSREVALEAQTSRYLNEFEEL
AILGKGGYGRVYKVRNKLDGQYYAIKKILIKGATKTVCMKVLREVKVLAGLQHPNIVGYHTAWIEHVHVIQPRADRAAIELPSLEVL
SDQEEDREQCGVKNDESSSSSIIFAEP**TP**EKE**E**KRFGESDTENQNNKSVKYTTNLVIRESGELESTLELQENGLAGLSASSIVEQQ
LPLRRNSHLEESFTSTEESSEENVNFLGQTEAQYHLMLHIQMQLCELSLWDWIVERNKRGREYVDESACPYVMANVATKIFQEL
VEGVFYIHNMGIVHRDLKPRNIFLHGPDQQVKIGDFGLACTDILQKNTDWTN**R**NGKR**TP**T**H**T**S**RVGTCLYA**SP**EQLEGSEYDAK
SDMYSLGVVLLELFQPFGTEERAEVLTGLRTGQLPESLRKRCPVQAKYIQHLTRRNSSQRPSAIQLLQSELFQNSGNVNLTLQM
KIIEQEKEIAELKKQLNLLSQDKGVRDDGKDGGVG

D- PERK

MERAI**SP**GLLVRALLLLLLLLGLAARTVAAGRARGLPAPTAEAAFGLGAAAAPTSATRVPAAGAVAAAEVTVEDAEALPAAAGEQ
EPRGPEPDDETELRPRGRSLVIISTLDGRIAALDPENHGKKQWDLDVGSGSLVSSSLSKPEVFGNKMIIPSLDGALFQWDQDRE
SMETVPFTVESLLESSYKFGDDVVLVGGKSLTTYGLSAYSGKVRYICSALGCRQWDSDEMEQEEDILLLQRTQKTVRAVGPRSG
NEKWNFSVGHFELRYIPDMETRAGFIESTFKPNENTEESKIISDVEEQEAAIMDIVIKVSVADWKVMAFSKKGGHLEWEYQFC**TP**I
A**S**AWLLKDGKVIPISLFDDTSYTSNDDVLEDEEDIVEAARGATENSVYLGMYRGQLYLQSSVRIS**E**KFPS**SP**KALESVTNENAIIP
LPTIKW**K**PLI**H**SPSRT**TP**VLVGSDEFDKCLSNDKFSHEEYSNGALSILQYPYDNGYYLPYYKRERNKRSTQITVRFLDNPHYNKNIR
KKDPVLLLHWWKEIVATILFCIIATTFIVRRLFHPHPHRQRKESETQCQTENKYDSVSGEANDSSWNDIKNSGYISRYLTDFEPIQC
LGRGGFGVVFEAKNKVDDCNYAIKRIRLPNRELAREKVMREVKALAKLEHPGIVRYFNAWLEAPPEKWQEKMDEIWLKDESTD
W**P**LS**SPSP**MDAPSVKIRRMDPFATKEHIEIIAP**SP**QRSRSFSVGISCDQTSSSESQF**SPL**EFSGMDHEDISESVDAAYNLQDSCL

TDCDVEDGTMDGNDEGHSFELCPSEA**SP**YVRSRERTSSSIVFEDSGCDNASSKEEPKTNRLHIGNHCANKLTAFKPTSSKSSS
EATLSI**SP**PRPTTLSLDLTKNTTEKLQPS**SP**KVYLYIQMQLCRKENLKDWMNGRCTIEERERSVCLHIFLQIAEAVEFLHSKGLMH
RDLKPSNIFFTMDDVVKVGDFGLVTAMDQDEEEQTVL**TP**MPAYARHTGQVGTKLYM**SP**EQIHGNSYSHKVDIFSLGLILFELLYP
FSTQMERVRTLTDVRNLKFPPLFTQKYPCEYVMVQDMLSPSPMERPEAINIIENAVFEDLDFPGKTVLRQRSRSLSSSGTKHSR
QSNNSH**SP**LP**S**N

E- PKR

MAGDLSAGFFMEELNTYRQKQGVVLKYQELPNSGPPHDRRFTFQVIIDGREFPEGEGRSKKEAKNAAAKLAVEILNKEKKAV**SP**
LLLTTTNSSEGLSMGNYIGLINRIAQKKRLTVNYEQCASGVHGPEGFHYKCKMGQKEYSIGTGSTKQEAKQLAAKLAYLQILSEE
TSVKSDYLSSGSFATTCESQSNSLVTSTLASESSSEGDFSADTSEINSNSDSLNSSSLLMNGLRNNQRKAKRSLAPRFDLPDMK
ETKYTVDKRFGMDFKEIELIGSGGFGQVFKAKHRIDGKTYVIKRVKYNNEKAEREVKALAKLDHVNIVHYNGCWDGFDYDPETS
DDSLESSDYDPENSKNSSRSKTKCLFIQMEFCDKGTLEQWIEKRRGEKLDKVLALELFEQITKGVDYIHSKKLIHRDLKPSNIFLVD
TKQVKIGDFGLVTSLKNDGKRTRSKGTLRYM**SP**EQISSQDYGKEVDLYALGLILAELLHVCDTAFETSKFFTDLRDGIISDIFDKKE
KTLLQKLLSKKPEDRPNTSEILRTLTVWKK**SP**EKNERHTC

Annex Figure 2: Possible CPDs in ABCB1 and ISR kinases. (**A-E**) Possible CPDs in ABCB1 (A) and ISR kinases (B-E) are marked. The optimal CPD is: φ, X, φ, φ, φ, T/S, P, P, X, T/S/D/E (positions -5 to +4). Basic positions are 0 T/S, +1 P and +4 T/S/D/E, and are marked in bold. In yellow are highlighted the amino acids that correspond with the canonical CPD, in blue those that do not, and X amino acids are not highlighted. CPDs with more than two changes in the canonical CPD are considered a suboptimal CPD.

2. ANNEX TABLES

Annex Table 1: CRISPR-Cas9 screen types, applications and representative examples. Related to Introduction 1.3.3.

Type	Applications	Representative examples
Negative selection screens	Pathways negative regulators of	- LPS-cytokine response (Parnas et al., 2015) - PARKIN (Potting et al., 2018) - PD-L1 expression (Burr et al., 2017) - T-cell responses (Huang et al., 2021)
	Essential fitness genes	- In human ES cells (Shalem et al., 2014, Ihry et al., 2019, Mair et al., 2019) - In different human cancer cells (Shalem et al., 2014, Wang et al., 2014b, Gilbert et al., 2014, Hart et al., 2015, Yamauchi et al., 2018, Zhang et al., 2019c, MacLeod et al., 2019) - For oxidative phosphorylation (Arroyo et al., 2016) - Under different oxygen tensions (Jain et al., 2020)
	Map tumour dependencies	- Combinatorial screens for synthetic lethalities (Wong et al., 2016, Han et al., 2017, Shen et al., 2017, Najm et al., 2018) - CRISPR screens in thousands of cancer cell lines (Chan et al., 2019, Behan et al., 2019, Dharia et al., 2021)
	Therapy-sensitiser mutations in **Annex Table 2**	
Positive selection screens	Pathways positive regulators of	- LPS-cytokine response (Parnas et al., 2015) - PARKIN (Potting et al., 2018) - Hedgehog signalling (Breslow et al., 2018) - EMT transition (McFaline-Figueroa et al., 2019) - mTORC1 (Condon et al., 2021)
	Drivers of tumourigenesis in	- Lung cancer growth and metastasis (Chen et al., 2015) - Colorectal cancer (Takeda et al., 2019) - KRAS-mutated tumours (Huang et al., 2019) - TP53-deficient cells (Drainas et al., 2020) - Melanoma (Gautron et al., 2021)
	Therapy-resistant mutations in **Annex Table 2**	

Annex Table 2: Drug sensitivity or resistance CRISPR-Cas9 screens representative examples. Related to Introduction 1.3.3. Some relevant genes/mutations discovered through each screen are displayed inside parentheses. Knock-out (KO), overexpression (OE).

Drug type	Drug	Representative examples of resistance or sensitivity
Classic chemotherapy	6-thioguanine	Resistance (MMR genes KO) (Wang et al., 2014b, Koike-Yusa et al., 2014)
	Etoposide	Resistance (*CDK6* KO) (Wang et al., 2014b)
	Cisplatin	Resistance & sensitivity (*ZNRF3* KO as sensitiser) (Ko and Li, 2019)
	Temozolomide	Resistance & sensitivity (*MCM8/9* and *ZC3H7A* KO as sensitisers) (MacLeod et al., 2019)
	Gemcitabine	Sensitivity (*SH3D21* KO (Masoudi et al., 2019); *PRMT5* KO (Wei et al., 2020))
Targeted therapies	BRAF inhibitors	Resistance (*NF2* KO (Shalem et al., 2014); GPCRs and ITG receptors OE (Konermann et al., 2015); *SMAD3, BIRC3*, and *SLC9A5* OE (Gautron et al., 2021); *DOT1L* KO (Torre et al., 2021))
	EGFR inhibitors	Resistance & sensitivity (*RIC8A* KO as sensitiser, *ARIH2* KO in resistance) (Zeng et al., 2019)
	Multi-kinase inhibitors	Resistance & sensitivity (*KEAP1* KO in resistance (Zheng et al., 2019); *PHGDH* as sensitiser (Wei et al., 2019))
	Imatinib	Resistance (*BCR-ABL1* point mutations) (Ma et al., 2017)
	Venetoclax	Resistance & sensitivity (mitochondrial genes as *CLPB* KO as sensitisers) (Chen et al., 2019b)
	ATR inhibitors	Resistance (*CDC25A* KO) (Ruiz et al., 2016) / Sensitivity (*POLE3/4* KO) (Hustedt et al., 2019)
Immunotherapy	Anti-PD-1	Resistance & sensitivity (*PTPN2* KO as sensitiser) (Manguso et al., 2017)
	T-cell killing	Resistance & sensitivity (PBAF components KO as sensitisers (Pan et al., 2018); *FITM2* and autophagy components KO as sensitisers (Lawson et al., 2020))
Multiple compounds screens	- 9 chemotherapeutic agents to find antagonistic pleiotropy (PRC2–NSD2/3-mediated MYC axis as BRD4i resistant but BCL2i sensitivity) (Lin et al., 2020) - 27 genotoxic agents to find novel DNA repair genes (*ERCC6L2, ELOF1*) and drug response (Olivieri et al., 2020) - 41 compounds response upon ubiquitin pathway loss (*FBXO42* KO in mitosis inhibitors sensitivity) (Hundley et al., 2021) - DNA damaging agents, PARPi and BH3 mimetics base editing screens for specific mutations (Cuella-Martin et al., 2021, Hanna et al., 2021)	

Annex Table 3: FBXW7 substrates. Related to Introduction 2.1.2. CPD type, substrate and reference are displayed in alphabetical order in each CPD type. (*) pseudo-substrate; (**) not degraded.

CPD type	Substrate	Reference
Optimal CPD	BBF2H7	(Yumimoto et al., 2013)
	C-MYC	(Yada et al., 2004, Welcker et al., 2004a, Welcker et al., 2004b)
	Cyclin E1	(Koepp et al., 2001, Moberg et al., 2001, Strohmaier et al., 2001)
	DISC1	(Yalla et al., 2018)
	GATA2	(Nakajima et al., 2015)
	GATA3	(Kitagawa et al., 2014)
	KLF2	(Wang et al., 2013a)
	NFκB2	(Busino et al., 2012, Arabi et al., 2012, Fukushima et al., 2012)
	N-MYC	(Otto et al., 2009)
	NONO	(Alfano et al., 2018)
	OASIS	(Yumimoto et al., 2013)
	PGC1α	(Olson et al., 2008)
Semi-optimal CPD	Aurora-A	(Kwon et al., 2012)
	BLM	(Kharat et al., 2016)
	BRAF	(de la Cova and Greenwald, 2012)
	BRG1	(Huang et al., 2018)
	C/EBPα	(Bengoechea-Alonso and Ericsson, 2010b)
	C/EBPδ	(Balamurugan et al., 2013)
	CCDC6	(Zhao et al., 2012)
	CDX2	(Kumar et al., 2016)
	C-JUN	(Wei et al., 2005)
	C-MYB	(Kitagawa et al., 2009)
	CRY2	(Fang et al., 2015)
	Cyclin E2	(Klotz et al., 2009)
	DAB2IP	(Dai et al., 2014)
	DEK	(Babaei-Jadidi et al., 2011)
	EBP2*	(Welcker et al., 2011)
	EGLN2	(Takada et al., 2017)
	EZH2	(Jin et al., 2017)
	FAAP20	(Wang et al., 2016a)
	Fetuin-A	(Zhao et al., 2018)
	FOXM1	(Chen et al., 2016)
	GFI1	(Kuai et al., 2019)
	GRα	(Malyukova et al., 2013)
	HSF1	(Kourtis et al., 2015)
	IRF1	(Garvin et al., 2019)
	JUNB	(Pérez-Benavente et al., 2013)
	KLF5	(Liu et al., 2010, Zhao et al., 2010)
	KLF7	(Sugiyama et al., 2019)
	KLF10	(Yu et al., 2018)
	KLF13	(Kim et al., 2012)
	LSD1*	(Lan et al., 2019)
	MCL1	(Inuzuka et al., 2011, Wertz et al., 2011)
	MED13	(Davis et al., 2013)
	MED13L	(Davis et al., 2013)
	MyRF	(Nakayama et al., 2018)

CPD type	Substrate	Reference
Semi-optimal CPD	NCOA3	(Wu et al., 2007)
	NGN3	(Sancho et al., 2014)
	NOTCH1	(Oberg et al., 2001, Wu et al., 2001, Gupta-Rossi et al., 2001, Maruyama et al., 2001)
	NOTCH2	Conservation with NOTCH1 (Yumimoto and Nakayama, 2020)
	NOTCH3	Conservation with NOTCH1 (Yumimoto and Nakayama, 2020)
	NOTCH4	Conservation with NOTCH1 (Yumimoto and Nakayama, 2020)
	NRF1	(Biswas et al., 2011)
	P53	(Cui et al., 2020)
	Presenilin-1	(Li et al., 2002)
	REV-ERBα	(Zhao et al., 2016)
	RICTOR	(Koo et al., 2015)
	SETD3	(Cheng et al., 2017)
	SHOC2	(Xie et al., 2019)
	SNAIL	(Xiao et al., 2018a)
	SOX9	(Hong et al., 2016, Suryo Rahmanto et al., 2016)
	SOX10	(Lv et al., 2015)
	SREBP1	(Sundqvist et al., 2005)
	SREBP2	(Sundqvist et al., 2005)
	TGIF1	(Bengoechea-Alonso and Ericsson, 2010a)
	ZNF322A	(Liao et al., 2017)
	NF1	(Tan et al., 2011)
Others	Aurora-B	(Teng et al., 2012)
	ENO1	(Zhan et al., 2015)
	EYA1	(Sun and Li, 2014)
	GCSFR	(Lochab et al., 2013)
	HIF1α	(Cassavaugh et al., 2011)
	MTDH	(Chen et al., 2018)
	MTOR	(Mao et al., 2008)
	NDE1	(Maskey et al., 2015)
	NDRG1	(Gasser et al., 2014)
	NRF3	(Kannan et al., 2015)
	P63	(Galli et al., 2010)
	PLK1	(Giráldez et al., 2014)
	PLK2	Conservation with PLK1 (Yumimoto and Nakayama, 2020)
	PLK3	Conservation with PLK1 (Yumimoto and Nakayama, 2020)
	PLK4	Conservation with PLK1 (Yumimoto and Nakayama, 2020)
	PTPN11	(Song et al., 2017)
	RCAN1	(Lee et al., 2012)
	RHOGDIα	(Zhu et al., 2017)
	STAT3	(Yao et al., 2017)
	TOPOIIα	(Chen et al., 2011a)
	YAP	(Tu et al., 2014)
	ZEB2	(Li et al., 2019)
	ZFP36	(Zhang et al., 2020b)
Not degraded	XRCC4**	(Zhang et al., 2016a)
	γ-Catenin**	(Li et al., 2018b)

Annex Table 4: *FBXW7* alterations related to drug resistance. Related to Introduction 2.2.3. Studies are ordered by their mediators, and compound to which they are resistant, cancer type and *FBXW7* status. (*) is indicated for mediators that are suggested in the study, but for which there were no complete proofs for considering them as the only direct mediator. For *FBXW7* status: knock-out (KO), knock-down (KD, via siRNA, shRNAs or miRNAs), mutation (MUT) or FBXW7 up-regulation related with sensitivity (UP).

Study	Mediator	Compound	Cancer type	FBXW7 status
(Wertz et al., 2011)	MCL1	Vincristine / Taxol	Colorectal	KO
(Tong et al., 2017b)	MCL1	Regorafenib	Colorectal	KO / MUT
(Tong et al., 2017a)	MCL1	HSP90 inhibitor	Colorectal	KO / MUT
(Inuzuka et al., 2011)	MCL1	ABT-737 BCL2i / Etoposide / CPT / Taxol / Nocodazole	T-ALL	KO / MUT
(Ishii et al., 2017)	MCL1	Gemcitabine / Paclitaxel	Pancreas	KD (siRNA)
(Ye et al., 2017)	MCL1	Gefitinib / Crizotinib	Lung	KD (shRNA)
(Gombodorj et al., 2018)	MCL1*	Nedaplatin / Docetaxel / Radiation	Oesophageal	UP
(Gasca et al., 2016)	MCL1 and PLK1	Paclitaxel	Breast	KD (siRNA)
(Yu et al., 2013)	EMT – TGF-β	Cisplatin	Lung	KD (siRNA) / UP
(Xiao et al., 2018a)	EMT- SNAIL	Cisplatin / Sorafenib	Lung	KD (shRNA) / UP
(Li et al., 2016)	EMT - TWIST	Doxorubicin	Lung	KD (siRNA/shRNA)
(Li et al., 2019)	EMT – ZEB2	5-FU	Colorectal	KO
(Ding et al., 2018)	EMT pathway*	Doxorubicin	Colorectal	KD (miRNA)
(Yu et al., 2014)	EMT pathway*	Doxorubicin	Liver	KD (siRNA) / UP
(Jiang et al., 2020)	C-MYC	AURKBi	T-ALL	MUT
(Xi et al., 2016)	C-MYC	Guttiferone K	Prostate	KD (siRNA)
(O'Neil et al., 2007)	NOTCH*	γ-secretase inhibitors	T-ALL	MUT
(Zhang et al., 2017)	NOTCH*	Erlotinib	Lung	KD (miRNA/siRNA)
(Xiao et al., 2018b)	mTOR*	Gefitinib	Lung	KD (siRNA/shRNA)
(Hong et al., 2016)	SOX9	UV radiation	Colorectal	KO
(Li et al., 2015b)	P53*	Oxaliplatin	Colorectal	KO
(Fang et al., 2015)	CRY2*	Oxaliplatin	Colorectal	UP
(Song et al., 2015)	ABCB?*	Cisplatin	Nasopharyngeal	KD (siRNA)
(Hu et al., 2017)	ENT1*	Gemcitabine	Pancreas	UP
(Lorenzi et al., 2016)	-	5-FU	Colorectal	KO
(Yokobori et al., 2014)	-	Taxol	Lung	KD (siRNA)
(Eto et al., 2015)	-	Trastuzumab	Gastric	KD (miRNA)
(Lin et al., 2018)	-	Temozolamide	Glioblastoma	KD (shRNA) / UP
(Guo et al., 2020b)	-	Astragalus polysaccharide	Ovarian	KD (siRNA)
(Zhou et al., 2015)	-	Cisplatin	Gastric	KD (miRNA/siRNA) / UP

Annex Table 5: *FBXW7* alterations related to drug sensitivity. Related to Introduction 2.2.3. Studies are represented with compound to which they are sensitive, whether it rescues resistance to any compound, mediator, cancer type and *FBXW7* status. (*) is indicated for mediators that are suggested in the study, but for which there were no complete proofs for considering them as the only direct mediator. For *FBXW7* status: knock-out (KO), knock-down (KD, via siRNA, shRNAs or miRNAs), mutation (MUT), FBXW7 expression related with sensitivity (**).

Study	Compound	Resistance reversal	Mediator	Cancer type	FBXW7 status
(Tong et al., 2017b)	MCL1 inhibitors	Regorafenib	MCL1	Colorectal	KO/MUT
(Xiao et al., 2018b)	Rapamycin	Gefitinib	mTOR	Lung	KD (siRNA/shRNA)
(Yokobori et al., 2014)	MS-275	Taxol	-	Lung	KD (siRNA)
(Inuzuka et al., 2011)	Sorafenib	-	MCL1*	T-ALL	KO / MUT
(He et al., 2013)	Vorinostat HDACi	-	MCL1	Squamous CC	KD (siRNA)
(Ye et al., 2017)	Gefitinib + Oridonin	-	MCL1	Lung	KD (shRNA)
(Takeishi et al., 2013)	Imatinib	-	C-MYC	CML	KO
(Izumi et al., 2017)	Irinotecan / Oxaliplatin	-	C-MYC	LGR5+ CSC	KD (siRNA)
(Fiore et al., 2019)	N6-isopentenylad.	-	C-MYC*	Colorectal	Expression**
(Davis et al., 2018)	PHGDH inhibitor CBR5884 / TOFA acetyl-CoA carboxylase inhibitor	-	OXPHOS met.	Colorectal	KO / MUT
(Cui et al., 2020)	Radiation / Etoposide	-	P53	Colorectal / Lung	KO / siRNA
(Galindo-Moreno et al., 2019)	UV radiation	-	P53	Colorectal	KO
(Ding et al., 2017)	Cisplatin / MG132 / Paclitaxel / SAHA	-	ING5	Breast	Expression**
(Honma et al., 2019)	5-FU / Oxaliplatin / Irinotecan	-	-	Colorectal	KD (shRNA)
(Urick and Bell, 2018)	SI-2 SRCi / Dinaciclib	-	-	Endometrial	KO
(Shimizu et al., 2019)	Paclitaxel	-	-	Breast	KO

Annex Table 6: Hits obtained in the cisplatin screens in mESCs Cas9 libraries (pool). Results from the cisplatin screens at 1.5μM using mES Cas9 1 and 2 libraries. Genes identified with more than 150 reads and their number of reads are displayed.

CISPLATIN (1.5μM)			
Library 1		**Library 2**	
Genes identified	**Nº reads**	**Genes identified**	**Nº reads**
Fbxw7	362449	*Gpr176*	354821
Myh9	330392	*Pdcl*	192115
Fam115c	114294	*Tsc2*	170171
Bicd1	100892	*Tshz1*	111844
Mlf1	73840	*Lrrc10*	78165
1700029H14Rik	29063	*Rdh16*	72533
Vmn2r95	21422	*Ptgs1*	6180
2810453I06Rik	19702	*Grhl1*	4901
Epc2	15421	*U2af1l4*	3609
Ano8	12648	*Glod4*	2944
Obfc2a	12565	*Slc5a12*	2427
Git2	12555	*Pdzrn4*	2340
Fam198b	10276	*Dtnbp1*	2211
Smap2	9624	*Top2a*	1993
Gm5538	7699	*Sipa1l1*	1924
Igfn1	5353	*Arhgef6*	1837
Ttpal	4327	*Nyx*	1741
Ppfibp2	3300	*1700018F24Rik*	1701
Zfp462	3022	*Gyx*	1516
Olfr666	2870	*Fbxw7*	1465
Nr1h4	2383	*Pou5f1?*	1017
Braf	2352	*Egf*	974
Brwd1?	2023	*Lrrc57*	945
Tdrd9	1940	*Vmn2r81*	776
Glt8d1	1854	*Myh9*	656
Pou5f1?	1659	*Gm97*	618
Vmn1r71	1521	*Xiap*	588
B630005N14Rik	1511	*Obsl1*	521
Nhlrc2	1436	*Mgat1*	435
Sbf1	1423	*2310030N02Rik*	432
Ceacam16	1399	*Lypd6b*	432
4932438H23Rik	1212	*Gm4787*	424
Fbxo21	1187	*Tsga14*	359
Fabp9	1046	*Ptpn2*	340
Scp2	1039	*Asxl1*	337
H2-M2	932	*Tbck*	296
C230096C10Rik	803	*Olfr605*	279
Engase	798	*Serhl*	265
Rnf24	737	*Pcdh18*	257
C230081A13Rik	732	*Olfr1427*	253
Vmn2r66	679	*Crebbp*	238
Sugt1	658	*Fam115c*	217
Lrrc8a	557	*Bicd1*	214
Otud3	533	*Fbxw7 (2)*	178
Zfp566	524	*Mlf1*	172
Olfr549	518		
Mphosph6	501		
Skint7	464		
AF529169	372		
Papolb	319		
Dse	312		

CISPLATIN (1.5µM)			
Library 1		Library 2	
Genes identified	Nº reads	Genes identified	Nº reads
Naa30	290		
Rcan2	277		
4930568D16Rik	273		
Slc38a11	240		
Smg7	233		
Tmem111	231		
Drd1a	227		
Tmem194b	227		
Krt25	219		
Tas2r117	209		
Xrn1	188		
Prkaa1	187		
Fam122b	166		
Slc30a10	165		
Olfr459	153		

Annex Table 7: Hits obtained in the cisplatin screens in mESCs Cas9 libraries (clones). Results from the cisplatin screens using mES Cas9 1 and 2 libraries. Doses were 2µM and 2.5µM for 1 and 2, respectively. Clone number, gene identified and sgRNA sequence are displayed.

CISPLATIN (2-2.5 µM)					
Library 1 - 2 µM			Library 2 - 2.5 µM		
Clone number	Genes identified	sgRNA sequence	Clone number	Genes identified	sgRNA sequence
Clone 1	*?*	CTCAGTGATGCTGTTGATC	Clone 1	*Tbck*	AAATAGCCCTTACCCTATT
Clone 2	*Fbxw7*	AGTGTCTGAGAACGTTAGT	Clone 3	*?*	CTCAGTGATGCTGTTGATC
	Myh9	ATCCTCACCCCACGCATCA	Clone 4	*Tbck*	AAATAGCCCTTACCCTATT
Clone 3	*?*	CTCAGTGATGCTGTTGATC		*Tsga14*	GGCAAAGACAAGCCTTATC
Clone 8	*?*	CTCAGTGATGCTGTTGATC	Clone 7	*Fbxw7*	AGTGTCTGAGAACGTTAGT
	Fbxw7	AGTGTCTGAGAACGTTAGT	Clone 9	*Crebbp*	TTGCCAGTGAATCGCATGC
	Myh9	ATCCTCACCCCACGCATCA		*2310030N02 Rik*	GCACTGCGGGCCTTCAATG
Clone 11	*?*	CTCAGTGATGCTGTTGATC	Clone 10	*4933409G03 Rik*	CCAGGACAGTGGTAACTCT
	Fbxw7	AGTGTCTGAGAACGTTAGT		*Gm1673*	AGCAAGGACCTGAGCGCGG
	Myh9	ATCCTCACCCCACGCATCA	Clone 13	*Olfr605*	TGAGCAAGGCATGCATCGA
Clone 12	*?*	CTCAGTGATGCTGTTGATC	Clone 14	*Ptgs1*	CGAGAAGTACTCATGCGCC
Clone 15	*Fbxw7*	AGTGTCTGAGAACGTTAGT	Clone 15	*Rragc*	AAGATCATTTCGTAGTCAA
	Myh9	ATCCTCACCCCACGCATCA	Clone 17	*Ptsg1*	CGAGAAGTACTCATGCGCC
Clone 17	*Fbxw7*	AGTGTCTGAGAACGTTAGT		*Glod4*	CTGCAAAGCTGCATGCAAT
	Myh9	ATCCTCACCCCACGCATCA	Clone 20	*Olfr605*	TGAGCAAGGCATGCATCGA
Clone 25	*Fbxw7*	AGTGTCTGAGAACGTTAGT			
Clone 28	*Fbxw7*	AGTGTCTGAGAACGTTAGT			
	Ptpn2	GGCAGCATGTGTTCG GAAG			
Clone 32	*Fbxw7*	AGTGTCTGAGAACGTT AGT			
	Myh9	ATCCTCACCCCACGCA TCA			

Annex Table 8: Hits obtained in the UV screens in mESCs Cas9 libraries. (**A**) Results from the UV screens at 25J/m^2 using mES Cas9 2 library. Clone number, gene identified and sgRNA sequence are displayed. (**B**) Results from the UV screens at 25J/m^2 using mES Cas9 1 library. Genes identified with more than 150 reads and their number of reads are displayed.

A UV-C 25 J/m^2

Library 2

Clone number	Genes identified	sgRNA sequence	Clone number	Genes identified	sgRNA sequence
Clone 2	*Ptpn2*	GGCAGCATGTGTTCGGAAG	Clone 32	*Ptpn2*	GGCAGCATGTGTTCGGAAG
	Gm5595	ACCTGTTCTTTCATTTATT		*Nrp1*	CTCACATTGGGCGTTATTG
	?	CCAGAGGACAGCCACGACG	Clone 35	*Tbck*	AAATAGCCCTTACCCTATT
Clone 10	*Fbxw7*	AGTGTCTGAGAACGTTAGT		*Olfr605*	TGAGCAAGGCATGCATCGA
	Tsga14	GGCAAAGACAAGCCTTATC	Clone 38	*Gm4871*	AGTGCCATATTCAACTTTC
Clone 13	*Ptpn2*	GGCAGCATGTGTTCGGAAG	Clone 47	*Ptpn2 (2)*	TCACTTCCATTATACCACC
	Ptpn2 (2)	TCACTTCCATTATACCACC		*Olfr605*	TGAGCAAGGCATGCATCGA
Clone 15	*Ptpn2 (2)*	TCACTTCCATTATACCACC	Clone 53	*Tbck*	AAATAGCCCTTACCCTATT
	Olfr605	TGAGCAAGGCATGCATCGA	Clone 54	*Fbxw7 (2)*	GTGGCAACCGCATAGTTAG
Clone 16	*Ptpn2 (2)*	TCACTTCCATTATACCACC	Clone 55	*1700018F24Rik*	AGTGCCATATTCAGCTTTC
	Tsga14	GGCAAAGACAAGCCTTATC		*Tsga14*	AGTGCCATATTCAGCTTTC
Clone 17	*Ptpn2 (2)*	TCACTTCCATTATACCACC	Clone 56	*Ptpn2 (2)*	TCACTTCCATTATACCACC
	Olfr605	TGAGCAAGGCATGCATCGA		*Tbck*	AAATAGCCCTTACCCTATT
Clone 20	*Tbck*	AAATAGCCCTTACCCTATT		*Olfr605*	TGAGCAAGGCATGCATCGA
Clone 22	*Fbxw7*	AGTGTCTGAGAACGTTAGT	Clone 61	*Ubxn7*	CTTGTGCATCAAGTCGATT
	Tsga14	GGCAAAGACAAGCCTTATC		*Prkar1a*	GTCCTCCCTCGAGTCAGTA
Clone 23	*Fbxw7 (2)*	GTGGCAACCGCATAGTTAG	Clone 63	*Olfr605*	TGAGCAAGGCATGCATCGA
	Ttc3	CCAGAGGACAGTCACGACG	Clone 65	*Ttc3*	CCAGAGGACAGTCACGACG
Clone 25	*Socs3*	TTTCTTATCCGCGACAGCT	Clone 66	*Ptpn2 (3)*	CCATTTCTCTGTCATCCGT
	Gas6	TTAACTCACCTTGATATCG		*Arntl2*	TGCGTGGTCGCCCAGTGTA
Clone 29	*Fbxw7 (2)*	GTGGCAACCGCATAGTTAG	Clone 69	*Fbxw7*	AGTGTCTGAGAACGTTAGT
	1700018F24Rik	AGTGCCATATTCAGCTTTC		*Tsga14*	GGCAAAGACAAGCCTTATC
Clone 30	*Ptpn2 (3)*	CCATTTCTCTGTCATCCGT			
	Ptpn2 (4)	GCAGCATGTGTTCGGAAGT			

B UV-C 25 J/m^2

Library 1

Gene identified	Nº reads	sgRNA sequence	Gene identified	Nº reads	sgRNA sequence
Ptgs1	149217	CGAGAAGTACTCATGCGCCG	*Tmem62*	922	TGCACACCCGTCACTTCACG
Fam115c	140210	TTTGCTCAATGCTATACGCG	*Zfp534*	911	ATACTAAGTTTGGATTGTTG
Glod4	104891	CTGCAAAGCTGCATGCAATG	*Nfkbiz*	909	ATACTGGTACATTGACGCCG
Reps1	54861	GATTGCCTACGGATCTCATG	*Omg?*	908	ACTTGACTACATCACCACCG
Trp53inp1	50345	CTTGTTTCCACCTTGATAGG	*Slc15a2*	895	TTACCTTTCATGCCATAATG
Cyp3a11	42882	TTTCTCTTTCTAGGGTTTAG	*Myh9*	892	ATCCTCACCCCACGCATCAG
Fbxw7	38937	AGTGTCTGAGAACGTTAGTG	*Apc (3)*	888	GATCCTTCCCGACTTCCGTG
2200002K05Rik	37386	TGGAAGTACACTCCTAACTG	*Usp21*	869	CCTCAGGCTCTCGTCCTAGG
Fbxw7 (3)	35081	TGGTCAGCGGTCACGGGCAG	*Nup133*	866	GCTCCCGTGGAAATCGCTAG
Ifngr1	34855	GTATTCCCAGCATACGACAG	*F3*	851	CAGTGTAGGTATAGTTGGTG
A130010J15Rik	26878	CATCCTTCTGTCCGGTCGGG	*Apc (4)*	839	CTACTATCATCATGTCGATG
2810453I06Rik	25549	TGGAAAGTCACGGGCCACGG	*Efcab9*	830	GGGATGATATTTGACCTCCG

B UV-C 25 J/m²					
Library 1					
Gene identified	**Nº reads**	**sgRNA sequence**	**Gene identified**	**Nº reads**	**sgRNA sequence**
Nub1	25490	GCTATGGGATATCACGAGAG	*Cfb*	823	TTTCAAAGTCCTGCGGTCGG
1700029H14 Rik	25244	GGTGAGCCTAGAGGACGACG	*Defb21*	823	AAAAGATGCTTGAAAATTTG
Obfc2a	21965	ACAGACAGGGGATATTATTG	*Fabp4*	822	AAAGTACTCTCTGACCGGAG
Tubgcp4	21700	TTACTTTTCTAATGCGCTTT	*Mypn*	821	GATGCATGCTTCGTCTGGTG
Fbxo21	17678	TCTAACCAATTGACGTAGTG	*Scgb1a1*	817	GAATCAGAGTCTGGTTATGG
Ep300	14685	CATATGCTCGTAAAGTGGAG	*Pou4f3*	805	CGCATCACGCGGTACATCAG
Olfr749	11958	TTACCCTACCATCATGACTG	*Naa30*	791	CCAGAACTGCGACACCTCCG
Il17d	11016	CGTGTCGCCCTGGGCGTACG	*Fabp9*	783	GGAGATCTCTTTCAAGTTGG
Ccdc13	10907	CTTTCATTTTAGGGGCGTCG	*Mid2*	782	TCGCTGAATCACCGGGGCCG
Gm1673	10829	AGCAAGGACCTGAGCGCGGG	*Ccdc79*	779	TTTATTTCCGGGAAATTGGG
Slc22a19	9975	CATTTATCCGGTCTCAGGTG	*BC005561*	776	AACATAGATATCGCTTATAG
Slc22a2	9415	ACCAAATCGCCTTTACTGTG	*Epc2 (2)*	770	CGCTGAAATAGCTCGCTGTG
4933409G03 Rik	9392	CCAGGACAGTGGTAACTCTG	*1700018F24 Rik*	769	AGTGCCATATTCAGCTTTCG
Axin1	8932	GAGCTTATTCACCGTCTAGG	*Vmn1r68*	767	GCCATTACAATCAGTCATAG
Mlf1	8595	TCACGTTCTCGACGATTATG	*Prkcz*	755	TCTCTTGCAGGATATCGACG
Olfr441	8314	CCTCAGGATGAGAATTAAAG	*AU021092*	736	TGTTCCTAGTAGTTGCACCG
Lyar	7882	GTCAGAAGTACGGAGGCAAG	*3110082D06 Rik*	725	GTGTAAGTCCGAATAGAGCG
Pirt	7057	TTCCAGAAGTGAGTCTGTCG	*Nxf7*	713	CAGAGGCAATGCGAAAGTCG
Glipr1l2	6309	TTTGTCTAGATGAGTATTAG	*Hykk*	699	CCTTTAGTTCGGCATACGGG
Fbxw7 (2)	5733	GTGGCAACCGCATAGTTAGG	*Zfp518b*	698	TGACTACATCGTCAAGCACG
Elmod2	5591	GGGCCGTCAACTTTTTCGTG	*Hsd11b1*	689	CCTCTGCTCACTACATTGCG
Oct4?	5485	CTCAGTGATGCTGTTGATCG	*Ogfr*	687	GTCAGAGAGCGTCTTGTCCG
Apc	5119	GATCTGTATCCAGCCGTTCG	*Rnf2*	675	TGTTTACATCGGTTTTGCGG
Git2	4820	AAAGGGACGACGGTCGTCTG	*Col25a1*	661	TACTCCTGGCATTCCTCGGG
H2-M2	4609	CTGACGGTATGCGTGAAGTG	*Ssbp4*	651	TCTCTTTCATAGATCCGTTG
Nanog?	4245	CGTAAGTCTCATATTTCACC	*Acpl2*	639	CATAAACCGGGTCTACGGTG
Nmt1	4085	AACTGGTAGCTCCGTTTACG	*Olfr805*	632	TTACATCTTGAGCTTGATAG
Tmem136	3931	GCTACTTCATCTTCGACTTG	*Nell2*	625	ATGGAGTGCGCCAAGTCCCG
Tmem194b	3901	CGACTCACGCTTACTATGTG	*Egfl6*	618	CCAATTGCCTCAATACCCGG
Scp2	3875	CTGTTCCACTGCGGAGTAAG	*Dio3*	617	TGTCGTCTGATACGCATATG
Rbm17	3846	CTTTCTCTACAAGAGACGTG	*Nrp1 (2)*	613	TACGTGGAAGTAATCGATGG
Mrgprb1	3782	GTCATATGTACTGTGCTTTG	*Slc3a1*	610	GTTCCAATCGAGTAGGACAG
Olfr845	3757	TTGACAGCACTAATAGCCAG	*Olfr761*	608	TTTCTTTGCATCTTTTGCCG
Rictor	3597	CAATTAAGTCGAATAAATGG	*Gm14744*	606	CGCACCCTTTACATAGCTGG
Fam110b	3250	ACCTTCAGCGACTCTGCGAG	*Ephx2?*	589	CCTGTTGGTGCGTACCAGGT
Apc (2)	3224	CCGACTTCCGTAGGAGCGAG	*Olfr787*	582	ATCTTTCCACCATTAATGTG
Pde10a	3180	CGCTGCCTCGGCTCACTATG	*Nrp1*	580	CTCACATTGGGCGTTATTGG
Brwd1?	2953	GGTCTTCGAGAAGACGTTTT	*Vsig1*	579	TTCAAAGACCGAATAATTGG
Smap2	2941	ATTTCGGAGAGCTTTTCCGG	*Errfi1*	576	ATTTCAAATACGATGCTCCG
Otud3	2858	ACCGTAGCGGTAGGCGATGG	*Eif5a2*	563	CGGCTTCGTCGTGCTCAAAG
Cisd1	2727	GAAGGCATGCACCACCTTCG	*C9*	550	TGTCTTTTCGTCTCGTACCG
Lpar1	2714	CAGTCAGTCTCCGGGTATAG	*Fam65c*	544	TCCAGGTTCTCGTGCACCGG
Vmn1r71	2704	GAGAGAAGTATCACCAGATG	*Nup50*	544	AGGCAAAGCGCAGAAACGTG
2510002D24 Rik	2619	TACACCACTACTACGTCCAG	*Icos?*	534	CTGCAAAGCTGCATGTAATG
Pald1	2584	CTGCACCAGGTAGTGCTCGG	*Smad2*	533	ATATTGCCGGCTCTGGCGCG
Olfr605	2445	TGAGCAAGGCATGCATCGAG	*Tas2r117*	527	TATTCATTTGTCCACATGTG
Rcan2	2327	CTGTTTAAGAGTTTCCGACG	*D5Ertd577e*	510	CACATTTTGCTCCCTACATG
Ceacam16	2313	TTGCCTACAATTGGTACGCG	*Kcnt2*	499	TTCAGCATCTAGAACGAATG
Zfp113	2267	AGACTGACTTCTTGTTCGTG	*Myt1*	497	CTGGTTCAGGACATGTGCGG
Tdrd9	2249	CTCTTTCAGCGCTGTCCGCG	*Paqr8*	489	CTACTTTGTGGACTACGTCG

B UV-C 25 J/m²					
Library 1					
Gene identified	**Nº reads**	**sgRNA sequence**	**Gene identified**	**Nº reads**	**sgRNA sequence**
Rrp15	2225	GTCCCAGCACTCGACTCTGG	*Pde12?*	487	GATGTCTGCATTGCACGGTT
4930571K23 Rik	2141	TCATCCTTACCCAGCTTAGG	*Slc7a13*	486	TACTTTGCGTTTTCTGGCGG
Elovl3	2132	ATCTGTTGCTCATCGTTGTG	*Vmn1r78*	483	ATATTTACCGAATAATGAGG
Ppfibp2	1922	CACTCCGTAGTGTGTCGATG	*Oit1*	471	CAAACAGGCATAACCCCCAG
Nr1h4	1916	ACAGGTGAGCGCGTTGTAGG	*Necap1*	468	TTTATTGGCATCGGCTTCAG
Mtap7d3	1901	CAACTGGCGTTTTTGCTGAG	*Tmem120a?*	466	CGTCTTTGTAAGCGAACCGT
1700025E21 Rik	1858	TCTCTATTTTGTCGCTTACG	*Cldn4*	454	GCTGATGACCATAAGGGCTG
Sult1c2	1839	AGGCAGATTCAGACCTTCGG	*Dsg1c*	453	ACTCTGATCTGCAATAGTTG
Klk10	1822	TGATAGTCACGCTCGCACTG	*Ddx1*	447	AATTGGTGGCGTTGCGGCTG
Ctsq	1765	GGCAATAGAGGCTGTCGTTG	*1110054O05 Rik*	440	GGAAGTCCTTGGTAAGAGAG
Drd1a	1686	CATCCTGATTAGCGTAGCAG	*4930568D16 Rik*	437	ATGTTTTAAGTGTCCGAAGG
Braf	1679	CATAGGTACCCGCAAGATGG	*Ptpn2*	436	GGCAGCATGTGTTCGGAAGG
Lpar2	1665	AAAGGCTGGTTCCTGCGACG	*Jmjd5*	432	GTGGCTGCGCTTTTGCGGCG
Wash	1652	CAGAGCCCGCTCATCCAGTG	*Cacng3*	431	TCACTCTGCTGTTTTTCGGG
Fam198b	1642	CTTGGGTTTCACCGTGCCAG	*Ing2*	430	CTGCTGTAGGCGTTTTTTCG
Fbxo18	1582	ATGGGAACAAACGATGGCGG	*Rad51ap1*	412	GACGCCTCGAGTGTTGAAGG
Epc2	1524	ATCTGGTTGCTCGTTGTCTG	*Slc20a2*	412	GGATGGAGCTCGTCAAGATG
Smg7 (2)	1490	ACTCAGGTATACATGACCGG	*Sbf1*	410	CTCACATGTACCGTCCCATG
Jmjd7	1486	TTATGCGGACGCGGTGCGAG	*Lmbr1l*	408	ACTGGATGTAGTAGTTGCGG
Ptpn2 (2)	1393	TCACTTCCATTATACCACCG	*Myh9 (2)*	406	GGGTTGGTATTCCTCAACGG
Kat2a	1342	GCTACGGCACAACTCGCTCG	*Uchl4*	396	GGAGTAACACTGCGCACACG
Smg7 (3)	1313	TTCCTTGGTTCACTTCTCGG	*Gdap1*	394	TCCTTGTGGTTGCATAAGCG
1700074P13 Rik	1302	ACTCTCATTGACCCTCAGTG	*Slmo1*	394	TCACCGCTCGCACGAGGCCG
Csnk1a1	1260	TAACTTCCTAATGGGTATTG	*Epc2 (3)*	393	ATTACAATCGCTTGTACAAG
H2-DMb2	1217	TCAAATATCCTCAACGAACG	*Fibcd1*	375	GCAGCGAGGGTCGATGAGAG
Parp14	1211	GAGTTGTTGATTTGAGCGGG	*Enam*	374	TGTTCCCAGCGTTCGGCCCG
Krt2	1180	GCATCTCTAGTAGCGTGGCG	*Olfr102*	373	CACAGGCCAGATCCAACAAG
Syt4	1110	ATTTTGATGTACGGGTCAGG	*Fv1*	372	TCATCCTTTTCGAGCGGTAG
Trmt12	1101	CTGAGCAGGTGAACGAACCG	*Prkaa1*	366	ACTTCTGGTGCGGCATAATG
Fbxo18 (2)	1086	TTTGAAGGGCATTAACGTCG	*Apba1*	361	GCGGAGGCCGAGCACGTCGG
Dhtkd1	1080	GCTTAAGCCTCGCATTTTAG	*Sbp*	359	GACTGATGTCTATGGAACCG
Olfr31	1047	GCTAGTTGATTATCTTCTAG	*BC048502*	351	TGGGTGAGTAATCTTTTGAG
Olfr922	1029	TGGTAACAGTGTACAACAGG	*2610029G23 Rik*	349	CCTGATATTGAAATGGCTTG
Cst10	1026	TTCACTATAGGTTGTGGCTG	*Ubqlnl*	346	ATTGTTGGTTACCAGGTTCG
Bcl7b	1016	CCTCCTTGCTATCTGTCACG	*Fbxw7 (4)*	340	GGCTCAGACTTGTCGATACG
Fkbp5	1002	GGGCTTTGTCGATCCCAATG	*Esco2*	338	GCTTATAGGTCACTTGATTG
Endou	996	AGCAGCGATGCCGTCACTAG	*Engase*	337	GTAACCACCCATCATGTCGG
Hoxb2	989	CCGAGGTCGGATCACCATCG	*Ick*	336	TTCCAGATCGGACACCCACG
Zp2	985	CACACGCTATCTGCGCACCG	*Slc38a8*	324	GACAGATGCTGCGTAGCCCG
Satl1	972	TTGTTTTCATATCGGAAGTG	*Htr3b*	319	CAATACAGCATGGACGCAAG
Olfr606	966	TCTACATTATTGGGGTAACG	*Slco4a1*	316	GCTGGCGATGAGCCCGCTCG
Npsr1	959	GCTATTCCGATGAGGACTTG	*Olfr173*	309	ATTTTAGGGGTAATAGCACG
Tagap	947	CCCCACAGATGATCGACAAG	*Ermap*	307	TGTGGTCTTGCCCGTCTTGG
Ly6g5c	936	CTAGGTGATACCAAGCTCGG	*Rnf7*	306	GTTTTCAGCTTGACATCGAG
Tbck	922	AAATAGCCCTTACCCTATTG	*Muc15*	300	ATCACCAGAAAACTTTACTG

Annex Tables 9-11: Proteomics, Kinome Scan and CMap data.

Annex Table 9 displays the complete list of the proteins upregulated in DLD1 *FBXW7* KO cells and their log Fold Change (FC), p-value (pval), and their log FC in mESCs. The proteins in bold indicate FBXW7 substrates. In the mESCs, the upregulated proteins are shown in a scale of reds and the downregulated ones in green.

Annex Table 10 contains the Kinome Scan for PLX-4720, ID:20024, downloaded from the following link: https://lincs.hms.harvard.edu/db/datasets/20024/ (Fabian et al., 2005). Proteins ID, proteins name, and their corresponding % Control at 10 µM of PLX-4720 are displayed.

Annex Table 11 contains the complete CMap analysis of PLX-4720, downloaded from the following link: https://clue.io/connection?url=macchiato.clue.io/builds/touchstone/v1.1/arfs/BRD-K16478699. Rank, Score, Type of perturbagen, Compounds ID and name, and their mechanism of action (MOA, showed as description) are displayed. The different perturbagen categories displayed in Type are the following: compounds (cp), gene knock-down (kd), gene overexpression (oe), and CMap class (cc).

These files can be found in the following link:

https://www.dropbox.com/sh/peeyxtkadibdmut/AAC_43s5doV19aKykpGHP2XJa?dl=0

Bibliography

AAS, T., BØRRESEN, A.-L., GEISLER, S., SMITH-SØRENSEN, B., JOHNSEN, H., VARHAUG, J. E., AKSLEN, L. A. & LØNNING, P. E. 1996. Specific P53 mutations are associated with de novo resistance to doxorubicin in breast cancer patients. *Nature Medicine,* 2**,** 811-814.

ABBATE, F., BADAL, B., MENDELSON, K., AYDIN, I. T., SERASINGHE, M. N., IQBAL, R., MOHAMMED, J. N., SOLOVYOV, A., GREENBAUM, B. D., CHIPUK, J. E. & CELEBI, J. T. 2018. FBXW7 regulates a mitochondrial transcription program by modulating MITF. *Pigment Cell Melanoma Res,* 31**,** 636-640.

ABOLHODA, A., WILSON, A. E., ROSS, H., DANENBERG, P. V., BURT, M. & SCOTTO, K. W. 1999. Rapid activation of MDR1 gene expression in human metastatic sarcoma after in vivo exposure to doxorubicin. *Clinical Cancer Research,* 5**,** 3352-3356.

ACEVEDO-AROZENA, A., WELLS, S., POTTER, P., KELLY, M., COX, R. D. & BROWN, S. D. 2008. ENU mutagenesis, a way forward to understand gene function. *Annu Rev Genomics Hum Genet,* 9**,** 49-69.

ADLER, S., PELLIZZER, C., HARENG, L., HARTUNG, T. & BREMER, S. 2008. First steps in establishing a developmental toxicity test method based on human embryonic stem cells. *Toxicology in Vitro,* 22**,** 200-211.

AKHOONDI, S., SUN, D., VON DER LEHR, N., APOSTOLIDOU, S., KLOTZ, K., MALJUKOVA, A., CEPEDA, D., FIEGL, H., DAFOU, D., MARTH, C., MUELLER-HOLZNER, E., CORCORAN, M., DAGNELL, M., NEJAD, S. Z., NAYER, B. N., ZALI, M. R., HANSSON, J., EGYHAZI, S., PETERSSON, F., SANGFELT, P., NORDGREN, H., GRANDER, D., REED, S. I., WIDSCHWENDTER, M., SANGFELT, O. & SPRUCK, C. 2007. FBXW7/hCDC4 is a general tumor suppressor in human cancer. *Cancer Res,* 67**,** 9006-9012.

ALASIRI, G., JIRAMONGKOL, Y., ZONA, S., FAN, L. Y., MAHMUD, Z., GONG, G., LEE, H. J. & LAM, E. W. 2019. Regulation of PERK expression by FOXO3: a vulnerability of drug-resistant cancer cells. *Oncogene,* 38**,** 6382-6398.

ALBERTS, B., JOHNSON, A., LEWIS, J., RAFF, M., ROBERTS, K. & WALTER, P. 2005. *Molecular Biology of the Cell*, New York: Garland Publishing Inc.

ALFANO, L., CAPORASO, A., ALTIERI, A., COSTA, C., FORTE, I. M., IANNUZZI, C. A., BARONE, D., ESPOSITO, L., GIORDANO, A. & PENTIMALLI, F. 2018. NONO ubiquitination is mediated by FBW7 and GSK3 beta via a degron lost upon chromosomal rearrangement in cancer. *J Cell Physiol,* 233**,** 4338-4344.

ALLEY, M. C., SCUDIERO, D. A., MONKS, A., HURSEY, M. L., CZERWINSKI, M. J., FINE, D. L., ABBOTT, B. J., MAYO, J. G., SHOEMAKER, R. H. & BOYD, M. R. 1988. Feasibility of Drug Screening with Panels of Human Tumor Cell Lines Using a Microculture Tetrazolium Assay. *Cancer Research,* 48**,** 589-601.

ANDERSON, S., BANKIER, A. T., BARRELL, B. G., DE BRUIJN, M. H. L., COULSON, A. R., DROUIN, J., EPERON, I. C., NIERLICH, D. P., ROE, B. A., SANGER, F., SCHREIER, P. H., SMITH, A. J. H., STADEN, R. & YOUNG, I. G. 1981. Sequence and organization of the human mitochondrial genome. *Nature,* 290**,** 457-465.

ANDRAE, B., KEMETLI, L., SPAREN, P., SILFVERDAL, L., STRANDER, B., RYD, W., DILLNER, J. & TORNBERG, S. 2008. Screening-preventable cervical cancer risks: evidence from a nationwide audit in Sweden. *J Natl Cancer Inst,* 100**,** 622-629.

ARABI, A., ULLAH, K., BRANCA, R. M., JOHANSSON, J., BANDARRA, D., HANEKLAUS, M., FU, J., ARIES, I., NILSSON, P., DEN BOER, M. L., POKROVSKAJA, K., GRANDER, D., XIAO, G., ROCHA, S., LEHTIO, J. & SANGFELT, O. 2012. Proteomic screen reveals Fbw7 as a modulator of the NF-kappaB pathway. *Nat Commun,* 3**,** 976.

ARITA, H., NAGATA, M., YOSHIDA, R., MATSUOKA, Y., HIROSUE, A., KAWAHARA, K., SAKATA, J., NAKASHIMA, H., KOJIMA, T., TOYA, R., MURAKAMI, R., HIRAKI, A., SHINOHARA, M. & NAKAYAMA, H. 2017. FBXW7 expression affects the response to chemoradiotherapy and overall survival among patients with oral squamous cell carcinoma: A single-center retrospective study. *Tumour Biol,* 39**,** 1010428317731771.

ARROYO, J. D., JOURDAIN, A. A., CALVO, S. E., BALLARANO, C. A., DOENCH, J. G., ROOT, D. E. & MOOTHA, V. K. 2016. A Genome-wide CRISPR Death Screen Identifies Genes Essential for Oxidative Phosphorylation. *Cell Metab,* 24**,** 875-885.

ARUMUGAM, T., RAMACHANDRAN, V., FOURNIER, K. F., WANG, H., MARQUIS, L., ABBRUZZESE, J. L., GALLICK, G. E., LOGSDON, C. D., MCCONKEY, D. J. & CHOI, W. 2009. Epithelial to mesenchymal transition contributes to drug resistance in pancreatic cancer. *Cancer Res,* 69**,** 5820-5828.

ASHTON, T. M., MCKENNA, W. G., KUNZ-SCHUGHART, L. A. & HIGGINS, G. S. 2018. Oxidative Phosphorylation as an Emerging Target in Cancer Therapy. *Clin Cancer Res,* 24**,** 2482-2490.

AVRIL, T., VAULÉON, E. & CHEVET, E. 2017. Endoplasmic reticulum stress signaling and chemotherapy resistance in solid cancers. *Oncogenesis,* 6**,** e373.

BABAEI-JADIDI, R., LI, N., SAADEDDIN, A., SPENCER-DENE, B., JANDKE, A., MUHAMMAD, B., IBRAHIM, E. E., MURALEEDHARAN, R., ABUZINADAH, M., DAVIS, H., LEWIS, A., WATSON, S., BEHRENS, A., TOMLINSON, I. & NATERI, A. S. 2011. FBXW7 influences murine intestinal homeostasis and cancer, targeting Notch, Jun, and DEK for degradation. *J Exp Med,* 208**,** 295-312.

BAER, M. R., GEORGE, S. L., DODGE, R. K., O'LOUGHLIN, K. L., MINDERMAN, H., CALIGIURI, M. A., ANASTASI, J., POWELL, B. L., KOLITZ, J. E., SCHIFFER, C. A., BLOOMFIELD, C. D. & LARSON, R. A. 2002. Phase 3 study of the multidrug resistance modulator PSC-833 in previously untreated patients 60 years of age and older with acute myeloid leukemia: Cancer and Leukemia Group B Study 9720. *Blood,* 100**,** 1224-1232.

BAHRAM, F., VON DER LEHR, N., CETINKAYA, C. & LARSSON, L. G. 2000. c-Myc hot spot mutations in lymphomas result in inefficient ubiquitination and decreased proteasome-mediated turnover. *Blood,* 95**,** 2104-2110.

BAJAR, B. T., WANG, E. S., LAM, A. J., KIM, B. B., JACOBS, C. L., HOWE, E. S., DAVIDSON, M. W., LIN, M. Z. & CHU, J. 2016. Improving brightness and photostability of green and red fluorescent proteins for live cell imaging and FRET reporting. *Scientific Reports,* 6**,** 20889.

BALAMURUGAN, K., SHARAN, S., KLARMANN, K. D., ZHANG, Y., COPPOLA, V., SUMMERS, G. H., ROGER, T., MORRISON, D. K., KELLER, J. R. & STERNECK, E. 2013. FBXW7alpha attenuates inflammatory signalling by downregulating C/EBPdelta and its target gene Tlr4. *Nat Commun,* 4**,** 1662.

BALAMURUGAN, K., WANG, J. M., TSAI, H. H., SHARAN, S., ANVER, M., LEIGHTY, R. & STERNECK, E. 2010. The tumour suppressor C/EBPdelta inhibits FBXW7 expression and promotes mammary tumour metastasis. *EMBO J,* 29**,** 4106-4117.

BARRELL, B. G., ANDERSON, S., BANKIER, A. T., DE BRUIJN, M. H., CHEN, E., COULSON, A. R., DROUIN, J., EPERON, I. C., NIERLICH, D. P., ROE, B. A., SANGER, F., SCHREIER, P. H., SMITH, A. J., STADEN, R. & YOUNG, I. G. 1980. Different pattern of codon recognition by mammalian mitochondrial tRNAs. *Proc Natl Acad Sci U S A,* 77**,** 3164-3166.

BARRETINA, J., CAPONIGRO, G., STRANSKY, N., VENKATESAN, K., MARGOLIN, A. A., KIM, S., WILSON, C. J., LEHAR, J., KRYUKOV, G. V., SONKIN, D., REDDY, A., LIU, M., MURRAY, L., BERGER, M. F., MONAHAN, J. E., MORAIS, P., MELTZER, J., KOREJWA, A., JANE-VALBUENA, J., MAPA, F. A., THIBAULT, J., BRIC-FURLONG, E., RAMAN, P., SHIPWAY, A., ENGELS, I. H., CHENG, J., YU, G. K., YU, J., ASPESI, P., JR., DE SILVA, M., JAGTAP, K., JONES, M. D., WANG, L., HATTON, C., PALESCANDOLO, E., GUPTA, S., MAHAN, S., SOUGNEZ, C., ONOFRIO, R. C., LIEFELD, T., MACCONAILL, L., WINCKLER, W., REICH, M., LI, N., MESIROV, J. P., GABRIEL, S. B., GETZ, G., ARDLIE, K., CHAN, V., MYER, V. E., WEBER, B. L., PORTER, J., WARMUTH, M., FINAN, P., HARRIS, J. L., MEYERSON, M., GOLUB, T. R., MORRISSEY, M. P., SELLERS, W. R., SCHLEGEL, R. & GARRAWAY, L. A. 2012. The Cancer Cell Line Encyclopedia enables predictive modelling of anticancer drug sensitivity. *Nature,* 483**,** 603-607.

BASU, A., BODYCOMBE, N. E., CHEAH, J. H., PRICE, E. V., LIU, K., SCHAEFER, G. I., EBRIGHT, R. Y., STEWART, M. L., ITO, D., WANG, S., BRACHA, A. L., LIEFELD, T., WAWER, M., GILBERT, J. C., WILSON, A. J., STRANSKY, N., KRYUKOV, G. V., DANCIK, V., BARRETINA, J., GARRAWAY, L. A., HON, C. S., MUNOZ, B., BITTKER, J. A., STOCKWELL, B. R., KHABELE, D., STERN, A. M., CLEMONS, P. A., SHAMJI, A. F. & SCHREIBER, S. L. 2013. An interactive resource to identify cancer genetic and lineage dependencies targeted by small molecules. *Cell,* 154**,** 1151-1161.

BEDARD, P. L., HYMAN, D. M., DAVIDS, M. S. & SIU, L. L. 2020. Small molecules, big impact: 20 years of targeted therapy in oncology. *The Lancet,* 395**,** 1078-1088.

BEHAN, F. M., IORIO, F., PICCO, G., GONÇALVES, E., BEAVER, C. M., MIGLIARDI, G., SANTOS, R., RAO, Y., SASSI, F., PINNELLI, M., ANSARI, R., HARPER, S., JACKSON, D. A., MCRAE, R., POOLEY, R., WILKINSON, P., VAN DER MEER, D., DOW, D., BUSER-DOEPNER, C., BERTOTTI, A., TRUSOLINO, L., STRONACH, E. A., SAEZ-RODRIGUEZ, J., YUSA, K. & GARNETT, M. J. 2019. Prioritization of cancer therapeutic targets using CRISPR–Cas9 screens. *Nature,* 568**,** 511-516.

BENGOECHEA-ALONSO, M. T. & ERICSSON, J. 2010a. Tumor suppressor Fbxw7 regulates TGFbeta signaling by targeting TGIF1 for degradation. *Oncogene,* 29**,** 5322-5328.

BENGOECHEA-ALONSO, M. T. & ERICSSON, J. 2010b. The ubiquitin ligase Fbxw7 controls adipocyte differentiation by targeting C/EBPalpha for degradation. *Proc Natl Acad Sci U S A,* 107**,** 11817-11822.

BENSLIMANE, Y., BERTOMEU, T., COULOMBE-HUNTINGTON, J., MCQUAID, M., SANCHEZ-OSUNA, M., PAPADOPOLI, D., AVIZONIS, D., RUSSO, M. S. T., HUARD, C., TOPISIROVIC, I., WURTELE, H., TYERS, M. & HARRINGTON, L. 2020. Genome-Wide Screens Reveal that Resveratrol Induces Replicative Stress in Human Cells. *Mol Cell,* 79**,** 846-856 e8.

BERWICK, M., LACHIEWICZ, A., PESTAK, C. & THOMAS, N. 2008. Solar UV Exposure and Mortality from Skin Tumors. *In:* REICHRATH, J. (ed.) *Sunlight, Vitamin D and Skin Cancer.* New York, NY: Springer New York.

BI, K., NISHIHARA, K., MACHLEIDT, T., HERMANSON, S., WANG, J., SAKAMURU, S., HUANG, R. & XIA, M. 2015. Identification of known drugs targeting the endoplasmic reticulum stress response. *Analytical and Bioanalytical Chemistry,* 407**,** 5343-5351.

BI, M., NACZKI, C., KORITZINSKY, M., FELS, D., BLAIS, J., HU, N., HARDING, H., NOVOA, I., VARIA, M., RALEIGH, J., SCHEUNER, D., KAUFMAN, R. J., BELL, J., RON, D., WOUTERS, B. G. & KOUMENIS, C. 2005. ER stress-regulated translation increases tolerance to extreme hypoxia and promotes tumor growth. *EMBO J,* 24**,** 3470-3481.

BIAN, W. P., CHEN, Y. L., LUO, J. J., WANG, C., XIE, S. L. & PEI, D. S. 2019. Knock-In Strategy for Editing Human and Zebrafish Mitochondrial DNA Using Mito-CRISPR/Cas9 System. *ACS Synth Biol,* 8**,** 621-632.

BIRKENMEIER, K., DROSE, S., WITTIG, I., WINKELMANN, R., KAFER, V., DORING, C., HARTMANN, S., WENZ, T., REICHERT, A. S., BRANDT, U. & HANSMANN, M. L. 2016. Hodgkin and Reed-Sternberg cells of classical Hodgkin lymphoma are highly dependent on oxidative phosphorylation. *Int J Cancer,* 138**,** 2231-2246.

BISWAS, M., PHAN, D., WATANABE, M. & CHAN, J. Y. 2011. The Fbw7 tumor suppressor regulates nuclear factor E2-related factor 1 transcription factor turnover through proteasome-mediated proteolysis. *J Biol Chem,* 286**,** 39282-39289.

BLEYER, A. & WELCH, H. G. 2012. Effect of Three Decades of Screening Mammography on Breast-Cancer Incidence. *New England Journal of Medicine,* 367**,** 1998-2005.

BOCH, J., SCHOLZE, H., SCHORNACK, S., LANDGRAF, A., HAHN, S., KAY, S., LAHAYE, T., NICKSTADT, A. & BONAS, U. 2009. Breaking the Code of DNA Binding Specificity of TAL-Type III Effectors. *Science,* 326**,** 1509-1512.

BONADONNA, G., BRUSAMOLINO, E., VALAGUSSA, P., ROSSI, A., BRUGNATELLI, L., BRAMBILLA, C., DE LENA, M., TANCINI, G., BAJETTA, E., MUSUMECI, R. & VERONESI, U. 1976. Combination Chemotherapy as an Adjuvant Treatment in Operable Breast Cancer. *New England Journal of Medicine,* 294**,** 405-410.

BONEKAMP, N. A., PETER, B., HILLEN, H. S., FELSER, A., BERGBREDE, T., CHOIDAS, A., HORN, M., UNGER, A., DI LUCREZIA, R., ATANASSOV, I., LI, X., KOCH, U., MENNINGER, S., BOROS, J., HABENBERGER, P., GIAVALISCO, P., CRAMER, P., DENZEL, M. S., NUSSBAUMER, P., KLEBL, B., FALKENBERG, M., GUSTAFSSON, C. M. & LARSSON, N. G. 2020. Small-molecule inhibitors of human mitochondrial DNA transcription. *Nature,* 588**,** 712-716.

BOOKER, M., SAMSONOVA, A. A., KWON, Y., FLOCKHART, I., MOHR, S. E. & PERRIMON, N. 2011. False negative rates in Drosophila cell-based RNAi screens: a case study. *BMC Genomics,* 12**,** 50.

BOSL, G. J., GLUCKMAN, R., GELLER, N. L., GOLBEY, R. B., WHITMORE, W. F., HERR, H., SOGANI, P., MORSE, M., MARTINI, N. & BAINS, M. 1986. VAB-6: an effective chemotherapy regimen for patients with germ-cell tumors. *Journal of Clinical Oncology,* 4**,** 1493-1499.

BOYCE, M., BRYANT, K. F., JOUSSE, C., LONG, K., HARDING, H. P., SCHEUNER, D., KAUFMAN, R. J., MA, D., COEN, D. M., RON, D. & YUAN, J. 2005. A selective inhibitor of eIF2alpha dephosphorylation protects cells from ER stress. *Science,* 307**,** 935-939.

BRESLOW, D. K., HOOGENDOORN, S., KOPP, A. R., MORGENS, D. W., VU, B. K., KENNEDY, M. C., HAN, K., LI, A., HESS, G. T., BASSIK, M. C., CHEN, J. K. & NACHURY, M. V. 2018. A CRISPR-based screen for Hedgehog signaling provides insights into ciliary function and ciliopathies. *Nat Genet,* 50**,** 460-471.

BROCKMAN, R. W. 1963. Mechanisms of Resistance to Anticancer Agents. *Advances in Cancer Research,* 7**,** 129-234.

BRUMMELKAMP, T. R., BERNARDS, R. & AGAMI, R. 2002. A System for Stable Expression of Short Interfering RNAs in Mammalian Cells. *Science,* 296**,** 550-553.

BRYANT, H. E., SCHULTZ, N., THOMAS, H. D., PARKER, K. M., FLOWER, D., LOPEZ, E., KYLE, S., MEUTH, M., CURTIN, N. J. & HELLEDAY, T. 2005. Specific killing of BRCA2-deficient tumours with inhibitors of poly(ADP-ribose) polymerase. *Nature,* 434**,** 913-917.

BUCKLEY, SHANNON M., ARANDA-ORGILLES, B., STRIKOUDIS, A., APOSTOLOU, E., LOIZOU, E., MORAN-CRUSIO, K., FARNSWORTH, CHARLES L., KOLLER, ANTONIUS A., DASGUPTA, R., SILVA, JEFFREY C., STADTFELD, M., HOCHEDLINGER, K., CHEN, EMILY I. & AIFANTIS, I. 2012. Regulation of Pluripotency and Cellular Reprogramming by the Ubiquitin-Proteasome System. *Cell Stem Cell,* 11**,** 783-798.

BUNPO, P., DUDLEY, A., CUNDIFF, J. K., CAVENER, D. R., WEK, R. C. & ANTHONY, T. G. 2009. GCN2 protein kinase is required to activate amino acid deprivation responses in mice treated with the anti-cancer agent L-asparaginase. *J Biol Chem,* 284**,** 32742-32749.

BURGER, H., CAPELLO, A., SCHENK, P. W., STOTER, G., BROUWER, J. & NOOTER, K. 2000. A genome-wide screening in Saccharomyces cerevisiae for genes that confer resistance to the anticancer agent cisplatin. *Biochem Biophys Res Commun,* 269**,** 767-774.

BURR, M. L., SPARBIER, C. E., CHAN, Y. C., WILLIAMSON, J. C., WOODS, K., BEAVIS, P. A., LAM, E. Y. N., HENDERSON, M. A., BELL, C. C., STOLZENBURG, S., GILAN, O., BLOOR, S., NOORI, T., MORGENS, D. W., BASSIK, M. C., NEESON, P. J., BEHREN, A., DARCY, P. K., DAWSON, S. J., VOSKOBOINIK, I., TRAPANI, J. A., CEBON, J., LEHNER, P. J. & DAWSON, M. A. 2017. CMTM6 maintains the expression of PD-L1 and regulates anti-tumour immunity. *Nature,* 549**,** 101-105.

BUSINO, L., MILLMAN, S. E., SCOTTO, L., KYRATSOUS, C. A., BASRUR, V., O'CONNOR, O., HOFFMANN, A., ELENITOBA-JOHNSON, K. S. & PAGANO, M. 2012. Fbxw7alpha- and GSK3-mediated degradation of p100 is a pro-survival mechanism in multiple myeloma. *Nat Cell Biol,* 14**,** 375-385.

CARDOZO, T. & PAGANO, M. 2004. The SCF ubiquitin ligase: insights into a molecular machine. *Nat Rev Mol Cell Biol,* 5**,** 739-751.

CARO, P., KISHAN, A. U., NORBERG, E., STANLEY, I. A., CHAPUY, B., FICARRO, S. B., POLAK, K., TONDERA, D., GOUNARIDES, J., YIN, H., ZHOU, F., GREEN, M. R., CHEN, L., MONTI, S., MARTO, J. A., SHIPP, M. A. & DANIAL, N. N. 2012. Metabolic signatures uncover distinct targets in molecular subsets of diffuse large B cell lymphoma. *Cancer Cell,* 22**,** 547-560.

CASSAVAUGH, J. M., HALE, S. A., WELLMAN, T. L., HOWE, A. K., WONG, C. & LOUNSBURY, K. M. 2011. Negative regulation of HIF-1alpha by an FBW7-mediated degradation pathway during hypoxia. *J Cell Biochem,* 112**,** 3882-3890.

CENCIARELLI, C., CHIAUR, D. S., GUARDAVACCARO, D., PARKS, W., VIDAL, M. & PAGANO, M. 1999. Identification of a family of human F-box proteins. *Current Biology,* 9**,** 1177-1179.

CERAMI, E., GAO, J., DOGRUSOZ, U., GROSS, B. E., SUMER, S. O., AKSOY, B. A., JACOBSEN, A., BYRNE, C. J., HEUER, M. L., LARSSON, E., ANTIPIN, Y., REVA, B., GOLDBERG, A. P., SANDER, C. & SCHULTZ, N. 2012. The cBio cancer genomics portal: an open platform for exploring multidimensional cancer genomics data. *Cancer Discov,* 2**,** 401-404.

CHAN, D. C. 2006. Mitochondria: dynamic organelles in disease, aging, and development. *Cell,* 125**,** 1241-1252.

CHAN, E. M., SHIBUE, T., MCFARLAND, J. M., GAETA, B., GHANDI, M., DUMONT, N., GONZALEZ, A., MCPARTLAN, J. S., LI, T., ZHANG, Y., BIN LIU, J., LAZARO, J.-B., GU, P., PIETT, C. G., APFFEL, A., ALI, S. O., DEASY, R., KESKULA, P., NG, R. W. S., ROBERTS, E. A., REZNICHENKO, E., LEUNG, L., ALIMOVA, M., SCHENONE, M., ISLAM, M., MARUVKA, Y. E., LIU, Y., ROPER, J., RAGHAVAN, S., GIANNAKIS, M., TSENG, Y.-Y., NAGEL, Z. D., D'ANDREA, A., ROOT, D. E., BOEHM, J. S., GETZ, G., CHANG, S., GOLUB, T. R., TSHERNIAK, A., VAZQUEZ, F. & BASS, A. J. 2019. WRN helicase is a synthetic lethal target in microsatellite unstable cancers. *Nature,* 568**,** 551-556.

CHEN, J., XU, X. & FAN, M. 2019a. Inhibition of mitochondrial translation selectively targets osteosarcoma. *Biochem Biophys Res Commun,* 515**,** 9-15.

CHEN, M. C., CHEN, C. H., CHUANG, H. C., KULP, S. K., TENG, C. M. & CHEN, C. S. 2011a. Novel mechanism by which histone deacetylase inhibitors facilitate topoisomerase IIα degradation in hepatocellular carcinoma cells. *Hepatology,* 53**,** 148-159.

CHEN, S., SANJANA, N. E., ZHENG, K., SHALEM, O., LEE, K., SHI, X., SCOTT, D. A., SONG, J., PAN, J. Q., WEISSLEDER, R., LEE, H., ZHANG, F. & SHARP, P. A. 2015. Genome-wide CRISPR screen in a mouse model of tumor growth and metastasis. *Cell,* 160**,** 1246-1260.

CHEN, T., OZEL, D., QIAO, Y., HARBINSKI, F., CHEN, L., DENOYELLE, S., HE, X., ZVEREVA, N., SUPKO, J. G., CHOREV, M., HALPERIN, J. A. & AKTAS, B. H. 2011b. Chemical genetics

identify eIF2alpha kinase heme-regulated inhibitor as an anticancer target. *Nat Chem Biol,* 7**,** 610-616.

CHEN, X., GLYTSOU, C., ZHOU, H., NARANG, S., REYNA, D. E., LOPEZ, A., SAKELLAROPOULOS, T., GONG, Y., KLOETGEN, A., YAP, Y. S., WANG, E., GAVATHIOTIS, E., TSIRIGOS, A., TIBES, R. & AIFANTIS, I. 2019b. Targeting Mitochondrial Structure Sensitizes Acute Myeloid Leukemia to Venetoclax Treatment. *Cancer Discov,* 9**,** 890-909.

CHEN, X., LI, X. Y., LONG, M., WANG, X., GAO, Z. W., CUI, Y., REN, J., ZHANG, Z., LIU, C., DONG, K. & ZHANG, H. 2018. The FBXW7 tumor suppressor inhibits breast cancer proliferation and promotes apoptosis by targeting MTDH for degradation. *Neoplasma,* 65**,** 201-209.

CHEN, Y., LI, Y., XUE, J., GONG, A., YU, G., ZHOU, A., LIN, K., ZHANG, S., ZHANG, N., GOTTARDI, C. J. & HUANG, S. 2016. Wnt-induced deubiquitination FoxM1 ensures nucleus beta-catenin transactivation. *EMBO J,* 35**,** 668-684.

CHENG, G. Z., CHAN, J., WANG, Q., ZHANG, W., SUN, C. D. & WANG, L. H. 2007. Twist transcriptionally up-regulates AKT2 in breast cancer cells leading to increased migration, invasion, and resistance to paclitaxel. *Cancer Res,* 67**,** 1979-1987.

CHENG, X., HAO, Y., SHU, W., ZHAO, M., ZHAO, C., WU, Y., PENG, X., YAO, P., XIAO, D., QING, G., PAN, Z., YIN, L., HU, D. & DU, H. N. 2017. Cell cycle-dependent degradation of the methyltransferase SETD3 attenuates cell proliferation and liver tumorigenesis. *J Biol Chem,* 292**,** 9022-9033.

CHONGHAILE, T. N., SAROSIEK, K. A., VO, T.-T., RYAN, J. A., TAMMAREDDI, A., MOORE, V. D. G., DENG, J., ANDERSON, K. C., RICHARDSON, P., TAI, Y.-T., MITSIADES, C. S., MATULONIS, U. A., DRAPKIN, R., STONE, R., DEANGELO, D. J., MCCONKEY, D. J., SALLAN, S. E., SILVERMAN, L., HIRSCH, M. S., CARRASCO, D. R. & LETAI, A. 2011. Pretreatment Mitochondrial Priming Correlates with Clinical Response to Cytotoxic Chemotherapy. *Science,* 334**,** 1129-1133.

CLINGEN, P. H., ARLETT, C. F., ROZA, L., MORI, T., NIKAIDO, O. & GREEN, M. H. L. 1995. Induction of Cyclobutane Pyrimidine Dimers, Pyrimidine(6-4)pyrimidone Photoproducts, and Dewar Valence Isomers by Natural Sunlight in Normal Human Mononuclear Cells. *Cancer Research,* 55**,** 2245-2248.

CONDON, K. J., OROZCO, J. M., ADELMANN, C. H., SPINELLI, J. B., VAN DER HELM, P. W., ROBERTS, J. M., KUNCHOK, T. & SABATINI, D. M. 2021. Genome-wide CRISPR screens reveal multitiered mechanisms through which mTORC1 senses mitochondrial dysfunction. *Proc Natl Acad Sci U S A,* 118**,** e2022120118.

CONG, L., RAN, F. A., COX, D., LIN, S., BARRETTO, R., HABIB, N., HSU, P. D., WU, X., JIANG, W., MARRAFFINI, L. A. & ZHANG, F. 2013. Multiplex genome engineering using CRISPR/Cas systems. *Science,* 339**,** 819-823.

CORMAN, A., KANELLIS, D. C., MICHALSKA, P., HÄGGBLAD, M., LAFARGA, V., BARTEK, J., CARRERAS-PUIGVERT, J. & FERNANDEZ-CAPETILLO, O. 2021. A chemical screen for modulators of mRNA translation identifies a novel mechanism of toxicity for sphingosine kinase inhibitors. *PLOS Biology,* (in press).

CORNWELL, M. M., PASTAN, I. & GOTTESMAN, M. M. 1987. Certain calcium channel blockers bind specifically to multidrug-resistant human KB carcinoma membrane vesicles and inhibit drug binding to P-glycoprotein. *J Biol Chem,* 262**,** 2166-2170.

COSTANZO, M., VANDERSLUIS, B., KOCH, E. N., BARYSHNIKOVA, A., PONS, C., TAN, G., WANG, W., USAJ, M., HANCHARD, J., LEE, S. D., PELECHANO, V., STYLES, E. B., BILLMANN, M., VAN LEEUWEN, J., VAN DYK, N., LIN, Z.-Y., KUZMIN, E., NELSON, J., PIOTROWSKI, J. S., SRIKUMAR, T., BAHR, S., CHEN, Y., DESHPANDE, R., KURAT, C. F., LI, S. C., LI, Z., USAJ, M. M., OKADA, H., PASCOE, N., SAN LUIS, B.-J., SHARIFPOOR, S., SHUTERIQI, E., SIMPKINS, S. W., SNIDER, J., SURESH, H. G., TAN, Y., ZHU, H., MALOD-DOGNIN, N., JANJIC, V., PRZULJ, N., TROYANSKAYA, O. G., STAGLJAR, I., XIA, T., OHYA, Y., GINGRAS, A.-C., RAUGHT, B., BOUTROS, M., STEINMETZ, L. M., MOORE, C. L., ROSEBROCK, A. P., CAUDY, A. A., MYERS, C. L., ANDREWS, B. & BOONE, C. 2016. A global genetic interaction network maps a wiring diagram of cellular function. *Science,* 353**,** 1381-1396 aaf1420.

CRUZ-BERMUDEZ, A., LAZA-BRIVIESCA, R., VICENTE-BLANCO, R. J., GARCIA-GRANDE, A., CORONADO, M. J., LAINE-MENENDEZ, S., PALACIOS-ZAMBRANO, S., MORENO-VILLA, M. R., RUIZ-VALDEPENAS, A. M., LENDINEZ, C., ROMERO, A., FRANCO, F., CALVO, V., ALFARO, C., ACOSTA, P. M., SALAS, C., GARCIA, J. M. & PROVENCIO, M. 2019. Cisplatin resistance involves a metabolic reprogramming through ROS and PGC-1alpha in NSCLC which can be overcome by OXPHOS inhibition. *Free Radic Biol Med,* 135**,** 167-181.

CUELLA-MARTIN, R., HAYWARD, S. B., FAN, X., CHEN, X., HUANG, J. W., TAGLIALATELA, A., LEUZZI, G., ZHAO, J., RABADAN, R., LU, C., SHEN, Y. & CICCIA, A. 2021. Functional interrogation of DNA damage response variants with base editing screens. *Cell,* 184**,** 1081-1097 e19.

CUI, D., XIONG, X., SHU, J., DAI, X., SUN, Y. & ZHAO, Y. 2020. FBXW7 Confers Radiation Survival by Targeting p53 for Degradation. *Cell Rep,* 30**,** 497-509 e4.

D'ANTONIO, M., MUSNER, N., SCAPIN, C., UNGARO, D., DEL CARRO, U., RON, D., FELTRI, M. L. & WRABETZ, L. 2013. Resetting translational homeostasis restores myelination in Charcot-Marie-Tooth disease type 1B mice. *J Exp Med,* 210**,** 821-838.

D'ANDREA, A., GRITTI, I., NICOLI, P., GIORGIO, M., DONI, M., CONTI, A., BIANCHI, V., CASOLI, L., SABÒ, A., MIRONOV, A., BEZNOUSSENKO, G. V. & AMATI, B. 2016. The mitochondrial translation machinery as a therapeutic target in Myc-driven lymphomas. *Oncotarget,* 7**,** 72415-72430.

DAI, W. & JIANG, L. 2019. Dysregulated Mitochondrial Dynamics and Metabolism in Obesity, Diabetes, and Cancer. *Front Endocrinol (Lausanne),* 10**,** 570.

DAI, X., NORTH, B. J. & INUZUKA, H. 2014. Negative regulation of DAB2IP by Akt and SCFFbw7 pathways. *Oncotarget,* 5**,** 3307-3315.

DAS, I., KRZYZOSIAK, A., SCHNEIDER, K., WRABETZ, L., D'ANTONIO, M., BARRY, N., SIGURDARDOTTIR, A. & BERTOLOTTI, A. 2015. Preventing proteostasis diseases by selective inhibition of a phosphatase regulatory subunit. *Science,* 348**,** 239-242.

DASH, P. K., HYLIN, M. J., HOOD, K. N., ORSI, S. A., ZHAO, J., REDELL, J. B., TSVETKOV, A. S. & MOORE, A. N. 2015. Inhibition of Eukaryotic Initiation Factor 2 Alpha Phosphatase Reduces Tissue Damage and Improves Learning and Memory after Experimental Traumatic Brain Injury. *J Neurotrauma,* 32**,** 1608-1620.

DAVIS, H., LEWIS, A., BEHRENS, A. & TOMLINSON, I. 2014a. Investigation of the atypical FBXW7 mutation spectrum in human tumours by conditional expression of a heterozygous propellor tip missense allele in the mouse intestines. *Gut,* 63**,** 792-799.

DAVIS, H., LEWIS, A., SPENCER-DENE, B., TATEOSSIAN, H., STAMP, G., BEHRENS, A. & TOMLINSON, I. 2011. FBXW7 mutations typically found in human cancers are distinct from null alleles and disrupt lung development. *J Pathol,* 224**,** 180-189.

DAVIS, M. A., LARIMORE, E. A., FISSEL, B. M., SWANGER, J., TAATJES, D. J. & CLURMAN, B. E. 2013. The SCF-Fbw7 ubiquitin ligase degrades MED13 and MED13L and regulates CDK8 module association with Mediator. *Genes Dev,* 27**,** 151-156.

DAVIS, R. J., GONEN, M., MARGINEANTU, D. H., HANDELI, S., SWANGER, J., HOELLERBAUER, P., PADDISON, P. J., GU, H., RAFTERY, D., GRIM, J. E., HOCKENBERY, D. M., MARGOLIN, A. A. & CLURMAN, B. E. 2018. Pan-cancer transcriptional signatures predictive of oncogenic mutations reveal that Fbw7 regulates cancer cell oxidative metabolism. *Proc Natl Acad Sci U S A,* 115**,** 5462-5467.

DAVIS, R. J., WELCKER, M. & CLURMAN, B. E. 2014b. Tumor suppression by the Fbw7 ubiquitin ligase: mechanisms and opportunities. *Cancer Cell,* 26**,** 455-464.

DE GRUIJL, F. R. & FORBES, P. D. 1995. UV-induced skin cancer in a hairless mouse model. *BioEssays,* 17**,** 651-660.

DE LA COVA, C. & GREENWALD, I. 2012. SEL-10/Fbw7-dependent negative feedback regulation of LIN-45/Braf signaling in C. elegans via a conserved phosphodegron. *Genes Dev,* 26**,** 2524-2535.

DEAN, M., FOJO, T. & BATES, S. 2005. Tumour stem cells and drug resistance. *Nat Rev Cancer,* 5**,** 275-284.

DEVITA, V. T., JR., SIMON, R. M., HUBBARD, S. M., YOUNG, R. C., BERARD, C. W., MOXLEY, J. H., III, FREI, E., III, CARBONE, P. P. & CANELLOS, G. P. 1980. Curability of Advanced Hodgkin's Disease with Chemotherapy: Long-Term Follow-up of MOPP-Treated Patients at the National Cancer Institute. *Annals of Internal Medicine,* 92**,** 587-595.

DEWEIRDT, P. C., SANGREE, A. K., HANNA, R. E., SANSON, K. R., HEGDE, M., STRAND, C., PERSKY, N. S. & DOENCH, J. G. 2020. Genetic screens in isogenic mammalian cell lines without single cell cloning. *Nat Commun,* 11**,** 752.

DHARIA, N. V., KUGENER, G., GUENTHER, L. M., MALONE, C. F., DURBIN, A. D., HONG, A. L., HOWARD, T. P., BANDOPADHAYAY, P., WECHSLER, C. S., FUNG, I., WARREN, A. C., DEMPSTER, J. M., KRILL-BURGER, J. M., PAOLELLA, B. R., MOH, P., JHA, N., TANG, A., MONTGOMERY, P., BOEHM, J. S., HAHN, W. C., ROBERTS, C. W. M., MCFARLAND, J. M., TSHERNIAK, A., GOLUB, T. R., VAZQUEZ, F. & STEGMAIER, K. 2021. A first-generation pediatric cancer dependency map. *Nat Genet***,** 529-538.

DIJK, S. N., PROTASONI, M., ELPIDOROU, M., KROON, A. M. & TAANMAN, J. W. 2020. Mitochondria as target to inhibit proliferation and induce apoptosis of cancer cells: the effects of doxycycline and gemcitabine. *Sci Rep,* 10**,** 4363.

DING, J., ZHAO, Z., SONG, J., LUO, B. & HUANG, L. 2018. MiR-223 promotes the doxorubicin resistance of colorectal cancer cells via regulating epithelial-mesenchymal transition by targeting FBXW7. *Acta Biochim Biophys Sin (Shanghai),* 50**,** 597-604.

DING, X.-Q., ZHAO, S., YANG, L., ZHAO, X., ZHAO, G.-F., ZHAO, S.-P., LI, Z.-J. & ZHENG, H.-C. 2017. The nucleocytoplasmic translocation and up-regulation of ING5 protein in breast cancer: a potential target for gene therapy. *Oncotarget,* 8**,** 81953-81966.

DIXIT, D., MADDURI, R. P. & SHARMA, R. 2014. The role of tigecycline in the treatment of infections in light of the new black box warning. *Expert Rev Anti Infect Ther,* 12**,** 397-400.

DOENCH, J. G., FUSI, N., SULLENDER, M., HEGDE, M., VAIMBERG, E. W., DONOVAN, K. F., SMITH, I., TOTHOVA, Z., WILEN, C., ORCHARD, R., VIRGIN, H. W., LISTGARTEN, J. & ROOT, D. E. 2016. Optimized sgRNA design to maximize activity and minimize off-target effects of CRISPR-Cas9. *Nat Biotechnol,* 34**,** 184-191.

DONATI, G., RAVÀ, M., FILIPUZZI, M., NICOLI, P., CASSINA, L., VERRECCHIA, A., DONI, M., RODIGHIERO, S., PARODI, F., BOLETTA, A., VELLANO, C. P., MARSZALEK, J. R., DRAETTA, G. F. & AMATI, B. 2020. Targeting mitochondrial respiration and the BCL2 family in MYC-associated B-cell lymphoma. *bioRxiv***,** 2020.11.22.390922.

DRAINAS, A. P., LAMBUTA, R. A., IVANOVA, I., SERCIN, O., SARROPOULOS, I., SMITH, M. L., EFTHYMIOPOULOS, T., RAEDER, B., STUTZ, A. M., WASZAK, S. M., MARDIN, B. R. & KORBEL, J. O. 2020. Genome-wide Screens Implicate Loss of Cullin Ring Ligase 3 in Persistent Proliferation and Genome Instability in TP53-Deficient Cells. *Cell Rep,* 31**,** 107465.

DULBECCO, R. 1949. Reactivation of Ultra-Violet-Inactivated Bacteriophage by Visible Light. *Nature,* 163**,** 949-950.

EKHOLM-REED, S., GOLDBERG, M. S., SCHLOSSMACHER, M. G. & REED, S. I. 2013. Parkin-dependent degradation of the F-box protein Fbw7beta promotes neuronal survival in response to oxidative stress by stabilizing Mcl-1. *Mol Cell Biol,* 33**,** 3627-3643.

EPSTEIN, J. H. 1983. Photocarcinogenesis, skin cancer, and aging. *Journal of the American Academy of Dermatology,* 9**,** 487-502.

ERROL, C. F., GRAHAM, C. W., WOLFRAM, S., RICHARD, D. W., ROGER, A. S. & TOM, E. 2006. *DNA Repair and Mutagenesis, Second Edition*, American Society of Microbiology.

ESTELL, C., STAMATIDOU, E., EL-MESSEIRY, S. & HAMILTON, A. 2017. In situ imaging of mitochondrial translation shows weak correlation with nucleoid DNA intensity and no suppression during mitosis. *J Cell Sci,* 130**,** 4193-4199.

ETO, K., IWATSUKI, M., WATANABE, M., ISHIMOTO, T., IDA, S., IMAMURA, Y., IWAGAMI, S., BABA, Y., SAKAMOTO, Y., MIYAMOTO, Y., YOSHIDA, N. & BABA, H. 2015. The sensitivity of gastric cancer to trastuzumab is regulated by the miR-223/FBXW7 pathway. *Int J Cancer,* 136**,** 1537-1545.

FANG, L., YANG, Z., ZHOU, J., TUNG, J. Y., HSIAO, C. D., WANG, L., DENG, Y., WANG, P., WANG, J. & LEE, M. H. 2015. Circadian Clock Gene CRY2 Degradation Is Involved in Chemoresistance of Colorectal Cancer. *Mol Cancer Ther,* 14**,** 1476-1487.

FARBER, S., DIAMOND, L. K., MERCER, R. D., SYLVESTER, R. F. & WOLFF, J. A. 1948. Temporary Remissions in Acute Leukemia in Children Produced by Folic Acid Antagonist, 4-Aminopteroyl-Glutamic Acid (Aminopterin). *New England Journal of Medicine,* 238**,** 787-793.

FARES, C. M., VAN ALLEN, E. M., DRAKE, C. G., ALLISON, J. P. & HU-LIESKOVAN, S. 2019. Mechanisms of Resistance to Immune Checkpoint Blockade: Why Does Checkpoint Inhibitor Immunotherapy Not Work for All Patients? *American Society of Clinical Oncology Educational Book***,** 147-164.

FARGE, T., SALAND, E., DE TONI, F., AROUA, N., HOSSEINI, M., PERRY, R., BOSC, C., SUGITA, M., STUANI, L., FRAISSE, M., SCOTLAND, S., LARRUE, C., BOUTZEN, H., FELIU, V., NICOLAU-TRAVERS, M. L., CASSANT-SOURDY, S., BROIN, N., DAVID, M., SERHAN, N., SARRY, A., TAVITIAN, S., KAOMA, T., VALLAR, L., IACOVONI, J., LINARES, L. K., MONTERSINO, C., CASTELLANO, R., GRIESSINGER, E., COLLETTE, Y., DUCHAMP, O., BARREIRA, Y., HIRSCH, P., PALAMA, T., GALES, L., DELHOMMEAU, F., GARMY-SUSINI, B. H., PORTAIS, J. C., VERGEZ, F., SELAK, M., DANET-DESNOYERS, G., CARROLL, M., RECHER, C. & SARRY, J. E. 2017. Chemotherapy-Resistant Human Acute Myeloid Leukemia Cells Are Not Enriched for Leukemic Stem Cells but Require Oxidative Metabolism. *Cancer Discov,* 7**,** 716-735.

FARMER, H., MCCABE, N., LORD, C. J., TUTT, A. N., JOHNSON, D. A., RICHARDSON, T. B., SANTAROSA, M., DILLON, K. J., HICKSON, I., KNIGHTS, C., MARTIN, N. M., JACKSON, S. P., SMITH, G. C. & ASHWORTH, A. 2005. Targeting the DNA repair defect in BRCA mutant cells as a therapeutic strategy. *Nature,* 434**,** 917-921.

FARNIE, G., SOTGIA, F. & LISANTI, M. P. 2015. High mitochondrial mass identifies a sub-population of stem-like cancer cells that are chemo-resistant. *Oncotarget,* 6**,** 30472–30486.

FERRIS, J., ESPONA-FIEDLER, M., HAMILTON, C., HOLOHAN, C., CRAWFORD, N., MCINTYRE, A. J., ROBERTS, J. Z., WAPPETT, M., MCDADE, S. S., LONGLEY, D. B. & COYLE, V. 2020. Pevonedistat (MLN4924): mechanism of cell death induction and therapeutic potential in colorectal cancer. *Cell Death Discov,* 6**,** 61.

FESSLER, E., ECKL, E. M., SCHMITT, S., MANCILLA, I. A., MEYER-BENDER, M. F., HANF, M., PHILIPPOU-MASSIER, J., KREBS, S., ZISCHKA, H. & JAE, L. T. 2020. A pathway coordinated by DELE1 relays mitochondrial stress to the cytosol. *Nature,* 579**,** 433-437.

FIEBIG, H. H., NEUMANN, H. A., HENß, H., KOCH, H., KAISER, D. & ARNOLD, H. 1985. Development of Three Human Small Cell Lung Cancer Models in Nude Mice. *In:* SEEBER, S. (ed.) *Small Cell Lung Cancer.* Berlin, Heidelberg: Springer Berlin Heidelberg.

FINN, R. S., MARTIN, M., RUGO, H. S., JONES, S., IM, S.-A., GELMON, K., HARBECK, N., LIPATOV, O. N., WALSHE, J. M., MOULDER, S., GAUTHIER, E., LU, D. R., RANDOLPH, S., DIÉRAS, V. & SLAMON, D. J. 2016. Palbociclib and Letrozole in Advanced Breast Cancer. *New England Journal of Medicine,* 375**,** 1925-1936.

FIORE, D., PISCOPO, C., PROTO, M. C., VASATURO, M., DAL PIAZ, F., FUSCO, B. M., PAGANO, C., LAEZZA, C., BIFULCO, M. & GAZZERRO, P. 2019. N6-Isopentenyladenosine Inhibits Colorectal Cancer and Improves Sensitivity to 5-Fluorouracil-Targeting FBXW7 Tumor Suppressor. *Cancers (Basel),* 11**,** 1456.

FIRE, A., XU, S., MONTGOMERY, M. K., KOSTAS, S. A., DRIVER, S. E. & MELLO, C. C. 1998. Potent and specific genetic interference by double-stranded RNA in Caenorhabditis elegans. *Nature,* 391**,** 806-811.

FISCHER, K. R., DURRANS, A., LEE, S., SHENG, J., LI, F., WONG, S. T., CHOI, H., EL RAYES, T., RYU, S., TROEGER, J., SCHWABE, R. F., VAHDAT, L. T., ALTORKI, N. K., MITTAL, V. & GAO, D. 2015. Epithelial-to-mesenchymal transition is not required for lung metastasis but contributes to chemoresistance. *Nature,* 527**,** 472-476.

FOUFELLE, F. & FROMENTY, B. 2016. Role of endoplasmic reticulum stress in drug-induced toxicity. *Pharmacology research & perspectives,* 4**,** e00211.

FOX, E., WIDEMANN, B. C., PASTAKIA, D., CHEN, C. C., YANG, S. X., COLE, D. & BALIS, F. M. 2015. Pharmacokinetic and pharmacodynamic study of tariquidar (XR9576), a P-glycoprotein inhibitor, in combination with doxorubicin, vinorelbine, or docetaxel in children and adolescents with refractory solid tumors. *Cancer Chemother Pharmacol,* 76**,** 1273-1283.

FRIBERG, A., VIGIL, D., ZHAO, B., DANIELS, R. N., BURKE, J. P., GARCIA-BARRANTES, P. M., CAMPER, D., CHAUDER, B. A., LEE, T., OLEJNICZAK, E. T. & FESIK, S. W. 2013. Discovery of potent myeloid cell leukemia 1 (Mcl-1) inhibitors using fragment-based methods and structure-based design. *J Med Chem,* 56**,** 15-30.

FRIEDBERG, E. C. 2008. A brief history of the DNA repair field. *Cell Res,* 18**,** 3-7.

FU, X., LIU, W., HUANG, Q., WANG, Y., LI, H. & XIONG, Y. 2017. Targeting mitochondrial respiration selectively sensitizes pediatric acute lymphoblastic leukemia cell lines and patient samples to standard chemotherapy. *American journal of cancer research,* 7**,** 2395-2405.

FU, X., WAN, S., LYU, Y. L., LIU, L. F. & QI, H. 2008. Etoposide induces ATM-dependent mitochondrial biogenesis through AMPK activation. *PLoS One,* 3**,** e2009.

FUKUOKA, M., YANO, S., GIACCONE, G., TAMURA, T., NAKAGAWA, K., DOUILLARD, J. Y., NISHIWAKI, Y., VANSTEENKISTE, J., KUDOH, S., RISCHIN, D., EEK, R., HORAI, T., NODA, K., TAKATA, I., SMIT, E., AVERBUCH, S., MACLEOD, A., FEYEREISLOVA, A., DONG, R. P. & BASELGA, J. 2003. Multi-institutional randomized phase II trial of gefitinib for previously treated patients with advanced non-small-cell lung cancer (The IDEAL 1 Trial). *J Clin Oncol,* 21**,** 2237-2246.

FUKUSHIMA, H., MATSUMOTO, A., INUZUKA, H., ZHAI, B., LAU, A. W., WAN, L., GAO, D., SHAIK, S., YUAN, M., GYGI, S. P., JIMI, E., ASARA, J. M., NAKAYAMA, K., NAKAYAMA, K. I. & WEI, W. 2012. SCF(Fbw7) modulates the NFkB signaling pathway by targeting NFkB2 for ubiquitination and destruction. *Cell Rep,* 1**,** 434-443.

GALINDO-MORENO, M., GIRALDEZ, S., LIMON-MORTES, M. C., BELMONTE-FERNANDEZ, A., REED, S. I., SAEZ, C., JAPON, M. A., TORTOLERO, M. & ROMERO, F. 2019. SCF(FBXW7)-

mediated degradation of p53 promotes cell recovery after UV-induced DNA damage. *FASEB J,* 33**,** 11420-11430.

GALLI, F., ROSSI, M., D'ALESSANDRA, Y., DE SIMONE, M., LOPARDO, T., HAUPT, Y., ALSHEICH-BARTOK, O., ANZI, S., SHAULIAN, E., CALABRO, V., LA MANTIA, G. & GUERRINI, L. 2010. MDM2 and Fbw7 cooperate to induce p63 protein degradation following DNA damage and cell differentiation. *J Cell Sci,* 123**,** 2423-2433.

GALLO, D., YOUNG, J. T. F., FOURTOUNIS, J., MARTINO, G., ÁLVAREZ-QUILÓN, A., BERNIER, C., DUFFY, N. M., PAPP, R., ROULSTON, A., STOCCO, R., SZYCHOWSKI, J., VELOSO, A., ALAM, H., BARUAH, P. S., FORTIN, A. B., BOWLAN, J., CHAUDHARY, N., DESJARDINS, J., DIETRICH, E., FOURNIER, S., FUGÈRE-DESJARDINS, C., DE RUGY, T. G., LECLAIRE, M.-E., LIU, B., MELO, H., NICOLAS, O., SINGHANIA, A., SZILARD, R. K., TKÁČ, J., YIN, S. Y., MORRIS, S. J., ZINDA, M., GARY MARSHALL, C. & DUROCHER, D. 2021. CCNE1 amplification is synthetic-lethal with PKMYT1 kinase inhibition. *bioRxiv***,** 2021.04.08.438361.

GALLUZZI, L., SENOVILLA, L., VITALE, I., MICHELS, J., MARTINS, I., KEPP, O., CASTEDO, M. & KROEMER, G. 2012. Molecular mechanisms of cisplatin resistance. *Oncogene,* 31**,** 1869-1883.

GALLUZZI, L., VITALE, I., MICHELS, J., BRENNER, C., SZABADKAI, G., HAREL-BELLAN, A., CASTEDO, M. & KROEMER, G. 2014. Systems biology of cisplatin resistance: past, present and future. *Cell Death Dis,* 5**,** e1257.

GAMMAGE, P. A., MORAES, C. T. & MINCZUK, M. 2018. Mitochondrial Genome Engineering: The Revolution May Not Be CRISPR-Ized. *Trends in Genetics,* 34**,** 101-110.

GAO, J., AKSOY, B. A., DOGRUSOZ, U., DRESDNER, G., GROSS, B., SUMER, S. O., SUN, Y., JACOBSEN, A., SINHA, R., LARSSON, E., CERAMI, E., SANDER, C. & SCHULTZ, N. 2013. Integrative analysis of complex cancer genomics and clinical profiles using the cBioPortal. *Sci Signal,* 6**,** pl1.

GAO, Y., KIM, S., LEE, Y.-I. & LEE, J. 2019. Cellular Stress-Modulating Drugs Can Potentially Be Identified by in Silico Screening with Connectivity Map (CMap). *International journal of molecular sciences,* 20**,** 5601.

GARRAWAY, L. A. & JANNE, P. A. 2012. Circumventing cancer drug resistance in the era of personalized medicine. *Cancer Discov,* 2**,** 214-226.

GARRIDO-MESA, N., ZARZUELO, A. & GÁLVEZ, J. 2013. Minocycline: far beyond an antibiotic. *British journal of pharmacology,* 169**,** 337-352.

GARVIN, A. J., KHALAF, A. H. A., RETTINO, A., XICLUNA, J., BUTLER, L., MORRIS, J. R., HEERY, D. M. & CLARKE, N. M. 2019. GSK3beta-SCFFBXW7alpha mediated phosphorylation and ubiquitination of IRF1 are required for its transcription-dependent turnover. *Nucleic Acids Res,* 47**,** 4476-4494.

GASCA, J., FLORES, M. L., GIRÁLDEZ, S., RUIZ-BORREGO, M., TORTOLERO, M., ROMERO, F., JAPÓN, M. A. & SÁEZ, C. 2016. Loss of FBXW7 and accumulation of MCL1 and PLK1 promote paclitaxel resistance in breast cancer. *Oncotarget,* 7**,** 52751-52765.

GASSER, J. A., INUZUKA, H., LAU, A. W., WEI, W., BEROUKHIM, R. & TOKER, A. 2014. SGK3 mediates INPP4B-dependent PI3K signaling in breast cancer. *Mol Cell,* 56**,** 595-607.

GAUTRON, A., BACHELOT, L., AUBRY, M., LECLERC, D., QUEMENER, A. M., CORRE, S., RAMBOW, F., PARIS, A., TARDIF, N., LECLAIR, H. M., MARIN-BEJAR, O., COULOUARN, C., MARINE, J. C., GALIBERT, M. D. & GILOT, D. 2021. CRISPR screens identify tumor-promoting genes conferring melanoma cell plasticity and resistance. *EMBO Mol Med***,** e13466.

GERHARDS, N. M., BLOMEN, V. A., MUTLU, M., NIEUWENHUIS, J., HOWALD, D., GUYADER, C., JONKERS, J., BRUMMELKAMP, T. R. & ROTTENBERG, S. 2018. Haploid genetic screens identify genetic vulnerabilities to microtubule-targeting agents. *Mol Oncol,* 12**,** 953-971.

GHANDI, M., HUANG, F. W., JANE-VALBUENA, J., KRYUKOV, G. V., LO, C. C., MCDONALD, E. R., 3RD, BARRETINA, J., GELFAND, E. T., BIELSKI, C. M., LI, H., HU, K., ANDREEV-DRAKHLIN, A. Y., KIM, J., HESS, J. M., HAAS, B. J., AGUET, F., WEIR, B. A., ROTHBERG, M. V., PAOLELLA, B. R., LAWRENCE, M. S., AKBANI, R., LU, Y., TIV, H. L., GOKHALE, P. C., DE WECK, A., MANSOUR, A. A., OH, C., SHIH, J., HADI, K., ROSEN, Y., BISTLINE, J., VENKATESAN, K., REDDY, A., SONKIN, D., LIU, M., LEHAR, J., KORN, J. M., PORTER, D. A., JONES, M. D., GOLJI, J., CAPONIGRO, G., TAYLOR, J. E., DUNNING, C. M., CREECH, A. L., WARREN, A. C., MCFARLAND, J. M., ZAMANIGHOMI, M., KAUFFMANN, A., STRANSKY, N., IMIELINSKI, M., MARUVKA, Y. E., CHERNIACK, A. D., TSHERNIAK, A., VAZQUEZ, F., JAFFE, J. D., LANE, A. A., WEINSTOCK, D. M., JOHANNESSEN, C. M., MORRISSEY, M. P., STEGMEIER, F., SCHLEGEL, R., HAHN, W. C., GETZ, G., MILLS, G.

B., BOEHM, J. S., GOLUB, T. R., GARRAWAY, L. A. & SELLERS, W. R. 2019. Next-generation characterization of the Cancer Cell Line Encyclopedia. *Nature,* 569**,** 503-508.

GIAEVER, G., CHU, A. M., NI, L., CONNELLY, C., RILES, L., VÉRONNEAU, S., DOW, S., LUCAU-DANILA, A., ANDERSON, K., ANDRÉ, B., ARKIN, A. P., ASTROMOFF, A., EL BAKKOURY, M., BANGHAM, R., BENITO, R., BRACHAT, S., CAMPANARO, S., CURTISS, M., DAVIS, K., DEUTSCHBAUER, A., ENTIAN, K.-D., FLAHERTY, P., FOURY, F., GARFINKEL, D. J., GERSTEIN, M., GOTTE, D., GÜLDENER, U., HEGEMANN, J. H., HEMPEL, S., HERMAN, Z., JARAMILLO, D. F., KELLY, D. E., KELLY, S. L., KÖTTER, P., LABONTE, D., LAMB, D. C., LAN, N., LIANG, H., LIAO, H., LIU, L., LUO, C., LUSSIER, M., MAO, R., MENARD, P., OOI, S. L., REVUELTA, J. L., ROBERTS, C. J., ROSE, M., ROSS-MACDONALD, P., SCHERENS, B., SCHIMMACK, G., SHAFER, B., SHOEMAKER, D. D., SOOKHAI-MAHADEO, S., STORMS, R. K., STRATHERN, J. N., VALLE, G., VOET, M., VOLCKAERT, G., WANG, C.-Y., WARD, T. R., WILHELMY, J., WINZELER, E. A., YANG, Y., YEN, G., YOUNGMAN, E., YU, K., BUSSEY, H., BOEKE, J. D., SNYDER, M., PHILIPPSEN, P., DAVIS, R. W. & JOHNSTON, M. 2002. Functional profiling of the Saccharomyces cerevisiae genome. *Nature,* 418**,** 387-391.

GILBERT, L. A., HORLBECK, M. A., ADAMSON, B., VILLALTA, J. E., CHEN, Y., WHITEHEAD, E. H., GUIMARAES, C., PANNING, B., PLOEGH, H. L., BASSIK, M. C., QI, L. S., KAMPMANN, M. & WEISSMAN, J. S. 2014. Genome-Scale CRISPR-Mediated Control of Gene Repression and Activation. *Cell,* 159**,** 647-661.

GIRÁLDEZ, S., HERRERO-RUIZ, J., MORA-SANTOS, M., JAPÓN, M., TORTOLERO, M. & ROMERO, F. 2014. SCF(FBXW7α) modulates the intra-S-phase DNA-damage checkpoint by regulating Polo like kinase-1 stability. *Oncotarget,* 5**,** 4370-4383.

GOMBODORJ, N., YOKOBORI, T., TANAKA, N., SUZUKI, S., KURIYAMA, K., KUMAKURA, Y., YOSHIDA, T., SAKAI, M., SOHDA, M., BAATAR, S., MIYAZAKI, T., NISHIYAMA, M., SHIRABE, K. & KUWANO, H. 2018. Correlation between high FBXW7 expression in pretreatment biopsy specimens and good response to chemoradiation therapy in patients with locally advanced esophageal cancer: A retrospective study. *J Surg Oncol,* 118**,** 101-108.

GOODMAN, L. S., WINTROBE, M. M., DAMESHEK, W., GOODMAN, M. J., GILMAN, A. & MCLENNAN, M. T. 1946. Nitrogen mustard therapy: Use of Methyl-Bis(Beta-Chloroethyl)amine Hydrochloride and Tris(Beta-Chloroethyl)amine Hydrochloride for Hodgkin's Disease, Lymphosarcoma, Leukemia and Certain Allied and Miscellaneous Disorders. *Journal of the American Medical Association,* 132**,** 126-132.

GOODSPEED, A., JEAN, A. & COSTELLO, J. C. 2019. A Whole-genome CRISPR Screen Identifies a Role of MSH2 in Cisplatin-mediated Cell Death in Muscle-invasive Bladder Cancer. *European Urology,* 75**,** 242-250.

GORRE, M. E., MOHAMMED, M., ELLWOOD, K., HSU, N., PAQUETTE, R., RAO, P. N. & SAWYERS, C. L. 2001. Clinical Resistance to STI-571 Cancer Therapy Caused by BCR-ABL Gene Mutation or Amplification. *Science,* 293**,** 876-880.

GRAVES, J. A., WANG, Y., SIMS-LUCAS, S., CHEROK, E., ROTHERMUND, K., BRANCA, M. F., ELSTER, J., BEER-STOLZ, D., VAN HOUTEN, B., VOCKLEY, J. & PROCHOWNIK, E. V. 2012. Mitochondrial structure, function and dynamics are temporally controlled by c-Myc. *PLoS One,* 7**,** e37699.

GRAY, M. W., BURGER, G. & LANG, B. F. 1999. Mitochondrial Evolution. *Science,* 283**,** 1476-1481.

GRAY, W. M., KEPINSKI, S., ROUSE, D., LEYSER, O. & ESTELLE, M. 2001. Auxin regulates SCFTIR1-dependent degradation of AUX/IAA proteins. *Nature,* 414**,** 271-276.

GRIM, J. E., GUSTAFSON, M. P., HIRATA, R. K., HAGAR, A. C., SWANGER, J., WELCKER, M., HWANG, H. C., ERICSSON, J., RUSSELL, D. W. & CLURMAN, B. E. 2008. Isoform- and cell cycle-dependent substrate degradation by the Fbw7 ubiquitin ligase. *J Cell Biol,* 181**,** 913-920.

GROHMANN, K., AMALRIC, F., CREWS, S. & ATTARDI, G. 1978. Failure to detect “cap” structures in mitochondrial DNA-coded poly(A)-containing RNA from HeLa cells. *Nucleic Acids Research,* 5**,** 637-651.

GRUBER, A., BJÖRKHOLM, M., BRINCH, L., EVENSEN, S., GUSTAVSSON, B., HEDENUS, M., JULIUSSON, G., LÖFVENBERG, E., NESTHUS, I., SIMONSSON, B., SJO, M., STENKE, L., TANGEN, J. M., TIDEFELT, U., UDÉN, A.-M., PAUL, C. & LILIEMARK, J. 2003. A phase I/II study of the MDR modulator Valspodar (PSC 833) combined with daunorubicin and cytarabine in patients with relapsed and primary refractory acute myeloid leukemia. *Leukemia Research,* 27**,** 323-328.

GSTALDER, C., LIU, D., MIAO, D., LUTTERBACH, B., DEVINE, A. L., LIN, C., SHETTIGAR, M., PANCHOLI, P., BUCHBINDER, E. I., CARTER, S. L., MANOS, M. P., ROJAS-RUDILLA, V., BRENNICK, R., GJINI, E., CHEN, P. H., LAKO, A., RODIG, S., YOON, C. H., FREEMAN, G.

J., BARBIE, D. A., HODI, F. S., MILES, W., VAN ALLEN, E. M. & HAQ, R. 2020. Inactivation of Fbxw7 Impairs dsRNA Sensing and Confers Resistance to PD-1 Blockade. *Cancer Discov,* 10**,** 1296-1311.

GUO, X., AVILES, G., LIU, Y., TIAN, R., UNGER, B. A., LIN, Y. T., WIITA, A. P., XU, K., CORREIA, M. A. & KAMPMANN, M. 2020a. Mitochondrial stress is relayed to the cytosol by an OMA1-DELE1-HRI pathway. *Nature,* 579**,** 427-432.

GUO, Y., ZHANG, Z., WANG, Z., LIU, G., LIU, Y. & WANG, H. 2020b. Astragalus polysaccharides inhibit ovarian cancer cell growth via microRNA-27a/FBXW7 signaling pathway. *Biosci Rep,* 40**,** BSR20193396.

GUPTA-ROSSI, N., LE BAIL, O., GONEN, H., BROU, C., LOGEAT, F., SIX, E., CIECHANOVER, A. & ISRAEL, A. 2001. Functional interaction between SEL-10, an F-box protein, and the nuclear form of activated Notch1 receptor. *J Biol Chem,* 276**,** 34371-34378.

HAN, H., JAIN, A. D., TRUICA, M. I., IZQUIERDO-FERRER, J., ANKER, J. F., LYSY, B., SAGAR, V., LUAN, Y., CHALMERS, Z. R., UNNO, K., MOK, H., VATAPALLI, R., YOO, Y. A., RODRIGUEZ, Y., KANDELA, I., PARKER, J. B., CHAKRAVARTI, D., MISHRA, R. K., SCHILTZ, G. E. & ABDULKADIR, S. A. 2019. Small-Molecule MYC Inhibitors Suppress Tumor Growth and Enhance Immunotherapy. *Cancer Cell,* 36**,** 483-497 e15.

HAN, K., JENG, E. E., HESS, G. T., MORGENS, D. W., LI, A. & BASSIK, M. C. 2017. Synergistic drug combinations for cancer identified in a CRISPR screen for pairwise genetic interactions. *Nat Biotechnol,* 35**,** 463-474.

HAN, Q., ZHANG, C., ZHANG, J. & TIAN, Z. 2011. Involvement of activation of PKR in HBx-siRNA-mediated innate immune effects on HBV inhibition. *PLoS One,* 6**,** e27931.

HANAHAN, D. & WEINBERG, R. A. 2000. The Hallmarks of Cancer. *Cell,* 100**,** 57-70.

HANAHAN, D. & WEINBERG, R. A. 2011. Hallmarks of cancer: the next generation. *Cell,* 144**,** 646-674.

HANGAUER, M. J., VISWANATHAN, V. S., RYAN, M. J., BOLE, D., EATON, J. K., MATOV, A., GALEAS, J., DHRUV, H. D., BERENS, M. E., SCHREIBER, S. L., MCCORMICK, F. & MCMANUS, M. T. 2017. Drug-tolerant persister cancer cells are vulnerable to GPX4 inhibition. *Nature,* 551**,** 247-250.

HANNA, R. E., HEGDE, M., FAGRE, C. R., DEWEIRDT, P. C., SANGREE, A. K., SZEGLETES, Z., GRIFFITH, A., FEELEY, M. N., SANSON, K. R., BAIDI, Y., KOBLAN, L. W., LIU, D. R., NEAL, J. T. & DOENCH, J. G. 2021. Massively parallel assessment of human variants with base editor screens. *Cell,* 184**,** 1064-1080 e20.

HAQ, R., SHOAG, J., ANDREU-PEREZ, P., YOKOYAMA, S., EDELMAN, H., ROWE, G. C., FREDERICK, D. T., HURLEY, A. D., NELLORE, A., KUNG, A. L., WARGO, J. A., SONG, J. S., FISHER, D. E., ARANY, Z. & WIDLUND, H. R. 2013. Oncogenic BRAF regulates oxidative metabolism via PGC1alpha and MITF. *Cancer Cell,* 23**,** 302-315.

HART, T., CHANDRASHEKHAR, M., AREGGER, M., STEINHART, Z., BROWN, K. R., MACLEOD, G., MIS, M., ZIMMERMANN, M., FRADET-TURCOTTE, A., SUN, S., MERO, P., DIRKS, P., SIDHU, S., ROTH, F. P., RISSLAND, O. S., DUROCHER, D., ANGERS, S. & MOFFAT, J. 2015. High-Resolution CRISPR Screens Reveal Fitness Genes and Genotype-Specific Cancer Liabilities. *Cell,* 163**,** 1515-1526.

HARTWELL, L. H., MORTIMER, R. K., CULOTTI, J. & CULOTTI, M. 1973. Genetic Control of the Cell Division Cycle in Yeast: V. Genetic Analysis of cdc Mutants. *Genetics,* 74**,** 267-286.

HE, J., SONG, Y., LI, G., XIAO, P., LIU, Y., XUE, Y., CAO, Q., TU, X., PAN, T., JIANG, Z., CAO, X., LAI, L. & WANG, Q. 2019. Fbxw7 increases CCL2/7 in CX3CR1hi macrophages to promote intestinal inflammation. *J Clin Invest,* 129**,** 3877-3893.

HE, L., TORRES-LOCKHART, K., FORSTER, N., RAMAKRISHNAN, S., GRENINGER, P., GARNETT, M. J., MCDERMOTT, U., ROTHENBERG, S. M., BENES, C. H. & ELLISEN, L. W. 2013. Mcl-1 and FBW7 control a dominant survival pathway underlying HDAC and Bcl-2 inhibitor synergy in squamous cell carcinoma. *Cancer Discov,* 3**,** 324-337.

HEPBURN, A. C., STEELE, R. E., VEERATTERAPILLAY, R., WILSON, L., KOUNATIDOU, E. E., BARNARD, A., BERRY, P., CASSIDY, J. R., MOAD, M., EL-SHERIF, A., GAUGHAN, L., MILLS, I. G., ROBSON, C. N. & HEER, R. 2019. The induction of core pluripotency master regulators in cancers defines poor clinical outcomes and treatment resistance. *Oncogene,* 38**,** 4412-4424.

HERSHKO, A. & CIECHANOVER, A. 1998. The ubiquitin system. *Annu Rev Biochem,* 67**,** 425-479.

HIDALGO, M., AMANT, F., BIANKIN, A. V., BUDINSKA, E., BYRNE, A. T., CALDAS, C., CLARKE, R. B., DE JONG, S., JONKERS, J., MAELANDSMO, G. M., ROMAN-ROMAN, S., SEOANE, J.,

TRUSOLINO, L. & VILLANUEVA, A. 2014. Patient-derived xenograft models: an emerging platform for translational cancer research. *Cancer Discov,* 4**,** 998-1013.

HIRPARA, J., EU, J. Q., TAN, J. K. M., WONG, A. L., CLEMENT, M. V., KONG, L. R., OHI, N., TSUNODA, T., QU, J., GOH, B. C. & PERVAIZ, S. 2019. Metabolic reprogramming of oncogene-addicted cancer cells to OXPHOS as a mechanism of drug resistance. *Redox Biol,* 25**,** 101076.

HOCHSTRASSER, M. 2009. Origin and function of ubiquitin-like proteins. *Nature,* 458**,** 422-429.

HODGES, L. M., MARKOVA, S. M., CHINN, L. W., GOW, J. M., KROETZ, D. L., KLEIN, T. E. & ALTMAN, R. B. 2011. Very important pharmacogene summary: ABCB1 (MDR1, P-glycoprotein). *Pharmacogenet Genomics,* 21**,** 152-161.

HØJLUND, K., MOGENSEN, M., SAHLIN, K. & BECK-NIELSEN, H. 2008. Mitochondrial Dysfunction in Type 2 Diabetes and Obesity. *Endocrinology and Metabolism Clinics of North America,* 37**,** 713-731.

HOLOHAN, C., VAN SCHAEYBROECK, S., LONGLEY, D. B. & JOHNSTON, P. G. 2013. Cancer drug resistance: an evolving paradigm. *Nat Rev Cancer,* 13**,** 714-726.

HOLZ, M. S., JANNING, A., RENNÉ, C., GATTENLÖHNER, S., SPIEKER, T. & BRÄUNINGER, A. 2013. Induction of endoplasmic reticulum stress by sorafenib and activation of NF-κB by lestaurtinib as a novel resistance mechanism in Hodgkin lymphoma cell lines. *Mol Cancer Ther,* 12**,** 173-183.

HONG, X., LIU, W., SONG, R., SHAH, J. J., FENG, X., TSANG, C. K., MORGAN, K. M., BUNTING, S. F., INUZUKA, H., ZHENG, X. F., SHEN, Z., SABAAWY, H. E., LIU, L. & PINE, S. R. 2016. SOX9 is targeted for proteasomal degradation by the E3 ligase FBW7 in response to DNA damage. *Nucleic Acids Res,* 44**,** 8855-8869.

HONMA, S., HISAMORI, S., NISHIUCHI, A., ITATANI, Y., OBAMA, K., SHIMONO, Y. & SAKAI, Y. 2019. F-Box/WD Repeat Domain-Containing 7 Induces Chemotherapy Resistance in Colorectal Cancer Stem Cells. *Cancers (Basel),* 11**,** 635.

HOUSMAN, G., BYLER, S., HEERBOTH, S., LAPINSKA, K., LONGACRE, M., SNYDER, N. & SARKAR, S. 2014. Drug resistance in cancer: an overview. *Cancers (Basel),* 6**,** 1769-1792.

HU, B. & GUO, Y. 2019. Inhibition of mitochondrial translation as a therapeutic strategy for human ovarian cancer to overcome chemoresistance. *Biochem Biophys Res Commun,* 509**,** 373-378.

HU, H., DONG, Z., TAN, P., ZHANG, Y., LIU, L., YANG, L., LIU, Y. & CUI, H. 2016. Antibiotic drug tigecycline inhibits melanoma progression and metastasis in a p21CIP1/Waf1-dependent manner. *Oncotarget,* 7**,** 3171-3185.

HU, J., LOCASALE, J. W., BIELAS, J. H., O'SULLIVAN, J., SHEAHAN, K., CANTLEY, L. C., VANDER HEIDEN, M. G. & VITKUP, D. 2013. Heterogeneity of tumor-induced gene expression changes in the human metabolic network. *Nat Biotechnol,* 31**,** 522-529.

HU, Q., QIN, Y., ZHANG, B., LIANG, C., JI, S., SHI, S., XU, W., XIANG, J., LIANG, D., NI, Q., YU, X. & XU, J. 2017. FBW7 increases the chemosensitivity of pancreatic cancer cells to gemcitabine through upregulation of ENT1. *Oncol Rep,* 38**,** 2069-2077.

HU, W., HOFSTETTER, W., WEI, X., GUO, W., ZHOU, Y., PATAER, A., LI, H., FANG, B. & SWISHER, S. G. 2009. Double-stranded RNA-dependent protein kinase-dependent apoptosis induction by a novel small compound. *J Pharmacol Exp Ther,* 328**,** 866-872.

HUANG, H., ZHOU, P., WEI, J., LONG, L., SHI, H., DHUNGANA, Y., CHAPMAN, N. M., FU, G., SARAVIA, J., RAYNOR, J. L., LIU, S., PALACIOS, G., WANG, Y. D., QIAN, C., YU, J. & CHI, H. 2021. In vivo CRISPR screening reveals nutrient signaling processes underpinning CD8(+) T cell fate decisions. *Cell,* 184**,** 1245-1261 e21.

HUANG, J., CHEN, M., XU, E. S., LUO, L., MA, Y., HUANG, W., FLOYD, W., KLANN, T. S., KIM, S. Y., GERSBACH, C. A., CARDONA, D. M. & KIRSCH, D. G. 2019. Genome-wide CRISPR Screen to Identify Genes that Suppress Transformation in the Presence of Endogenous Kras(G12D). *Sci Rep,* 9**,** 17220.

HUANG, L. Y., ZHAO, J., CHEN, H., WAN, L., INUZUKA, H., GUO, J., FU, X., ZHAI, Y., LU, Z., WANG, X., HAN, Z. G., SUN, Y. & WEI, W. 2018. SCF(FBW7)-mediated degradation of Brg1 suppresses gastric cancer metastasis. *Nat Commun,* 9**,** 3569.

HUNDLEY, F. V., SANVISENS DELGADO, N., MARIN, H. C., CARR, K. L., TIAN, R. & TOCZYSKI, D. P. 2021. A comprehensive phenotypic CRISPR-Cas9 screen of the ubiquitin pathway uncovers roles of ubiquitin ligases in mitosis. *Mol Cell,* 81**,** 1319-1336 e9.

HUSTEDT, N., ALVAREZ-QUILON, A., MCEWAN, A., YUAN, J. Y., CHO, T., KOOB, L., HART, T. & DUROCHER, D. 2019. A consensus set of genetic vulnerabilities to ATR inhibition. *Open Biol,* 9**,** 190156.

HWANG, W. Y., FU, Y., REYON, D., MAEDER, M. L., TSAI, S. Q., SANDER, J. D., PETERSON, R. T., YEH, J. R. J. & JOUNG, J. K. 2013. Efficient genome editing in zebrafish using a CRISPR-Cas system. *Nature Biotechnology,* 31**,** 227-229.

IARC 1992. *IARC monographs on the evaluation of carcinogenic risks to humans. Solar and UV radiation*, IARC.

IHRY, R. J., SALICK, M. R., HO, D. J., SONDEY, M., KOMMINENI, S., PAULA, S., RAYMOND, J., HENRY, B., FRIAS, E., WANG, Q., WORRINGER, K. A., YE, C., RUSS, C., REECE-HOYES, J. S., ALTSHULER, R. C., RANDHAWA, R., YANG, Z., MCALLISTER, G., HOFFMAN, G. R., DOLMETSCH, R. & KAYKAS, A. 2019. Genome-Scale CRISPR Screens Identify Human Pluripotency-Specific Genes. *Cell Rep,* 27**,** 616-630 e6.

IKENOUE, T., TERAKADO, Y., ZHU, C., LIU, X., OHSUGI, T., MATSUBARA, D., FUJII, T., KAKUTA, S., KUBO, S., SHIBATA, T., YAMAGUCHI, K., IWAKURA, Y. & FURUKAWA, Y. 2018. Establishment and analysis of a novel mouse line carrying a conditional knockin allele of a cancer-specific FBXW7 mutation. *Sci Rep,* 8**,** 2021.

INUZUKA, H., SHAIK, S., ONOYAMA, I., GAO, D., TSENG, A., MASER, R. S., ZHAI, B., WAN, L., GUTIERREZ, A., LAU, A. W., XIAO, Y., CHRISTIE, A. L., ASTER, J., SETTLEMAN, J., GYGI, S. P., KUNG, A. L., LOOK, T., NAKAYAMA, K. I., DEPINHO, R. A. & WEI, W. 2011. SCF(FBW7) regulates cellular apoptosis by targeting MCL1 for ubiquitylation and destruction. *Nature,* 471**,** 104-109.

IPPOLITO, L., MARINI, A., CAVALLINI, L., MORANDI, A., PIETROVITO, L., PINTUS, G., GIANNONI, E., SCHRADER, T., PUHR, M., CHIARUGI, P. & TADDEI, M. L. 2016. Metabolic shift toward oxidative phosphorylation in docetaxel resistant prostate cancer cells. *Oncotarget,* 7**,** 61890-61904.

ISHII, N., ARAKI, K., YOKOBORI, T., GANTUMUR, D., YAMANAKA, T., ALTAN, B., TSUKAGOSHI, M., IGARASHI, T., WATANABE, A., KUBO, N., HOSOUCHI, Y., KUWANO, H. & SHIRABE, K. 2017. Reduced FBXW7 expression in pancreatic cancer correlates with poor prognosis and chemotherapeutic resistance via accumulation of MCL1. *Oncotarget,* 8**,** 112636-112646.

IWAI, Y., ISHIDA, M., TANAKA, Y., OKAZAKI, T., HONJO, T. & MINATO, N. 2002. Involvement of PD-L1 on tumor cells in the escape from host immune system and tumor immunotherapy by PD-L1 blockade. *Proceedings of the National Academy of Sciences,* 99**,** 12293-12297.

IZUMI, D., ISHIMOTO, T., MIYAKE, K., ETO, T., ARIMA, K., KIYOZUMI, Y., UCHIHARA, T., KURASHIGE, J., IWATSUKI, M., BABA, Y., SAKAMOTO, Y., MIYAMOTO, Y., YOSHIDA, N., WATANABE, M., GOEL, A., TAN, P. & BABA, H. 2017. Colorectal Cancer Stem Cells Acquire Chemoresistance Through the Upregulation of F-Box/WD Repeat-Containing Protein 7 and the Consequent Degradation of c-Myc. *Stem Cells,* 35**,** 2027-2036.

JAIN, I. H., CALVO, S. E., MARKHARD, A. L., SKINNER, O. S., TO, T. L., AST, T. & MOOTHA, V. K. 2020. Genetic Screen for Cell Fitness in High or Low Oxygen Highlights Mitochondrial and Lipid Metabolism. *Cell,* 181**,** 716-727 e11.

JENNER, L., STAROSTA, A. L., TERRY, D. S., MIKOLAJKA, A., FILONAVA, L., YUSUPOV, M., BLANCHARD, S. C., WILSON, D. N. & YUSUPOVA, G. 2013. Structural basis for potent inhibitory activity of the antibiotic tigecycline during protein synthesis. *Proc Natl Acad Sci U S A,* 110**,** 3812-3816.

JEONG, K. W., KU, J. M., PARK, M. W., PARK, S. M., YANG, J. E. & NAM, T. G. 2013. Hydroxynaphthoic acids identified in a high throughput screening potently ameliorate endoplasmic reticulum stress as novel chemical chaperones. *Chem Pharm Bull (Tokyo),* 61**,** 740-746.

JI, S., QIN, Y., SHI, S., LIU, X., HU, H., ZHOU, H., GAO, J., ZHANG, B., XU, W., LIU, J., LIANG, D., LIU, L., LIU, C., LONG, J., ZHOU, H., CHIAO, P. J., XU, J., NI, Q., GAO, D. & YU, X. 2015. ERK kinase phosphorylates and destabilizes the tumor suppressor FBW7 in pancreatic cancer. *Cell Res,* 25**,** 561-573.

JIA, X., GU, Z., CHEN, W. & JIAO, J. 2016. Tigecycline targets nonsmall cell lung cancer through inhibition of mitochondrial function. *Fundam Clin Pharmacol,* 30**,** 297-306.

JIANG, H. Q., REN, M., JIANG, H. Z., WANG, J., ZHANG, J., YIN, X., WANG, S. Y., QI, Y., WANG, X. D. & FENG, H. L. 2014. Guanabenz delays the onset of disease symptoms, extends lifespan, improves motor performance and attenuates motor neuron loss in the SOD1 G93A mouse model of amyotrophic lateral sclerosis. *Neuroscience,* 277**,** 132-138.

JIANG, J., WANG, J., YUE, M., CAI, X., WANG, T., WU, C., SU, H., WANG, Y., HAN, M., ZHANG, Y., ZHU, X., JIANG, P., LI, P., SUN, Y., XIAO, W., FENG, H., QING, G. & LIU, H. 2020. Direct Phosphorylation and Stabilization of MYC by Aurora B Kinase Promote T-cell Leukemogenesis. *Cancer Cell,* 37**,** 200-215 e5.

JIANG, Y., QI, X., LIU, X., ZHANG, J., JI, J., ZHU, Z., REN, J. & YU, Y. 2017. Fbxw7 haploinsufficiency loses its protection against DNA damage and accelerates MNU-induced gastric carcinogenesis. *Oncotarget,* 8**,** 33444-33456.

JIN, J. 2004. Systematic analysis and nomenclature of mammalian F-box proteins. *Genes & Development,* 18**,** 2573-2580.

JIN, L., CHUN, J., PAN, C., LI, D., LIN, R., ALESI, G. N., WANG, X., KANG, H. B., SONG, L., WANG, D., ZHANG, G., FAN, J., BOGGON, T. J., ZHOU, L., KOWALSKI, J., QU, C. K., STEUER, C. E., CHEN, G. Z., SABA, N. F., BOISE, L. H., OWONIKOKO, T. K., KHURI, F. R., MAGLIOCCA, K. R., SHIN, D. M., LONIAL, S. & KANG, S. 2018. MAST1 Drives Cisplatin Resistance in Human Cancers by Rewiring cRaf-Independent MEK Activation. *Cancer Cell,* 34**,** 315-330 e7.

JIN, X., YANG, C., FAN, P., XIAO, J., ZHANG, W., ZHAN, S., LIU, T., WANG, D. & WU, H. 2017. CDK5/FBW7-dependent ubiquitination and degradation of EZH2 inhibits pancreatic cancer cell migration and invasion. *J Biol Chem,* 292**,** 6269-6280.

JINEK, M., CHYLINSKI, K., FONFARA, I., HAUER, M., DOUDNA, J. A. & CHARPENTIER, E. 2012. A Programmable Dual-RNA–Guided DNA Endonuclease in Adaptive Bacterial Immunity. *Science,* 337**,** 816-821.

JITKOVA, Y., GRONDA, M., HURREN, R., WANG, X., GOARD, C. A., JHAS, B. & SCHIMMER, A. D. 2014. A novel formulation of tigecycline has enhanced stability and sustained antibacterial and antileukemic activity. *PLoS One,* 9**,** e95281.

JONAS, O., LANDRY, H. M., FULLER, J. E., SANTINI, J. T., BASELGA, J., TEPPER, R. I., CIMA, M. J. & LANGER, R. 2015. An implantable microdevice to perform high-throughput in vivo drug sensitivity testing in tumors. *Science Translational Medicine,* 7**,** 284ra57.

JONES, R. A., ROBINSON, T. J., LIU, J. C., SHRESTHA, M., VOISIN, V., JU, Y., CHUNG, P. E., PELLECCHIA, G., FELL, V. L., BAE, S., MUTHUSWAMY, L., DATTI, A., EGAN, S. E., JIANG, Z., LEONE, G., BADER, G. D., SCHIMMER, A. & ZACKSENHAUS, E. 2016. RB1 deficiency in triple-negative breast cancer induces mitochondrial protein translation. *J Clin Invest,* 126**,** 3739-3757.

JOSE, C., BELLANCE, N. & ROSSIGNOL, R. 2011. Choosing between glycolysis and oxidative phosphorylation: a tumor's dilemma? *Biochim Biophys Acta,* 1807**,** 552-561.

JOST, M., CHEN, Y., GILBERT, L. A., HORLBECK, M. A., KRENNING, L., MENCHON, G., RAI, A., CHO, M. Y., STERN, J. J., PROTA, A. E., KAMPMANN, M., AKHMANOVA, A., STEINMETZ, M. O., TANENBAUM, M. E. & WEISSMAN, J. S. 2020. Pharmaceutical-Grade Rigosertib Is a Microtubule-Destabilizing Agent. *Molecular Cell,* 79**,** 191-198.e3.

JUNG, P. S., KIM, D. Y., KIM, M. B., LEE, S. W., KIM, J. H., KIM, Y. M., KIM, Y. T., HOFFMAN, R. M. & NAM, J. H. 2013. Progression-free survival is accurately predicted in patients treated with chemotherapy for epithelial ovarian cancer by the histoculture drug response assay in a prospective correlative clinical trial at a single institution. *Anticancer Res,* 33**,** 1029-1034.

JUNTTILA, M. R. & DE SAUVAGE, F. J. 2013. Influence of tumour micro-environment heterogeneity on therapeutic response. *Nature,* 501**,** 346-354.

KAELIN, W. G. 2012. Use and Abuse of RNAi to Study Mammalian Gene Function. *Science,* 337**,** 421-422.

KAISER, J. 2017. When less is more. *Science,* 355**,** 1144-1146.

KALKAVAN, H. & GREEN, D. R. 2018. MOMP, cell suicide as a BCL-2 family business. *Cell Death Differ,* 25**,** 46-55.

KANATSU-SHINOHARA, M., ONOYAMA, I., NAKAYAMA, K. I. & SHINOHARA, T. 2014. Skp1-Cullin-F-box (SCF)-type ubiquitin ligase FBXW7 negatively regulates spermatogonial stem cell self-renewal. *Proc Natl Acad Sci U S A,* 111**,** 8826-8831.

KANNAN, M. B., DODARD-FRIEDMAN, I. & BLANK, V. 2015. Stringent Control of NFE2L3 (Nuclear Factor, Erythroid 2-Like 3; NRF3) Protein Degradation by FBW7 (F-box/WD Repeat-containing Protein 7) and Glycogen Synthase Kinase 3 (GSK3). *Journal of Biological Chemistry,* 290**,** 26292-26302.

KANTARJIAN, H., SAWYERS, C., HOCHHAUS, A., GUILHOT, F., SCHIFFER, C., GAMBACORTI-PASSERINI, C., NIEDERWIESER, D., RESTA, D., CAPDEVILLE, R., ZOELLNER, U., TALPAZ, M. & DRUKER, B. 2002. Hematologic and Cytogenetic Responses to Imatinib Mesylate in Chronic Myelogenous Leukemia. *New England Journal of Medicine,* 346**,** 645-652.

KARTNER, N., RIORDAN & LING, V. 1983a. Cell surface P-glycoprotein associated with multidrug resistance in mammalian cell lines. *Science,* 221**,** 1285-1288.

KARTNER, N., SHALES, M., RIORDAN, J. R. & LING, V. 1983b. Daunorubicin-resistant Chinese Hamster Ovary Cells Expressing Multidrug Resistance and a Cell-Surface P-Glycoprotein. *Cancer Research,* 43**,** 4413-4419.

KAS, S. M., DE RUITER, J. R., SCHIPPER, K., ANNUNZIATO, S., SCHUT, E., KLARENBEEK, S., DRENTH, A. P., VAN DER BURG, E., KLIJN, C., TEN HOEVE, J. J., ADAMS, D. J., KOUDIJS, M. J., WESSELING, J., NETHE, M., WESSELS, L. F. A. & JONKERS, J. 2017. Insertional mutagenesis identifies drivers of a novel oncogenic pathway in invasive lobular breast carcinoma. *Nat Genet,* 49**,** 1219-1230.

KAS, S. M., DE RUITER, J. R., SCHIPPER, K., SCHUT, E., BOMBARDELLI, L., WIENTJENS, E., DRENTH, A. P., DE KORTE-GRIMMERINK, R., MAHAKENA, S., PHILLIPS, C., SMITH, P. D., KLARENBEEK, S., VAN DE WETERING, K., BERNS, A., WESSELS, L. F. A. & JONKERS, J. 2018. Transcriptomics and Transposon Mutagenesis Identify Multiple Mechanisms of Resistance to the FGFR Inhibitor AZD4547. *Cancer Res,* 78**,** 5668-5679.

KEENAN, A. B., JENKINS, S. L., JAGODNIK, K. M., KOPLEV, S., HE, E., TORRE, D., WANG, Z., DOHLMAN, A. B., SILVERSTEIN, M. C., LACHMANN, A., KULESHOV, M. V., MA'AYAN, A., STATHIAS, V., TERRYN, R., COOPER, D., FORLIN, M., KOLETI, A., VIDOVIC, D., CHUNG, C., SCHURER, S. C., VASILIAUSKAS, J., PILARCZYK, M., SHAMSAEI, B., FAZEL, M., REN, Y., NIU, W., CLARK, N. A., WHITE, S., MAHI, N., ZHANG, L., KOURIL, M., REICHARD, J. F., SIVAGANESAN, S., MEDVEDOVIC, M., MELLER, J., KOCH, R. J., BIRTWISTLE, M. R., IYENGAR, R., SOBIE, E. A., AZELOGLU, E. U., KAYE, J., OSTERLOH, J., HASTON, K., KALRA, J., FINKBIENER, S., LI, J., MILANI, P., ADAM, M., ESCALANTE-CHONG, R., SACHS, K., LENAIL, A., RAMAMOORTHY, D., FRAENKEL, E., DAIGLE, G., HUSSAIN, U., COYE, A., ROTHSTEIN, J., SAREEN, D., ORNELAS, L., BANUELOS, M., MANDEFRO, B., HO, R., SVENDSEN, C. N., LIM, R. G., STOCKSDALE, J., CASALE, M. S., THOMPSON, T. G., WU, J., THOMPSON, L. M., DARDOV, V., VENKATRAMAN, V., MATLOCK, A., VAN EYK, J. E., JAFFE, J. D., PAPANASTASIOU, M., SUBRAMANIAN, A., GOLUB, T. R., ERICKSON, S. D., FALLAHI-SICHANI, M., HAFNER, M., GRAY, N. S., LIN, J. R., MILLS, C. E., MUHLICH, J. L., NIEPEL, M., SHAMU, C. E., WILLIAMS, E. H., WROBEL, D., SORGER, P. K., HEISER, L. M., GRAY, J. W., KORKOLA, J. E., MILLS, G. B., LABARGE, M., FEILER, H. S., DANE, M. A., BUCHER, E., NEDERLOF, M., SUDAR, D., GROSS, S., et al. 2018. The Library of Integrated Network-Based Cellular Signatures NIH Program: System-Level Cataloging of Human Cells Response to Perturbations. *Cell Syst,* 6**,** 13-24.

KELLER, T. L., ZOCCO, D., SUNDRUD, M. S., HENDRICK, M., EDENIUS, M., YUM, J., KIM, Y. J., LEE, H. K., CORTESE, J. F., WIRTH, D. F., DIGNAM, J. D., RAO, A., YEO, C. Y., MAZITSCHEK, R. & WHITMAN, M. 2012. Halofuginone and other febrifugine derivatives inhibit prolyl-tRNA synthetase. *Nat Chem Biol,* 8**,** 311-317.

KELNER, A. 1949. Effect of Visible Light on the Recovery of Streptomyces Griseus Conidia from Ultra-violet Irradiation Injury. *Proceedings of the National Academy of Sciences,* 35**,** 73-79.

KHAN, O. M., ALMAGRO, J., NELSON, J. K., HORSWELL, S., ENCHEVA, V., KEYAN, K. S., CLURMAN, B. E., SNIJDERS, A. P. & BEHRENS, A. 2021. Proteasomal degradation of the tumour suppressor FBW7 requires branched ubiquitylation by TRIP12. *Nat Commun,* 12**,** 2043.

KHAN, O. M., CARVALHO, J., SPENCER-DENE, B., MITTER, R., FRITH, D., SNIJDERS, A. P., WOOD, S. A. & BEHRENS, A. 2018. The deubiquitinase USP9X regulates FBW7 stability and suppresses colorectal cancer. *J Clin Invest,* 128**,** 1326-1337.

KHARAT, S. S., TRIPATHI, V., DAMODARAN, A. P., PRIYADARSHINI, R., CHANDRA, S., TIKOO, S., NANDHAKUMAR, R., SRIVASTAVA, V., PRIYA, S., HUSSAIN, M., KAUR, S., FISHMAN, J. B. & SENGUPTA, S. 2016. Mitotic phosphorylation of Bloom helicase at Thr182 is required for its proteasomal degradation and maintenance of chromosomal stability. *Oncogene,* 35**,** 1025-1038.

KIM, D. J., TREMBLAY, M. L. & DIGIOVANNI, J. 2010. Protein tyrosine phosphatases, TC-PTP, SHP1, and SHP2, cooperate in rapid dephosphorylation of Stat3 in keratinocytes following UVB irradiation. *PLoS One,* 5**,** e10290.

KIM, D. S., ZHANG, W., MILLMAN, S. E., HWANG, B. J., KWON, S. J., CLAYBERGER, C., PAGANO, M. & KRENSKY, A. M. 2012. Fbw7γ-mediated degradation of KLF13 prevents RANTES expression in resting human but not murine T lymphocytes. *Blood,* 120**,** 1658-1667.

KIM, H. J., MAITI, P. & BARRIENTOS, A. 2017a. Mitochondrial ribosomes in cancer. *Semin Cancer Biol,* 47**,** 67-81.

KIM, K. H., JEONG, Y. T., KIM, S. H., JUNG, H. S., PARK, K. S., LEE, H. Y. & LEE, M. S. 2013. Metformin-induced inhibition of the mitochondrial respiratory chain increases FGF21 expression via ATF4 activation. *Biochem Biophys Res Commun,* 440**,** 76-81.

KIM, M., MORALES, L. D., BAEK, M., SLAGA, T. J., DIGIOVANNI, J. & KIM, D. J. 2017b. UVB-induced nuclear translocation of TC-PTP by AKT/14-3-3σ axis inhibits keratinocyte survival and proliferation. *Oncotarget,* 8**,** 90674-90692.

KIMURA, T., GOTOH, M., NAKAMURA, Y. & ARAKAWA, H. 2003. hCDC4b, a regulator of cyclin E, as a direct transcriptional target of p53. *Cancer Sci,* 94**,** 431-436.

KITADA, S., ANDERSEN, J., AKAR, S., ZAPATA, J. M., TAKAYAMA, S., KRAJEWSKI, S., WANG, H.-G., ZHANG, X., BULLRICH, F., CROCE, C. M., RAI, K., HINES, J. & REED, J. C. 1998. Expression of Apoptosis-Regulating Proteins in Chronic Lymphocytic Leukemia: Correlations With In Vitro and In Vivo Chemoresponses. *Blood,* 91**,** 3379-3389.

KITAGAWA, K., HIRAMATSU, Y., UCHIDA, C., ISOBE, T., HATTORI, T., ODA, T., SHIBATA, K., NAKAMURA, S., KIKUCHI, A. & KITAGAWA, M. 2009. Fbw7 promotes ubiquitin-dependent degradation of c-Myb: involvement of GSK3-mediated phosphorylation of Thr-572 in mouse c-Myb. *Oncogene,* 28**,** 2393-2405.

KITAGAWA, K., SHIBATA, K., MATSUMOTO, A., MATSUMOTO, M., OHHATA, T., NAKAYAMA, K. I., NIIDA, H. & KITAGAWA, M. 2014. Fbw7 targets GATA3 through cyclin-dependent kinase 2-dependent proteolysis and contributes to regulation of T-cell development. *Mol Cell Biol,* 34**,** 2732-2744.

KLOTZ, K., CEPEDA, D., TAN, Y., SUN, D., SANGFELT, O. & SPRUCK, C. 2009. SCF(Fbxw7/hCdc4) targets cyclin E2 for ubiquitin-dependent proteolysis. *Exp Cell Res,* 315**,** 1832-1839.

KO, T. & LI, S. 2019. Genome-wide screening identifies novel genes and biological processes implicated in cisplatin resistance. *FASEB J,* 33**,** 7143-7154.

KOBAYASHI, S., BOGGON, T. J., DAYARAM, T., JÄNNE, P. A., KOCHER, O., MEYERSON, M., JOHNSON, B. E., ECK, M. J., TENEN, D. G. & HALMOS, B. 2005. EGFR Mutation and Resistance of Non–Small-Cell Lung Cancer to Gefitinib. *New England Journal of Medicine,* 352**,** 786-792.

KOEPP, D. M., SCHAEFER, L. K., YE, X., KEYOMARSI, K., CHU, C., HARPER, J. W. & ELLEDGE, S. J. 2001. Phosphorylation-Dependent Ubiquitination of Cyclin E by the SCFFbw7 Ubiquitin Ligase. *Science,* 294**,** 173-177.

KOIKE-YUSA, H., LI, Y., TAN, E. P., VELASCO-HERRERA MDEL, C. & YUSA, K. 2014. Genome-wide recessive genetic screening in mammalian cells with a lentiviral CRISPR-guide RNA library. *Nat Biotechnol,* 32**,** 267-273.

KOMANDER, D. & RAPE, M. 2012. The ubiquitin code. *Annu Rev Biochem,* 81**,** 203-229.

KONERMANN, S., BRIGHAM, M. D., TREVINO, A. E., JOUNG, J., ABUDAYYEH, O. O., BARCENA, C., HSU, P. D., HABIB, N., GOOTENBERG, J. S., NISHIMASU, H., NUREKI, O. & ZHANG, F. 2015. Genome-scale transcriptional activation by an engineered CRISPR-Cas9 complex. *Nature,* 517**,** 583-588.

KOO, J., WU, X., MAO, Z., KHURI, F. R. & SUN, S. Y. 2015. Rictor Undergoes Glycogen Synthase Kinase 3 (GSK3)-dependent, FBXW7-mediated Ubiquitination and Proteasomal Degradation. *J Biol Chem,* 290**,** 14120-14129.

KOROTKEVICH, G., SUKHOV, V. & SERGUSHICHEV, A. 2019. Fast gene set enrichment analysis. *bioRxiv***,** 060012.

KOURTIS, N., MOUBARAK, R. S., ARANDA-ORGILLES, B., LUI, K., AYDIN, I. T., TRIMARCHI, T., DARVISHIAN, F., SALVAGGIO, C., ZHONG, J., BHATT, K., CHEN, E. I., CELEBI, J. T., LAZARIS, C., TSIRIGOS, A., OSMAN, I., HERNANDO, E. & AIFANTIS, I. 2015. FBXW7 modulates cellular stress response and metastatic potential through HSF1 post-translational modification. *Nat Cell Biol,* 17**,** 322-332.

KRAEMER, K. H. 1997. Sunlight and skin cancer: Another link revealed. *Proceedings of the National Academy of Sciences,* 94**,** 11-14.

KRIS, M. G., NATALE, R. B., HERBST, R. S., LYNCH, J. T. J., PRAGER, D., BELANI, C. P., SCHILLER, J. H., KELLY, K., SPIRIDONIDIS, H., SANDLER, A., ALBAIN, K. S., CELLA, D., WOLF, M. K., AVERBUCH, S. D., OCHS, J. J. & KAY, A. C. 2003. Efficacy of Gefitinib, an Inhibitor of the Epidermal Growth Factor Receptor Tyrosine Kinase, in Symptomatic Patients With Non–Small Cell Lung Cancer: A Randomized Trial. *JAMA,* 290**,** 2149-2158.

KROKOWSKI, D., HAN, J., SAIKIA, M., MAJUMDER, M., YUAN, C. L., GUAN, B. J., BEVILACQUA, E., BUSSOLATI, O., BRÖER, S., ARVAN, P., TCHÓRZEWSKI, M., SNIDER, M. D., PUCHOWICZ, M., CRONIGER, C. M., KIMBALL, S. R., PAN, T., KOROMILAS, A. E., KAUFMAN, R. J. & HATZOGLOU, M. 2013. A self-defeating anabolic program leads to β-cell apoptosis in endoplasmic reticulum stress-induced diabetes via regulation of amino acid flux. *J Biol Chem,* 288**,** 17202-17213.

KROON, A. M., DONTJE, B. H. J., HOLTROP, M. & VAN DEN BOGERT, C. 1984. The mitochondrial genetic system as a target for chemotherapy: Tetracyclines as cytostatics. *Cancer Letters,* 25**,** 33-40.

KUAI, X., LI, L., CHEN, R., WANG, K., CHEN, M., CUI, B., ZHANG, Y., LI, J., ZHU, H., ZHOU, H., HUANG, J., QIN, J., WANG, Z., WEI, W. & GAO, D. 2019. SCF(FBXW7)/GSK3beta-Mediated GFI1 Degradation Suppresses Proliferation of Gastric Cancer Cells. *Cancer Res,* 79**,** 4387-4398.

KUMAR, Y., SHUKLA, N., THACKER, G., KAPOOR, I., LOCHAB, S., BHATT, M. L., CHATTOPADHYAY, N., SANYAL, S. & TRIVEDI, A. K. 2016. Ubiquitin Ligase, Fbw7, Targets CDX2 for Degradation via Two Phosphodegron Motifs in a GSK3beta-Dependent Manner. *Mol Cancer Res,* 14**,** 1097-1109.

KUNTZ, E. M., BAQUERO, P., MICHIE, A. M., DUNN, K., TARDITO, S., HOLYOAKE, T. L., HELGASON, G. V. & GOTTLIEB, E. 2017. Targeting mitochondrial oxidative phosphorylation eradicates therapy-resistant chronic myeloid leukemia stem cells. *Nat Med,* 23**,** 1234-1240.

KWON, Y. W., KIM, I. J., WU, D., LU, J., STOCK, W. A., JR., LIU, Y., HUANG, Y., KANG, H. C., DELROSARIO, R., JEN, K. Y., PEREZ-LOSADA, J., WEI, G., BALMAIN, A. & MAO, J. H. 2012. Pten regulates Aurora-A and cooperates with Fbxw7 in modulating radiation-induced tumor development. *Mol Cancer Res,* 10**,** 834-844.

LAGADINOU, E. D., SACH, A., CALLAHAN, K., ROSSI, R. M., NEERING, S. J., MINHAJUDDIN, M., ASHTON, J. M., PEI, S., GROSE, V., O'DWYER, K. M., LIESVELD, J. L., BROOKES, P. S., BECKER, M. W. & JORDAN, C. T. 2013. BCL-2 inhibition targets oxidative phosphorylation and selectively eradicates quiescent human leukemia stem cells. *Cell Stem Cell,* 12**,** 329-341.

LAI, A. C. & CREWS, C. M. 2017. Induced protein degradation: an emerging drug discovery paradigm. *Nat Rev Drug Discov,* 16**,** 101-114.

LAMB, J., CRAWFORD, E. D., PECK, D., MODELL, J. W., BLAT, I. C., WROBEL, M. J., LERNER, J., BRUNET, J. P., SUBRAMANIAN, A., ROSS, K. N., REICH, M., HIERONYMUS, H., WEI, G., ARMSTRONG, S. A., HAGGARTY, S. J., CLEMONS, P. A., WEI, R., CARR, S. A., LANDER, E. S. & GOLUB, T. R. 2006. The Connectivity Map: using gene-expression signatures to connect small molecules, genes, and disease. *Science,* 313**,** 1929-1935.

LAMB, R., OZSVARI, B., LISANTI, C. L., TANOWITZ, H. B., HOWELL, A., MARTINEZ-OUTSCHOORN, U. E., SOTGIA, F. & LISANTI, M. P. 2015. Antibiotics that target mitochondria effectively eradicate cancer stem cells, across multiple tumor types: Treating cancer like an infectious disease. *Oncotarget,* 6**,** 4569-4584.

LAN, H., TAN, M., ZHANG, Q., YANG, F., WANG, S., LI, H., XIONG, X. & SUN, Y. 2019. LSD1 destabilizes FBXW7 and abrogates FBXW7 functions independent of its demethylase activity. *Proc Natl Acad Sci U S A,* 116**,** 12311-12320.

LARMAN, T. C., DEPALMA, S. R., HADJIPANAYIS, A. G., CANCER GENOME ATLAS RESEARCH, N., PROTOPOPOV, A., ZHANG, J., GABRIEL, S. B., CHIN, L., SEIDMAN, C. E., KUCHERLAPATI, R. & SEIDMAN, J. G. 2012. Spectrum of somatic mitochondrial mutations in five cancers. *Proc Natl Acad Sci U S A,* 109**,** 14087-14091.

LASSOT, I., SEGERAL, E., BERLIOZ-TORRENT, C., DURAND, H., GROUSSIN, L., HAI, T., BENAROUS, R. & MARGOTTIN-GOGUET, F. 2001. ATF4 degradation relies on a phosphorylation-dependent interaction with the SCF(betaTrCP) ubiquitin ligase. *Mol Cell Biol,* 21**,** 2192-2202.

LAWRENCE, M. S., STOJANOV, P., POLAK, P., KRYUKOV, G. V., CIBULSKIS, K., SIVACHENKO, A., CARTER, S. L., STEWART, C., MERMEL, C. H., ROBERTS, S. A., KIEZUN, A., HAMMERMAN, P. S., MCKENNA, A., DRIER, Y., ZOU, L., RAMOS, A. H., PUGH, T. J., STRANSKY, N., HELMAN, E., KIM, J., SOUGNEZ, C., AMBROGIO, L., NICKERSON, E., SHEFLER, E., CORTES, M. L., AUCLAIR, D., SAKSENA, G., VOET, D., NOBLE, M., DICARA, D., LIN, P., LICHTENSTEIN, L., HEIMAN, D. I., FENNELL, T., IMIELINSKI, M., HERNANDEZ, B., HODIS, E., BACA, S., DULAK, A. M., LOHR, J., LANDAU, D. A., WU, C. J., MELENDEZ-ZAJGLA, J., HIDALGO-MIRANDA, A., KOREN, A., MCCARROLL, S. A., MORA, J., CROMPTON, B., ONOFRIO, R., PARKIN, M., WINCKLER, W., ARDLIE, K., GABRIEL, S. B., ROBERTS, C. W. M., BIEGEL, J. A., STEGMAIER, K., BASS, A. J., GARRAWAY, L. A., MEYERSON, M., GOLUB, T. R., GORDENIN, D. A., SUNYAEV, S., LANDER, E. S. & GETZ, G. 2013. Mutational heterogeneity in cancer and the search for new cancer-associated genes. *Nature,* 499**,** 214-218.

LAWSON, K. A., SOUSA, C. M., ZHANG, X., KIM, E., AKTHAR, R., CAUMANNS, J. J., YAO, Y., MIKOLAJEWICZ, N., ROSS, C., BROWN, K. R., ZID, A. A., FAN, Z. P., HUI, S., KRALL, J. A., SIMONS, D. M., SLATER, C. J., DE JESUS, V., TANG, L., SINGH, R., GOLDFORD, J. E., MARTIN, S., HUANG, Q., FRANCIS, E. A., HABSID, A., CLIMIE, R., TIEU, D., WEI, J., LI, R., TONG, A. H. Y., AREGGER, M., CHAN, K. S., HAN, H., WANG, X., MERO, P., BRUMELL, J. H., FINELLI, A., AILLES, L., BADER, G., SMOLEN, G. A., KINGSBURY, G. A., HART, T.,

KUNG, C. & MOFFAT, J. 2020. Functional genomic landscape of cancer-intrinsic evasion of killing by T cells. *Nature,* 586**,** 120-126.

LEACH, D. R., KRUMMEL, M. F. & ALLISON, J. P. 1996. Enhancement of Antitumor Immunity by CTLA-4 Blockade. *Science,* 271**,** 1734-1736.

LEE, H., KIM, M., BAEK, M., MORALES, L. D., JANG, I. S., SLAGA, T. J., DIGIOVANNI, J. & KIM, D. J. 2017a. Targeted disruption of TC-PTP in the proliferative compartment augments STAT3 and AKT signaling and skin tumor development. *Sci Rep,* 7**,** 45077.

LEE, H., MORALES, L. D., SLAGA, T. J. & KIM, D. J. 2015. Activation of T-cell protein-tyrosine phosphatase suppresses keratinocyte survival and proliferation following UVB irradiation. *J Biol Chem,* 290**,** 13-24.

LEE, J. W., KANG, H. S., LEE, J. Y., LEE, E. J., RHIM, H., YOON, J. H., SEO, S. R. & CHUNG, K. C. 2012. The transcription factor STAT2 enhances proteasomal degradation of RCAN1 through the ubiquitin E3 ligase FBW7. *Biochem Biophys Res Commun,* 420**,** 404-410.

LEE, K. M., GILTNANE, J. M., BALKO, J. M., SCHWARZ, L. J., GUERRERO-ZOTANO, A. L., HUTCHINSON, K. E., NIXON, M. J., ESTRADA, M. V., SANCHEZ, V., SANDERS, M. E., LEE, T., GOMEZ, H., LLUCH, A., PEREZ-FIDALGO, J. A., WOLF, M. M., ANDREJEVA, G., RATHMELL, J. C., FESIK, S. W. & ARTEAGA, C. L. 2017b. MYC and MCL1 Cooperatively Promote Chemotherapy-Resistant Breast Cancer Stem Cells via Regulation of Mitochondrial Oxidative Phosphorylation. *Cell Metab,* 26**,** 633-647 e7.

LEEZENBERG, J. A., WESSELING, H. & KROON, A. M. 1979. Possible cytostatic action of tetracyclines in the treatment of tumors of the nasopharynx and larynx. *European Journal of Clinical Pharmacology,* 16**,** 237-241.

LEITER, U., KEIM, U. & GARBE, C. 2020. Epidemiology of Skin Cancer: Update 2019. *In:* REICHRATH, J. (ed.) *Sunlight, Vitamin D and Skin Cancer.* Cham: Springer International Publishing.

LETAI, A. G. 2008. Diagnosing and exploiting cancer's addiction to blocks in apoptosis. *Nat Rev Cancer,* 8**,** 121-132.

LETTNIN, A. P., WAGNER, E. F., CARRETT-DIAS, M., DOS SANTOS MACHADO, K., WERHLI, A., CANEDO, A. D., TRINDADE, G. S. & DE SOUZA VOTTO, A. P. 2019. Silencing the OCT4-PG1 pseudogene reduces OCT-4 protein levels and changes characteristics of the multidrug resistance phenotype in chronic myeloid leukemia. *Mol Biol Rep,* 46**,** 1873-1884.

LEY, R. D. 1993. Photoreactivation in humans. *Proceedings of the National Academy of Sciences of the United States of America,* 90**,** 4337-4337.

LI, F., WANG, Y., ZELLER, K. I., POTTER, J. J., WONSEY, D. R., O'DONNELL, K. A., KIM, J. W., YUSTEIN, J. T., LEE, L. A. & DANG, C. V. 2005. Myc stimulates nuclearly encoded mitochondrial genes and mitochondrial biogenesis. *Mol Cell Biol,* 25**,** 6225-6234.

LI, H., JIAO, S., LI, X., BANU, H., HAMAL, S. & WANG, X. 2015a. Therapeutic effects of antibiotic drug tigecycline against cervical squamous cell carcinoma by inhibiting Wnt/beta-catenin signaling. *Biochem Biophys Res Commun,* 467**,** 14-20.

LI, J., PAULEY, A. M., MYERS, R. L., SHUANG, R., BRASHLER, J. R., YAN, R., BUHL, A. E., RUBLE, C. & GURNEY, M. E. 2002. SEL-10 interacts with presenilin1, facilitates its ubiquitination, and alters A-beta peptide production. *Journal of Neurochemistry,* 82**,** 1540-1548.

LI, M. R., ZHU, C. C., LING, T. L., ZHANG, Y. Q., XU, J., ZHAO, E. H. & ZHAO, G. 2017. FBXW7 expression is associated with prognosis and chemotherapeutic outcome in Chinese patients with gastric adenocarcinoma. *BMC Gastroenterol,* 17**,** 60.

LI, N., BABAEI-JADIDI, R., LORENZI, F., SPENCER-DENE, B., CLARKE, P., DOMINGO, E., TULCHINSKY, E., VRIES, R. G. J., KERR, D., PAN, Y., HE, Y., BATES, D. O., TOMLINSON, I., CLEVERS, H. & NATERI, A. S. 2019. An FBXW7-ZEB2 axis links EMT and tumour microenvironment to promote colorectal cancer stem cells and chemoresistance. *Oncogenesis,* 8**,** 13.

LI, N., LORENZI, F., KALAKOUTI, E., NORMATOVA, M., BABAEI-JADIDI, R., TOMLINSON, I. & NATERI, A. S. 2015b. FBXW7-mutated colorectal cancer cells exhibit aberrant expression of phosphorylated-p53 at Serine-15. *Oncotarget,* 6**,** 9240-9256.

LI, Q., LI, Y., LI, J., MA, Y., DAI, W., MO, S., XU, Y., LI, X. & CAI, S. 2018a. FBW7 suppresses metastasis of colorectal cancer by inhibiting HIF1alpha/CEACAM5 functional axis. *Int J Biol Sci,* 14**,** 726-735.

LI, R., WU, S., CHEN, X., XU, H., TENG, P. & LI, W. 2016. miR-223/FBW7 axis regulates doxorubicin sensitivity through epithelial mesenchymal transition in non-small cell lung cancer. *American journal of translational research,* 8**,** 2512-2524.

LI, Y., HU, K., XIAO, X., WU, W., YAN, H., CHEN, H., CHEN, Z. & YIN, D. 2018b. FBW7 suppresses cell proliferation and G2/M cell cycle transition via promoting gamma-catenin K63-linked ubiquitylation. *Biochem Biophys Res Commun,* 497**,** 473-479.

LIAO, H. X. & SPREMULLI, L. L. 1989. Interaction of bovine mitochondrial ribosomes with messenger RNA. *J Biol Chem,* 264**,** 7518-7522.

LIAO, S., MAERTENS, O., CICHOWSKI, K. & ELLEDGE, S. J. 2018. Genetic modifiers of the BRD4-NUT dependency of NUT midline carcinoma uncovers a synergism between BETis and CDK4/6is. *Genes Dev,* 32**,** 1188-1200.

LIAO, S. Y., CHIANG, C. W., HSU, C. H., CHEN, Y. T., JEN, J., JUAN, H. F., LAI, W. W. & WANG, Y. C. 2017. CK1δ/GSK3β/FBXW7α axis promotes degradation of the ZNF322A oncoprotein to suppress lung cancer progression. *Oncogene,* 36**,** 5722-5733.

LIN, J., JI, A., QIU, G., FENG, H., LI, J., LI, S., ZOU, Y., CUI, Y., SONG, C., HE, H. & LU, Y. 2018. FBW7 is associated with prognosis, inhibits malignancies and enhances temozolomide sensitivity in glioblastoma cells. *Cancer Sci,* 109**,** 1001-1011.

LIN, K. H., RUTTER, J. C., XIE, A., PARDIEU, B., WINN, E. T., BELLO, R. D., FORGET, A., ITZYKSON, R., AHN, Y. R., DAI, Z., SOBHAN, R. T., ANDERSON, G. R., SINGLETON, K. R., DECKER, A. E., WINTER, P. S., LOCASALE, J. W., CRAWFORD, L., PUISSANT, A. & WOOD, K. C. 2020. Using antagonistic pleiotropy to design a chemotherapy-induced evolutionary trap to target drug resistance in cancer. *Nat Genet,* 52**,** 408-417.

LIN, M., XU, Y., GAO, Y., PAN, C., ZHU, X. & WANG, Z. W. 2019. Regulation of F-box proteins by noncoding RNAs in human cancers. *Cancer Lett,* 466**,** 61-70.

LIU, C., BANISTER, C. E. & BUCKHAULTS, P. J. 2019. Spindle Assembly Checkpoint Inhibition Can Resensitize p53-Null Stem Cells to Cancer Chemotherapy. *Cancer Res,* 79**,** 2392-2403.

LIU, H., REN, C., LIU, W., JIANG, X., WANG, L., ZHU, B., JIA, W., LIN, J., TAN, J. & LIU, X. 2017. Embryotoxicity estimation of commonly used compounds with embryonic stem cell test. *Mol Med Rep,* 16**,** 263-271.

LIU, L., JIANG, H., WANG, X., WANG, X. & ZOU, L. 2020. STYX/FBXW7 axis participates in the development of endometrial cancer cell via Notch-mTOR signaling pathway. *Biosci Rep,* 40**,** BSR20200057.

LIU, N., LI, H., LI, S., SHEN, M., XIAO, N., CHEN, Y., WANG, Y., WANG, W., WANG, R., WANG, Q., SUN, J. & WANG, P. 2010. The Fbw7/human CDC4 tumor suppressor targets proproliferative factor KLF5 for ubiquitination and degradation through multiple phosphodegron motifs. *J Biol Chem,* 285**,** 18858-18867.

LOCHAB, S., PAL, P., KAPOOR, I., KANAUJIYA, J. K., SANYAL, S., BEHRE, G. & TRIVEDI, A. K. 2013. E3 ubiquitin ligase Fbw7 negatively regulates granulocytic differentiation by targeting G-CSFR for degradation. *Biochim Biophys Acta,* 1833**,** 2639-2652.

LONERGAN, T., BAVISTER, B. & BRENNER, C. 2007. Mitochondria in stem cells. *Mitochondrion,* 7**,** 289-296.

LONG, Y., TSAI, W. B., WANGPAICHITR, M., TSUKAMOTO, T., SAVARAJ, N., FEUN, L. G. & KUO, M. T. 2013. Arginine deiminase resistance in melanoma cells is associated with metabolic reprogramming, glucose dependence, and glutamine addiction. *Mol Cancer Ther,* 12**,** 2581-2590.

LONGLEY, D. B. & JOHNSTON, P. G. 2005. Molecular mechanisms of drug resistance. *J Pathol,* 205**,** 275-292.

LOPEZ-CAMARILLO, C., OCAMPO, E. A., CASAMICHANA, M. L., PEREZ-PLASENCIA, C., ALVAREZ-SANCHEZ, E. & MARCHAT, L. A. 2012. Protein kinases and transcription factors activation in response to UV-radiation of skin: implications for carcinogenesis. *Int J Mol Sci,* 13**,** 142-172.

LORENZI, F., BABAEI-JADIDI, R., SHEARD, J., SPENCER-DENE, B. & NATERI, A. S. 2016. Fbxw7-associated drug resistance is reversed by induction of terminal differentiation in murine intestinal organoid culture. *Mol Ther Methods Clin Dev,* 3**,** 16024.

LOS, G. V., ENCELL, L. P., MCDOUGALL, M. G., HARTZELL, D. D., KARASSINA, N., ZIMPRICH, C., WOOD, M. G., LEARISH, R., OHANA, R. F., URH, M., SIMPSON, D., MENDEZ, J., ZIMMERMAN, K., OTTO, P., VIDUGIRIS, G., ZHU, J., DARZINS, A., KLAUBERT, D. H., BULLEIT, R. F. & WOOD, K. V. 2008. HaloTag: A Novel Protein Labeling Technology for Cell Imaging and Protein Analysis. *ACS Chemical Biology,* 3**,** 373-382.

LU, D., DAVIS, M. P., ABREU-GOODGER, C., WANG, W., CAMPOS, L. S., SIEDE, J., VIGORITO, E., SKARNES, W. C., DUNHAM, I., ENRIGHT, A. J. & LIU, P. 2012. MiR-25 regulates Wwp2 and Fbxw7 and promotes reprogramming of mouse fibroblast cells to iPSCs. *PLoS One,* 7**,** e40938.

LU, Z., XU, N., HE, B., PAN, C., LAN, Y., ZHOU, H. & LIU, X. 2017. Inhibition of autophagy enhances the selective anti-cancer activity of tigecycline to overcome drug resistance in the treatment of chronic myeloid leukemia. *J Exp Clin Cancer Res,* 36**,** 43.

LUM, P. Y., ARMOUR, C. D., STEPANIANTS, S. B., CAVET, G., WOLF, M. K., BUTLER, J. S., HINSHAW, J. C., GARNIER, P., PRESTWICH, G. D., LEONARDSON, A., GARRETT-ENGELE, P., RUSH, C. M., BARD, M., SCHIMMACK, G., PHILLIPS, J. W., ROBERTS, C. J. & SHOEMAKER, D. D. 2004. Discovering Modes of Action for Therapeutic Compounds Using a Genome-Wide Screen of Yeast Heterozygotes. *Cell,* 116**,** 121-137.

LV, X. B., WU, W., TANG, X., WU, Y., ZHU, Y., LIU, Y., CUI, X., CHU, J., HU, P., LI, J., GUO, Q., CAI, Z., WU, J., HU, K. & OUYANG, N. 2015. Regulation of SOX10 stability via ubiquitination-mediated degradation by Fbxw7α modulates melanoma cell migration. *Oncotarget,* 6**,** 36370-36382.

MA, L., BOUCHER, J. I., PAULSEN, J., MATUSZEWSKI, S., EIDE, C. A., OU, J., EICKELBERG, G., PRESS, R. D., ZHU, L. J., DRUKER, B. J., BRANFORD, S., WOLFE, S. A., JENSEN, J. D., SCHIFFER, C. A., GREEN, M. R. & BOLON, D. N. 2017. CRISPR-Cas9-mediated saturated mutagenesis screen predicts clinical drug resistance with improved accuracy. *Proc Natl Acad Sci U S A,* 114**,** 11751-11756.

MA, R., ZHANG, Y., WANG, W., WU, J., YANG, Q., XU, W., JIANG, S., HAN, Y., YU, K. & ZHANG, S. 2018. Inhibition of autophagy enhances the antitumour activity of tigecycline in multiple myeloma. *J Cell Mol Med,* 22**,** 5955-5963.

MACLEOD, G., BOZEK, D. A., RAJAKULENDRAN, N., MONTEIRO, V., AHMADI, M., STEINHART, Z., KUSHIDA, M. M., YU, H., COUTINHO, F. J., CAVALLI, F. M. G., RESTALL, I., HAO, X., HART, T., LUCHMAN, H. A., WEISS, S., DIRKS, P. B. & ANGERS, S. 2019. Genome-Wide CRISPR-Cas9 Screens Expose Genetic Vulnerabilities and Mechanisms of Temozolomide Sensitivity in Glioblastoma Stem Cells. *Cell Rep,* 27**,** 971-986 e9.

MAIR, B., TOMIC, J., MASUD, S. N., TONGE, P., WEISS, A., USAJ, M., TONG, A. H. Y., KWAN, J. J., BROWN, K. R., TITUS, E., ATKINS, M., CHAN, K. S. K., MUNSIE, L., HABSID, A., HAN, H., KENNEDY, M., COHEN, B., KELLER, G. & MOFFAT, J. 2019. Essential Gene Profiles for Human Pluripotent Stem Cells Identify Uncharacterized Genes and Substrate Dependencies. *Cell Rep,* 27**,** 599-615 e12.

MAJUMDER, B., BARANEEDHARAN, U., THIYAGARAJAN, S., RADHAKRISHNAN, P., NARASIMHAN, H., DHANDAPANI, M., BRIJWANI, N., PINTO, D. D., PRASATH, A., SHANTHAPPA, B. U., THAYAKUMAR, A., SURENDRAN, R., BABU, G. K., SHENOY, A. M., KURIAKOSE, M. A., BERGTHOLD, G., HOROWITZ, P., LODA, M., BEROUKHIM, R., AGARWAL, S., SENGUPTA, S., SUNDARAM, M. & MAJUMDER, P. K. 2015. Predicting clinical response to anticancer drugs using an ex vivo platform that captures tumour heterogeneity. *Nat Commun,* 6**,** 6169.

MALET-MARTINO, M. & MARTINO, R. 2002. Clinical Studies of Three Oral Prodrugs of 5-Fluorouracil (Capecitabine, UFT, S-1): A Review. *The Oncologist,* 7**,** 288-323.

MALI, P., YANG, L., ESVELT, K. M., AACH, J., GUELL, M., DICARLO, J. E., NORVILLE, J. E. & CHURCH, G. M. 2013. RNA-Guided Human Genome Engineering via Cas9. *Science,* 339**,** 823-826.

MALYUKOVA, A., BROWN, S., PAPA, R., O'BRIEN, R., GILES, J., TRAHAIR, T. N., DALLA POZZA, L., SUTTON, R., LIU, T., HABER, M., NORRIS, M. D., LOCK, R. B., SANGFELT, O. & MARSHALL, G. M. 2013. FBXW7 regulates glucocorticoid response in T-cell acute lymphoblastic leukaemia by targeting the glucocorticoid receptor for degradation. *Leukemia,* 27**,** 1053-1062.

MALYUKOVA, A., DOHDA, T., VON DER LEHR, N., AKHOONDI, S., CORCORAN, M., HEYMAN, M., SPRUCK, C., GRANDER, D., LENDAHL, U. & SANGFELT, O. 2007. The tumor suppressor gene hCDC4 is frequently mutated in human T-cell acute lymphoblastic leukemia with functional consequences for Notch signaling. *Cancer Res,* 67**,** 5611-5616.

MANDEMAKERS, W., MORAIS, V. A. & DE STROOPER, B. 2007. A cell biological perspective on mitochondrial dysfunction in Parkinson disease and other neurodegenerative diseases. *Journal of Cell Science,* 120**,** 1707-1716.

MANGUSO, R. T., POPE, H. W., ZIMMER, M. D., BROWN, F. D., YATES, K. B., MILLER, B. C., COLLINS, N. B., BI, K., LAFLEUR, M. W., JUNEJA, V. R., WEISS, S. A., LO, J., FISHER, D. E., MIAO, D., VAN ALLEN, E., ROOT, D. E., SHARPE, A. H., DOENCH, J. G. & HAINING, W. N. 2017. In vivo CRISPR screening identifies Ptpn2 as a cancer immunotherapy target. *Nature,* 547**,** 413-418.

MANI, S. A., GUO, W., LIAO, M. J., EATON, E. N., AYYANAN, A., ZHOU, A. Y., BROOKS, M., REINHARD, F., ZHANG, C. C., SHIPITSIN, M., CAMPBELL, L. L., POLYAK, K., BRISKEN, C., YANG, J. & WEINBERG, R. A. 2008. The epithelial-mesenchymal transition generates cells with properties of stem cells. *Cell,* 133**,** 704-715.

MANSOORI, B., MOHAMMADI, A., DAVUDIAN, S., SHIRJANG, S. & BARADARAN, B. 2017. The Different Mechanisms of Cancer Drug Resistance: A Brief Review. *Adv Pharm Bull,* 7**,** 339-348.

MAO, J.-H., KIM, I.-J., WU, D., CLIMENT, J., KANG, H. C., DELROSARIO, R. & BALMAIN, A. 2008. FBXW7 Targets mTOR for Degradation and Cooperates with PTEN in Tumor Suppression. *Science,* 321**,** 1499-1502.

MAO, J.-H., PEREZ-LOSADA, J., WU, D., DELROSARIO, R., TSUNEMATSU, R., NAKAYAMA, K. I., BROWN, K., BRYSON, S. & BALMAIN, A. 2004. Fbxw7/Cdc4 is a p53-dependent, haploinsufficient tumour suppressor gene. *Nature,* 432**,** 775-779.

MARGULIS, L. 1970. *Origin of eukaryotic cells: evidence and research implications for a theory of the origin and evolution of microbial, plant, and animal cells on the Precambrian earth*, New Haven: Yale University Press.

MARINIELLO, M., PETRUZZELLI, R., WANDERLINGH, L. G., LA MONTAGNA, R., CARISSIMO, A., PANE, F., AMORESANO, A., ILYECHOVA, E. Y., GALAGUDZA, M. M., CATALANO, F., CRISPINO, R., PUCHKOVA, L. V., MEDINA, D. L. & POLISHCHUK, R. S. 2020. Synthetic Lethality Screening Identifies FDA-Approved Drugs that Overcome ATP7B-Mediated Tolerance of Tumor Cells to Cisplatin. *Cancers (Basel),* 12**,** 608.

MARKOVIC, D. S., VINNAKOTA, K., VAN ROOIJEN, N., KIWIT, J., SYNOWITZ, M., GLASS, R. & KETTENMANN, H. 2011. Minocycline reduces glioma expansion and invasion by attenuating microglial MT1-MMP expression. *Brain, Behavior, and Immunity,* 25**,** 624-628.

MARQUES-SANTOS, L. F., OLIVEIRA, J. G., MAIA, R. C. & RUMJANEK, V. M. 2003. Mitotracker green is a P-glycoprotein substrate. *Biosci Rep,* 23**,** 199-212.

MARTEIJN, J. A., LANS, H., VERMEULEN, W. & HOEIJMAKERS, J. H. 2014. Understanding nucleotide excision repair and its roles in cancer and ageing. *Nat Rev Mol Cell Biol,* 15**,** 465-481.

MARTIN, T. D., COOK, D. R., CHOI, M. Y., LI, M. Z., HAIGIS, K. M. & ELLEDGE, S. J. 2017. A Role for Mitochondrial Translation in Promotion of Viability in K-Ras Mutant Cells. *Cell Rep,* 20**,** 427-438.

MARTÍNEZ-JIMÉNEZ, F., MUIÑOS, F., LÓPEZ-ARRIBILLAGA, E., LOPEZ-BIGAS, N. & GONZALEZ-PEREZ, A. 2019. Systematic analysis of alterations in the ubiquitin proteolysis system reveals its contribution to driver mutations in cancer. *Nature Cancer,* 1**,** 122-135.

MARUYAMA, S., HATAKEYAMA, S., NAKAYAMA, K., ISHIDA, N., KAWAKAMI, K. & NAKAYAMA, K. 2001. Characterization of a mouse gene (Fbxw6) that encodes a homologue of Caenorhabditis elegans SEL-10. *Genomics,* 78**,** 214-222.

MARZIO, A., PUCCINI, J., KWON, Y., MAVERAKIS, N. K., ARBINI, A., SUNG, P., BAR-SAGI, D. & PAGANO, M. 2019. The F-Box Domain-Dependent Activity of EMI1 Regulates PARPi Sensitivity in Triple-Negative Breast Cancers. *Mol Cell,* 73**,** 224-237 e6.

MASKEY, D., MARLIN, M. C., KIM, S., KIM, S., ONG, E. C., LI, G. & TSIOKAS, L. 2015. Cell cycle-dependent ubiquitylation and destruction of NDE1 by CDK5-FBW7 regulates ciliary length. *EMBO J,* 34**,** 2424-2440.

MASOUDI, M., SEKI, M., YAZDANPARAST, R., YACHIE, N. & ABURATANI, H. 2019. A genome-scale CRISPR/Cas9 knockout screening reveals SH3D21 as a sensitizer for gemcitabine. *Sci Rep,* 9**,** 19188.

MATSUMOTO, A., ONOYAMA, I. & NAKAYAMA, K. I. 2006. Expression of mouse Fbxw7 isoforms is regulated in a cell cycle- or p53-dependent manner. *Biochem Biophys Res Commun,* 350**,** 114-119.

MATSUMOTO, A., ONOYAMA, I., SUNABORI, T., KAGEYAMA, R., OKANO, H. & NAKAYAMA, K. I. 2011. Fbxw7-dependent degradation of Notch is required for control of "stemness" and neuronal-glial differentiation in neural stem cells. *J Biol Chem,* 286**,** 13754-13764.

MATSUOKA, S., OIKE, Y., ONOYAMA, I., IWAMA, A., ARAI, F., TAKUBO, K., MASHIMO, Y., OGURO, H., NITTA, E., ITO, K., MIYAMOTO, K., YOSHIWARA, H., HOSOKAWA, K., NAKAMURA, Y., GOMEI, Y., IWASAKI, H., HAYASHI, Y., MATSUZAKI, Y., NAKAYAMA, K., IKEDA, Y., HATA, A., CHIBA, S., NAKAYAMA, K. I. & SUDA, T. 2008. Fbxw7 acts as a critical fail-safe against premature loss of hematopoietic stem cells and development of T-ALL. *Genes Dev,* 22**,** 986-991.

MAYOR-RUIZ, C., BAUER, S., BRAND, M., KOZICKA, Z., SIKLOS, M., IMRICHOVA, H., KALTHEUNER, I. H., HAHN, E., SEILER, K., KOREN, A., PETZOLD, G., FELLNER, M., BOCK,

C., MÜLLER, A. C., ZUBER, J., GEYER, M., THOMÄ, N. H., KUBICEK, S. & WINTER, G. E. 2020. Rational discovery of molecular glue degraders via scalable chemical profiling. *Nature Chemical Biology,* 16**,** 1199-1207.

MAYOR-RUIZ, C., OLBRICH, T., DROSTEN, M., LECONA, E., VEGA-SENDINO, M., ORTEGA, S., DOMINGUEZ, O., BARBACID, M., RUIZ, S. & FERNANDEZ-CAPETILLO, O. 2018. ERF deletion rescues RAS deficiency in mouse embryonic stem cells. *Genes Dev,* 32**,** 568-576.

MCDONALD, E. R., 3RD, DE WECK, A., SCHLABACH, M. R., BILLY, E., MAVRAKIS, K. J., HOFFMAN, G. R., BELUR, D., CASTELLETTI, D., FRIAS, E., GAMPA, K., GOLJI, J., KAO, I., LI, L., MEGEL, P., PERKINS, T. A., RAMADAN, N., RUDDY, D. A., SILVER, S. J., SOVATH, S., STUMP, M., WEBER, O., WIDMER, R., YU, J., YU, K., YUE, Y., ABRAMOWSKI, D., ACKLEY, E., BARRETT, R., BERGER, J., BERNARD, J. L., BILLIG, R., BRACHMANN, S. M., BUXTON, F., CAOTHIEN, R., CAUSHI, J. X., CHUNG, F. S., CORTES-CROS, M., DEBEAUMONT, R. S., DELAUNAY, C., DESPLAT, A., DUONG, W., DWOSKE, D. A., ELDRIDGE, R. S., FARSIDJANI, A., FENG, F., FENG, J., FLEMMING, D., FORRESTER, W., GALLI, G. G., GAO, Z., GAUTER, F., GIBAJA, V., HAAS, K., HATTENBERGER, M., HOOD, T., HUROV, K. E., JAGANI, Z., JENAL, M., JOHNSON, J. A., JONES, M. D., KAPOOR, A., KORN, J., LIU, J., LIU, Q., LIU, S., LIU, Y., LOO, A. T., MACCHI, K. J., MARTIN, T., MCALLISTER, G., MEYER, A., MOLLE, S., PAGLIARINI, R. A., PHADKE, T., REPKO, B., SCHOUWEY, T., SHANAHAN, F., SHEN, Q., STAMM, C., STEPHAN, C., STUCKE, V. M., TIEDT, R., VARADARAJAN, M., VENKATESAN, K., VITARI, A. C., WALLROTH, M., WEILER, J., ZHANG, J., MICKANIN, C., MYER, V. E., PORTER, J. A., LAI, A., BITTER, H., LEES, E., KEEN, N., KAUFFMANN, A., STEGMEIER, F., HOFMANN, F., SCHMELZLE, T. & SELLERS, W. R. 2017. Project DRIVE: A Compendium of Cancer Dependencies and Synthetic Lethal Relationships Uncovered by Large-Scale, Deep RNAi Screening. *Cell,* 170**,** 577-592 e10.

MCFALINE-FIGUEROA, J. L., HILL, A. J., QIU, X., JACKSON, D., SHENDURE, J. & TRAPNELL, C. 2019. A pooled single-cell genetic screen identifies regulatory checkpoints in the continuum of the epithelial-to-mesenchymal transition. *Nat Genet,* 51**,** 1389-1398.

MCKEOWN, M. R. & BRADNER, J. E. 2014. Therapeutic strategies to inhibit MYC. *Cold Spring Harbor perspectives in medicine,* 4**,** a014266.

MENGWASSER, K. E., ADEYEMI, R. O., LENG, Y., CHOI, M. Y., CLAIRMONT, C., D'ANDREA, A. D. & ELLEDGE, S. J. 2019. Genetic Screens Reveal FEN1 and APEX2 as BRCA2 Synthetic Lethal Targets. *Mol Cell,* 73**,** 885-899 e6.

MENSSEN, A. & HERMEKING, H. 2002. Characterization of the c-MYC-regulated transcriptome by SAGE: identification and analysis of c-MYC target genes. *Proc Natl Acad Sci U S A,* 99**,** 6274-6279.

MESSNER, M., SCHMITT, S., ARDELT, M. A., FROHLICH, T., MULLER, M., PEIN, H., HUBER-CANTONATI, P., ORTLER, C., KOENIG, L. M., ZOBEL, L., KOEBERLE, A., ARNOLD, G. J., ROTHENFUSSER, S., KIEMER, A. K., GERBES, A. L., ZISCHKA, H., VOLLMAR, A. M. & PACHMAYR, J. 2020. Metabolic implication of tigecycline as an efficacious second-line treatment for sorafenib-resistant hepatocellular carcinoma. *FASEB J,* 34**,** 11860-11882.

MEYER, N. & PENN, L. Z. 2008. Reflecting on 25 years with MYC. *Nature Reviews Cancer,* 8**,** 976-990.

MICHEL, S., CANONNE, M., ARNOULD, T. & RENARD, P. 2015. Inhibition of mitochondrial genome expression triggers the activation of CHOP-10 by a cell signaling dependent on the integrated stress response but not the mitochondrial unfolded protein response. *Mitochondrion,* 21**,** 58-68.

MICK, E., TITOV, D. V., SKINNER, O. S., SHARMA, R., JOURDAIN, A. A. & MOOTHA, V. K. 2020. Distinct mitochondrial defects trigger the integrated stress response depending on the metabolic state of the cell. *Elife,* 9**,** e49178.

MIKELSAAR, R. 1983. Human mitochondrial genome and the evolution of methionine transfer ribonucleic acids. *J Theor Biol,* 105**,** 221-232.

MILLER, D. M., THOMAS, S. D., ISLAM, A., MUENCH, D. & SEDORIS, K. 2012. c-Myc and cancer metabolism. *Clin Cancer Res,* 18**,** 5546-5553.

MILLER, R. E., BROUGH, R., BAJRAMI, I., WILLIAMSON, C. T., MCDADE, S., CAMPBELL, J., KIGOZI, A., RAFIQ, R., PEMBERTON, H., NATRAJAN, R., JOEL, J., ASTLEY, H., MAHONEY, C., MOORE, J. D., TORRANCE, C., GORDAN, J. D., WEBBER, J. T., LEVIN, R. S., SHOKAT, K. M., BANDYOPADHYAY, S., LORD, C. J. & ASHWORTH, A. 2016. Synthetic Lethal Targeting of ARID1A-Mutant Ovarian Clear Cell Tumors with Dasatinib. *Mol Cancer Ther,* 15**,** 1472-1484.

MIYASHITA, T. & REED, J. C. 1992. bcl2 Gene Transfer Increases Relative Resistance of S49.1 and WEHI7.2 Lymphoid Cells to Cell Death and DNA Fragmentation Induced by Glucocorticoids and Multiple Chemotherapeutic Drugs. *Cancer Research,* 52**,** 5407-5411.

MOBERG, K. H., BELL, D. W., WAHRER, D. C. R., HABER, D. A. & HARIHARAN, I. K. 2001. Archipelago regulates Cyclin E levels in Drosophila and is mutated in human cancer cell lines. *Nature,* 413**,** 311-316.

MOENS, S., ZHAO, P., BAIETTI, M. F., MARINELLI, O., VAN HAVER, D., IMPENS, F., FLORIS, G., MARANGONI, E., NEVEN, P., ANNIBALI, D., SABLINA, A. A. & AMANT, F. 2021. The mitotic checkpoint is a targetable vulnerability of carboplatin-resistant triple negative breast cancers. *Sci Rep,* 11**,** 3176.

MOLINA, J. R., SUN, Y., PROTOPOPOVA, M., GERA, S., BANDI, M., BRISTOW, C., MCAFOOS, T., MORLACCHI, P., ACKROYD, J., AGIP, A. A., AL-ATRASH, G., ASARA, J., BARDENHAGEN, J., CARRILLO, C. C., CARROLL, C., CHANG, E., CIUREA, S., CROSS, J. B., CZAKO, B., DEEM, A., DAVER, N., DE GROOT, J. F., DONG, J. W., FENG, N., GAO, G., GAY, J., DO, M. G., GREER, J., GIULIANI, V., HAN, J., HAN, L., HENRY, V. K., HIRST, J., HUANG, S., JIANG, Y., KANG, Z., KHOR, T., KONOPLEV, S., LIN, Y. H., LIU, G., LODI, A., LOFTON, T., MA, H., MAHENDRA, M., MATRE, P., MULLINAX, R., PEOPLES, M., PETROCCHI, A., RODRIGUEZ-CANALE, J., SERRELI, R., SHI, T., SMITH, M., TABE, Y., THEROFF, J., TIZIANI, S., XU, Q., ZHANG, Q., MULLER, F., DEPINHO, R. A., TONIATTI, C., DRAETTA, G. F., HEFFERNAN, T. P., KONOPLEVA, M., JONES, P., DI FRANCESCO, M. E. & MARSZALEK, J. R. 2018. An inhibitor of oxidative phosphorylation exploits cancer vulnerability. *Nat Med,* 24**,** 1036-1046.

MONTOYA, J., OJALA, D. & ATTARDI, G. 1981. Distinctive features of the 5′-terminal sequences of the human mitochondrial mRNAs. *Nature,* 290**,** 465-470.

MORENO-SANCHEZ, R., RODRIGUEZ-ENRIQUEZ, S., MARIN-HERNANDEZ, A. & SAAVEDRA, E. 2007. Energy metabolism in tumor cells. *FEBS J,* 274**,** 1393-1418.

MORICEAU, G., HUGO, W., HONG, A., SHI, H., KONG, X., YU, C. C., KOYA, R. C., SAMATAR, A. A., KHANLOU, N., BRAUN, J., RUCHALSKI, K., SEIFERT, H., LARKIN, J., DAHLMAN, K. B., JOHNSON, D. B., ALGAZI, A., SOSMAN, J. A., RIBAS, A. & LO, R. S. 2015. Tunable-combinatorial mechanisms of acquired resistance limit the efficacy of BRAF/MEK cotargeting but result in melanoma drug addiction. *Cancer Cell,* 27**,** 240-256.

MORRISH, F. & HOCKENBERY, D. 2014. MYC and mitochondrial biogenesis. *Cold Spring Harb Perspect Med,* 4**,** a014225.

MOSCOU, M. J. & BOGDANOVE, A. J. 2009. A Simple Cipher Governs DNA Recognition by TAL Effectors. *Science,* 326**,** 1501.

MUN, G. I., CHOI, E., LEE, Y. & LEE, Y. S. 2020. Decreased expression of FBXW7 by ERK1/2 activation in drug-resistant cancer cells confers transcriptional activation of MDR1 by suppression of ubiquitin degradation of HSF1. *Cell Death Dis,* 11**,** 395.

MUNCH, C. & HARPER, J. W. 2016. Mitochondrial unfolded protein response controls matrix pre-RNA processing and translation. *Nature,* 534**,** 710-713.

NAGUIB, A., MATHEW, G., RECZEK, C. R., WATRUD, K., AMBRICO, A., HERZKA, T., SALAS, I. C., LEE, M. F., EL-AMINE, N., ZHENG, W., DI FRANCESCO, M. E., MARSZALEK, J. R., PAPPIN, D. J., CHANDEL, N. S. & TROTMAN, L. C. 2018. Mitochondrial Complex I Inhibitors Expose a Vulnerability for Selective Killing of Pten-Null Cells. *Cell Rep,* 23**,** 58-67.

NAJM, F. J., STRAND, C., DONOVAN, K. F., HEGDE, M., SANSON, K. R., VAIMBERG, E. W., SULLENDER, M. E., HARTENIAN, E., KALANI, Z., FUSI, N., LISTGARTEN, J., YOUNGER, S. T., BERNSTEIN, B. E., ROOT, D. E. & DOENCH, J. G. 2018. Orthologous CRISPR-Cas9 enzymes for combinatorial genetic screens. *Nat Biotechnol,* 36**,** 179-189.

NAKAJIMA, T., KITAGAWA, K., OHHATA, T., SAKAI, S., UCHIDA, C., SHIBATA, K., MINEGISHI, N., YUMIMOTO, K., NAKAYAMA, K. I., MASUMOTO, K., KATOU, F., NIIDA, H. & KITAGAWA, M. 2015. Regulation of GATA-binding protein 2 levels via ubiquitin-dependent degradation by Fbw7: involvement of cyclin B-cyclin-dependent kinase 1-mediated phosphorylation of THR176 in GATA-binding protein 2. *J Biol Chem,* 290**,** 10368-10381.

NAKAYAMA, S., YUMIMOTO, K., KAWAMURA, A. & NAKAYAMA, K. I. 2018. Degradation of the endoplasmic reticulum-anchored transcription factor MyRF by the ubiquitin ligase SCF(Fbxw7) in a manner dependent on the kinase GSK-3. *J Biol Chem,* 293**,** 5705-5714.

NASH, P., TANG, X., ORLICKY, S., CHEN, Q., GERTLER, F. B., MENDENHALL, M. D., SICHERI, F., PAWSON, T. & TYERS, M. 2001. Multisite phosphorylation of a CDK inhibitor sets a threshold for the onset of DNA replication. *Nature,* 414**,** 514-521.

NIJWENING, J. H., KUIKEN, H. J. & BEIJERSBERGEN, R. L. 2011. Screening for modulators of cisplatin sensitivity: unbiased screens reveal common themes. *Cell Cycle,* 10**,** 380-386.

NISSANKA, N., BACMAN, S. R., PLASTINI, M. J. & MORAES, C. T. 2018. The mitochondrial DNA polymerase gamma degrades linear DNA fragments precluding the formation of deletions. *Nature Communications,* 9**,** 2491.

NITA, M. E., NAGAWA, H., TOMINAGA, O., TSUNO, N., FUJII, S., SASAKI, S., FU, C. G., TAKENOUE, T., TSURUO, T. & MUTO, T. 1998. 5-Fluorouracil induces apoptosis in human colon cancer cell lines with modulation of Bcl-2 family proteins. *British Journal of Cancer,* 78**,** 986-992.

NOLFI-DONEGAN, D., BRAGANZA, A. & SHIVA, S. 2020. Mitochondrial electron transport chain: Oxidative phosphorylation, oxidant production, and methods of measurement. *Redox Biol,* 37**,** 101674.

NOOTER, K., BRUTEL DE LA RIVIERE, G., LOOK, M. P., VAN WINGERDEN, K. E., HENZEN-LOGMANS, S. C., SCHEPER, R. J., FLENS, M. J., KLIJN, J. G. M., STOTER, G. & FOEKENS, J. A. 1997. The prognostic significance of expression of the multidrug resistance-associated protein (MRP) in primary breast cancer. *British Journal of Cancer,* 76**,** 486-493.

NORBERG, E., LAKO, A., CHEN, P. H., STANLEY, I. A., ZHOU, F., FICARRO, S. B., CHAPUY, B., CHEN, L., RODIG, S., SHIN, D., CHOI, D. W., LEE, S., SHIPP, M. A., MARTO, J. A. & DANIAL, N. N. 2017. Differential contribution of the mitochondrial translation pathway to the survival of diffuse large B-cell lymphoma subsets. *Cell Death Differ,* 24**,** 251-262.

NUNES, T., HAMDAN, D., LEBOEUF, C., EL BOUCHTAOUI, M., GAPIHAN, G., NGUYEN, T. T., MELES, S., ANGELI, E., RATAJCZAK, P., LU, H., DI BENEDETTO, M., BOUSQUET, G. & JANIN, A. 2018. Targeting Cancer Stem Cells to Overcome Chemoresistance. *Int J Mol Sci,* 19.

NUSINOW, D. P., SZPYT, J., GHANDI, M., ROSE, C. M., MCDONALD, E. R., 3RD, KALOCSAY, M., JANE-VALBUENA, J., GELFAND, E., SCHWEPPE, D. K., JEDRYCHOWSKI, M., GOLJI, J., PORTER, D. A., REJTAR, T., WANG, Y. K., KRYUKOV, G. V., STEGMEIER, F., ERICKSON, B. K., GARRAWAY, L. A., SELLERS, W. R. & GYGI, S. P. 2020. Quantitative Proteomics of the Cancer Cell Line Encyclopedia. *Cell,* 180**,** 387-402 e16.

O'NEIL, J., GRIM, J., STRACK, P., RAO, S., TIBBITTS, D., WINTER, C., HARDWICK, J., WELCKER, M., MEIJERINK, J. P., PIETERS, R., DRAETTA, G., SEARS, R., CLURMAN, B. E. & LOOK, A. T. 2007. FBW7 mutations in leukemic cells mediate NOTCH pathway activation and resistance to gamma-secretase inhibitors. *J Exp Med,* 204**,** 1813-1824.

OBERG, C., LI, J., PAULEY, A., WOLF, E., GURNEY, M. & LENDAHL, U. 2001. The Notch intracellular domain is ubiquitinated and negatively regulated by the mammalian Sel-10 homolog. *J Biol Chem,* 276**,** 35847-35853.

OKITA, Y., MATSUMOTO, A., YUMIMOTO, K., ISOSHITA, R. & NAKAYAMA, K. I. 2012. Increased efficiency in the generation of induced pluripotent stem cells by Fbxw7 ablation. *Genes Cells,* 17**,** 768-777.

OLBRICH, T., VEGA-SENDINO, M., MURGA, M., DE CARCER, G., MALUMBRES, M., ORTEGA, S., RUIZ, S. & FERNANDEZ-CAPETILLO, O. 2019. A Chemical Screen Identifies Compounds Capable of Selecting for Haploidy in Mammalian Cells. *Cell Rep,* 28**,** 597-604 e4.

OLIVERAS-FERRAROS, C., COROMINAS-FAJA, B., CUFI, S., VAZQUEZ-MARTIN, A., MARTIN-CASTILLO, B., IGLESIAS, J. M., LOPEZ-BONET, E., MARTIN, A. G. & MENENDEZ, J. A. 2012. Epithelial-to-mesenchymal transition (EMT) confers primary resistance to trastuzumab (Herceptin). *Cell Cycle,* 11**,** 4020-4032.

OLIVIERI, M., CHO, T., ÁLVAREZ-QUILÓN, A., LI, K., SCHELLENBERG, M. J., ZIMMERMANN, M., HUSTEDT, N., ROSSI, S. E., ADAM, S., MELO, H., HEIJINK, A. M., SASTRE-MORENO, G., MOATTI, N., SZILARD, R. K., MCEWAN, A., LING, A. K., SERRANO-BENITEZ, A., UBHI, T., FENG, S., PAWLING, J., DELGADO-SAINZ, I., FERGUSON, M. W., DENNIS, J. W., BROWN, G. W., CORTÉS-LEDESMA, F., WILLIAMS, R. S., MARTIN, A., XU, D. & DUROCHER, D. 2020. A Genetic Map of the Response to DNA Damage in Human Cells. *Cell,* 182**,** 481-496.e21.

OLSON, B. L., HOCK, M. B., EKHOLM-REED, S., WOHLSCHLEGEL, J. A., DEV, K. K., KRALLI, A. & REED, S. I. 2008. SCFCdc4 acts antagonistically to the PGC-1alpha transcriptional coactivator by targeting it for ubiquitin-mediated proteolysis. *Genes & development,* 22**,** 252-264.

OLTERSDORF, T., ELMORE, S. W., SHOEMAKER, A. R., ARMSTRONG, R. C., AUGERI, D. J., BELLI, B. A., BRUNCKO, M., DECKWERTH, T. L., DINGES, J., HAJDUK, P. J., JOSEPH, M. K., KITADA, S., KORSMEYER, S. J., KUNZER, A. R., LETAI, A., LI, C., MITTEN, M. J., NETTESHEIM, D. G., NG, S., NIMMER, P. M., O'CONNOR, J. M., OLEKSIJEW, A., PETROS, A. M., REED, J. C., SHEN, W., TAHIR, S. K., THOMPSON, C. B., TOMASELLI, K. J., WANG, B., WENDT, M. D., ZHANG, H., FESIK, S. W. & ROSENBERG, S. H. 2005. An inhibitor of Bcl-2 family proteins induces regression of solid tumours. *Nature,* 435**,** 677-681.

ONOYAMA, I., SUZUKI, A., MATSUMOTO, A., TOMITA, K., KATAGIRI, H., OIKE, Y., NAKAYAMA, K. & NAKAYAMA, K. I. 2011. Fbxw7 regulates lipid metabolism and cell fate decisions in the mouse liver. *J Clin Invest,* 121**,** 342-354.

ONOYAMA, I., TSUNEMATSU, R., MATSUMOTO, A., KIMURA, T., DE ALBORAN, I. M., NAKAYAMA, K. & NAKAYAMA, K. I. 2007. Conditional inactivation of Fbxw7 impairs cell-cycle exit during T cell differentiation and results in lymphomatogenesis. *J Exp Med,* 204**,** 2875-2888.

ORAN, A. R., ADAMS, C. M., ZHANG, X.-Y., GENNARO, V. J., PFEIFFER, H. K., MELLERT, H. S., SEIDEL, H. E., MASCIOLI, K., KAPLAN, J., GABALLA, M. R., SHEN, C., RIGOUTSOS, I., KING, M. P., COTNEY, J. L., ARNOLD, J. J., SHARMA, S. D., MARTINEZ-OUTSCHOORN, U. E., VAKOC, C. R., CHODOSH, L. A., THOMPSON, J. E., BRADNER, J. E., CAMERON, C. E., SHADEL, G. S., EISCHEN, C. M. & MCMAHON, S. B. 2016. Multi-focal control of mitochondrial gene expression by oncogenic MYC provides potential therapeutic targets in cancer. *Oncotarget,* 7**,** 72395-72414.

ORLICKY, S., TANG, X., NEDUVA, V., ELOWE, N., BROWN, E. D., SICHERI, F. & TYERS, M. 2010. An allosteric inhibitor of substrate recognition by the SCF(Cdc4) ubiquitin ligase. *Nat Biotechnol,* 28**,** 733-737.

OSAWA, S., JUKES, T. H., WATANABE, K. & MUTO, A. 1992. Recent evidence for evolution of the genetic code. *Microbiological Reviews,* 56**,** 229-264.

OTTO, T., HORN, S., BROCKMANN, M., EILERS, U., SCHÜTTRUMPF, L., POPOV, N., KENNEY, A. M., SCHULTE, J. H., BEIJERSBERGEN, R., CHRISTIANSEN, H., BERWANGER, B. & EILERS, M. 2009. Stabilization of N-Myc Is a Critical Function of Aurora A in Human Neuroblastoma. *Cancer Cell,* 15**,** 67-78.

OUYANG, Q., LIU, Y., TAN, J., LI, J., YANG, D., ZENG, F., HUANG, W., KONG, Y., LIU, Z., ZHOU, H. & LIU, Y. 2019. Loss of ZNF587B and SULF1 contributed to cisplatin resistance in ovarian cancer cell lines based on Genome-scale CRISPR/Cas9 screening. *American journal of cancer research,* 9**,** 988-998.

PAKOS-ZEBRUCKA, K., KORYGA, I., MNICH, K., LJUJIC, M., SAMALI, A. & GORMAN, A. M. 2016. The integrated stress response. *EMBO reports,* 17**,** 1374-1395.

PALASKAS, N., LARSON, S. M., SCHULTZ, N., KOMISOPOULOU, E., WONG, J., ROHLE, D., CAMPOS, C., YANNUZZI, N., OSBORNE, J. R., LINKOV, I., KASTENHUBER, E. R., TASCHEREAU, R., PLAISIER, S. B., TRAN, C., HEGUY, A., WU, H., SANDER, C., PHELPS, M. E., BRENNAN, C., PORT, E., HUSE, J. T., GRAEBER, T. G. & MELLINGHOFF, I. K. 2011. 18F-fluorodeoxy-glucose positron emission tomography marks MYC-overexpressing human basal-like breast cancers. *Cancer Res,* 71**,** 5164-5174.

PAN, C., JIN, L., WANG, X., LI, Y., CHUN, J., BOESE, A. C., LI, D., KANG, H. B., ZHANG, G., ZHOU, L., CHEN, G. Z., SABA, N. F., SHIN, D. M., MAGLIOCCA, K. R., OWONIKOKO, T. K., MAO, H., LONIAL, S. & KANG, S. 2019. Inositol-triphosphate 3-kinase B confers cisplatin resistance by regulating NOX4-dependent redox balance. *J Clin Invest,* 129**,** 2431-2445.

PAN, D., KOBAYASHI, A., JIANG, P., FERRARI DE ANDRADE, L., TAY, R. E., LUOMA, A. M., TSOUCAS, D., QIU, X., LIM, K., RAO, P., LONG, H. W., YUAN, G.-C., DOENCH, J., BROWN, M., LIU, X. S. & WUCHERPFENNIG, K. W. 2018. A major chromatin regulator determines resistance of tumor cells to T cell–mediated killing. *Science,* 359**,** 770-775.

PANINA, Y., YAMANE, J., KOBAYASHI, K., SONE, H. & FUJIBUCHI, W. 2021. Human ES and iPS cells display less drug resistance than differentiated cells, and naïve-state induction further decreases drug resistance. *The Journal of Toxicological Sciences,* 46**,** 131-142.

PAO, W., MILLER, V. A., POLITI, K. A., RIELY, G. J., SOMWAR, R., ZAKOWSKI, M. F., KRIS, M. G. & VARMUS, H. 2005. Acquired resistance of lung adenocarcinomas to gefitinib or erlotinib is associated with a second mutation in the EGFR kinase domain. *PLoS Med,* 2**,** e73.

PAPATHEODOROU, I., FONSECA, N. A., KEAYS, M., TANG, Y. A., BARRERA, E., BAZANT, W., BURKE, M., FULLGRABE, A., FUENTES, A. M., GEORGE, N., HUERTA, L., KOSKINEN, S., MOHAMMED, S., GENIZA, M., PREECE, J., JAISWAL, P., JARNUCZAK, A. F., HUBER, W., STEGLE, O., VIZCAINO, J. A., BRAZMA, A. & PETRYSZAK, R. 2018. Expression Atlas: gene and protein expression across multiple studies and organisms. *Nucleic Acids Res,* 46**,** D246-D251.

PARNAS, O., JOVANOVIC, M., EISENHAURE, T. M., HERBST, R. H., DIXIT, A., YE, C. J., PRZYBYLSKI, D., PLATT, R. J., TIROSH, I., SANJANA, N. E., SHALEM, O., SATIJA, R., RAYCHOWDHURY, R., MERTINS, P., CARR, S. A., ZHANG, F., HACOHEN, N. & REGEV, A. 2015. A Genome-wide CRISPR Screen in Primary Immune Cells to Dissect Regulatory Networks. *Cell,* 162**,** 675-686.

PEDERSEN, P. L. 1978. Tumor mitochondria and the bioenergetics of cancer cells. *Prog Exp Tumor Res,* 22**,** 190-274.

PEEVA, V., BLEI, D., TROMBLY, G., CORSI, S., SZUKSZTO, M. J., REBELO-GUIOMAR, P., GAMMAGE, P. A., KUDIN, A. P., BECKER, C., ALTMÜLLER, J., MINCZUK, M., ZSURKA, G. & KUNZ, W. S. 2018. Linear mitochondrial DNA is rapidly degraded by components of the replication machinery. *Nature Communications,* 9**,** 1727.

PÉREZ-BENAVENTE, B., GARCÍA, J. L., RODRÍGUEZ, M. S., PINEDA-LUCENA, A., PIECHACZYK, M., FONT DE MORA, J. & FARRÀS, R. 2013. GSK3-SCF(FBXW7) targets JunB for degradation in G2 to preserve chromatid cohesion before anaphase. *Oncogene,* 32**,** 2189-2199.

PERKINS, G., DRURY, L. S. & DIFFLEY, J. F. X. 2001. Separate SCFCDC4 recognition elements target Cdc6 for proteolysis in S phase and mitosis. *The EMBO Journal,* 20**,** 4836-4845.

PETERS, S., CAMIDGE, D. R., SHAW, A. T., GADGEEL, S., AHN, J. S., KIM, D.-W., OU, S.-H. I., PÉROL, M., DZIADZIUSZKO, R., ROSELL, R., ZEAITER, A., MITRY, E., GOLDING, S., BALAS, B., NOE, J., MORCOS, P. N. & MOK, T. 2017. Alectinib versus Crizotinib in Untreated ALK-Positive Non–Small-Cell Lung Cancer. *New England Journal of Medicine,* 377**,** 829-838.

PFEIFER, G. P., YOU, Y.-H. & BESARATINIA, A. 2005. Mutations induced by ultraviolet light. *Mutation Research/Fundamental and Molecular Mechanisms of Mutagenesis,* 571**,** 19-31.

PIÑEIRO-YÁÑEZ, E., REBOIRO-JATO, M., GÓMEZ-LÓPEZ, G., PERALES-PATÓN, J., TROULÉ, K., RODRÍGUEZ, J. M., TEJERO, H., SHIMAMURA, T., LÓPEZ-CASAS, P. P., CARRETERO, J., VALENCIA, A., HIDALGO, M., GLEZ-PEÑA, D. & AL-SHAHROUR, F. 2018. PanDrugs: a novel method to prioritize anticancer drug treatments according to individual genomic data. *Genome Medicine,* 10**,** 41.

PLJESA-ERCEGOVAC, M., SAVIC-RADOJEVIC, A., MATIC, M., CORIC, V., DJUKIC, T., RADIC, T. & SIMIC, T. 2018. Glutathione Transferases: Potential Targets to Overcome Chemoresistance in Solid Tumors. *International Journal of Molecular Sciences,* 19**,** 3785.

POPOV, N., WANZEL, M., MADIREDJO, M., ZHANG, D., BEIJERSBERGEN, R., BERNARDS, R., MOLL, R., ELLEDGE, S. J. & EILERS, M. 2007. The ubiquitin-specific protease USP28 is required for MYC stability. *Nat Cell Biol,* 9**,** 765-774.

POTTING, C., CROCHEMORE, C., MORETTI, F., NIGSCH, F., SCHMIDT, I., MANNEVILLE, C., CARBONE, W., KNEHR, J., DEJESUS, R., LINDEMAN, A., MAHER, R., RUSS, C., MCALLISTER, G., REECE-HOYES, J. S., HOFFMAN, G. R., ROMA, G., MULLER, M., SAILER, A. W. & HELLIWELL, S. B. 2018. Genome-wide CRISPR screen for PARKIN regulators reveals transcriptional repression as a determinant of mitophagy. *Proc Natl Acad Sci U S A,* 115**,** E180-E189.

PRESTAYKO, A. W., D'AOUST, J. C., ISSELL, B. F. & CROOKE, S. T. 1979. Cisplatin (cis-diamminedichloroplatinum II). *Cancer Treatment Reviews,* 6**,** 17-39.

PUSZTAI, L., WAGNER, P., IBRAHIM, N., RIVERA, E., THERIAULT, R., BOOSER, D., SYMMANS, F. W., WONG, F., BLUMENSCHEIN, G., FLEMING, D. R., ROUZIER, R., BONIFACE, G. & HORTOBAGYI, G. N. 2005. Phase II study of tariquidar, a selective P-glycoprotein inhibitor, in patients with chemotherapy-resistant, advanced breast carcinoma. *Cancer,* 104**,** 682-691.

PUTHENVEETIL, S., WHITBY, L., REN, J., KELNAR, K., KREBS, J. F. & BEAL, P. A. 2006. Controlling activation of the RNA-dependent protein kinase by siRNAs using site-specific chemical modification. *Nucleic Acids Res,* 34**,** 4900-4911.

QIN, Y., HU, Q., XU, J., JI, S., DAI, W., LIU, W., XU, W., SUN, Q., ZHANG, Z., NI, Q., ZHANG, B., YU, X. & XU, X. 2019. PRMT5 enhances tumorigenicity and glycolysis in pancreatic cancer via the FBW7/cMyc axis. *Cell Commun Signal,* 17**,** 30.

QUIRÓS, P. M., PRADO, M. A., ZAMBONI, N., D'AMICO, D., WILLIAMS, R. W., FINLEY, D., GYGI, S. P. & AUWERX, J. 2017. Multi-omics analysis identifies ATF4 as a key regulator of the mitochondrial stress response in mammals. *Journal of Cell Biology,* 216**,** 2027-2045.

RACHIGLIO, A. M., LAMBIASE, M., FENIZIA, F., ROMA, C., CARDONE, C., IANNACCONE, A., DE LUCA, A., CAROTENUTO, M., FREZZETTI, D., MARTINELLI, E., MAIELLO, E., CIARDIELLO, F. & NORMANNO, N. 2019. Genomic Profiling of KRAS/NRAS/BRAF/PIK3CA Wild-Type Metastatic Colorectal Cancer Patients Reveals Novel Mutations in Genes Potentially Associated with Resistance to Anti-EGFR Agents. *Cancers (Basel),* 11**,** 859.

RAJAGOPALAN, H., JALLEPALLI, P. V., RAGO, C., VELCULESCU, V. E., KINZLER, K. W., VOGELSTEIN, B. & LENGAUER, C. 2004. Inactivation of hCDC4 can cause chromosomal instability. *Nature,* 428**,** 77-81.

RANGREZ, A. Y., POTT, J., KLUGE, A., FRAUEN, R., STIEBELING, K., HOPPE, P., SOSSALLA, S., FREY, N. & FRANK, D. 2017. Myeloid leukemia factor-1 is a novel modulator of neonatal rat

cardiomyocyte proliferation. *Biochimica et Biophysica Acta (BBA) - Molecular Cell Research,* 1864**,** 634-644.

RAVÀ, M., D'ANDREA, A., NICOLI, P., GRITTI, I., DONATI, G., DONI, M., GIORGIO, M., OLIVERO, D. & AMATI, B. 2018. Therapeutic synergy between tigecycline and venetoclax in a preclinical model of MYC/BCL2 double-hit B cell lymphoma. *Science Translational Medicine,* 10**,** eaan8723.

REAVIE, L., BUCKLEY, SHANNON M., LOIZOU, E., TAKEISHI, S., ARANDA-ORGILLES, B., NDIAYE-LOBRY, D., ABDEL-WAHAB, O., IBRAHIM, S., NAKAYAMA, KEIICHI I. & AIFANTIS, I. 2013. Regulation of c-Myc Ubiquitination Controls Chronic Myelogenous Leukemia Initiation and Progression. *Cancer Cell,* 23**,** 362-375.

REED, G. A., SCHILLER, G. J., KAMBHAMPATI, S., TALLMAN, M. S., DOUER, D., MINDEN, M. D., YEE, K. W., GUPTA, V., BRANDWEIN, J., JITKOVA, Y., GRONDA, M., HURREN, R., SHAMAS-DIN, A., SCHUH, A. C. & SCHIMMER, A. D. 2016. A Phase 1 study of intravenous infusions of tigecycline in patients with acute myeloid leukemia. *Cancer Med,* 5**,** 3031-3040.

REES, M. G., SEASHORE-LUDLOW, B., CHEAH, J. H., ADAMS, D. J., PRICE, E. V., GILL, S., JAVAID, S., COLETTI, M. E., JONES, V. L., BODYCOMBE, N. E., SOULE, C. K., ALEXANDER, B., LI, A., MONTGOMERY, P., KOTZ, J. D., HON, C. S., MUNOZ, B., LIEFELD, T., DANČÍK, V., HABER, D. A., CLISH, C. B., BITTKER, J. A., PALMER, M., WAGNER, B. K., CLEMONS, P. A., SHAMJI, A. F. & SCHREIBER, S. L. 2016. Correlating chemical sensitivity and basal gene expression reveals mechanism of action. *Nat Chem Biol,* 12**,** 109-116.

REITERER, V., FIGUERAS-PUIG, C., LE GUERROUE, F., CONFALONIERI, S., VECCHI, M., JALAPOTHU, D., KANSE, S. M., DESHAIES, R. J., DI FIORE, P. P., BEHRENDS, C. & FARHAN, H. 2017. The pseudophosphatase STYX targets the F-box of FBXW7 and inhibits SCFFBXW7 function. *EMBO J,* 36**,** 260-273.

REITZER, L. J., WICE, B. M. & KENNELL, D. 1979. Evidence that glutamine, not sugar, is the major energy source for cultured HeLa cells. *Journal of Biological Chemistry,* 254**,** 2669-2676.

REN, A., QIU, Y., CUI, H. & FU, G. 2015. Tigecycline exerts an antitumoral effect in oral squamous cell carcinoma. *Oral Diseases,* 21**,** 558-564.

REN, H., KOO, J., GUAN, B., YUE, P., DENG, X., CHEN, M., KHURI, F. R. & SUN, S. Y. 2013a. The E3 ubiquitin ligases β-TrCP and FBXW7 cooperatively mediates GSK3-dependent Mcl-1 degradation induced by the Akt inhibitor API-1, resulting in apoptosis. *Mol Cancer,* 12**,** 146.

REN, J., CHEN, Y., SONG, H., CHEN, L. & WANG, R. 2013b. Inhibition of ZEB1 reverses EMT and chemoresistance in docetaxel-resistant human lung adenocarcinoma cell line. *J Cell Biochem,* 114**,** 1395-1403.

RIESBECK, K., BREDBERG, A. & FORSGREN, A. 1990. Ciprofloxacin does not inhibit mitochondrial functions but other antibiotics do. *Antimicrobial agents and chemotherapy,* 34**,** 167-169.

RITCHIE, M. E., PHIPSON, B., WU, D., HU, Y., LAW, C. W., SHI, W. & SMYTH, G. K. 2015. limma powers differential expression analyses for RNA-sequencing and microarray studies. *Nucleic Acids Res,* 43**,** e47.

RITT, D. A., ABREU-BLANCO, M. T., BINDU, L., DURRANT, D. E., ZHOU, M., SPECHT, S. I., STEPHEN, A. G., HOLDERFIELD, M. & MORRISON, D. K. 2016. Inhibition of Ras/Raf/MEK/ERK Pathway Signaling by a Stress-Induced Phospho-Regulatory Circuit. *Molecular Cell,* 64**,** 875-887.

ROE, M., FOLKES, A., ASHWORTH, P., BRUMWELL, J., CHIMA, L., HUNJAN, S., PRETSWELL, I., DANGERFIELD, W., RYDER, H. & CHARLTON, P. 1999. Reversal of P-glycoprotein mediated multidrug resistance by novel anthranilamide derivatives. *Bioorganic & Medicinal Chemistry Letters,* 9**,** 595-600.

ROESCH, A., VULTUR, A., BOGESKI, I., WANG, H., ZIMMERMANN, K. M., SPEICHER, D., KORBEL, C., LASCHKE, M. W., GIMOTTY, P. A., PHILIPP, S. E., KRAUSE, E., PATZOLD, S., VILLANUEVA, J., KREPLER, C., FUKUNAGA-KALABIS, M., HOTH, M., BASTIAN, B. C., VOGT, T. & HERLYN, M. 2013. Overcoming intrinsic multidrug resistance in melanoma by blocking the mitochondrial respiratory chain of slow-cycling JARID1B(high) cells. *Cancer Cell,* 23**,** 811-825.

ROMERO-MIGUEL, D., LAMANNA-RAMA, N., CASQUERO-VEIGA, M., GÓMEZ-RANGEL, V., DESCO, M. & SOTO-MONTENEGRO, M. L. 2021. Minocycline in neurodegenerative and psychiatric diseases: An update. *European Journal of Neurology,* 28**,** 1056-1081.

ROSENBERG, B., VAN CAMP, L. & KRIGAS, T. 1965. Inhibition of Cell Division in Escherichia coli by Electrolysis Products from a Platinum Electrode. *Nature,* 205**,** 698-699.

ROSENBERG, B., VANCAMP, L., TROSKO, J. E. & MANSOUR, V. H. 1969. Platinum Compounds: a New Class of Potent Antitumour Agents. *Nature,* 222**,** 385-386.

RUIZ, C. F., MONTAL, E. D., HALEY, J. A., BOTT, A. J. & HALEY, J. D. 2020. SREBP1 regulates mitochondrial metabolism in oncogenic KRAS expressing NSCLC. *The FASEB Journal,* 34**,** 10574-10589.

RUIZ, E. J., DIEFENBACHER, M. E., NELSON, J. K., SANCHO, R., PUCCI, F., CHAKRABORTY, A., MORENO, P., ANNIBALDI, A., LICCARDI, G., ENCHEVA, V., MITTER, R., ROSENFELDT, M., SNIJDERS, A. P., MEIER, P., CALZADO, M. A. & BEHRENS, A. 2019. LUBAC determines chemotherapy resistance in squamous cell lung cancer. *J Exp Med,* 216**,** 450-465.

RUIZ, S., MAYOR-RUIZ, C., LAFARGA, V., MURGA, M., VEGA-SENDINO, M., ORTEGA, S. & FERNANDEZ-CAPETILLO, O. 2016. A Genome-wide CRISPR Screen Identifies CDC25A as a Determinant of Sensitivity to ATR Inhibitors. *Mol Cell,* 62**,** 307-313.

RUIZ, S., PANOPOULOS, A. D., HERRERIAS, A., BISSIG, K. D., LUTZ, M., BERGGREN, W. T., VERMA, I. M. & IZPISUA BELMONTE, J. C. 2011. A high proliferation rate is required for cell reprogramming and maintenance of human embryonic stem cell identity. *Curr Biol,* 21**,** 45-52.

RUSSELL, W. L., KELLY, E. M., HUNSICKER, P. R., BANGHAM, J. W., MADDUX, S. C. & PHIPPS, E. L. 1979. Specific-locus test shows ethylnitrosourea to be the most potent mutagen in the mouse. *Proceedings of the National Academy of Sciences,* 76**,** 5818-5819.

SAKAMOTO, K. M., KIM, K. B., KUMAGAI, A., MERCURIO, F., CREWS, C. M. & DESHAIES, R. J. 2001. Protacs: Chimeric molecules that target proteins to the Skp1–Cullin–F box complex for ubiquitination and degradation. *Proceedings of the National Academy of Sciences,* 98**,** 8554-8559.

SALE, M. J., BALMANNO, K., SAXENA, J., OZONO, E., WOJDYLA, K., MCINTYRE, R. E., GILLEY, R., WORONIUK, A., HOWARTH, K. D., HUGHES, G., DRY, J. R., ARENDS, M. J., CARO, P., OXLEY, D., ASHTON, S., ADAMS, D. J., SAEZ-RODRIGUEZ, J., SMITH, P. D. & COOK, S. J. 2019. MEK1/2 inhibitor withdrawal reverses acquired resistance driven by BRAF(V600E) amplification whereas KRAS(G13D) amplification promotes EMT-chemoresistance. *Nat Commun,* 10**,** 2030.

SANCHEZ-BURGOS, L., GOMEZ-LOPEZ, G., AL-SHAHROUR, F. & FERNANDEZ-CAPETILLO, O. 2020. An In-Silico Analysis of Drugs Potentially Modulating the Cytokine Storm Triggered by SARS-CoV-2 Infection. *Preprints,* 2020**,** 2020060087.

SANCHO, R., GRUBER, R., GU, G. & BEHRENS, A. 2014. Loss of Fbw7 reprograms adult pancreatic ductal cells into alpha, delta, and beta cells. *Cell Stem Cell,* 15**,** 139-153.

SANJANA, N. E., SHALEM, O. & ZHANG, F. 2014. Improved vectors and genome-wide libraries for CRISPR screening. *Nature Methods,* 11**,** 783-784.

SANSON, K. R., HANNA, R. E., HEGDE, M., DONOVAN, K. F., STRAND, C., SULLENDER, M. E., VAIMBERG, E. W., GOODALE, A., ROOT, D. E., PICCIONI, F. & DOENCH, J. G. 2018. Optimized libraries for CRISPR-Cas9 genetic screens with multiple modalities. *Nat Commun,* 9**,** 5416.

SAWYERS, C. L., HOCHHAUS, A., FELDMAN, E., GOLDMAN, J. M., MILLER, C. B., OTTMANN, O. G., SCHIFFER, C. A., TALPAZ, M., GUILHOT, F., DEININGER, M. W. N., FISCHER, T., O'BRIEN, S. G., STONE, R. M., GAMBACORTI-PASSERINI, C. B., RUSSELL, N. H., REIFFERS, J. J., SHEA, T. C., CHAPUIS, B., COUTRE, S., TURA, S., MORRA, E., LARSON, R. A., SAVEN, A., PESCHEL, C., GRATWOHL, A., MANDELLI, F., BEN-AM, M., GATHMANN, I., CAPDEVILLE, R., PAQUETTE, R. L. & DRUKER, B. J. 2002. Imatinib induces hematologic and cytogenetic responses in patients with chronic myelogenous leukemia in myeloid blast crisis: results of a phase II study: Presented in part at the 43rd Annual Meeting of The American Society of Hematology, Orlando, FL, December 11, 2001. *Blood,* 99**,** 3530-3539.

SAYERS, C. M., PAPANDREOU, I., GUTTMANN, D. M., MAAS, N. L., DIEHL, J. A., WITZE, E. S., KOONG, A. C. & KOUMENIS, C. 2013. Identification and characterization of a potent activator of p53-independent cellular senescence via a small-molecule screen for modifiers of the integrated stress response. *Mol Pharmacol,* 83**,** 594-604.

SCHEDLBAUER, A., KAMINISHI, T., OCHOA-LIZARRALDE, B., DHIMOLE, N., ZHOU, S., LOPEZ-ALONSO, J. P., CONNELL, S. R. & FUCINI, P. 2015. Structural characterization of an alternative mode of tigecycline binding to the bacterial ribosome. *Antimicrob Agents Chemother,* 59**,** 2849-2854.

SCHRAMEK, D., SENDOEL, A., SEGAL, J. P., BERONJA, S., HELLER, E., ORISTIAN, D., REVA, B. & FUCHS, E. 2014. Direct in Vivo RNAi Screen Unveils Myosin IIa as a Tumor Suppressor of Squamous Cell Carcinomas. *Science,* 343**,** 309-313.

SCHULEIN-VOLK, C., WOLF, E., ZHU, J., XU, W., TARANETS, L., HELLMANN, A., JANICKE, L. A., DIEFENBACHER, M. E., BEHRENS, A., EILERS, M. & POPOV, N. 2014. Dual regulation of Fbw7 function and oncogenic transformation by Usp28. *Cell Rep,* 9**,** 1099-1109.

SCHULEIN, C., EILERS, M. & POPOV, N. 2011. PI3K-dependent phosphorylation of Fbw7 modulates substrate degradation and activity. *FEBS Lett,* 585**,** 2151-2157.

SCHWARTZ, P. M., MOIR, R. D., HYDE, C. M., TUREK, P. J. & HANDSCHUMACHER, R. E. 1985. Role of uridine phosphorylase in the anabolism of 5-fluorouracil. *Biochemical Pharmacology,* 34**,** 3585-3589.

SCOTLAND, S., SALAND, E., SKULI, N., DE TONI, F., BOUTZEN, H., MICKLOW, E., SENEGAS, I., PEYRAUD, R., PEYRIGA, L., THEODORO, F., DUMON, E., MARTINEAU, Y., DANET-DESNOYERS, G., BONO, F., ROCHER, C., LEVADE, T., MANENTI, S., JUNOT, C., PORTAIS, J. C., ALET, N., RECHER, C., SELAK, M. A., CARROLL, M. & SARRY, J. E. 2013. Mitochondrial energetic and AKT status mediate metabolic effects and apoptosis of metformin in human leukemic cells. *Leukemia,* 27**,** 2129-2138.

SEASHORE-LUDLOW, B., REES, M. G., CHEAH, J. H., COKOL, M., PRICE, E. V., COLETTI, M. E., JONES, V., BODYCOMBE, N. E., SOULE, C. K., GOULD, J., ALEXANDER, B., LI, A., MONTGOMERY, P., WAWER, M. J., KURU, N., KOTZ, J. D., HON, C. S., MUNOZ, B., LIEFELD, T., DANČÍK, V., BITTKER, J. A., PALMER, M., BRADNER, J. E., SHAMJI, A. F., CLEMONS, P. A. & SCHREIBER, S. L. 2015. Harnessing Connectivity in a Large-Scale Small-Molecule Sensitivity Dataset. *Cancer Discov,* 5**,** 1210-1223.

SHAH, N. P., NICOLL, J. M., NAGAR, B., GORRE, M. E., PAQUETTE, R. L., KURIYAN, J. & SAWYERS, C. L. 2002. Multiple BCR-ABL kinase domain mutations confer polyclonal resistance to the tyrosine kinase inhibitor imatinib (STI571) in chronic phase and blast crisis chronic myeloid leukemia. *Cancer Cell,* 2**,** 117-125.

SHALEM, O., SANJANA, N. E., HARTENIAN, E., SHI, X., SCOTT, D. A., MIKKELSEN, T. S., HECKL, D., EBERT, B. L., ROOT, D. E., DOENCH, J. G. & ZHANG, F. 2014. Genome-Scale CRISPR-Cas9 Knockout Screening in Human Cells. *Science,* 343**,** 84-87.

SHARMA, P., HU-LIESKOVAN, S., WARGO, J. A. & RIBAS, A. 2017. Primary, Adaptive, and Acquired Resistance to Cancer Immunotherapy. *Cell,* 168**,** 707-723.

SHARON, D., CATHELIN, S., MIRALI, S., DI TRANI, J. M., YANOFSKY, D. J., KEON, K. A., RUBINSTEIN, J. L., SCHIMMER, A. D., KETELA, T. & CHAN, S. M. 2019. Inhibition of mitochondrial translation overcomes venetoclax resistance in AML through activation of the integrated stress response. *Science Translational Medicine,* 11**,** eaax2863.

SHEN, J. P., ZHAO, D., SASIK, R., LUEBECK, J., BIRMINGHAM, A., BOJORQUEZ-GOMEZ, A., LICON, K., KLEPPER, K., PEKIN, D., BECKETT, A. N., SANCHEZ, K. S., THOMAS, A., KUO, C.-C., DU, D., ROGUEV, A., LEWIS, N. E., CHANG, A. N., KREISBERG, J. F., KROGAN, N., QI, L., IDEKER, T. & MALI, P. 2017. Combinatorial CRISPR–Cas9 screens for de novo mapping of genetic interactions. *Nature Methods,* 14**,** 573-576.

SHETH, A., ESCOBAR-ALVAREZ, S., GARDNER, J., RAN, L., HEANEY, M. L. & SCHEINBERG, D. A. 2014. Inhibition of human mitochondrial peptide deformylase causes apoptosis in c-myc-overexpressing hematopoietic cancers. *Cell Death Dis,* 5**,** e1152.

SHIMIZU, H., TAKEISHI, S., NAKATSUMI, H. & NAKAYAMA, K. I. 2019. Prevention of cancer dormancy by Fbxw7 ablation eradicates disseminated tumor cells. *JCI Insight,* 4**,** e125138.

SHOEMAKER, R. H., CURT, G. A. & CARNEY, D. N. 1983. Evidence for multidrug-resistant cells in human tumor cell populations. *Cancer treatment reports,* 67**,** 883-888.

SHUKLA, S., CHEN, Z.-S. & AMBUDKAR, S. V. 2012. Tyrosine kinase inhibitors as modulators of ABC transporter-mediated drug resistance. *Drug Resistance Updates,* 15**,** 70-80.

SIDRAUSKI, C., ACOSTA-ALVEAR, D., KHOUTORSKY, A., VEDANTHAM, P., HEARN, B. R., LI, H., GAMACHE, K., GALLAGHER, C. M., ANG, K. K. H., WILSON, C., OKREGLAK, V., ASHKENAZI, A., HANN, B., NADER, K., ARKIN, M. R., RENSLO, A. R., SONENBERG, N. & WALTER, P. 2013. Pharmacological brake-release of mRNA translation enhances cognitive memory. *eLife,* 2**,** e00498.

SIDRAUSKI, C., MCGEACHY, A. M., INGOLIA, N. T. & WALTER, P. 2015. The small molecule ISRIB reverses the effects of eIF2α phosphorylation on translation and stress granule assembly. *eLife,* 4**,** e05033.

SIEKEVITZ, P. 1957. Powerhouse of the Cell. *Scientific American,* 197**,** 131-144.

SIMONETTA, K. R., TAYGERLY, J., BOYLE, K., BASHAM, S. E., PADOVANI, C., LOU, Y., CUMMINS, T. J., YUNG, S. L., VON SOLY, S. K., KAYSER, F., KURIYAN, J., RAPE, M., CARDOZO, M., GALLOP, M. A., BENCE, N. F., BARSANTI, P. A. & SAHA, A. 2019. Prospective discovery of small molecule enhancers of an E3 ligase-substrate interaction. *Nat Commun,* 10**,** 1402.

SINHA, R. P. & HÄDER, D.-P. 2002. UV-induced DNA damage and repair: a review. *Photochemical & Photobiological Sciences,* 1**,** 225-236.

SINHA, S., CHENG, K., SCHAFFER, A. A., ALDAPE, K., SCHIFF, E. & RUPPIN, E. 2020. In vitro and in vivo identification of clinically approved drugs that modify ACE2 expression. *Mol Syst Biol,* 16**,** e9628.

SKRTIC, M., SRISKANTHADEVAN, S., JHAS, B., GEBBIA, M., WANG, X., WANG, Z., HURREN, R., JITKOVA, Y., GRONDA, M., MACLEAN, N., LAI, C. K., EBERHARD, Y., BARTOSZKO, J., SPAGNUOLO, P., RUTLEDGE, A. C., DATTI, A., KETELA, T., MOFFAT, J., ROBINSON, B. H., CAMERON, J. H., WRANA, J., EAVES, C. J., MINDEN, M. D., WANG, J. C., DICK, J. E., HUMPHRIES, K., NISLOW, C., GIAEVER, G. & SCHIMMER, A. D. 2011. Inhibition of mitochondrial translation as a therapeutic strategy for human acute myeloid leukemia. *Cancer Cell,* 20**,** 674-688.

SMITH, J., GRIZOT, S., ARNOULD, S., DUCLERT, A., EPINAT, J. C., CHAMES, P., PRIETO, J., REDONDO, P., BLANCO, F. J., BRAVO, J., MONTOYA, G., PAQUES, F. & DUCHATEAU, P. 2006. A combinatorial approach to create artificial homing endonucleases cleaving chosen sequences. *Nucleic Acids Res,* 34**,** e149.

SMITS, P., SMEITINK, J. & VAN DEN HEUVEL, L. 2010. Mitochondrial translation and beyond: processes implicated in combined oxidative phosphorylation deficiencies. *J Biomed Biotechnol,* 2010**,** 737385.

SOMMERS, C. L., HECKFORD, S. E., SKERKER, J. M., WORLAND, P., TORRI, J. A., THOMPSON, E. W., BYERS, S. W. & GELMANN, E. P. 1992. Loss of Epithelial Markers and Acquisition of Vimentin Expression in Adriamycin- and Vinblastine-resistant Human Breast Cancer Cell Lines. *Cancer Research,* 52**,** 5190-5197.

SONG, K. A., NIEDERST, M. J., LOCHMANN, T. L., HATA, A. N., KITAI, H., HAM, J., FLOROS, K. V., HICKS, M. A., HU, H., MULVEY, H. E., DRIER, Y., HEISEY, D. A. R., HUGHES, M. T., PATEL, N. U., LOCKERMAN, E. L., GARCIA, A., GILLEPSIE, S., ARCHIBALD, H. L., GOMEZ-CARABALLO, M., NULTON, T. J., WINDLE, B. E., PIOTROWSKA, Z., SAHINGUR, S. E., TAYLOR, S. M., DOZMOROV, M., SEQUIST, L. V., BERNSTEIN, B., EBI, H., ENGELMAN, J. A. & FABER, A. C. 2018. Epithelial-to-Mesenchymal Transition Antagonizes Response to Targeted Therapies in Lung Cancer by Suppressing BIM. *Clin Cancer Res,* 24**,** 197-208.

SONG, Y., LAI, L., CHONG, Z., HE, J., ZHANG, Y., XUE, Y., XIE, Y., CHEN, S., DONG, P., CHEN, L., CHEN, Z., DAI, F., WAN, X., XIAO, P., CAO, X., LIU, Y. & WANG, Q. 2017. E3 ligase FBXW7 is critical for RIG-I stabilization during antiviral responses. *Nat Commun,* 8**,** 14654.

SONG, Y., ZHOU, X., BAI, W. & MA, X. 2015. FBW7 increases drug sensitivity to cisplatin in human nasopharyngeal carcinoma by downregulating the expression of multidrug resistance-associated protein. *Tumour Biol,* 36**,** 4197-4202.

SORIA, J.-C., OHE, Y., VANSTEENKISTE, J., REUNGWETWATTANA, T., CHEWASKULYONG, B., LEE, K. H., DECHAPHUNKUL, A., IMAMURA, F., NOGAMI, N., KURATA, T., OKAMOTO, I., ZHOU, C., CHO, B. C., CHENG, Y., CHO, E. K., VOON, P. J., PLANCHARD, D., SU, W.-C., GRAY, J. E., LEE, S.-M., HODGE, R., MAROTTI, M., RUKAZENKOV, Y. & RAMALINGAM, S. S. 2017. Osimertinib in Untreated EGFR-Mutated Advanced Non–Small-Cell Lung Cancer. *New England Journal of Medicine,* 378**,** 113-125.

SOTGIA, F., WHITAKER-MENEZES, D., MARTINEZ-OUTSCHOORN, U. E., SALEM, A. F., TSIRIGOS, A., LAMB, R., SNEDDON, S., HULIT, J., HOWELL, A. & LISANTI, M. P. 2012. Mitochondria "fuel" breast cancer metabolism: fifteen markers of mitochondrial biogenesis label epithelial cancer cells, but are excluded from adjacent stromal cells. *Cell Cycle,* 11**,** 4390-4401.

SOTOMAYOR, E. A., TEICHER, B. A., SCHWARTZ, G. N., HOLDEN, S. A., MENON, K., HERMAN, T. S. & FREI, E., 3RD 1992. Minocycline in combination with chemotherapy or radiation therapy in vitro and in vivo. *Cancer Chemother Pharmacol,* 30**,** 377-384.

SOUERS, A. J., LEVERSON, J. D., BOGHAERT, E. R., ACKLER, S. L., CATRON, N. D., CHEN, J., DAYTON, B. D., DING, H., ENSCHEDE, S. H., FAIRBROTHER, W. J., HUANG, D. C., HYMOWITZ, S. G., JIN, S., KHAW, S. L., KOVAR, P. J., LAM, L. T., LEE, J., MAECKER, H. L., MARSH, K. C., MASON, K. D., MITTEN, M. J., NIMMER, P. M., OLEKSIJEW, A., PARK, C. H., PARK, C. M., PHILLIPS, D. C., ROBERTS, A. W., SAMPATH, D., SEYMOUR, J. F., SMITH, M. L., SULLIVAN, G. M., TAHIR, S. K., TSE, C., WENDT, M. D., XIAO, Y., XUE, J. C., ZHANG, H., HUMERICKHOUSE, R. A., ROSENBERG, S. H. & ELMORE, S. W. 2013. ABT-199, a potent and selective BCL-2 inhibitor, achieves antitumor activity while sparing platelets. *Nat Med,* 19**,** 202-208.

SPRUCK, C. H., STROHMAIER, H., SANGFELT, O., MÜLLER, H. M., HUBALEK, M., MÜLLER-HOLZNER, E., MARTH, C., WIDSCHWENDTER, M. & REED, S. I. 2002. hCDC4 Gene Mutations in Endometrial Cancer. *Cancer Research,* 62**,** 4535-4359.

STARLING, J. J., SHEPARD, R. L., CAO, J., LAW, K. L., NORMAN, B. H., KROIN, J. S., EHLHARDT, W. J., BAUGHMAN, T. M., WINTER, M. A., BELL, M. G., SHIH, C., GRUBER, J., ELMQUIST, W. F. & DANTZIG, A. H. 1997. Pharmacological characterization of LY335979: a potent cyclopropyldibenzosuberane modulator of P-glycoprotein. *Adv Enzyme Regul,* 37**,** 335-347.

STEHELIN, D., VARMUS, H. E., BISHOP, J. M. & VOGT, P. K. 1976. DNA related to the transforming gene(s) of avian sarcoma viruses is present in normal avian DNA. *Nature,* 260**,** 170-173.

STOCKWELL, S. R., PLATT, G., BARRIE, S. E., ZOUMPOULIDOU, G., TE POELE, R. H., AHERNE, G. W., WILSON, S. C., SHELDRAKE, P., MCDONALD, E., VENET, M., SOUDY, C., ELUSTONDO, F., RIGOREAU, L., BLAGG, J., WORKMAN, P., GARRETT, M. D. & MITTNACHT, S. 2012. Mechanism-based screen for G1/S checkpoint activators identifies a selective activator of EIF2AK3/PERK signalling. *PLoS One,* 7**,** e28568.

STOVER, E. H., BACO, M. B., COHEN, O., LI, Y. Y., CHRISTIE, E. L., BAGUL, M., GOODALE, A., LEE, Y., PANTEL, S., REES, M. G., WEI, G., PRESSER, A. G., GELBARD, M. K., ZHANG, W., ZERVANTONAKIS, I. K., BHOLA, P. D., RYAN, J., GUERRIERO, J. L., MONTERO, J., LIANG, F. J., CHERNIACK, A. D., PICCIONI, F., MATULONIS, U. A., BOWTELL, D. D. L., SAROSIEK, K. A., LETAI, A., GARRAWAY, L. A., JOHANNESSEN, C. M. & MEYERSON, M. 2019. Pooled Genomic Screens Identify Anti-apoptotic Genes as Targetable Mediators of Chemotherapy Resistance in Ovarian Cancer. *Mol Cancer Res,* 17**,** 2281-2293.

STROHMAIER, H., SPRUCK, C. H., KAISER, P., WON, K.-A., SANGFELT, O. & REED, S. I. 2001. Human F-box protein hCdc4 targets cyclin E for proteolysis and is mutated in a breast cancer cell line. *Nature,* 413**,** 316-322.

STROZYK, E. & KULMS, D. 2013. The role of AKT/mTOR pathway in stress response to UV-irradiation: implication in skin carcinogenesis by regulation of apoptosis, autophagy and senescence. *Int J Mol Sci,* 14**,** 15260-15285.

SU, G., BURANT, C. F., BEECHER, C. W., ATHEY, B. D. & MENG, F. 2011. Integrated metabolome and transcriptome analysis of the NCI60 dataset. *BMC Bioinformatics,* 12**,** S36.

SUBRAMANIAN, A., NARAYAN, R., CORSELLO, S. M., PECK, D. D., NATOLI, T. E., LU, X., GOULD, J., DAVIS, J. F., TUBELLI, A. A., ASIEDU, J. K., LAHR, D. L., HIRSCHMAN, J. E., LIU, Z., DONAHUE, M., JULIAN, B., KHAN, M., WADDEN, D., SMITH, I. C., LAM, D., LIBERZON, A., TODER, C., BAGUL, M., ORZECHOWSKI, M., ENACHE, O. M., PICCIONI, F., JOHNSON, S. A., LYONS, N. J., BERGER, A. H., SHAMJI, A. F., BROOKS, A. N., VRCIC, A., FLYNN, C., ROSAINS, J., TAKEDA, D. Y., HU, R., DAVISON, D., LAMB, J., ARDLIE, K., HOGSTROM, L., GREENSIDE, P., GRAY, N. S., CLEMONS, P. A., SILVER, S., WU, X., ZHAO, W. N., READ-BUTTON, W., WU, X., HAGGARTY, S. J., RONCO, L. V., BOEHM, J. S., SCHREIBER, S. L., DOENCH, J. G., BITTKER, J. A., ROOT, D. E., WONG, B. & GOLUB, T. R. 2017. A Next Generation Connectivity Map: L1000 Platform and the First 1,000,000 Profiles. *Cell,* 171**,** 1437-1452 e17.

SUGIYAMA, S., YUMIMOTO, K., INOUE, I. & NAKAYAMA, K. I. 2019. SCF(Fbxw7) ubiquitylates KLF7 for degradation in a manner dependent on GSK-3-mediated phosphorylation. *Genes Cells,* 24**,** 354-365.

SUIZU, F., HIRAMUKI, Y., OKUMURA, F., MATSUDA, M., OKUMURA, A. J., HIRATA, N., NARITA, M., KOHNO, T., YOKOTA, J., BOHGAKI, M., OBUSE, C., HATAKEYAMA, S., OBATA, T. & NOGUCHI, M. 2009. The E3 ligase TTC3 facilitates ubiquitination and degradation of phosphorylated Akt. *Dev Cell,* 17**,** 800-810.

SUN, C.-Y., NIE, J., HUANG, J.-P., ZHENG, G.-J. & FENG, B. 2019. Targeting STAT3 inhibition to reverse cisplatin resistance. *Biomedicine & Pharmacotherapy,* 117**,** 109135.

SUN, Y. & LI, X. 2014. The canonical wnt signal restricts the glycogen synthase kinase 3/fbw7-dependent ubiquitination and degradation of eya1 phosphatase. *Mol Cell Biol,* 34**,** 2409-2417.

SUNDQVIST, A., BENGOECHEA-ALONSO, M. T., YE, X., LUKIYANCHUK, V., JIN, J., HARPER, J. W. & ERICSSON, J. 2005. Control of lipid metabolism by phosphorylation-dependent degradation of the SREBP family of transcription factors by SCF(Fbw7). *Cell Metab,* 1**,** 379-391.

SURYO RAHMANTO, A., SAVOV, V., BRUNNER, A., BOLIN, S., WEISHAUPT, H., MALYUKOVA, A., ROSEN, G., CANCER, M., HUTTER, S., SUNDSTROM, A., KAWAUCHI, D., JONES, D. T., SPRUCK, C., TAYLOR, M. D., CHO, Y. J., PFISTER, S. M., KOOL, M., KORSHUNOV, A., SWARTLING, F. J. & SANGFELT, O. 2016. FBW7 suppression leads to SOX9 stabilization and increased malignancy in medulloblastoma. *EMBO J,* 35**,** 2192-2212.

TAKADA, M., ZHUANG, M., INUZUKA, H., ZHANG, J., ZURLO, G., ZHANG, J. & ZHANG, Q. 2017. EglN2 contributes to triple negative breast tumorigenesis by functioning as a substrate for the FBW7 tumor suppressor. *Oncotarget,* 8**,** 6787-6795.

TAKEDA, H., KATAOKA, S., NAKAYAMA, M., ALI, M. A. E., OSHIMA, H., YAMAMOTO, D., PARK, J. W., TAKEGAMI, Y., AN, T., JENKINS, N. A., COPELAND, N. G. & OSHIMA, M. 2019. CRISPR-Cas9-mediated gene knockout in intestinal tumor organoids provides functional validation for colorectal cancer driver genes. *Proc Natl Acad Sci U S A,* 116**,** 15635-15644.

TAKEISHI, S., MATSUMOTO, A., ONOYAMA, I., NAKA, K., HIRAO, A. & NAKAYAMA, K. I. 2013. Ablation of Fbxw7 eliminates leukemia-initiating cells by preventing quiescence. *Cancer Cell,* 23**,** 347-361.

TAMEIRE, F., VERGINADIS, I. I., LELI, N. M., POLTE, C., CONN, C. S., OJHA, R., SALAS SALINAS, C., CHINGA, F., MONROY, A. M., FU, W., WANG, P., KOSSENKOV, A., YE, J., AMARAVADI, R. K., IGNATOVA, Z., FUCHS, S. Y., DIEHL, J. A., RUGGERO, D. & KOUMENIS, C. 2019. ATF4 couples MYC-dependent translational activity to bioenergetic demands during tumour progression. *Nature Cell Biology,* 21**,** 889-899.

TAN, J., SONG, M., ZHOU, M. & HU, Y. 2017. Antibiotic tigecycline enhances cisplatin activity against human hepatocellular carcinoma through inducing mitochondrial dysfunction and oxidative damage. *Biochemical and Biophysical Research Communications,* 483**,** 17-23.

TAN, M., ZHAO, Y., KIM, S. J., LIU, M., JIA, L., SAUNDERS, T. L., ZHU, Y. & SUN, Y. 2011. SAG/RBX2/ROC2 E3 ubiquitin ligase is essential for vascular and neural development by targeting NF1 for degradation. *Dev Cell,* 21**,** 1062-1076.

TAN, X., CALDERON-VILLALOBOS, L. I., SHARON, M., ZHENG, C., ROBINSON, C. V., ESTELLE, M. & ZHENG, N. 2007. Mechanism of auxin perception by the TIR1 ubiquitin ligase. *Nature,* 446**,** 640-645.

TANDON, S. & JYOTI, S. 2012. Embryonic stem cells: An alternative approach to developmental toxicity testing. *J Pharm Bioallied Sci,* 4**,** 96-100.

TANG, C., YANG, L., JIANG, X., XU, C., WANG, M., WANG, Q., ZHOU, Z., XIANG, Z. & CUI, H. 2014. Antibiotic drug tigecycline inhibited cell proliferation and induced autophagy in gastric cancer cells. *Biochem Biophys Res Commun,* 446**,** 105-112.

TANG, X., ORLICKY, S., LIN, Z., WILLEMS, A., NECULAI, D., CECCARELLI, D., MERCURIO, F., SHILTON, B. H., SICHERI, F. & TYERS, M. 2007. Suprafacial orientation of the SCFCdc4 dimer accommodates multiple geometries for substrate ubiquitination. *Cell,* 129**,** 1165-1176.

TANSEY, W. P. 2014. Mammalian MYC Proteins and Cancer. *New Journal of Science,* 2014**,** 757534.

TELANG, S., LANE, A. N., NELSON, K. K., ARUMUGAM, S. & CHESNEY, J. 2007. The oncoprotein H-RasV12 increases mitochondrial metabolism. *Mol Cancer,* 6**,** 77.

TENG, C. L., HSIEH, Y. C., PHAN, L., SHIN, J., GULLY, C., VELAZQUEZ-TORRES, G., SKERL, S., YEUNG, S. C., HSU, S. L. & LEE, M. H. 2012. FBXW7 is involved in Aurora B degradation. *Cell Cycle,* 11**,** 4059-4068.

TETZLAFF, M. T., YU, W., LI, M., ZHANG, P., FINEGOLD, M., MAHON, K., HARPER, J. W., SCHWARTZ, R. J. & ELLEDGE, S. J. 2004. Defective cardiovascular development and elevated cyclin E and Notch proteins in mice lacking the Fbw7 F-box protein. *Proceedings of the National Academy of Sciences of the United States of America,* 101**,** 3338-3345.

THOMPSON, B. J., JANKOVIC, V., GAO, J., BUONAMICI, S., VEST, A., LEE, J. M., ZAVADIL, J., NIMER, S. D. & AIFANTIS, I. 2008. Control of hematopoietic stem cell quiescence by the E3 ubiquitin ligase Fbw7. *J Exp Med,* 205**,** 1395-1408.

TOLEDO, L. I., MURGA, M., ZUR, R., SORIA, R., RODRIGUEZ, A., MARTINEZ, S., OYARZABAL, J., PASTOR, J., BISCHOFF, J. R. & FERNANDEZ-CAPETILLO, O. 2011. A cell-based screen identifies ATR inhibitors with synthetic lethal properties for cancer-associated mutations. *Nat Struct Mol Biol,* 18**,** 721-727.

TONG, J., TAN, S., NIKOLOVSKA-COLESKA, Z., YU, J., ZOU, F. & ZHANG, L. 2017a. FBW7-Dependent Mcl-1 Degradation Mediates the Anticancer Effect of Hsp90 Inhibitors. *Mol Cancer Ther,* 16**,** 1979-1988.

TONG, J., TAN, S., ZOU, F., YU, J. & ZHANG, L. 2017b. FBW7 mutations mediate resistance of colorectal cancer to targeted therapies by blocking Mcl-1 degradation. *Oncogene,* 36**,** 787-796.

TORRE, E. A., ARAI, E., BAYATPOUR, S., JIANG, C. L., BECK, L. E., EMERT, B. L., SHAFFER, S. M., MELLIS, I. A., FANE, M. E., ALICEA, G. M., BUDINICH, K. A., WEERARATNA, A. T., SHI, J. & RAJ, A. 2021. Genetic screening for single-cell variability modulators driving therapy resistance. *Nat Genet,* 53**,** 76-85.

TOWNSEND, D. M. & TEW, K. D. 2003. The role of glutathione-S-transferase in anti-cancer drug resistance. *Oncogene,* 22**,** 7369-7375.

TRAUSCH-AZAR, J. S., ABED, M., ORIAN, A. & SCHWARTZ, A. L. 2015. Isoform-specific SCF(Fbw7) ubiquitination mediates differential regulation of PGC-1alpha. *J Cell Physiol,* 230**,** 842-852.

TRILLER, N., KOROŠEC, P., KERN, I., KOŠNIK, M. & DEBELJAK, A. 2006. Multidrug resistance in small cell lung cancer: Expression of P-glycoprotein, multidrug resistance protein 1 and lung resistance protein in chemo-naive patients and in relapsed disease. *Lung Cancer,* 54**,** 235-240.

TSAI, J., LEE, J. T., WANG, W., ZHANG, J., CHO, H., MAMO, S., BREMER, R., GILLETTE, S., KONG, J., HAASS, N. K., SPROESSER, K., LI, L., SMALLEY, K. S. M., FONG, D., ZHU, Y.-L., MARIMUTHU, A., NGUYEN, H., LAM, B., LIU, J., CHEUNG, I., RICE, J., SUZUKI, Y., LUU, C., SETTACHATGUL, C., SHELLOOE, R., CANTWELL, J., KIM, S.-H., SCHLESSINGER, J., ZHANG, K. Y. J., WEST, B. L., POWELL, B., HABETS, G., ZHANG, C., IBRAHIM, P. N., HIRTH, P., ARTIS, D. R., HERLYN, M. & BOLLAG, G. 2008. Discovery of a selective inhibitor of oncogenic B-Raf kinase with potent antimelanoma activity. *Proceedings of the National Academy of Sciences,* 105**,** 3041-3046.

TSAYTLER, P. & BERTOLOTTI, A. 2013. Exploiting the selectivity of protein phosphatase 1 for pharmacological intervention. *FEBS J,* 280**,** 766-770.

TSAYTLER, P., HARDING, H. P., RON, D. & BERTOLOTTI, A. 2011. Selective inhibition of a regulatory subunit of protein phosphatase 1 restores proteostasis. *Science,* 332**,** 91-94.

TSHERNIAK, A., VAZQUEZ, F., MONTGOMERY, P. G., WEIR, B. A., KRYUKOV, G., COWLEY, G. S., GILL, S., HARRINGTON, W. F., PANTEL, S., KRILL-BURGER, J. M., MEYERS, R. M., ALI, L., GOODALE, A., LEE, Y., JIANG, G., HSIAO, J., GERATH, W. F. J., HOWELL, S., MERKEL, E., GHANDI, M., GARRAWAY, L. A., ROOT, D. E., GOLUB, T. R., BOEHM, J. S. & HAHN, W. C. 2017. Defining a Cancer Dependency Map. *Cell,* 170**,** 564-576 e16.

TSUJI, A., AKAO, T., MASUYA, T., MURAI, M. & MIYOSHI, H. 2020. IACS-010759, a potent inhibitor of glycolysis-deficient hypoxic tumor cells, inhibits mitochondrial respiratory complex I through a unique mechanism. *J Biol Chem,* 295**,** 7481-7491.

TSUNEMATSU, R., NAKAYAMA, K., OIKE, Y., NISHIYAMA, M., ISHIDA, N., HATAKEYAMA, S., BESSHO, Y., KAGEYAMA, R., SUDA, T. & NAKAYAMA, K. I. 2004. Mouse Fbw7/Sel-10/Cdc4 is required for notch degradation during vascular development. *J Biol Chem,* 279**,** 9417-9423.

TU, K., YANG, W., LI, C., ZHENG, X., LU, Z., GUO, C., YAO, Y. & LIU, Q. 2014. Fbxw7 is an independent prognostic marker and induces apoptosis and growth arrest by regulating YAP abundance in hepatocellular carcinoma. *Molecular Cancer,* 13**,** 110.

TZELEPIS, K., KOIKE-YUSA, H., DE BRAEKELEER, E., LI, Y., METZAKOPIAN, E., DOVEY, O. M., MUPO, A., GRINKEVICH, V., LI, M., MAZAN, M., GOZDECKA, M., OHNISHI, S., COOPER, J., PATEL, M., MCKERRELL, T., CHEN, B., DOMINGUES, A. F., GALLIPOLI, P., TEICHMANN, S., PONSTINGL, H., MCDERMOTT, U., SAEZ-RODRIGUEZ, J., HUNTLY, B. J. P., IORIO, F., PINA, C., VASSILIOU, G. S. & YUSA, K. 2016. A CRISPR Dropout Screen Identifies Genetic Vulnerabilities and Therapeutic Targets in Acute Myeloid Leukemia. *Cell Rep,* 17**,** 1193-1205.

URICK, M. E. & BELL, D. W. 2018. In vitro effects of FBXW7 mutation in serous endometrial cancer: Increased levels of potentially druggable proteins and sensitivity to SI-2 and dinaciclib. *Mol Carcinog,* 57**,** 1445-1457.

URNOV, F. D., MILLER, J. C., LEE, Y. L., BEAUSEJOUR, C. M., ROCK, J. M., AUGUSTUS, S., JAMIESON, A. C., PORTEUS, M. H., GREGORY, P. D. & HOLMES, M. C. 2005. Highly efficient endogenous human gene correction using designed zinc-finger nucleases. *Nature,* 435**,** 646-651.

VAN DELFT, M. F., WEI, A. H., MASON, K. D., VANDENBERG, C. J., CHEN, L., CZABOTAR, P. E., WILLIS, S. N., SCOTT, C. L., DAY, C. L., CORY, S., ADAMS, J. M., ROBERTS, A. W. & HUANG, D. C. 2006. The BH3 mimetic ABT-737 targets selective Bcl-2 proteins and efficiently induces apoptosis via Bak/Bax if Mcl-1 is neutralized. *Cancer Cell,* 10**,** 389-399.

VAN DER BLIEK, A. M., SEDENSKY, M. M. & MORGAN, P. G. 2017. Cell Biology of the Mitochondrion. *Genetics,* 207**,** 843-871.

VANNESTE, M., HUANG, Q., LI, M., MOOSE, D., ZHAO, L., STAMNES, M. A., SCHULTZ, M., WU, M. & HENRY, M. D. 2019. High content screening identifies monensin as an EMT-selective cytotoxic compound. *Sci Rep,* 9**,** 1200.

VASAN, N., BASELGA, J. & HYMAN, D. M. 2019. A view on drug resistance in cancer. *Nature,* 575**,** 299-309.

VAZQUEZ-DOMINGUEZ, I., GONZALEZ-SANCHEZ, L., LOPEZ-NIEVA, P., FERNANDEZ-NAVARRO, P., VILLA-MORALES, M., COBOS-FERNANDEZ, M. A., SASTRE, I., M, F. F., A, F. F., MALUMBRES, M., SALAZAR-ROA, M., GRANA-CASTRO, O., SANTOS, J., LLAMAS, P., LOPEZ-LORENZO, J. L. & FERNANDEZ-PIQUERAS, J. 2019. Downregulation of specific FBXW7 isoforms with differential effects in T-cell lymphoblastic lymphoma. *Oncogene,* 38**,** 4620-4636.

VAZQUEZ, F., LIM, J. H., CHIM, H., BHALLA, K., GIRNUN, G., PIERCE, K., CLISH, C. B., GRANTER, S. R., WIDLUND, H. R., SPIEGELMAN, B. M. & PUIGSERVER, P. 2013. PGC1alpha expression defines a subset of human melanoma tumors with increased mitochondrial capacity and resistance to oxidative stress. *Cancer Cell,* 23**,** 287-301.

VEGA-NAREDO, I., LOUREIRO, R., MESQUITA, K. A., BARBOSA, I. A., TAVARES, L. C., BRANCO, A. F., ERICKSON, J. R., HOLY, J., PERKINS, E. L., CARVALHO, R. A. & OLIVEIRA, P. J. 2014. Mitochondrial metabolism directs stemness and differentiation in P19 embryonal carcinoma stem cells. *Cell Death Differ,* 21**,** 1560-1574.

VELLINGA, T. T., BOROVSKI, T., DE BOER, V. C., FATRAI, S., VAN SCHELVEN, S., TRUMPI, K., VERHEEM, A., SNOEREN, N., EMMINK, B. L., KOSTER, J., RINKES, I. H. & KRANENBURG, O. 2015. SIRT1/PGC1alpha-Dependent Increase in Oxidative Phosphorylation Supports Chemotherapy Resistance of Colon Cancer. *Clin Cancer Res,* 21**,** 2870-2879.

VOGTLE, F. N. 2021. Open questions on the mitochondrial unfolded protein response. *FEBS J,* 288**,** 2856-2869.

WALCZAK, A., GRADZIK, K., KABZINSKI, J., PRZYBYLOWSKA-SYGUT, K. & MAJSTEREK, I. 2019. The Role of the ER-Induced UPR Pathway and the Efficacy of Its Inhibitors and Inducers in the Inhibition of Tumor Progression. *Oxid Med Cell Longev,* 2019**,** 5729710.

WANG, G.-Q., GASTMAN, B. R., WIECKOWSKI, E., GOLDSTEIN, L. A., GAMBOTTO, A., KIM, T.-H., FANG, B., RABINOVITZ, A., YIN, X.-M. & RABINOWICH, H. 2001. A Role for Mitochondrial Bak in Apoptotic Response to Anticancer Drugs. *Journal of Biological Chemistry,* 276**,** 34307-34317.

WANG, J., JO, U., JOO, S. Y. & KIM, H. 2016a. FBW7 regulates DNA interstrand cross-link repair by modulating FAAP20 degradation. *Oncotarget,* 7**,** 35724-35740.

WANG, L., POPKO, B. & ROOS, R. P. 2014a. An enhanced integrated stress response ameliorates mutant SOD1-induced ALS. *Hum Mol Genet,* 23**,** 2629-2638.

WANG, R., WANG, Y., LIU, N., REN, C., JIANG, C., ZHANG, K., YU, S., CHEN, Y., TANG, H., DENG, Q., FU, C., WANG, Y., LI, R., LIU, M., PAN, W. & WANG, P. 2013a. FBW7 regulates endothelial functions by targeting KLF2 for ubiquitination and degradation. *Cell Res,* 23**,** 803-819.

WANG, T., LANDER, E. S. & SABATINI, D. M. 2016b. Large-Scale Single Guide RNA Library Construction and Use for CRISPR-Cas9-Based Genetic Screens. *Cold Spring Harb Protoc,* 2016**,** pdb.top086892.

WANG, T., WEI, J. J., SABATINI, D. M. & LANDER, E. S. 2014b. Genetic Screens in Human Cells Using the CRISPR-Cas9 System. *Science,* 343**,** 80-84.

WANG, X., ZHAI, H. & WANG, F. 2018. 6-OHDA Induces Oxidation of F-box Protein Fbw7beta by Chaperone-Mediated Autophagy in Parkinson's Model. *Mol Neurobiol,* 55**,** 4825-4833.

WANG, Y., LIU, Y., LU, J., ZHANG, P., WANG, Y., XU, Y., WANG, Z., MAO, J. H. & WEI, G. 2013b. Rapamycin inhibits FBXW7 loss-induced epithelial-mesenchymal transition and cancer stem cell-like characteristics in colorectal cancer cells. *Biochem Biophys Res Commun,* 434**,** 352-356.

WANG, Y., XIE, F., CHEN, D. & WANG, L. 2019. Inhibition of mitochondrial respiration by tigecycline selectively targets thyroid carcinoma and increases chemosensitivity. *Clin Exp Pharmacol Physiol,* 46**,** 890-897.

WANG, Z., MONTEIRO, C. D., JAGODNIK, K. M., FERNANDEZ, N. F., GUNDERSEN, G. W., ROUILLARD, A. D., JENKINS, S. L., FELDMANN, A. S., HU, K. S., MCDERMOTT, M. G., DUAN, Q., CLARK, N. R., JONES, M. R., KOU, Y., GOFF, T., WOODLAND, H., AMARAL, F. M. R., SZETO, G. L., FUCHS, O., SCHUSSLER-FIORENZA ROSE, S. M., SHARMA, S., SCHWARTZ, U., BAUSELA, X. B., SZYMKIEWICZ, M., MAROULIS, V., SALYKIN, A., BARRA, C. M., KRUTH, C. D., BONGIO, N. J., MATHUR, V., TODORIC, R. D., RUBIN, U. E., MALATRAS, A., FULP, C. T., GALINDO, J. A., MOTIEJUNAITE, R., JUSCHKE, C., DISHUCK, P. C., LAHL, K., JAFARI, M., AIBAR, S., ZARAVINOS, A., STEENHUIZEN, L. H., ALLISON, L. R., GAMALLO, P., DE ANDRES SEGURA, F., DAE DEVLIN, T., PEREZ-GARCIA, V. & MA'AYAN, A. 2016c. Extraction and analysis of signatures from the Gene Expression Omnibus by the crowd. *Nat Commun,* 7**,** 12846.

WARBURG, O. 1956. On the Origin of Cancer Cells. *Science,* 123**,** 309-314.

WARBURG, O., WIND, F. & NEGELEIN, E. 1927. The metabolism of tumors in the body. *The Journal of general physiology,* 8**,** 519-530.

WAY, S. W., PODOJIL, J. R., CLAYTON, B. L., ZAREMBA, A., COLLINS, T. L., KUNJAMMA, R. B., ROBINSON, A. P., BRUGAROLAS, P., MILLER, R. H., MILLER, S. D. & POPKO, B. 2015. Pharmaceutical integrated stress response enhancement protects oligodendrocytes and provides a potential multiple sclerosis therapeutic. *Nat Commun,* 6**,** 6532.

WEI, L., LEE, D., LAW, C. T., ZHANG, M. S., SHEN, J., CHIN, D. W., ZHANG, A., TSANG, F. H., WONG, C. L., NG, I. O., WONG, C. C. & WONG, C. M. 2019. Genome-wide CRISPR/Cas9 library screening identified PHGDH as a critical driver for Sorafenib resistance in HCC. *Nat Commun,* 10**,** 4681.

WEI, W., JIN, J., SCHLISIO, S., HARPER, J. W. & KAELIN, W. G., JR. 2005. The v-Jun point mutation allows c-Jun to escape GSK3-dependent recognition and destruction by the Fbw7 ubiquitin ligase. *Cancer Cell,* 8**,** 25-33.

WEI, X., YANG, J., ADAIR, S. J., OZTURK, H., KUSCU, C., LEE, K. Y., KANE, W. J., O'HARA, P. E., LIU, D., DEMIRLENK, Y. M., HABIEB, A. H., YILMAZ, E., DUTTA, A., BAUER, T. W. & ADLI, M. 2020. Targeted CRISPR screening identifies PRMT5 as synthetic lethality combinatorial target with gemcitabine in pancreatic cancer cells. *Proc Natl Acad Sci U S A,* 117**,** 28068-28079.

WEINBERG, R. A. 2014. *The biology of cancer*, New York : Garland Science, Taylor & Francis Group.

WEINHOUSE, S., WARBURG, O., BURK, D. & SCHADE, A. L. 1956. On Respiratory Impairment in Cancer Cells. *Science,* 124**,** 267-269.

WELCKER, M. & CLURMAN, B. E. 2008. FBW7 ubiquitin ligase: a tumour suppressor at the crossroads of cell division, growth and differentiation. *Nat Rev Cancer,* 8**,** 83-93.

WELCKER, M., LARIMORE, E. A., FRAPPIER, L. & CLURMAN, B. E. 2011. Nucleolar targeting of the fbw7 ubiquitin ligase by a pseudosubstrate and glycogen synthase kinase 3. *Mol Cell Biol,* 31**,** 1214-1224.

WELCKER, M., LARIMORE, E. A., SWANGER, J., BENGOECHEA-ALONSO, M. T., GRIM, J. E., ERICSSON, J., ZHENG, N. & CLURMAN, B. E. 2013. Fbw7 dimerization determines the specificity and robustness of substrate degradation. *Genes Dev,* 27**,** 2531-2536.

WELCKER, M., ORIAN, A., GRIM, J. E., EISENMAN, R. N. & CLURMAN, B. E. 2004a. A nucleolar isoform of the Fbw7 ubiquitin ligase regulates c-Myc and cell size. *Curr Biol,* 14**,** 1852-1857.

WELCKER, M., ORIAN, A., JIN, J., GRIM, J. A., HARPER, J. W., EISENMAN, R. N. & CLURMAN, B. E. 2004b. The Fbw7 tumor suppressor regulates glycogen synthase kinase 3 phosphorylation-dependent c-Myc protein degradation. *Proceedings of the National Academy of Sciences,* 101**,** 9085-9090.

WERTZ, I. E., KUSAM, S., LAM, C., OKAMOTO, T., SANDOVAL, W., ANDERSON, D. J., HELGASON, E., ERNST, J. A., EBY, M., LIU, J., BELMONT, L. D., KAMINKER, J. S., O'ROURKE, K. M., PUJARA, K., KOHLI, P. B., JOHNSON, A. R., CHIU, M. L., LILL, J. R., JACKSON, P. K., FAIRBROTHER, W. J., SESHAGIRI, S., LUDLAM, M. J., LEONG, K. G., DUEBER, E. C., MAECKER, H., HUANG, D. C. & DIXIT, V. M. 2011. Sensitivity to antitubulin chemotherapeutics is regulated by MCL1 and FBW7. *Nature,* 471**,** 110-114.

WHITAKER-MENEZES, D., MARTINEZ-OUTSCHOORN, U. E., FLOMENBERG, N., BIRBE, R. C., WITKIEWICZ, A. K., HOWELL, A., PAVLIDES, S., TSIRIGOS, A., ERTEL, A., PESTELL, R. G., BRODA, P., MINETTI, C., LISANTI, M. P. & SOTGIA, F. 2011. Hyperactivation of oxidative mitochondrial metabolism in epithelial cancer cells in situ: visualizing the therapeutic effects of metformin in tumor tissue. *Cell Cycle,* 10**,** 4047-4064.

WHO, W. H. O. 2018. *Global Cancer Observatory* [Online]. Available: https://gco.iarc.fr/ [Accessed].

WIECZOREK, S., COMBES, F., LAZAR, C., GIAI GIANETTO, Q., GATTO, L., DORFFER, A., HESSE, A.-M., COUTÉ, Y., FERRO, M., BRULEY, C. & BURGER, T. 2017. DAPAR & ProStaR: software to perform statistical analyses in quantitative discovery proteomics. *Bioinformatics,* 33**,** 135-136.

WINSTON, J. T., KOEPP, D. M., ZHU, C., ELLEDGE, S. J. & HARPER, J. W. 1999. A family of mammalian F-box proteins. *Current Biology,* 9**,** 1180-1182.

WOLKING, S., SCHAEFFELER, E., LERCHE, H., SCHWAB, M. & NIES, A. T. 2015. Impact of Genetic Polymorphisms of ABCB1 (MDR1, P-Glycoprotein) on Drug Disposition and Potential Clinical Implications: Update of the Literature. *Clin Pharmacokinet,* 54**,** 709-735.

WONG, A. S., CHOI, G. C., CUI, C. H., PREGERNIG, G., MILANI, P., ADAM, M., PERLI, S. D., KAZER, S. W., GAILLARD, A., HERMANN, M., SHALEK, A. K., FRAENKEL, E. & LU, T. K. 2016. Multiplexed barcoded CRISPR-Cas9 screening enabled by CombiGEM. *Proc Natl Acad Sci U S A,* 113**,** 2544-2549.

WU, C. P., HSIAO, S. H., SIM, H. M., LUO, S. Y., TUO, W. C., CHENG, H. W., LI, Y. Q., HUANG, Y. H. & AMBUDKAR, S. V. 2013. Human ABCB1 (P-glycoprotein) and ABCG2 mediate resistance to BI 2536, a potent and selective inhibitor of Polo-like kinase 1. *Biochem Pharmacol,* 86**,** 904-913.

WU, G., LYAPINA, S., DAS, I., LI, J., GURNEY, M., PAULEY, A., CHUI, I., DESHAIES, R. J. & KITAJEWSKI, J. 2001. SEL-10 Is an Inhibitor of Notch Signaling That Targets Notch for Ubiquitin-Mediated Protein Degradation. *Molecular and Cellular Biology,* 21**,** 7403-7415.

WU, H. I., BROWN, J. A., DORIE, M. J., LAZZERONI, L. & BROWN, J. M. 2004. Genome-Wide Identification of Genes Conferring Resistance to the Anticancer Agents Cisplatin, Oxaliplatin, and Mitomycin C. *Cancer Research,* 64**,** 3940-3948.

WU, R. C., FENG, Q., LONARD, D. M. & O'MALLEY, B. W. 2007. SRC-3 coactivator functional lifetime is regulated by a phospho-dependent ubiquitin time clock. *Cell,* 129**,** 1125-1140.

XI, Z., YAO, M., LI, Y., XIE, C., HOLST, J., LIU, T., CAI, S., LAO, Y., TAN, H., XU, H. X. & DONG, Q. 2016. Guttiferone K impedes cell cycle re-entry of quiescent prostate cancer cells via stabilization of FBXW7 and subsequent c-MYC degradation. *Cell Death Dis,* 7**,** e2252.

XIAO, D., YUE, M., SU, H., REN, P., JIANG, J., LI, F., HU, Y., DU, H., LIU, H. & QING, G. 2016. Polo-like Kinase-1 Regulates Myc Stabilization and Activates a Feedforward Circuit Promoting Tumor Cell Survival. *Mol Cell,* 64**,** 493-506.

XIAO, G., LI, Y., WANG, M., LI, X., QIN, S., SUN, X., LIANG, R., ZHANG, B., DU, N., XU, C., REN, H. & LIU, D. 2018a. FBXW7 suppresses epithelial-mesenchymal transition and chemo-resistance of non-small-cell lung cancer cells by targeting snai1 for ubiquitin-dependent degradation. *Cell Prolif,* 51**,** e12473.

XIAO, Y., YIN, C., WANG, Y., LV, H., WANG, W., HUANG, Y., PEREZ-LOSADA, J., SNIJDERS, A. M., MAO, J. H. & ZHANG, P. 2018b. FBXW7 deletion contributes to lung tumor development and confers resistance to gefitinib therapy. *Mol Oncol,* 12**,** 883-895.

XIE, C. M., TAN, M., LIN, X. T., WU, D., JIANG, Y., TAN, Y., LI, H., MA, Y., XIONG, X. & SUN, Y. 2019. The FBXW7-SHOC2-Raptor Axis Controls the Cross-Talks between the RAS-ERK and mTORC1 Signaling Pathways. *Cell Rep,* 26**,** 3037-3050 e4.

XIONG, Y., LIU, W., HUANG, Q., WANG, J., WANG, Y., LI, H. & FU, X. 2018. Tigecycline as a dual inhibitor of retinoblastoma and angiogenesis via inducing mitochondrial dysfunctions and oxidative damage. *Sci Rep,* 8**,** 11747.

XU, D., LIANG, S. Q., YANG, H., BRUGGMANN, R., BEREZOWSKA, S., YANG, Z., MARTI, T. M., HALL, S. R. R., GAO, Y., KOCHER, G. J., SCHMID, R. A. & PENG, R. W. 2020. CRISPR Screening Identifies WEE1 as a Combination Target for Standard Chemotherapy in Malignant Pleural Mesothelioma. *Mol Cancer Ther,* 19**,** 661-672.

XU, W., TARANETS, L. & POPOV, N. 2016. Regulating Fbw7 on the road to cancer. *Semin Cancer Biol,* 36**,** 62-70.

XU, Y., GAO, W., ZHANG, Y., WU, S., LIU, Y., DENG, X., XIE, L., YANG, J., YU, H., SU, J. & SUN, L. 2018. ABT737 reverses cisplatin resistance by targeting glucose metabolism of human ovarian cancer cells. *Int J Oncol,* 53**,** 1055-1068.

YADA, M., HATAKEYAMA, S., KAMURA, T., NISHIYAMA, M., TSUNEMATSU, R., IMAKI, H., ISHIDA, N., OKUMURA, F., NAKAYAMA, K. & NAKAYAMA, K. I. 2004. Phosphorylation-dependent degradation of c-Myc is mediated by the F-box protein Fbw7. *EMBO J,* 23**,** 2116-2125.

YALLA, K., ELLIOTT, C., DAY, J. P., FINDLAY, J., BARRATT, S., HUGHES, Z. A., WILSON, L., WHITELEY, E., POPIOLEK, M., LI, Y., DUNLOP, J., KILLICK, R., ADAMS, D. R., BRANDON, N. J., HOUSLAY, M. D., HAO, B. & BAILLIE, G. S. 2018. FBXW7 regulates DISC1 stability via the ubiquitin-proteosome system. *Mol Psychiatry,* 23**,** 1278-1286.

YAMAUCHI, T., MASUDA, T., CANVER, M. C., SEILER, M., SEMBA, Y., SHBOUL, M., AL-RAQAD, M., MAEDA, M., SCHOONENBERG, V. A. C., COLE, M. A., MACIAS-TREVINO, C., ISHIKAWA, Y., YAO, Q., NAKANO, M., ARAI, F., ORKIN, S. H., REVERSADE, B., BUONAMICI, S., PINELLO, L., AKASHI, K., BAUER, D. E. & MAEDA, T. 2018. Genome-wide CRISPR-Cas9 Screen Identifies Leukemia-Specific Dependence on a Pre-mRNA Metabolic Pathway Regulated by DCPS. *Cancer Cell,* 33**,** 386-400 e5.

YAN, J., XIE, Y., WANG, F., CHEN, Y., ZHANG, J., DOU, Z., GAN, L., LI, H., SI, J., SUN, C., DI, C. & ZHANG, H. 2020a. Carbon ion combined with tigecycline inhibits lung cancer cell proliferation by inducing mitochondrial dysfunction. *Life Sci,* 263**,** 118586.

YAN, L., LIN, M., PAN, S., ASSARAF, Y. G., WANG, Z. W. & ZHU, X. 2020b. Emerging roles of F-box proteins in cancer drug resistance. *Drug Resist Updat,* 49**,** 100673.

YANG, H., LU, X., LIU, Z., CHEN, L., XU, Y., WANG, Y., WEI, G. & CHEN, Y. 2015. FBXW7 suppresses epithelial-mesenchymal transition, stemness and metastatic potential of cholangiocarcinoma cells. *Oncotarget,* 6**,** 6310-6325.

YANG, R., YI, L., DONG, Z., OUYANG, Q., ZHOU, J., PANG, Y., WU, Y., XU, L. & CUI, H. 2016. Tigecycline Inhibits Glioma Growth by Regulating miRNA-199b-5p–HES1–AKT Pathway. *Molecular Cancer Therapeutics,* 15**,** 421-429.

YAO, C. H., WANG, R., WANG, Y., KUNG, C. P., WEBER, J. D. & PATTI, G. J. 2019. Mitochondrial fusion supports increased oxidative phosphorylation during cell proliferation. *Elife,* 8**,** e41351.

YAO, S., XU, F., CHEN, Y., GE, Y., ZHANG, F., HUANG, H., LI, L., LIN, D., LUO, X., XU, J., LUO, D., ZHU, X. & LIU, Y. 2017. Fbw7 regulates apoptosis in activated B-cell like diffuse large B-cell lymphoma by targeting Stat3 for ubiquitylation and degradation. *J Exp Clin Cancer Res,* 36**,** 10.

YE, J., KUMANOVA, M., HART, L. S., SLOANE, K., ZHANG, H., DE PANIS, D. N., BOBROVNIKOVA-MARJON, E., DIEHL, J. A., RON, D. & KOUMENIS, C. 2010. The GCN2-ATF4 pathway is critical for tumour cell survival and proliferation in response to nutrient deprivation. *EMBO J,* 29**,** 2082-2096.

YE, M., ZHANG, Y., ZHANG, X., ZHANG, J., JING, P., CAO, L., LI, N., LI, X., YAO, L., ZHANG, J. & ZHANG, J. 2017. Targeting FBW7 as a Strategy to Overcome Resistance to Targeted Therapy in Non-Small Cell Lung Cancer. *Cancer Res,* 77**,** 3527-3539.

YEH, C. H., BELLON, M. & NICOT, C. 2018. FBXW7: a critical tumor suppressor of human cancers. *Mol Cancer,* 17**,** 115.

YOKOBORI, T., YOKOYAMA, Y., MOGI, A., ENDOH, H., ALTAN, B., KOSAKA, T., YAMAKI, E., YAJIMA, T., TOMIZAWA, K., AZUMA, Y., ONOZATO, R., MIYAZAKI, T., TANAKA, S. & KUWANO, H. 2014. FBXW7 mediates chemotherapeutic sensitivity and prognosis in NSCLCs. *Mol Cancer Res,* 12**,** 32-37.

YOON, J.-H., LEE, C.-S., O'CONNOR, T. R., YASUI, A. & PFEIFER, G. P. 2000. The DNA damage spectrum produced by simulated sunlight. *Journal of Molecular Biology,* 299**,** 681-693.

YU, H. G., WEI, W., XIA, L. H., HAN, W. L., ZHAO, P., WU, S. J., LI, W. D. & CHEN, W. 2013. FBW7 upregulation enhances cisplatin cytotoxicity in non- small cell lung cancer cells. *Asian Pac J Cancer Prev,* 14**,** 6321-6326.

YU, J., ZHANG, W., GAO, F., LIU, Y.-X., CHEN, Z.-Y., CHENG, L.-Y., XIE, S.-F. & ZHENG, S.-S. 2014. FBW7 increases chemosensitivity in hepatocellular carcinoma cells through suppression of epithelial-mesenchymal transition. *Hepatobiliary & Pancreatic Diseases International,* 13**,** 184-191.

YU, S., WANG, F., TAN, X., GAO, G. L., PAN, W. J., LUAN, Y. & GE, X. 2018. FBW7 targets KLF10 for ubiquitin-dependent degradation. *Biochem Biophys Res Commun,* 495**,** 2092-2097.

YUMIMOTO, K., AKIYOSHI, S., UEO, H., SAGARA, Y., ONOYAMA, I., UEO, H., OHNO, S., MORI, M., MIMORI, K. & NAKAYAMA, K. I. 2015. F-box protein FBXW7 inhibits cancer metastasis in a non-cell-autonomous manner. *J Clin Invest,* 125**,** 621-35.

YUMIMOTO, K., MATSUMOTO, M., ONOYAMA, I., IMAIZUMI, K. & NAKAYAMA, K. I. 2013. F-box and WD Repeat Domain-containing-7 (Fbxw7) Protein Targets Endoplasmic Reticulum-anchored Osteogenic and Chondrogenic Transcriptional Factors for Degradation. *Journal of Biological Chemistry,* 288**,** 28488-28502.

YUMIMOTO, K., MATSUMOTO, M., OYAMADA, K., MOROISHI, T. & NAKAYAMA, K. I. 2012. Comprehensive identification of substrates for F-box proteins by differential proteomics analysis. *J Proteome Res,* 11**,** 3175-3185.

YUMIMOTO, K. & NAKAYAMA, K. I. 2020. Recent insight into the role of FBXW7 as a tumor suppressor. *Semin Cancer Biol,* 67**,** 1-15.

YUN, C. W., HAN, Y. S. & LEE, S. H. 2019. PGC-1alpha Controls Mitochondrial Biogenesis in Drug-Resistant Colorectal Cancer Cells by Regulating Endoplasmic Reticulum Stress. *Int J Mol Sci,* 20**,** 1707.

ZACKSENHAUS, E., SHRESTHA, M., LIU, J. C., VOROBIEVA, I., CHUNG, P. E. D., JU, Y., NIR, U. & JIANG, Z. 2017. Mitochondrial OXPHOS Induced by RB1 Deficiency in Breast Cancer: Implications for Anabolic Metabolism, Stemness, and Metastasis. *Trends Cancer,* 3**,** 768-779.

ZENG, H., CASTILLO-CABRERA, J., MANSER, M., LU, B., YANG, Z., STRANDE, V., BEGUE, D., ZAMPONI, R., QIU, S., SIGOILLOT, F., WANG, Q., LINDEMAN, A., REECE-HOYES, J. S., RUSS, C., BONENFANT, D., JIANG, X., WANG, Y. & CONG, F. 2019. Genome-wide CRISPR screening reveals genetic modifiers of mutant EGFR dependence in human NSCLC. *Elife,* 8**,** e50223.

ZHAN, P., WANG, Y., ZHAO, S., LIU, C., WANG, Y., WEN, M., MAO, J. H., WEI, G. & ZHANG, P. 2015. FBXW7 negatively regulates ENO1 expression and function in colorectal cancer. *Lab Invest,* 95**,** 995-1004.

ZHANG, C., CHEN, F., FENG, L., SHAN, Q., ZHENG, G. H., WANG, Y. J., LU, J., FAN, S. H., SUN, C. H., WU, D. M., LI, M. Q., HU, B., WANG, Q. Q., ZHANG, Z. F. & ZHENG, Y. L. 2019a. FBXW7 suppresses HMGB1-mediated innate immune signaling to attenuate hepatic inflammation and insulin resistance in a mouse model of nonalcoholic fatty liver disease. *Mol Med,* 25**,** 29.

ZHANG, H., CHEN, F., HE, Y., YI, L., GE, C., SHI, X., TANG, C., WANG, D., WU, Y. & NIAN, W. 2017. Sensitivity of non-small cell lung cancer to erlotinib is regulated by the Notch/miR-223/FBXW7 pathway. *Biosci Rep,* 37**,** BSR20160478.

ZHANG, L., GING, N. C., KOMODA, T., HANADA, T., SUZUKI, T. & WATANABE, K. 2005. Antibiotic susceptibility of mammalian mitochondrial translation. *FEBS Lett,* 579**,** 6423-6427.

ZHANG, L., YAO, Y., ZHANG, S., LIU, Y., GUO, H., AHMED, M., BELL, T., ZHANG, H., HAN, G., LORENCE, E., BADILLO, M., ZHOU, S., SUN, Y., DI FRANCESCO, M. E., FENG, N., HAUN, R., LAN, R., MACKINTOSH, S. G., MAO, X., SONG, X., ZHANG, J., PHAM, L. V., LORENZI, P. L., MARSZALEK, J., HEFFERNAN, T., DRAETTA, G., JONES, P., FUTREAL, A., NOMIE, K., WANG, L. & WANG, M. 2019b. Metabolic reprogramming toward oxidative phosphorylation identifies a therapeutic target for mantle cell lymphoma. *Science Translational Medicine,* 11**,** eaau1167.

ZHANG, P., MCGRATH, B. C., REINERT, J., OLSEN, D. S., LEI, L., GILL, S., WEK, S. A., VATTEM, K. M., WEK, R. C., KIMBALL, S. R., JEFFERSON, L. S. & CAVENER, D. R. 2002. The GCN2 eIF2alpha kinase is required for adaptation to amino acid deprivation in mice. *Mol Cell Biol,* 22**,** 6681-6688.

ZHANG, Q., KARNAK, D., TAN, M., LAWRENCE, T. S., MORGAN, M. A. & SUN, Y. 2016a. FBXW7 Facilitates Nonhomologous End-Joining via K63-Linked Polyubiquitylation of XRCC4. *Mol Cell,* 61**,** 419-433.

ZHANG, Q., LI, X., CUI, K., LIU, C., WU, M., PROCHOWNIK, E. V. & LI, Y. 2020a. The MAP3K13-TRIM25-FBXW7alpha axis affects c-Myc protein stability and tumor development. *Cell Death Differ,* 27**,** 420-433.

ZHANG, Q., ZHANG, Y., PARSELS, J. D., LOHSE, I., LAWRENCE, T. S., PASCA DI MAGLIANO, M., SUN, Y. & MORGAN, M. A. 2016b. Fbxw7 Deletion Accelerates Kras(G12D)-Driven Pancreatic Tumorigenesis via Yap Accumulation. *Neoplasia,* 18**,** 666-673.

ZHANG, Y., DING, H., WANG, X. & YE, S. D. 2018a. Modulation of STAT3 phosphorylation by PTPN2 inhibits naive pluripotency of embryonic stem cells. *FEBS Lett,* 592**,** 2227-2237.

ZHANG, Y., TAO, Y., JI, H., LI, W., GUO, X., NG, D. M., HALEEM, M., XI, Y., DONG, C., ZHAO, J., ZHANG, L., ZHANG, X., XIE, Y., DAI, X. & LIAO, Q. 2019c. Genome-wide identification of the essential protein-coding genes and long non-coding RNAs for human pan-cancer. *Bioinformatics,* 35**,** 4344-4349.

ZHANG, Y., ZHANG, X., YE, M., JING, P., XIONG, J., HAN, Z., KONG, J., LI, M., LAI, X., CHANG, N., ZHANG, J. & ZHANG, J. 2018b. FBW7 loss promotes epithelial-to-mesenchymal transition in non-small cell lung cancer through the stabilization of Snail protein. *Cancer Lett,* 419**,** 75-83.

ZHANG, Z., GUO, M., LI, Y., SHEN, M., KONG, D., SHAO, J., DING, H., TAN, S., CHEN, A., ZHANG, F. & ZHENG, S. 2020b. RNA-binding protein ZFP36/TTP protects against ferroptosis by regulating autophagy signaling pathway in hepatic stellate cells. *Autophagy,* 16**,** 1482-1505.

ZHAO, D., ZHENG, H. Q., ZHOU, Z. & CHEN, C. 2010. The Fbw7 tumor suppressor targets KLF5 for ubiquitin-mediated degradation and suppresses breast cell proliferation. *Cancer Res,* 70**,** 4728-4738.

ZHAO, J., TANG, J., MEN, W. & REN, K. 2012. FBXW7-mediated degradation of CCDC6 is impaired by ATM during DNA damage response in lung cancer cells. *FEBS Lett,* 586**,** 4257-4263.

ZHAO, J., XIONG, X., LI, Y., LIU, X., WANG, T., ZHANG, H., JIAO, Y., JIANG, J., ZHANG, H., TANG, Q., GAO, X., LI, X., LU, Y., LIU, B., HU, C. & LI, X. 2018. Hepatic F-Box Protein FBXW7 Maintains Glucose Homeostasis Through Degradation of Fetuin-A. *Diabetes,* 67**,** 818-830.

ZHAO, Q., WANG, J., LEVICHKIN, I. V., STASINOPOULOS, S., RYAN, M. T. & HOOGENRAAD, N. J. 2002. A mitochondrial specific stress response in mammalian cells. *The EMBO journal,* 21**,** 4411-4419.

ZHAO, X., HIROTA, T., HAN, X., CHO, H., CHONG, L. W., LAMIA, K., LIU, S., ATKINS, A. R., BANAYO, E., LIDDLE, C., YU, R. T., YATES, J. R., 3RD, KAY, S. A., DOWNES, M. & EVANS, R. M. 2016. Circadian Amplitude Regulation via FBXW7-Targeted REV-ERBalpha Degradation. *Cell,* 165**,** 1644-1657.

ZHENG, A., CHEVALIER, N., CALDERONI, M., DUBUIS, G., DORMOND, O., ZIROS, P. G., SYKIOTIS, G. P. & WIDMANN, C. 2019. CRISPR/Cas9 genome-wide screening identifies KEAP1 as a sorafenib, lenvatinib, and regorafenib sensitivity gene in hepatocellular carcinoma. *Oncotarget,* 10**,** 7058-7070.

ZHENG, N., SCHULMAN, B. A., SONG, L., MILLER, J. J., JEFFREY, P. D., WANG, P., CHU, C., KOEPP, D. M., ELLEDGE, S. J., PAGANO, M., CONAWAY, R. C., CONAWAY, J. W., HARPER, J. W. & PAVLETICH, N. P. 2002. Structure of the Cul1–Rbx1–Skp1–F boxSkp2 SCF ubiquitin ligase complex. *Nature,* 416**,** 703-709.

ZHENG, X., CARSTENS, J. L., KIM, J., SCHEIBLE, M., KAYE, J., SUGIMOTO, H., WU, C. C., LEBLEU, V. S. & KALLURI, R. 2015. Epithelial-to-mesenchymal transition is dispensable for metastasis but induces chemoresistance in pancreatic cancer. *Nature,* 527**,** 525-530.

ZHONG, X., ZHAO, E., TANG, C., ZHANG, W., TAN, J., DONG, Z., DING, H. F. & CUI, H. 2016. Antibiotic drug tigecycline reduces neuroblastoma cells proliferation by inhibiting Akt activation in vitro and in vivo. *Tumour Biol,* 37**,** 7615-7623.

ZHOU, X., JIN, W., JIA, H., YAN, J. & ZHANG, G. 2015. MiR-223 promotes the cisplatin resistance of human gastric cancer cells via regulating cell cycle by targeting FBXW7. *J Exp Clin Cancer Res,* 34**,** 28.

ZHOU, Y., ZHU, S., CAI, C., YUAN, P., LI, C., HUANG, Y. & WEI, W. 2014. High-throughput screening of a CRISPR/Cas9 library for functional genomics in human cells. *Nature,* 509**,** 487-491.

ZHU, J., LI, Y., CHEN, C., MA, J., SUN, W., TIAN, Z., LI, J., XU, J., LIU, C. S., ZHANG, D., HUANG, C. & HUANG, H. 2017. NF-κB p65 Overexpression Promotes Bladder Cancer Cell Migration via FBW7-Mediated Degradation of RhoGDIα Protein. *Neoplasia,* 19**,** 672-683.